



Thèse

2020

Open Access

This version of the publication is provided by the author(s) and made available in accordance with the copyright holder(s).

Mechanisms and Persistence of Chromatin-Mediated Antisense Transcription Interference

Kaur, Jatinder

How to cite

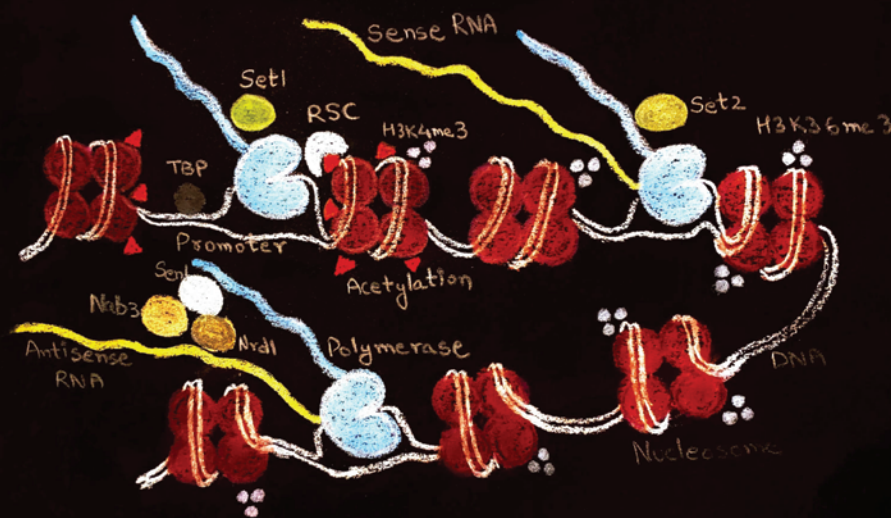
KAUR, Jatinder. Mechanisms and Persistence of Chromatin-Mediated Antisense Transcription Interference. 2020. doi: 10.13097/archive-ouverte/unige:148174

This publication URL: <https://archive-ouverte.unige.ch//unige:148174>

Publication DOI: [10.13097/archive-ouverte/unige:148174](https://doi.org/10.13097/archive-ouverte/unige:148174)



Mechanisms and Persistence of Chromatin-Mediated Antisense Transcription Interference



Jatinder Kaur

de

Punjab, India

Professeur Françoise Stutz

Dr. Julien Soudet

Thèse N° 80

Center d'impression de l'unige

2020

UNIVERSITÉ DE GENÈVE
Section de biologie
Département de Biologie Cellulaire

FACULTÉ DES SCIENCES
Professeur Françoise Stutz
Dr. Julien Soudet

Mechanisms and Persistence of Chromatin-Mediated Antisense Transcription Interference

THÈSE

présentée aux Facultés de médecine et des sciences de l'Université de Genève
pour obtenir le grade de Docteur ès sciences en sciences de la vie,
mention Biosciences moléculaires

par

Jatinder Kaur

de

Punjab, Inde

Thèse N° 80

GENÈVE

Center d'impression de l'unige

2020



DOCTORAT ÈS SCIENCES EN SCIENCES DE LA VIE DES
FACULTÉS DE MÉDECINE ET DES SCIENCES
MENTION BIOSCIENCES MOLECULAIRES

Thèse de Madame Jatinder KAUR

intitulée

**«Mechanisms and Persistence of Chromatin-Mediated
Antisense Transcription Interference»**

Les Facultés de médecine et des sciences, sur le préavis de Madame F STUTZ, professeure ordinaire et directeur de thèse (Département de biologie cellulaire), Monsieur J SOUDET, docteur et codirecteur de thèse (Département de biologie cellulaire), Monsieur D SHORE, professeur ordinaire (Département de biologie moléculaire), Monsieur N LUSCOMBE, docteur (Bioinformatics and Computational Biology Laboratory, The Francis Crick Institute, London, United Kingdom), Monsieur A. JACQUIER, docteur (Génétique des génomes, Génétique des Interactions Macromoléculaires, Institut Pasteur, Paris, France), autorisent l'impression de la présente thèse, sans exprimer d'opinion sur les propositions qui y sont énoncées.

Genève, le 19 octobre 2020

Thèse - 80 -

Le Doyen

Faculté de médecine

Le Doyen

Faculté des sciences

N.B. - La thèse doit porter la déclaration précédente et remplir les conditions énumérées dans les "Informations relatives aux thèses de doctorat à l'Université de Genève"

ACKNOWLEDGMENTS

I am grateful to my parents for teaching me to believe in myself. To my brothers and parents, who I know are with me, even if they are not close.

I am very grateful to both Françoise and Julien, for endless scientific discussions. They also read my TAC report, this thesis, which I know is not easy. I am grateful to them, as they motivate me to work when I couldn't see that it is worth it and logically contradicted me, when I was wrong. During my PhD, all the conversations helped me see things from other person's perspective. I also want to thank both Françoise and Julien, as they supported me in all the courses that I took during my PhD, to improve my ability to analyse large data sets. I also appreciate all the conversations I had at meetings with scientists and Françoise for giving me that opportunity.

I am very grateful to the people at SIB training unit, namely Diana Marek, Frédéric Schütz and Patricia Palagi. It is a very good network to learn new techniques and analysis. I would like to thank my TAC committee members, Dr. Florian Steiner, Dr. Michel Strubin, Dr. Ramesh Pillai, for reading the report thoroughly and giving me valuable feedback. I would also like to thank everyone in the selection committee of iGE3, Dr. David Shore, Dr. Emmanouil T. Dermitzakis, Dr. Denis Duboule, Dr. Emi Nagoshi, Dr. Dominique Soldati-Favre for selecting me for a two-year PhD salary grant.

The Department and Sciences III building represent a very collaborative environment. I asked for strains or samples from the Schalch, Shore, Loewith, Thanos, Picard and Martinou labs and they were very happy to share them with me. I also want to say that during the departmental presentations, once I presented a science paper in 13 minutes, I am grateful to you all, that you sat through it. I also want to thank you for important feedback during progress reports. I took bioinformatic classes with Dr. Mathias Currat and Dr. Jose Manuel Nunes from the department of Anthropology and it helped me a lot in the analyses presented in the thesis. I performed the Nascent RNA analyses with Dr. Nunez. I am grateful to both Dr. Nunez and Dr. Estella Poloni, as they gave me the opportunity to be a teaching assistant. It was a valuable experience.

In the lab, I will always remember the interesting conversations I had with Ivona, Geraldine, Julien, Audrey, Nataliia, Anna and Mariel. I would especially like to thank Geraldine, for making litres of

media, 100s of plates and also placing countless orders for me. I would like to thank all the lab members who helped me whenever I was stuck in an experiment, especially Julien. I also want to thank the PhD conference organising members, who worked with me during the organisation for 2019 conference. I am also grateful for all the social events like Easter and Christmas parties organised by the departments. I am thankful to Ms Carol and Ms Francesca for the help with paperwork during these 3.7 years. I am also grateful to Ms. Claudine for help in organising the PhD conference and for help with the administration work for setting-up deadlines for the thesis.

I would like to thank the Jury members, Dr. Alain Jacquier, Dr. David Shore, Dr. Nicholas Luscombe for agreeing to be in my thesis committee and critically reading the thesis manuscript.

I would like to thank everyone, who befriended me during my PhD and was a part of my social life. Everyone at the boxing club genevois, especially coach Samir. Please forgive me, if I forgot to mention anyone.

**Mechanisms and Persistence of
Chromatin-Mediated
Antisense Transcription Interference**

CONTENTS

ABSTRACT	1
RÉSUMÉ	3
INTRODUCTION	5
1 Chromatin and Transcription	7
1.1 Nucleosome: Basic Chromatin unit regulating DNA accessibility	7
1.1.1 Nucleosome Array: Format of Organisation of Eukaryotic Genome	9
1.1.2 Nucleosome Depleted Region: Break in the Array	9
1.2 Mechanisms of NDR formation	12
1.2.1 DNA sequence composition: Inherent determinant of an NDR	12
1.2.2 Role of General Regulatory Factors in NDR formation	13
1.2.3 Chromatin Remodelers shape NDRs	14
1.2.3.1 SWR1 and INO80 Govern -1/+1 Nucleosome Composition	14
1.2.3.2 RSC Regulate NDR Width	15
1.2.3.3 ISW1 and CHD1: Determinants of Nucleosome Array Spacing	17
1.3 Importance of Histone Acetylation at -1/+1 Nucleosomes	18
1.3.1 SAGA Histone Acetyl Transferase Complex	19
1.3.2 Rtt109 Histone Acetyl Transferase	20
1.3.3 NuA4 Histone Acetyl Transferase Complex	20
1.4 Pre-Initiation Complex Assembly	22
1.4.1 TFIID DNA Binding Initiates Assembly	23
1.4.2 Transcription Initiation	23
1.4.3 Mediator complex: Relay of Transcription Signals	24
1.5 Transcription Elongates with Co-conspirators	25
1.5.1 Transcription Initiation by Pol II CTD Phosphorylation	25
1.5.2 Transcription Bursts ON and OFF	27
1.5.3 Transcription Runs in both directions	27
1.6 Elongating polymerase re-write Chromatin Code	28
1.6.1 H3K4me Mark Active Promoters	28
1.6.2 H3K36me: Closing Chromatin After Polymerase	30
1.6.2.1 Rpd3 Histone Deacetylase recognises H3K36me3	30
1.7 Termination: pushing the break	31

2	Transcription of Non-Coding RNAs	32
2.1	Long Non-coding RNAs	32
2.2	<i>Cis-acting</i> LncRNA	33
2.2.1	Transcription Interference	34
2.2.2	Chromatin Mediates Transcription Interference	35
2.3	Antisense LncRNAs act in <i>Cis</i>	36
2.3.1	Nrd1-Nab3-Sen1 termination	37
2.3.2	Physiological Antisense Regulation	40
3	Objectives	41
	RESULTS	42
1	Antisense-Mediated Interference Mechanism	42
	Fine Chromatin-driven mechanism of transcription interference by antisense non-coding transcription	43
2	Alleviation of Antisense-Mediated Repression	62
2.1	Introduction	63
2.1.1	Mechanisms of Epigenetic Memory Maintenance	64
2.1.1.1	Non-coding RNAs Bind Chromatin Regulators	64
2.1.1.2	Reader-Modifier Reestablishment of Epigenetic Marks	65
2.1.1.3	Influence of Chromatin Domains on Epigenetics	66
2.1.2	Mechanisms of Erasure of Epigenetic Marks	67
2.1.2.1	Replication	67
2.1.2.2	Replication Independent Histone Exchange	68
2.1.2.3	Active Modification of PTMs	68
2.1.3	Antisense Transcription Modifies Chromatin PTMs	69
2.2	Antisense-Mediated Repression prime Sense Transcription for Activation	69
	Antisense-Mediated Repression primes Sense Transcript Promoter for Activation by Inducing Acetylation	70

DISCUSSION	91
1 Antisense Mediates Transcription Interference Through Changes in Chromatin at NDR	91
1.1 Precise Positioning of Nucleosomes Regulate Transcription Initiation	92
1.2 Binding of Chromatin Regulators to Antisense Modified NDR Chromatin	92
1.3 Collisions of Transcribing RNA Pol II	93
1.4 Formation of Antisense RNA Secondary Structure	94
2 Transcription Interference primes Sense Promoter for Activation	95
2.1 Time Series Analysis reveals Transcription and Chromatin Dynamics	95
2.2 Transcription Interference Recovery is Promoter Type Dependent	96
2.3 Higher Acetylation could mediate Recovery by Increasing Burst Size	97
2.4 Histone turnover as the fastest way of changing chromatin around +1	98
2.5 Different Methylation and Acetylation kinetics might play a role in Recovery	99
2.6 Ambivalence of Set1C mediated H3K4me	101
2.7 Cell Cycle Regulation of Histone PTMs	101
2.8 Transcription Interference from Sense or AS act in the same manner	101
2.9 TI during Physiological Nutrient Stress Response	102
2.10 Chromatin Marks Save the Information in the Chromatin Combinations	102
SUPPLEMENTARY	104
1 Antisense-Mediated Interference Mechanism	105
2 Antisense-Mediated Repression primes Sense Transcript Promoter for Activation	120
REFERENCES	129
APPENDIX	148
A R scripts	148
A.1 Calculating AS Repressed Genes and Defining Clusters	148
A.2 Calculating Acetylation for H3K18ac MNase ChIP-seq	150
A.3 NDR Size Calculation	151
A.4 +1 Nucleosome Distribution Calculation	151
B Non-coding Transcription Regulates Replication Program in <i>Cis</i>	153

Abstract

Eukaryotic genomes are transcribed almost entirely on both strands in an interleaved manner. This gives rise to many non-coding RNA (ncRNA) transcripts overlapping coding gene promoters. Most ncRNAs arise from divergent non-coding transcription by RNA polymerase II or from 3' end nucleosome depleted regions. In the compact genome of the yeast *S. cerevisiae*, these non-coding transcripts end up being in antisense orientation to the upstream mRNA. Nuclear surveillance mechanisms restrict non-coding transcription through early-termination and degradation by Nrd1/Nab3/Sen1 (NNS) pathway, by recognising small Nrd1 and Nab3 binding motifs on the non-coding RNA. NcRNAs that escape this control are rapidly degraded in the cytoplasm by the nonsense mediated decay (NMD) pathway. Non-coding transcripts are therefore barely detectable in a cell but the act of transcribing non-coding RNAs by itself causes gene repression by a poorly understood mechanism of transcription interference (TI).

To resolve the transcription interference mechanism, we dynamically disrupted early-termination by anchoring Nrd1 away from the nucleus in order to globally extend antisense transcription. Following the changes in both mRNA and antisense ncRNA levels using RNA-seq, we identified 217 genes that are downregulated due to AS extension into their promoters after Nrd1 depletion. AS extension lead to decreased binding of the Pre-Initiation Complex (PIC) at sense promoters indicating that TI occurs at the level of sense transcript initiation. Given the importance of chromatin-related factors in TI, we analysed changes in chromatin organization in coding promoters upon Nrd1 depletion. By MNase-seq and ATAC-seq, we observed a shift of -1 and +1 nucleosomes, the nucleosomes that flank the promoter Nucleosome Depleted Region (NDR), towards the TATA-binding site (TBS). This shift is accompanied by an increase of H3K36me3 at the TBS and a decrease of H3K18ac at the original -1/+1 nucleosome positions. The movement is also linked to a decreased binding of RSC, the major chromatin remodeler promoting NDRs.

Sense repression, decreased PIC and RSC binding, as well as -1/+1 nucleosome sliding can be partially alleviated by the loss of Rpd3 Histone DeAcetylase (HDAC). Thus, we propose a transcription interference mechanism - AS extension into promoters deposits H3K36me3 at the -1/+1 nucleosomes inducing their subsequent deacetylation. This decrease in acetylation reduces RSC binding, leading to -1/+1 nucleosome sliding towards the TBS, thereby hindering PIC binding and sense transcription initiation.

This mechanism, deciphered using an inducible system, is compatible with 20% of the *S. cerevisiae* genes being regulated by antisense non-coding transcription at steady-state.

AS-mediated transcription interference occurs through changes in chromatin at the promoter NDRs. Histone modifications act as epigenetic marks of gene expression and are independently inheritable traits. Chromatin is divided and distributed equally to daughter cells in a position specific manner during replication. Thus, once AS repression is established in the form of histone PTMs, it is not known whether it would be inherited by the next generation after the removal of overlapping AS readthrough. To address this question, we first extended AS using an Auxin-inducible degron tagged Nrd1 strain, followed by washing the cells to restore Nrd1 and resume early-termination. Using 4-tU-seq, we observed an instant upregulation of the sense transcription units following removal of AS. Antisense-mediated repression (AMR) was not maintained. Interestingly, sense transcription did not go back to its initial levels but it was hyper-activated over 30 min after removal of AS. These observations suggest that AMR may act as an activating signal for sense transcription.

TI occurs through chromatin modifications and we therefore examined H3K18ac as well as the MNase profile at the sense promoters during AS early-termination recovery. We observed a peak of acetylation at 30 min consistent with the peak of sense RNA expression. Over the following time points, we observed an oscillating pattern in RNA levels. There was also a remnant oscillating pattern in H3K18ac while Mnase-seq data showed a rapid opening of NDRs at 150 min, which remained open for the rest of the recovery timepoints. Importantly, the restoration of chromatin modifications was dependent on dilution of histone marks by replication and we observed that in G1-arrested cells, NDRs were still “closed” until the last experimental timepoint, after 180 min in recovery. Histone acetyl transferases (HATs) also contribute to the recovery as we observed delayed opening of NDRs when depleting the NuA4 HAT during the recovery. Thus, we conclude that recovery from TI depends both on PTM dilution by replication and active histone acetylation.

Résumé

Les génomes eucaryotes sont pervasivement transcrits sur les deux brins, les unités de transcription s'entrelaçant. Ainsi, de nombreux ARNs non-codants chevauchent les promoteurs de gènes codants. La plupart des ARNs non-codants proviennent de la transcription divergente par l'ARN polymérase II ou de régions pauvres en nucléosomes en 3' des gènes. Dans un génome compact comme celui de la levure *Saccharomyces cerevisiae* (*S. cerevisiae*), ces ARNs non-codants se trouvent être dans une configuration antisens vis-à-vis du gène codant en amont. Des mécanismes de surveillance nucléaires limitent la transcription non-codante *via* terminaison précoce et dégradation par le complexe Nrd1/Nab3/Sen1 (NNS) à travers la reconnaissance par Nrd1 et Nab3 de motifs sur l'ARN non-codant. Les ARNs non-codants qui échappent à ce contrôle sont rapidement dégradés dans le cytoplasme. Les ARNs non-codants sont donc difficilement détectables dans une cellule mais l'acte de transcription non-codante, par lui-même, peut induire une répression génique par un mécanisme encore mal compris d'interférence de transcription.

Afin de résoudre le mécanisme d'interférence de transcription, nous avons interrompu la terminaison précoce de manière dynamique grâce à la déplétion de Nrd1 du noyau et ainsi induit globalement l'extension de la transcription antisens. Nous avons suivi les changements à la fois des ARNm et des ARNs non-codants antisens par RNA-seq, révélant ainsi 217 gènes réprimés par l'extension d'antisens dans leurs promoteurs après déplétion de Nrd1. L'extension d'antisens entraîne une diminution de recrutement du complexe de pré-initiation au niveau des promoteurs des gènes sens indiquant ainsi que l'interférence de transcription se produit au moment de l'initiation de la transcription. Étant donnée l'importance de facteurs chromatinien dans l'interférence de transcription, nous avons analysé les changements d'organisation de la chromatine dans les promoteurs des gènes codants lors de la déplétion de Nrd1. Par MNase-seq et ATAC-seq, nous avons observé un décalage des nucléosomes -1 et +1, les nucléosomes entourant les régions pauvres en nucléosomes, vers les sites de liaison TATA. Ce changement de position est accompagné par une augmentation de H3K36me3 au site TATA et une diminution de H3K18ac aux positions

originales des nucléosomes -1/+1. Il est également associé à une diminution de la liaison de RSC, le remodeleur de chromatine essentiel à la maintenance des régions pauvres en nucléosomes.

La répression des gènes sens, la diminution des recrutements du complexe de pré-initiation et de RSC ainsi que le glissement des nucléosomes -1/+1 peuvent être partiellement atténués par la délétion de l'histone déacétylase Rpd3. Ainsi, nous proposons comme mécanisme d'interférence de transcription que l'extension d'antisens dans les promoteurs dépose H3K36me3 aux nucléosomes -1/+1 induisant leur déacétylation. Cette diminution en acétylation réduit la liaison de RSC entraînant un décalage des nucléosomes -1/+1 vers les sites de liaison TATA et ainsi bloquant la liaison du complexe de pré-initiation et l'initiation de la transcription. Ce mécanisme élucidé dans un système inductible est compatible avec le 20% des gènes de *S. cerevisiae* régulés par transcription non-codante antisens à l'équilibre.

L'interférence de transcription par antisens dépend de changements chromatiniens dans les régions pauvres en nucléosomes des promoteurs. Les modifications d'histones sont considérées comme des marques épigénétiques et peuvent être le modèle de traits hérités de manière épigénétiques. En considérant cela, nous avons voulu savoir combien de temps l'interférence de transcription peut être héritée de manière épigénétique. En d'autres termes, combien de temps l'interférence de transcription persiste après la suppression de l'extension de l'antisens. Afin d'étudier cela, nous avons tout d'abord induit l'extension d'antisens en utilisant une souche dans laquelle la dégradation de Nrd1 peut être déclenchée par addition d'auxine avant de rétablir la terminaison précoce par lavage des cellules. Nous observons par 4tu-seq une absence globale de persistance de l'interférence de transcription après suppression de l'antisens. La transcription sens ne revient pas à son niveau initial mais est surexprimée 30min après la suppression de la transcription antisens indiquant que l'interférence de transcription joue le rôle d'activateur pour la transcription sens subséquente.

L'interférence de transcription fait intervenir des modifications de la chromatine et nous avons donc analysé les profils H3K18ac et de nucléosomes par Mnase-seq durant le ré-établissement de la terminaison précoce. Nous observons un pic d'acétylation à 30min, en accord avec le pic d'expression de l'ARNm sens. Sur les points suivants, nous observons par 4tu-seq un patron d'expression en oscillation. Ce profil est aussi apprécié en ce qui concerne H3K18ac alors que la région pauvre en nucléosomes s'élargit rapidement et reste ouverte jusqu'au dernier point. La récupération de l'organisation de la chromatine dépend de la réplication puisque les cellules maintenues en phase G1 possèdent une région pauvre en nucléosomes moindre jusqu'au dernier point expérimental. Les Histone Acetyl Transferase (HATs) contribuent également à la récupération car nous observons un retard d'ouverture des régions pauvres en nucléosomes quand nous enlevons l'HAT NuA4 durant la récupération. Ainsi, nous concluons que la réversion de l'interférence de transcription dépend à la fois de la dilution des marques d'histones par réplication et d'une acétylation active.

Introduction

Eukaryotic organisms possess from 6000 protein coding genes in *S. cerevisiae* to 25000 in humans. They are co-regulated by multiple mechanisms that give rise to distinct expression patterns for each gene generating diversity. Gene expression regulation is essential for cell division, adapting to environment, fundamental for cell differentiation and development. Transcription regulation is the first and one of the major steps of gene expression regulation. Transcription initiation is highly controlled both temporally over the cell cycle and spatially in an organism. Studying transcription regulation is key to understand gene expression.

Transcription is a process in which gene sequence information is read from DNA into RNA by an RNA polymerase (Crick, 1958). There are three major classes of RNA polymerases, namely, RNA Polymerase I, II and III (Roeder and Rutter, 1969) that transcribe different types of RNAs (Sentenac, 1985). RNA Pol I produces ribosomal precursor RNAs (Engel et al., 2013), RNAPII transcribes messenger RNAs (mRNAs) and a variety of non-coding RNAs in eukaryotes (Kornberg, 2007), and Pol III synthesizes transfer RNAs and small nuclear RNAs (Paule and White, 2000).

Ribosomal RNAs along with ribosomal proteins form a platform for protein synthesis called Ribosomes (Palade, 1955). Transfer RNAs act as a translator for messenger RNA (mRNA) into proteins, with each tRNA having an anticodon for a triplet of bases on mRNA and an amino acid corresponding to it (Brenner et al., 1961; Hoagland et al., 1958). Later studies by Jacob & Monod and Gilbert proposed that gene expression is controlled by transcription regulation (Jacob and Monod, 1961) and is performed by a repressor polypeptide, now known as transcription factors (TF) (Gilbert and Muller-Hill, 1966). These studies led to a simple idea that proteins constitute the major part of the cellular machinery and the most important functional aspect of the genetic information. RNA was relegated to be acting just as an intermediary molecule passing the information.

These paradigms of transcription factors as gene expression regulators exist with the assumption that the combinatorial interactions of these factors would provide an enormous range of possibilities – enough for the very complex developmental gene expression program required in organisms such as humans (Levine and Tjian, 2003). This turned out to be false, as there is a mismatch between increased complexity required for human development and the observed scaling of regulatory genes (Mattick and Gagen, 2005). The genomes from *C. elegans* to humans have similar number of protein coding genes, although very different genome sizes (Liu et al., 2013). In humans, the coding genome only constitutes 1-2% of the total genome length (Djebali, 2012).

This prompted the idea that the required increased complexity might arise from non-protein-coding regions of the genome. However, the total transcriptional products measured at any time majorly consist of Ribosomal RNA constituting 75%, small tRNAs form 15% and mRNAs constitute the rest of the 10%. Transcripts from non-coding regions of the genome are not abundant but arguably the majority of transcribing RNAPII is potentially associated with these sequences (Struhl, 2007). This suggests that the total RNA analyses only identify abundant and stable RNAs while much of the transcriptional heterogeneity is hidden below the detection limit and is unobservable.

This view was strengthened with the advances in high throughput genome-wide techniques in the last decade that helped identify tens of thousands of long non-coding RNAs (>200 nt) from yeast to humans (Carninci, 2005; Fang, 2018). LncRNAs are transcribed by RNAPII and are essential for many key processes. LncRNA expression is developmentally regulated in metazoans, shows tissue specificity and has distinct subcellular localizations (Dinger, 2008; Mercer et al., 2008). A vast number of lncRNAs has been associated with human diseases (Chen, 2013). LncRNAs might contribute to the increased complexity in gene expression regulation that distinguishes humans from unicellular organisms.

LncRNAs further consist of many subclasses based on their production site and function. *Cis*-acting RNAs are functional at their site of transcription by regulating neighbouring gene expression and local chromatin organisation. Antisense long non-coding RNAs (AS lncRNAs) represent one class of functional lncRNAs. These non-coding RNAs are transcribed from the 3' end of genes in the antisense orientation towards the 5' end. Several AS lncRNAs have already been described as gene expression regulators, in yeast and higher eukaryotes (Gil and Ulitsky, 2020; Wu et al., 2020). In this study, we focus on antisense lncRNAs in the yeast *Saccharomyces cerevisiae*. We studied their mechanism of action on sense gene transcription and the long-term effects of their expression. I will first describe the molecular mechanism of RNAPII transcription through chromatin focusing on the yeast system before going to the non-coding RNAs and the specifics of antisense transcription.

1 Chromatin and Transcription

DNA is packed around repeating units of nucleosomes that form chromatin in the nucleus (Kornberg and Thomas, 1974). Nucleosomes were found to act as a barrier to transcription initiation by RNAPII (Han and Grunstein, 1988; Lorch et al., 1987). Interestingly, the chromatin isolated from yeast has been found to be better suited for transcription than naked DNA. (Kornberg and Lorch, 2020; Nagai et al., 2017). Furthermore, multiple factors such as chromatin remodelers, histone modifying enzymes and transcription factors regulate chromatin dynamics and promote gene expression from well-defined sites (Carey et al., 2006; Lemon et al., 2001; LeRoy et al., 1998). Hence, the paradigm of chromatin acting as a hurdle for transcription is shifting towards chromatin promoting transcription fidelity by specifying where to start, a process subjected to regulatory mechanisms. Transcription itself is known to regulate chromatin architecture (Hirota et al., 2008) and organisation (Steensel and Furlong, 2019). Together, these observations suggest that chromatin dynamics and transcription are interlinked mechanisms that work cooperatively.

1.1 Nucleosome: Basic Chromatin unit regulating DNA accessibility

Each nucleosome is made of two copies of each of four core histone proteins H2A, H2B, H3 and H4 and 147 bp of DNA wrapped around it in a left-handed superhelix (Fig. 1). In the histone core, H3 and H4 form a dimer through hydrophobic packing that assembles with another H3-H4 dimer using a four-helix-bundle structure. The core (H3-H4)₂ tetramer is flanked by two H2A-H2B dimers with similar interactions (Luger et al., 1997). In *S. cerevisiae* three additional histones exist: the linker histone H1 that plays a role in chromatin compaction (Schafer et al., 2008), the centromere specific H3 variant Cse4 (Meluh et al., 1998) and the H2A variant H2A.Z (Santisteban et al., 2000). The variants differ from canonical forms at certain residues mainly in the N-terminal regions.

All histones have disordered N-terminal chains about 40 amino acids in length protruding from the nucleosome. These chains are highly conserved, especially for H3 and H4 and they have well characterized post-translational modifications (PTMs) (Fig. 1). Histone PTMs play an important role in chromatin packaging, and are specifically recognised by chromatin binding proteins (Talbert and Henikoff, 2017; Zhang et al., 2015); reviewed in (Gates et al., 2017; Kouzarides, 2007; Li et al., 2007a). The interplay of PTMs with chromatin organization and transcription is discussed throughout the introduction. Some PTMs are mentioned in separate sections with a more detailed description of the corresponding ‘writer’ and ‘reader’ proteins.

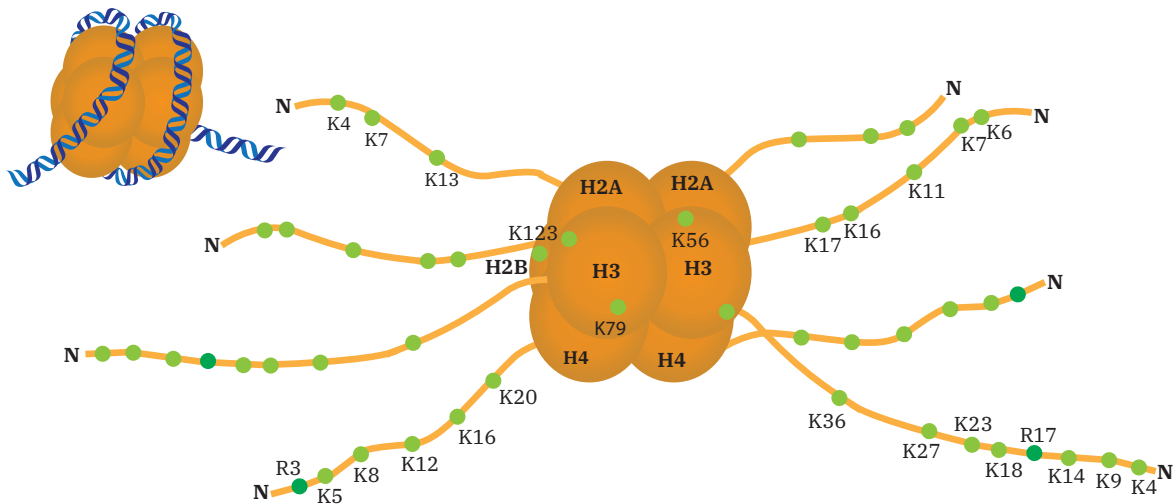


Figure 1. Structure of the nucleosome

Commonly modified lysine residues are shown in light green and a few arginine residues are shown in dark green. The inset at the top left shows the DNA wrapped around the histones in a left-handed manner with 1.65 turns around each histone octamer.

The DNA interacts with nucleosomes through histone-fold domains which render the DNA-nucleosome structure quite stable (Luger et al., 1997). Nucleosomes limit DNA accessibility and constrain DNA supercoiling (Struhl, 1999). Nucleosomes on DNA are dynamic structures undergoing conformational changes and are disassembled during transcription. Nucleosome unwrapping could occur spontaneously to provide access to DNA binding proteins (Poirier et al., 2008). In yeast, 30% of TF binding sites are located at the entry-exit region of the nucleosome that may be regulated by spontaneous unwrapping (North, 2012) or TF mediated sliding of a nucleosome.

Nucleosome disassembly involves the formation of nucleosome intermediates, which contain partially unwrapped nucleosomes that have lost proximal or distal H2A-H2B dimers in the promoter region (Ramachandran et al., 2017; Ramachandran et al., 2015). The nucleosomes are also able to interact *in vitro* and can form dinucleosomes spontaneously. An overlapping dinucleosome contains a hexasome lacking one H2A-H2B dimer, is associated with a canonical nucleosome, and has 250 bp of DNA wrapped around it, in three left handed turns (Engelholm et al., 2009; Kato et al., 2017).

Nucleosomes form the basis of chromatin organisation, as they arrange themselves in tetranucleosome units (Schalch et al., 2005). They interact to form chromatin fibres as two intertwined stacks of nucleosomes (Li et al., 2016). These units have been observed *in vivo* using Micro-C, a method involving MNase digestion (see below) of intact nuclei followed by sequencing the randomly re-ligated DNA in the close 3-dimensional vicinity (Hsieh, 2015).

1.1.1 Nucleosome Array: Format of Organisation of Eukaryotic Genomes

Nucleosomes are arranged on DNA as ‘beads on a string’. Partial chromatin digestion with the enzyme micrococcal nuclease (MNase), that cleaves linker DNA between nucleosomes, gives a ladder-like appearance on a DNA electrophoresis gel, illustrating the repetitive nature of the chromatin (Kornberg, 1977). Nucleosome arrays are usually visualized by sequencing the MNase-treated chromatin (Fig. 2). The development of sequencing technologies has provided precise nucleosome positioning for various organisms (Mavrich, 2008; Teif, 2012; Valouev, 2011). In yeast, nucleosomes are quite precisely mapped with ~165 bp distance between MNase peaks (Chereji et al., 2018; Weiner et al., 2015; Yuan et al., 2005). *S. cerevisiae* has an absolute nucleosome occupancy of ~90%, suggesting that almost all the nucleosome positions are occupied and there are very few gaps in nucleosome arrays in yeast (Oberbeckmann, 2019).

Well-spaced arrays are observed in the genic regions and are known to be inhibitory to transcription. These arrays act as a barrier and restrict search and binding of general transcription factors (Mirny, 2010). The linker regions between the nucleosomes of an array are less than 70 bp, which is the minimum requirement for the assembly of a transcription initiation complex. Thus, the global role of nucleosomes is transcription inhibition (Kornberg and Lorch, 2020). Gene expression is regulated by many mechanisms that remove or slide nucleosomes for creating a nucleosome free accessible region.

1.1.2 Nucleosome Depleted Region: Break in the Array

Nucleosome depleted regions or NDRs are stretches of DNA that are not occupied by nucleosomes *in vivo*. NDRs are usually observed at the 5' end of expressed genes. The nucleosome upstream of an NDR is termed -1 nucleosome and the one just downstream is called +1 nucleosome. The +1 nucleosome is followed by an array of well-defined, fixed linker-length nucleosomes (nucleosome array) throughout the gene body (Lai and Pugh, 2017; Zhang, 2011) (Fig 2). Promoter NDRs are sites of TF recruitment and pre-initiation complex (PIC) assembly.

NDRs also occur at non-promoter sites, where other proteins tightly interact with DNA, such as the origin-recognition complex (ORC) at replication origins (ARS) in yeast (Eaton et al., 2010). At these sites, the -1 and +1 nucleosomes are aligned to the barrier element, such as Orc in ARS or a transcription factor like Rap1 (Challal et al., 2018). NDR formation both at promoter and replication origin sites occurs through similar mechanisms. In yeast, NDRs also form at the transcription termination sites; these 3' NDRs can be shared with NDRs of neighbouring genes due to the compact

nature of the yeast genome and can lead to non-coding transcription in either direction. 3' NDRs are affected by neighbouring genes, growth conditions and transcription elongation (Fan, 2010).

In promoter NDRs, the -1 and +1 nucleosomes occupy well defined positions separated by a typical core promoter length of 100-200 bp, depending on the gene. The NDR size influences the recruitment of the transcription machinery. Few NDRs contain specific TF binding sites, which were initially called upstream activating sequences (UAS). Transcription initiates from a defined position, the transcription start site or TSS, which is located upstream of the +1 nucleosome dyad and is usually between 40-120 bp downstream of the TATA sequence or TATA-like element (Lee, 2007; Smale and Kadonaga, 2003; Vinayachandran et al., 2018). The +1 nucleosome positioning is important for proper TSS selection (Klein-Brill et al., 2019; Kubik, 2018; Malabat et al., 2015; Rhee and Pugh, 2012).

In yeast, genes show bimodal distribution of NDR sizes with peaks at 30 bp and 80 bp. Wide NDRs are usually ≥ 150 bp in size and associated with highly transcribed housekeeping (Weiner et al., 2010) and essential genes. Stress regulated genes usually have closed promoters with smaller NDRs (Tirosch and Barkai, 2008). Genes that have wide NDRs have well positioned -1 and +1 nucleosomes and are associated with TFs (Tirosch and Barkai, 2008). The stress regulated genes with small NDRs are TATA-containing promoters. These have more fuzzy positioning for nucleosomes flanking the NDR and they show more noisy expression in a population (Zenklusen et al., 2008). For, both types of NDRs, the +1 nucleosome is well positioned while the gene is expressed and becomes fuzzier in the off state. NDR sizes were shown to be a consistent property of the genes, irrespective of their transcriptional state. The genes keep their NDR sizes even when their expression level is changing due to changes in the media. The study concluded with the main determinants for promoter NDRs - work in *trans*, namely, TFs, TBP and chromatin remodelers like RSC, Swr1 (Zaugg and Luscombe, 2012). These are discussed in the following sections.

There are some reports that wide NDRs might be occupied by 'fragile' nucleosomes. The word 'fragile' comes from their sensitivity in the MNase digestion assay (Kubik et al., 2015). However these nucleosomes have been difficult to confirm and such MNase sensitive particles are detected in the NDR only when it is ~ 150 bp or larger, i.e., there is large enough open DNA segment to harbour a nucleosome (Kubik et al., 2017). These nucleosomes might correspond to the destabilised promoter nucleosomes that are undergoing remodelling (Brahma and Henikoff, 2019). This would explain the absence of H3- or H4-DNA contacts using traditional approaches of H3 ChIP-seq or chemical cleavage mapping at these sites respectively (Chereji et al., 2017; Henikoff et al., 2014). 'Fragile' nucleosomes are still under debate and discussed more in the section on chromatin remodelers.

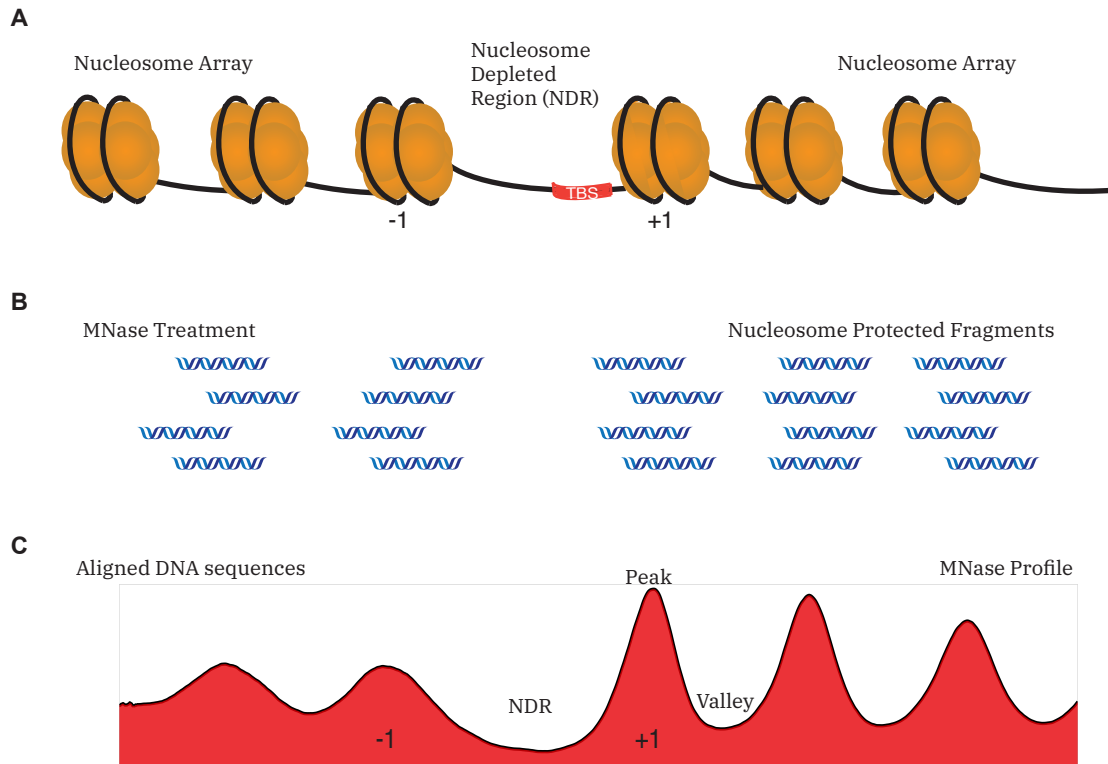


Figure 2. Nucleosome Array and Nucleosome Depleted Region

(A) Histones positioned on the DNA are shown in a linear format. Two well established patterns are observed - well spaced Nucleosome Arrays and Nucleosome Depleted Regions (NDR).

(B) Following MNase digestion of the chromatin, DNA bound by histones is protected while DNA from NDR regions is digested

(C) The protected fragments are aligned to their positions by the sequence information and they are observed by calculating and stacking the number of aligned reads on a given DNA sequence.

Nucleosome Dyad

It is the central bp of 147bp DNA wrapped around a nucleosome. In the MNase-treatment experiments the central bp of protected DNA fragment (Fig. 2B) is also known as nucleosome dyad. The coverage profile could be calculated by either adding the coverage using the whole protected DNA fragment which is usually termed Nucleosome Occupancy, or it is calculated using the defined number of bp in the center of the DNA fragment from paired-end sequencing.

In the thesis and most commonly in published work, the second calculation is used. Therefore, the MNase profile in Fig. 2C is the coverage calculated using middle 3 bp and then rolling mean was performed for smoothing of the curve. Hence, the fragment presented at +1 dyad is covering ~72 bp of DNA on either side of it.

1.2 Mechanisms of NDR formation

In an interesting study, when the core yeast nucleosomes were completely replaced with human nucleosomes– the yeast survived. The overall pattern of nucleosome spacing observed on the DNA was characteristic of yeast and not human – proving that DNA composition is an important determinant of nucleosome positioning (Truong and Boeke, 2017). However, the -1 nucleosome positioning was quite different from the wild-type yeast resulting in altered NDR sizes, and the cells took longer to respond to changes in transcription. Moreover, MNase profiles showed less difference between the peak and the valley (Fig. 2). These observations indicate that although the global positioning is determined by the underlying DNA sequence, the precise nucleosome positions are set by *trans* acting mechanisms. Indeed, because the human nucleosomes are different from their yeast counterparts, they are not recognised by yeast chromatin factors, or they may be recruited but cannot efficiently act on the human histones, which leads to overall reduced remodelling dynamics (Truong and Boeke, 2017).

1.2.1 DNA sequence composition: Inherent determinant of an NDR

The yeast promoters are enriched in poly(dA:dT) sequences. These sequence tracts are intrinsically stiff and are inhibitory to nucleosome formation (Kaplan, 2009; Suter et al., 2000). Furthermore, AT-rich DNA is incapable of bending around an histone octamer (Segal et al., 2006) and therefore promotes DNA accessibility and transcriptional activity (Hughes et al., 2012). Poly(dA:dT) sequences have been shown to recapitulate a nucleosome depleted region with purified histones *in vitro*, but other aspects of nucleosome positioning, such as nucleosome arrays or precise NDR flanking nucleosome positioning were not observed (Zhang, 2011).

Manipulating the arrangement and length of these AT-rich tracks was shown to regulate transcription levels (Raveh-Sadka, 2012). This intrinsic property has been used by organisms to regulate distinct classes of genes. Genes having higher occurrences of poly(dA:dT) are constitutively expressed and give rise to bidirectional transcription (Struhl, 1985). The class of genes with low poly(dA:dT) tracts is more enriched in stress response genes. These genes exhibit higher transcriptional regulation. Their expression is noisy and promoters have higher occupancy of chromatin remodelers or General Regulatory Factors (GRFs), which might indicate their regulation by competition between nucleosomes and factor binding under certain conditions (Tirosh and Barkai, 2008).

In vitro, nucleosomes with AT-rich DNA have been shown to preferably stimulate RSC activity and poly(dA:dT) tracts may therefore also help NDR formation by an active mechanism (Lorch et al.,

2014). Nucleosome positioning patterns were shown to be reconstituted *in vitro* if yeast crude extracts were added to purified histones. These observations support that *in vivo*, precise nucleosome positioning is determined by multiple *trans*-acting factors. The ATP-dependent remodelers were found to enhance depletion of nucleosomes in the cell free extract (Zhang, 2011) and GRFs such as Rap1, Reb1, and Abf1 act in nucleosome positioning (Kubik, 2018).

1.2.2 Role of General Regulatory Factors in NDR formation

Some transcription factors can invade compact chromatin structures consisting of closed nucleosome arrays or even tetranucleosome units (Zaret et al., 2016). They could recognize their binding sites partially accessible on the nucleosome surface (Soufi, 2015). Their binding results in opening of the chromatin structure making it accessible to other factors (Cirillo, 2002) leading to changes in transcriptional programs (Meers et al., 2019). The affinity of transcription factors for their binding sites and the position of the motif relative to the nucleosome dyad determine their nucleosome displacing capabilities (Meers et al., 2019; Yan et al., 2018).

Six yeast factors termed nucleosome-displacing factors (NDFs) are able to bind and deplete nucleosomes independently from a closed nucleosome array *in vivo*, namely the three GRFs Abf1, Rap1 and Reb1 as well as Cbf1, Mcm1 and Orc1, that is part of ORC (Yan et al., 2018). General regulatory factors (GRFs) are highly abundant factors that have strong DNA binding activity to short but specific DNA sequence motifs throughout the genome. They play a causal role in the establishment of NDRs and are known as pioneer factors (Hartley and Madhani, 2009; Yan et al., 2018). Their binding sites were found to be occupied by nucleosomes when reconstituted *in vitro*, but are highly nucleosome depleted *in vivo* (Badis, 2008; Kaplan, 2009; Tsankov et al., 2010; Yarragudi et al., 2007).

The establishment of an NDR by Reb1 was first shown by the Madhani laboratory, when they inserted a short stretch of poly(A) adjacent to a Reb1 binding site (Hartley and Madhani, 2009). This work suggested that GRFs might recruit the RSC chromatin remodeler to promote nucleosome eviction. Indeed, RSC binding motif was found ~100 bp upstream of TSS and deleting RSC resulted in increased nucleosome occupancy at these sites (Badis et al., 2008). Recently, it has been shown that deleting either GRFs, RSC or both, the +1 nucleosome is shifted upstream into the NDR with additive effects, indicating that they contribute independently to NDR formation (Kubik, 2018, 2019). GRFs and other TFs could also interact with histone acetyl transferases (HATs) to mediate acetylation of the surrounding histone tails, thereby promoting chromatin remodeler recruitment for establishment of an active NDR (Brown, 2001).

A more complete mechanism of action was observed by Mivelaz and colleagues for Rap1 GRF binding. Rap1 is able to bind its motif both on naked DNA and on nucleosome bound DNA, although with short residence time. Rap1 inhibits nucleosome stacking but Rap1 binding by itself does not promote NDR formation. Rap1 recruits the RSC chromatin remodeler that generates stably bound states by promoting nucleosome eviction (Mivelaz et al., 2020). Besides DNA binding domains (DBD), TFs possess intrinsically disordered regions (IDR). Recent analyses using the Msn2 and Yap1 transcription factors, showed that IDR regions outside of the DBD are sufficient and necessary for the localization of the TFs to their binding sites (Brodsky et al., 2020).

GRFs have also been shown to act as roadblocks for transcription. High resolution transcription maps revealed that these factors act as a failsafe mechanism for transcription termination and work independently of other termination pathways (Candelli et al., 2018). Rap1 and Reb1 have been shown independently to repress cryptic non-coding transcription from divergent promoters thereby also increasing transcription fidelity (Challal et al., 2018; Colin et al., 2014; Wu et al., 2018).

1.2.3 Chromatin Remodelers shape NDRs

Chromatin remodelling factors are protein complexes that can assemble, slide, evict or exchange nucleosomes on DNA (Cairns, 2005; Fazzio and Tsukiyama, 2003). Eukaryotes contain four families of chromatin remodelers SWI/SNF, ISWI, CHD and INO80. Remodelers possess a conserved ATP-dependent translocase subunit that slides DNA on the nucleosome surface (Saha et al., 2002) or evicts it completely by transferring the histone to a DNA chaperone (Lorch et al., 2006). Remodeler action on nucleosomes can give DNA binding factors access to important *cis-acting* DNA elements for gene regulation (Bowman, 2010). Remodelers are also important for the recruitment and the passage of RNA and DNA polymerases through nucleosomes (Clapier and Cairns, 2009).

1.2.3.1 SWR1 and INO80 govern -1/+1 Nucleosome Composition

The SWR1 complex contains 14 proteins and uses the ATPase/helicase domain of the Swr1 subunit to catalyse the exchange of histone H2A-H2B dimers with H2A.Z-H2B dimers (Kobor et al., 2004; Luk et al., 2010; Mizuguchi et al., 2004; Watanabe et al., 2013). The unidirectional replacement reaction occurs in two steps with the replacement of one H2A-H2B dimer with a H2A.Z containing dimer resulting in an intermediate heterotypic nucleosome. The second replacement reaction results in the formation of homotypic nucleosome containing two H2A.Z (Luk et al., 2010).

The specific targeting of H2A.Z to the acetylated promoters is performed by the Swr1 subunit, Bdf1, which via its bromodomains, binds to acetylated histones (including H3K14), at +1 and -1

nucleosomes in the promoter NDRs (Zhang et al., 2005). The H2A.Z-specific histone chaperone Chz1 delivers the H2A.Z-H2B dimer to the Swc2 and Swr1 subunits that interact directly with H2A.Z and facilitate the exchange (Luk et al., 2007; Wu et al., 2005; Wu et al., 2009).

H2A.Z is also preferentially evicted from promoters when genes are activated (Zhang et al., 2005). PIC assembly has been shown to be essential for the reverse reaction (Tramantano et al., 2016). INO80 complex catalyses this reverse reaction, exchanging H2A.Z containing dimers for H2A-H2B (Brahma, 2017; Papamichos-Chronakis et al., 2011). INO80 complex is one of the most evolutionarily conserved remodelling complexes which in yeast contains 15 subunits. The INO80 actin/Arp module serves as a conformational switch that regulates its binding to the nucleosomes (Zhang et al., 2019).

In yeast, INO80 activates inositol genes directly (Ford et al., 2008) and is a known nucleosome spacing factor (Udugama et al., 2011). It has been implicated in prevention of non-coding transcription invasion into silent chromatin (Xue et al., 2015). INO80 promotes efficient progression of replication fork, stabilizes the fork under stress and provide tolerance to DNA damage (Conaway and Conaway, 2009).

Histone variant H2A.Z

H2A.Z plays a role in the recruitment of the transcription initiation machinery - mediator, SAGA and general transcription factor and TATA-binding protein (Marques et al., 2010; Wan et al., 2009). It is also important in chromosome stability (Krogan et al., 2004). H2A.Z further marks the regions for RSC mediated nucleosome remodelling along with acetylation (Cakiroglu et al., 2019). H2A.Z acetylation by promoter associated HATs (SAGA) safeguards it from eviction by the INO80 remodeler (Papamichos-Chronakis et al., 2011).

The levels of H2A.Z are not directly related to transcriptional levels; instead, H2A.Z levels at a promoter indicate that the promoter is poised for transcription (Li et al., 2005). H2A.Z occupies well defined rotational settings in the promoter regions of transcription units that help in recognition of specific DNA sequences by the transcription machinery (Albert et al., 2007).

1.2.3.2 RSC regulates NDR Width

RSC stands for Remodell the Structure of Chromatin; it is homologous to the SWI/SNF chromatin remodelling complex but is ~10x more abundant and an essential nuclear protein complex (Cairns et al., 1996). It is important for transcription by all three RNA polymerases (Parnell et al., 2008). RSC contributes to the formation of NDRs in the majority of RNAPII promoters (Hartley and Madhani,

2009; Lorch et al., 2014). RSC utilizes its catalytic subunit Sth1 to slide and evict nucleosomes. Sth1 is a DNA translocase that pumps DNA around a nucleosome (Saha et al., 2002). RSC can evict complete nucleosomes in the presence of the histone chaperone Nap1 (Lorch et al., 2006).

RSC recruitment to DNA can be mediated by transcription factors (Badis, 2008; Hartley and Madhani, 2009) but RSC can also interact with both DNA and histones. RSC contains five putative DNA binding domains. The Zinc-finger domain in Rsc3 recognises a five bp motif CGCGC, although it requires multiple binding sites for it to displace nucleosomes (Yan et al., 2018). The other DNA binding domains are in Rsc30, an RFX domain in subunit Rsc9 and a ZZ zinc-finger domain in Rsc8 (Angus-Hill et al., 2001). The poly(dA:dT) sites were also found to act as a binding platform for the RSC complex and promote chromatin remodelling (Lorch et al., 2014).

RSC has six domains that interact with histones; it contains a bromodomain in Sth1, two bromodomains in Rsc2, a bromo-adjacent homology (BAH) domain that binds H3 (Chambers et al., 2013). Rsc4 has a tandem bromodomain that is known to interact with acetylated H3K14 (Kasten et al., 2004) and is acetylated at K25 itself. The Gcn5 histone acetyltransferase is adding both of these marks. Rsc4 K25ac inhibits the binding of H3K14ac suggesting that Gcn5 acetylation can promote or impair RSC activity (VanDemark et al., 2007).

RSC inactivation strongly affects the majority of NDRs in yeast. It leads to shifting of -1 and +1 nucleosomes towards each other eventually occluding NDRs. This leads to reduced RNAPII occupancy and TSS usage at a subset of genes and therefore reduced transcription (Badis, 2008; Hartley and Madhani, 2009; Klein-Brill et al., 2019; Kubik, 2018). RSC also plays a role after RNAPII initiation as it is found in the gene bodies of highly transcribed genes and promotes RNAPII elongation through acetylated nucleosomes (Carey et al., 2006). RSC works with SWI/SNF at a subset of promoters in remodelling/eviction of nucleosomes; specifically observed at Gcn4 regulated genes (Rawal, 2018). Recovery of RSC following depletion reverses the +1 and -1 nucleosome positioning to an open state in a replication independent manner (Klein-Brill et al., 2019).

The debated 'fragile' nucleosomes that could be present in the NDRs but are not found in nucleosome IPs; could be considered as partially unwrapped nucleosomes bound by remodelling factors. The partially unwrapped nucleosomes are defined as nucleosomes in which the DNA was released from one or both of the symmetric locations in the entry-exit site of the nucleosome, while central DNA gyre is attached to the DNA. They result in smaller than 147 bp DNA fragments after digestion with MNase and are normally observed at +1 and -1 promoter positions (Ramachandran et al., 2015) bound by RSC (Brahma and Henikoff, 2019). Recent work has provided some evidence that RSC occupies nucleosomes but is also present at the supposed fragile nucleosome in the NDR. This study asserted that fragile nucleosomes are not detected by histone ChIP-seq because these

nucleosomes are bound by RSC and probably other factors that results in it having reduced DNA contacts (Brahma and Henikoff, 2019). These ‘sub’ or ‘fragile’ nucleosomes might be highly dynamic nucleosome-remodeler intermediates. Recently, using a variant of an MNase-seq, MNase-SSP, subnucleosome structure was clearly detected (Ramani et al., 2019). These observations also suggest that there is requirement for improvement in current chromatin visualization methods.

Earlier studies revealed different outcomes when histones with modified N-terminal chains were remodelled by RSC (Somers and Owen-Hughes, 2009). A recent study supported the assertion that RSC remodelling of partially unwrapped nucleosomes can regulate the access of TFs. This work suggests that RSC contributes to gene regulation by specializing, i.e. RSC has evolved to recognize both complete and sub nucleosomes with different RSC subunits forming nucleosome specific modules (Schlichter et al., 2019). RSC has been shown to bind to sub nucleosome particles covering 180 bp of DNA *in vitro*, as an intermediate in its remodelling step (Shukla et al., 2010).

1.2.3.3 ISW1 and CHD1: Determinants of Nucleosome Array Spacing

Isw1 (Imitation-switch) and Chd1 (Chromodomain helicase DNA-binding protein 1) are the main determinants of global nucleosome spacing (Gkikopoulos, 2011; Ocampo et al., 2016). These remodelers determine linker lengths between nucleosomes in the gene bodies (Whitehouse et al., 2007). Individual deletions of Chd1, Isw1 or Isw2 showed little changes in the overall profile of the +1 or gene body nucleosomes, but combined deletions of Chd1 and Isw1 distorted the nucleosome profile after +1 (Gkikopoulos, 2011; Klein-Brill et al., 2019).

Isw1 possesses a SANT domain and interacts with Ioc3 to form Isw1a and Isw1b complexes (Vary et al., 2003). Chd1 contains a double chromodomain in the N-terminal region (Quan and Hartzog, 2010). Both Isw1 and Chd1 have been shown to bind H3K36me3 nucleosomes in the gene body and their binding prevents histone exchange in the ORF (Smolle, 2012). Functionally, in cells lacking both Isw1 and Chd1, RNAPII accumulates in gene bodies indicating that Isw1 and Chd1 facilitate elongation by separating closely packed nucleosomes (Ocampo et al., 2019).

The combined action of remodeler activities in establishing promoter nucleosome landscape has been systematically investigated in a study with single and combined deletions of remodelers (Kubik, 2019). In this study, RSC and SWI-SNF are described as acting redundantly as ‘pushers’ (pushing nucleosomes away from NDR) to increase NDR width, while Isw2 and INO80 are acting as ‘pullers’ to reduce NDR size. Their opposite activities on a same nucleosome is based on their overlapping occupancy. The authors hypothesized that their combined action resulted in the final +1 nucleosome position. This +1 is then used as a reference by Isw1 and Chd1 for proper positioning of downstream nucleosomes by equalizing linker lengths (Kubik, 2019).

1.3 Importance of Histone Acetylation at -1/+1 Nucleosomes

Evolutionarily conserved ϵ -lysine acetylation is a widespread and reversible PTM on proteins throughout the cell and is particularly enriched on chromatin. The level of acetylation is very strictly controlled by lysine (K) acetyl-transferases (KATs) and lysine (K) de-acetylases (KDACs), also referred to as histone acetyl-transferases, HATs and HDACs, named after their common substrate. HATs are found in molecular complexes that render them target specificity and capable of interacting with other proteins and to detect histones with specific PTMs (Sheikh and Akhtar, 2019; Wang, 2009b).

Acetylation modifications on the histone side chains neutralize the charge on the lysines, reducing their ability to form hydrogen bonds and therefore disrupt DNA-histone binding. Acetylation of H4K16 is known to disrupt interactions between nucleosomes. This leads to the formation of more open chromatin structure and favourable environment for transcription (Hong et al., 1993; Shogren-Knaak, 2006; Zhang et al., 2017).

Besides disrupting chromatin structure, acetylation is recognised by a range of chromatin binding proteins through their bromodomains and YEATS domains, that can further modify chromatin environment (Fujisawa and Filippakopoulos, 2017; Kanno, 2004; Li, 2014). The bromodomains of the SWI/SNF remodelling complex and RSC identify and associate with acetylated histones *in vitro*, and are found localized at acetylated -1/+1 nucleosomes *in vivo* (Brahma and Henikoff, 2019; Mitra et al., 2006). The YEATS domain protein Yaf9, component of the SWR1 complex, shows affinity for H3K14 and K3K27 acetylation residues and binds with higher affinity to histones with both modifications (Hsu, 2018; Wang, 2009a). Histone acetylation increases remodelling by the Snf2 family of remodelling enzymes (Ferreira et al., 2007). HATs can also modify chromatin remodelers themselves; thus acting both on factors and their substrates (Narita et al., 2018).

Histone acetylation is enriched at the promoters of highly transcribed genes, particularly H3K9ac, H3K18ac, H2AK9ac and H3K56ac (Wang, 2008; Weiner et al., 2015). Acetylation correlates with RNAPII occupancy and gene expression levels. H3K27ac is also known to associate with the increased release of RNAPII into transcription elongation (Carey et al., 2006; Protacio et al., 2000; Stasevich, 2014). Depleting histone acetyl transferases and therefore acetylation results in reduced gene expression (Bruzzone et al., 2018). In a separate study, individual and combinatorial mutants of all acetylated H4 lysines, showed that they work in a non-specific cumulative manner with smaller effects for individual mutants and larger effects for the combined mutants, except for H4K16ac, which is inhibitory to the spread of heterochromatin (Dion et al., 2005).

In humans, inhibition of either p300/CBP HAT or HDACs activity inhibits gene expression and reduces RNAPII activity suggesting that acetylation turnover is more important than static acetylation (Crump, 2011). Another study has shown that transcription is actually responsible for HAT targeting and HAT occupancy alone does not predict histone acetylation as it is regulated post-recruitment, which might in part be mediated by transcription (Martin et al., 2019). These studies suggest that HAT recruitment and acetylation is important for transcription and transcription in turn regulates acetylation.

1.3.1 SAGA Histone Acetyl Transferase Complex

In yeast, GCN5 was one of the first HATs to be identified (Kleff et al., 1995; Kuo, 1996). Gcn5 is a non-essential HAT in yeast and is a part of an acetylating module of the 1.8 MDa SAGA (Spt-Ada-Gcn5-Acetyltransferase) complex. The HAT module is composed of Gcn5, Ada2, Ada3, Sgf29. It acetylates multiple lysines of nucleosomal H3 and has been shown to acetylate H3K9, 14, 18, 23 *in vitro* (Grant, 1997; Suka et al., 2001). SAGA is recruited to gene loci by its interaction with Tra1, that forms the recruitment module (Tra1) (Brown, 2001; Grant et al., 1998). Gcn5 contains a bromodomain that interacts with acetylated histone tails (Hassan et al., 2002) and Sgf29 possess double Tudor domain that bind H3K4me2/3, both marks of actively transcribed genes (Vermeulen et al., 2010). Gcn5 and Swi1/Snf2 are required for stable occupancy of the SAGA transcription complex at promoter nucleosomes. Its Spt3 module forms the TBP interaction unit that facilitates TBP recruitment and promotes transcription (Mohibullah and Hahn, 2008). SAGA has an architecture module containing Spt5, Spt7, Ada1 and TAF proteins (Koutelou et al., 2010).

SAGA also consists of a deubiquitinating module (DUB) containing the ubiquitin hydrolase Ubp8 that is tightly regulated by Sgf73, Sgf11 and Sus1 and is activated by the interaction of the four subunits (Köhler et al., 2008; Köhler et al., 2010). Dub module and Gcn5 localize close to each other and form a chromatin-binding interface (Durand et al., 2014). H2B ubiquitination levels are dynamically associated with transcription, these transiently increase during activation, while they are lowered while the gene is being transcribed. This cycle of ubiquitination and de-ubiquitination is important for SAGA recruitment and gene activation (Henry et al., 2003). The DUB module promotes elongation by deubiquitinating the H2BK123ub1, which benefits the recruitment of Ctk1 kinase that promotes Ser2 phosphorylation of RNAPII (Wyce et al., 2007).

Eliminating HAT activity from the Gcn5 complex results in reduced mRNA levels for 10% of genes in the *mutant* strains. These genes were termed SAGA dominated genes and are positively regulated by Spt3 (Huisinga and Pugh, 2004). The SAGA dominated genes have a characteristic TATA box and are enriched in stress inducible genes. These genes have smaller NDRs and less well positioned

nucleosomes around 5' NDR (Lenstra et al., 2011). Although, at steady state expression level was affected for a small subset of genes in SAGA mutants, SAGA binds to the promoter regions of most genes and deubiquitinates almost all RNAPII transcribed regions (Bonnet et al., 2014). Recent study, performed using Nascent transcription analyses using 4-thiouracil labelling of RNA and dynamic depletion of SAGA showed that the transcription is globally reduced in Gcn5 mutants but the total RNA levels are buffered by an increased mRNA half-life. They further showed that removing the TBP interacting Spt3 subunit reduced the TBP binding at promoters. The effect of removing both Gcn5 activity and Spt3 from Gcn5 complex was larger than the individual effects. The study also observed lower H3K9ac in Gcn5 mutants. This study definitively and reliably showed that SAGA is a global regulator of gene transcription, and it acts independently of promoter architecture (Baptista et al., 2017). Earlier studies didn't measure this effect as it was probably masked by the global increase in RNA stability in the mutant strains which cannot be captured by steady state RNA-seq profiles. Although, we know that there is bimodal distribution in promoter NDRs and they possess different architectures (discussed in section on NDRs), but the naming of the classification 'SAGA' and 'TFIID' is confusing and a misnomer.

1.3.2 Rtt109 Histone Acetyl Transferase

Rtt109 is a HAT that forms complexes with different chaperones such as Vps75 or Asf1 that activate HAT activity and specify Rtt109 for selecting a specific substrate (Berndsen et al., 2008). The Rtt109 complex with Vps75 has been shown to catalyse acetylation on the histone H3-H4 heterodimers (Kolonko et al., 2010). Rtt109 has a different sequence compared to earlier described HATs but has structural homology with the human p300/CBP complex (Tang et al., 2008).

Rtt109 catalyses acetylation on H3K56 (Schneider et al., 2006). It uses free histones as substrate (Tsubota et al., 2007) and H3K56ac is consequently enriched on newly assembled histones which are usually promoter-proximal nucleosomes (Rufiange et al., 2007). H3K56ac enhances nucleosome turnover events and positively correlates with RNAPII distribution (Topal et al., 2019). In Asf1 mutants, H3K56ac is absent, suggesting that Asf1 is essential for H3K56ac (Tsubota et al., 2007).

1.3.3 NuA4 Histone Acetyl Transferase Complex

NuA4 (Nucleosome Acetyltransferase of H4) forms a multimeric histone acetyl transferase complex that is important for transcription and DNA damage repair (Squatrito et al., 2006). Esa1 corresponds to the catalytic subunit and is an essential HAT in yeast, required for cell cycle progression (Clarke et al., 1999; Smith, 1998). It is responsible for acetylation of H4, H2A and the H2A.Z histone variant on chromatin and many non-histone proteins (Allard et al., 1999; Downey, 2015; Keogh et al., 2006).

A recent study has shown that when Esa1 is dynamically anchored away from the nucleus, there is total loss of both acetylation and transcription (Bruzzone et al., 2018).

NuA4 contains five non-catalytic subunits: Epl1, Tra1, Arp4, Act1 and Swc4/Eaf2, which are broadly conserved (Doyon and Cote, 2004). NuA4 binds upstream of RNAPII transcribed genes (Kuang et al., 2014). Tra1 acts as a recruitment module that is shared between NuA4 and SAGA complexes. It could act as a scaffold for complex assembly or chromatin recruitment (Brown, 2001; Knutson and Hahn, 2011). NuA4 could also be recruited by its reader modules in the Yng2 and Eaf3 subunits. Yng2 contains a plant homeodomain (PHD) that identifies H3K4me3 and Eaf3 recognises H3K36me3 (Steunou, 2016). Eaf3 is a shared subunit with the Rpd3S HDAC (Carrozza et al., 2005). Both Gcn5 and Esa1 can bind promoters in the absence of a recruitment module, as HATs themselves have acetyl-binding domains called bromodomains, resulting in self-reinforcement (Boudreault et al., 2003; Grant, 1997; Hudson et al., 2000).

NuA4 exists in two independent complexes – piccolo-NuA4, composed of Esa1, Epl1, Yng2 and Eaf6 and the TINTIN complex composed of Eaf3/5/7 (Boudreault et al., 2003; Cheng and Cote, 2014; Friis, 2009). Eaf1 serves as a platform that helps assemble the four NuA4 modules: piccolo-NuA4, Tra1, Eaf3 and the Arp4 module (Mitchell, 2008). The Arp4 module containing Swc/Eaf2, Yaf9, Arp4 along with Act1 are also components of the SWR1 chromatin remodelling complex (Krogan et al., 2004). Arp4 and Act1 are also shared with the INO80 remodelling complex (Shen et al., 2000). In an interesting study, a chimeric protein Eaf1-Swr1 was shown to physically link NuA4 acetylation to H2A.Z remodelling by the SWR1 complex, which recapitulates the human TIP60 complex (Auger, 2008).

Acetylated histone tails are recognised by protein complexes containing bromodomains like RSC and SWI/SNF, as discussed before as well as by Bdf1, the primary bromodomain containing component of TFIID (Filippakopoulos, 2012; Kasten et al., 2004; Matangkasombut et al., 2000; Matangkasombut and Buratowski, 2003). This supports that NuA4 and SAGA acetylates histones that are then identified by multiple bromodomain containing proteins including Bdf1 that helps recruit TFIID, a component of the transcription pre-initiation complex or PIC (Durant and Pugh, 2007). Thus, most chromatin complexes collaborate on chromatin to give a precise transcriptional state in an 'hourglass' model of chromatin remodelling (Clapier et al., 2017). The final chromatin state determines the permissive or repressive regions for the assembly of a PIC and consequently the level of transcriptional activity.

1.4 Pre-Initiation Complex Assembly

RNA Polymerase II transcription machinery is a giant complex of 58 proteins with a total mass of 3.08 million daltons. Besides RNAPII and the mediator complex, it contains six general transcription factors (GTFs) which bind core promoter elements. Many laboratories around the world have been working on solving the structure and mechanism of RNAPII transcription with atomic resolution. For the scope of this thesis – I will discuss particular aspects of this mechanism relevant for our study.

Transcription is divided into three phases – initiation, elongation and termination. The first step in transcription initiation is the assembly of a functional PIC. The sequential model involves the recognition of core-promoter sequence elements and binding by TFIID, followed by the binding of TFIIA and TFIIB, the RNAPII-TFIIF complex binds to a pre-formed TFIIB-TBP-DNA resulting in the formation of the core initiation complex. This is followed by the binding of TFIIE and TFIIH complexes to form a complete PIC associated with double-stranded promoter DNA (Haberle and Stark, 2018; Sainsbury et al., 2015).

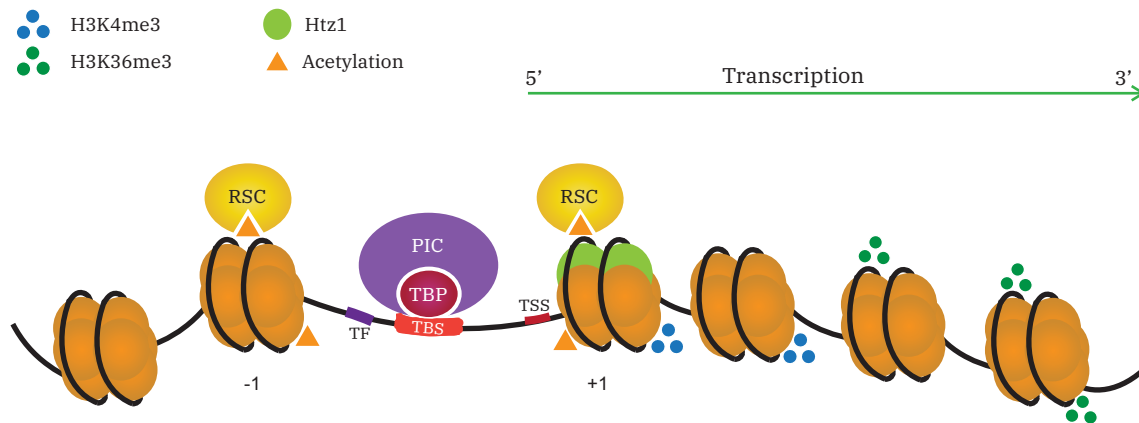


Figure 3. Promoters for Nucleosome Depleted Region

Characteristic representation of a promoter NDR, 5' to a gene. The nucleosome before the transcription start site is referred to as -1 and the +1 nucleosome is located just after the transcription start site (TSS). The +1 nucleosome contains the H2A variant Htz1 (light green) and is characterized by H3K4me3 (blue circles), while H3K36me3 (green circles) accumulates towards the 3' end of the gene. Nucleosomes surrounding the NDR are acetylated (orange triangles) and promote binding of the chromatin remodeler RSC to open the NDR. TBP binds TATA/TATA like sequences (TBS) and initiates pre-initiation complex (PIC) assembly.

1.4.1 TFIID DNA Binding Initiates Assembly

Promoter recognition and thus PIC assembly involves recognition of the promoter sequences by the TATA-binding protein (TBP). TBP specifically binds to the TATA box sequence or TATA-like sites that differ from TATA sites by two or more DNA bases (collectively termed as TBP binding sites or TBS) (Fig. 3). TBP has a saddle shaped structure and binds to the minor groove of the TATA box. DNA specificity of TBP binding results from A/T-rich DNA forming a hydrophobic surface (Vannini and Cramer, 2012). TBP functions by bending the AT-rich sequence at promoters by 90° (Blair et al., 2012).

TBP is functionally conserved from yeast to humans. TBP is present at most yeast gene promoters and it interacts with gene specific TFs and is known to interact with SAGA complex. TBP binds strongly to complete TATA sequences, but the transcription complex overlaps with the first nucleosome at these sites and gene expression is regulated by acetylation, that probably promote opening of NDRs. Most promoters in yeast have weak TATA-binding sites (~90%). The expression of these genes depends on 14 TBP-associated factors (TAFs) which, along with TBP, form TFIID (Cavallini, 1988; Rhee and Pugh, 2012).

Transcription is inhibited *in vitro* when nucleosome occludes the TBS (Lorch et al., 1987). Furthermore, recent studies have shown that repositioning of the +1 nucleosome towards the NDR results in a reduction of TBP binding. Genome-wide nucleosome occupancy changes at TBSs anti-correlate with changes in TBP binding (Kubik, 2018). Thus, TBS accessibility and occupancy are directly related to PIC assembly and transcription.

1.4.2 Transcription Initiation

The promoter-TBP complex interacts with TFIIB that acts as a bridge between RNAPII and the promoter. TFIIB binds 'dock' and 'wall' domains of the polymerase to recruit the RNAPII-TFIIF complex (Kostrewa, 2009). TFIIB functions to position the TBP-DNA complex over the RNAPII active site, which acts as a key for PIC architecture (Miller and Hahn, 2006).

Transition of the PIC into an open complex requires a conformational change. The DNA translocase XPB, a subunit of TFIIH, binds the DNA downstream of RNAPII and separates DNA strands. It propels the single stranded DNA template into the polymerase active centre. This leads to the formation of a transcription bubble (Grünberg et al., 2012; Kim et al., 2000).

Recent observations detected open PIC ~40 bp upstream of smaller NDR (SAGA-dominated) TSSs and about ~20 bp upstream of TFIID dominated TSSs (Vinayachandran et al., 2018). In both gene classes, the RNAPII active site is located ~30 bp downstream of the TATA sequence. This supports that yeast RNAPII melts DNA next to the TBS and scans downstream sequences for TSS selection (Kuehner and Brow, 2006). A model for translocating RNAPII might involve TFIIF-mediated DNA translocation in the form of ~10 bp bubble. Precise TSS selection is determined by the combined action of TFIIB, TFIIF, RNAPII and nucleosome positioning (Khapersky et al., 2008; Klein-Brill et al., 2019; Kostreva, 2009).

1.4.2.1 Mediator complex: Relay of Transcription Signal

Mediator is a 25-subunit co-activator complex that regulates RNAPII initiation. Mediator is composed of four modules – head, middle, tail and kinase. The Med14 subunit acts as a scaffold to hold the complex together. Mediator stabilizes the PIC *in vitro*; it binds RNAPII and the initiation factors TFIIB and TFIIF by its two modules – head and middle (Plaschka, 2015; Robinson, 2016; Tsai, 2017). The tail subunit of Mediator binds TFs (Jeronimo, 2016). Mediator is able to contact hundreds of transcription activators and transmits these signals with help of TFs (Poss et al., 2013). Mediator can also be recruited by nascent ncRNAs (Lai, 2013).

Mediator function is required for the expression of nearly all protein-coding genes and its interaction with RNAPII is essential (Soutourina et al., 2011). Based on *in vitro* data, a subset of GTFs and Mediator were shown to act as scaffold that remains bound on promoters, that promote transcription initiation, but this was never confirmed *in vivo* (Yudkovsky et al., 2000). Mediator acts as a bridge between TFs bound at enhancers and the general transcription machinery assembled at the promoters in higher Eukaryotes (Malik and Roeder, 2016). In yeast, Mediator interacts simultaneously with UAS and core promoters with a short-lived association and loses its kinase module while undergoing the compositional change in the formation of PIC (Petrenko et al., 2016).

Post-translation modifications (PTMs) of mediator subunits is highly regulated and modulates its activity. For examples, phosphorylation of Med15 in the tails module prevent stress-induced transcription by inhibiting mediator interaction with stress induced TFs (Miller, 2012; Soutourina, 2018) Mediator destabilizes the PIC for it to undergo ‘promoter escape’. It stimulates the phosphorylation of RNAPII CTD at Ser5 by the Kin28/Cdk7 kinase subunit of TFIIF to facilitate the transition of RNAPII to the elongation phase of transcription. Mediator is ejected by the XPB translocase activity of TFIIF that makes PICs transcriptionally competent (Kim et al., 1994; Malik et al., 2017). The +1 nucleosome is pushed downstream just after polymerase enters elongation phase and this is directly related to the increase in transcription level (Nocetti and Whitehouse, 2016).

1.5 Transcription Elongates with Co-conspirators

Transcription elongates at a rate of 30-40 nt/sec in yeast (Kos and Tollervey, 2010). RNAPII transcription elongation is associated with 5' capping, splicing, co-transcriptional changes in histone modifications and polyadenylation of the mRNA transcripts. After RNAPII release, promoter-proximal pausing of RNAPII is a characteristic phenomenon observed in higher eukaryotes. It acts as a quality control mechanism and also plays a role in synchronous activation of genes (Henriques, 2013).

Capping begins as soon as the mRNA 5' end emerges from the RNAPII exit channel (Tome et al., 2018). Capping of mRNA transcripts involves addition of the 5' inverted methylguanosine cap to the 5' most nucleotide. Capping provides protection from exonucleases. Capping enzymes bind to the Ser5P form of RNAPII CTD (McCracken et al., 1997). *S. cerevisiae* has ~250 intron-containing genes, most of which have one intron. The spliceosome identifies and completes splicing after RNAPII has travelled 26 nt downstream of the 3' splice site. This supports that yeast has strong intron definition motifs to demarcate splice sites (Oesterreich et al., 2016).

RNAPII CTD is continuously undergoing phosphorylation/dephosphorylation modulating its association with different factors. Elongating RNAPII has an impact on chromatin structure. The mean spacing between the nucleosomes is associated with the frequency of transcription and might be regulated by the RNAPII associated factors (Chereji et al., 2018; Rando and Winston, 2012; Zentner and Henikoff, 2013).

1.5.1 RNAPII-CTD Phosphorylation Co-regulate Elongation

RNAPII contains a repeated seven-residue motif (YSPTSPS) at the C terminus of Rpb1, termed C-terminal domain (CTD) (Buratowski, 2009). The number of CTD repeats varies from 26 in yeast to 52 in humans (Chapman et al., 2008). The residues Tyr1, Thr4, Ser2, Ser5 and Ser7 are phosphorylated and dephosphorylated by CTD kinases and phosphatases in a regulated manner during transcription. These changes are coupled with transitions in transcriptional stages (Jeronimo et al., 2013) (Fig. 4). The non-phosphorylated CTD form is preferentially associated with the PIC as it has a high affinity for the Mediator complex (Robinson, 2016).

CDK7 phosphorylates the RNAPII CTD at Ser5 and Ser7 residues of the repeats resulting in transcription initiation. Ser5P levels peak near the promoter and drop immediately after, whereas Ser2P, Thr4P and Tyr1P levels increase across gene bodies. Tyr1P levels decrease before the polyadenylation site (PAS) (Fig. 4). The phosphorylation patterns are crucial for recruitment of key

regulatory factors, changes in chromatin modifications and RNA processing during transcription (Harlen and Churchman, 2017) (Fig. 4). The phosphorylated form of RNAP II CTD promotes the recruitment of PAF1 complex and transcription elongation factors, such as Spt6 (Harlen et al., 2016).

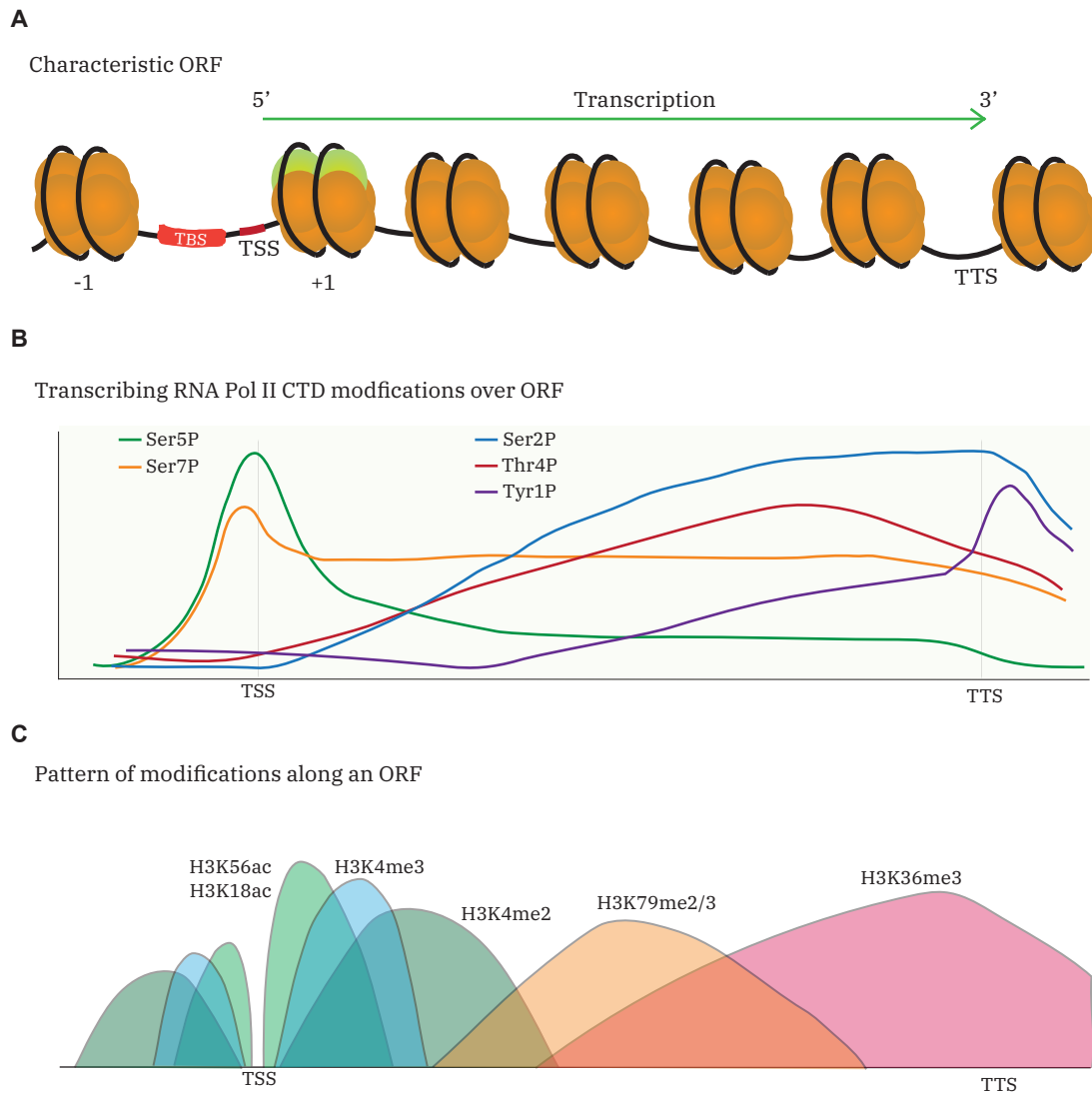


Figure 4. Co-transcriptional changes in RNA Pol II CTD and Histone PTMs

- (A) Representation of an Open Reading Frame with 5' NDR containing the TBS, TSS and +1 nucleosome with Htz1.
- (B) Levels of RNA Pol II CTD Phosphorylation states during transcription initiation and elongation, adapted from Harlen and Churchman, 2017.
- (C) Transcribing RNA Pol II associates with a variety of factors and deposits different modifications, resulting in a characteristic ORF profile of modifications.

1.5.2 Transcription Bursts ON and OFF

Transcription occurs in short bursts, which includes groups of initiation events separated by periods of inactivity (Chubb et al., 2006). Bursting depends on the organism and regulatory state of the gene (Lenstra et al., 2015). It contributes to transcriptional noise and increases cell-to-cell variability (Hornung, 2012; Tirosh et al., 2006). A single burst may contain between 2 – 100 transcribing RNAPII molecules (Tantale, 2016).

The stochastic nature of the transcription bursts defines the final transcriptional output in two ways – a. Burst size, i.e. the number of RNAPII molecules per burst and b. Burst frequency. The probability (frequency) of the burst positively correlates with the accessibility and priming of the promoter (Chen et al., 2019). The presence of a TATA-box in the promoter favors association with a large number of RNAPII molecules per burst (Larsson et al., 2019). The bursting frequency can be increased by changing the promoter chromatin to more easily recruit TFs or by inducing histone acetylation (Chen et al., 2019).

1.5.3 Transcription Runs in both Directions

The transcription that starts within the same NDR but elongates in the opposite direction is termed “divergent transcription”. Bidirectional transcription from coding gene promoters has been recognised to be a common phenomenon. Recent technological advances have revealed an abundance of non-coding transcripts near promoters of well-annotated genes in yeast (Neil et al., 2009; Xu et al., 2009). In humans, bidirectional transcription was observed at 55% of promoters by global run-on sequencing (GRO-seq) (Core et al., 2008). In humans, functionally, divergent gene pairs are usually the genes involved in the same pathway which mostly show positively correlated expression, which could be achieved by the binding of single TF (Lin et al., 2007).

Bidirectional transcripts arising from the same NDR originate from two distinct PICs, one for each transcribing direction, are associated within a relatively short region of ~120 bp, (Neil et al., 2009; Rhee and Pugh, 2012). In this study, PIC assembly was also observed at 3’ end NDRs of mRNA encoding genes. Furthermore, both ncRNAs and mRNAs transcribed from NDRs were observed to have compositionally homogenous PICs with regard to GTFs. Divergent transcription is regulated in a chromatin-dependent manner by CAF-1 and H3K56ac, and is promoted by the nucleosome remodeler SWI/SNF (Marquardt et al., 2014).

A recent study using native elongating transcript sequencing (NET-seq) observed transcription initiation upon introduction of a naïve DNA sequence from a closely related species into the *S.*

cerevisiae genome. Transcription initiation was observed to be bidirectional originating from either sides of randomly distributed yeast TF sequence motifs that were present in the DNA sequence. These observations support that new promoter regions are inherently bidirectional and that unidirectionality is an acquired trait (Jin et al., 2017).

1.6 Elongating polymerase re-write Chromatin Code

A variety of chromatin modifications are associated with different regions on the gene (Fig. 4). RNAPII CTD interacts with different factors co-transcriptionally to read/write the chromatin landscape in the gene bodies. This gives rise to an RNAPII CTD phosphorylation linked chromatin PTM landscape and to the different stages of transcription. Chromatin modifications also influence the speed of elongating RNAPII and the extent to which co-transcriptional factors could bind. It works as if RNAPII marks the transcription unit for the ‘next’ cycle of transcription; that in turn regulates the RNAPII binding and passage in the ‘next’ cycle.

Modifications can be broadly divided into two classes – a. modifications that are localised on repressed genes or transcriptionally inactive chromatin also known as heterochromatin. Heterochromatin modifications such as H3K9me and H3K27me localize to the transcriptionally inactive regions of the genome in higher organisms; b. modifications associated with active chromatin, which are referred to as euchromatin modifications.

The actively transcribed gene bodies are enriched with H2B ubiquitination (ub), methylations of H3K36, H3K79 and H3K4 (Fig. 4). Histone PTMs also present a high level of cross-talk among readers and writers. In steady state condition, the combinatorial complexity is reduced because of the co-occurrence of many modifications and a few strict non-occurring modifications. An analysis of the time resolved changes in modifications revealed changing kinetics of different modifications in response to transcriptional upregulation and revealed new combination states (Weiner et al., 2015). I will discuss few co-transcriptionally deposited modifications relevant for this work.

1.6.1 H3K4 Methylation marks Active Promoters

Active promoter regions have H3K4me besides multiple acetylated H3 and H4 Lysine residues. H3K4 monomethylation is enriched towards the 3’ end of the genes, dimethylation peaks in the middle of the gene body. Trimethylation occurs at the promoter regions of the gene, around the TSS and 5’ end of the open reading frame (ORF) (Pokholok et al., 2005; Weiner et al., 2015) (Fig. 4). Over successive transcription cycles, Set1 converts monomethylated into demethylated and finally into trimethylated residues. This methylation gradient depends on the transcription elongation rate,

frequency and time Set1 spends near a nucleosome (Soares et al., 2017). H3K4me3 provides a memory of recent transcriptional activity and helps maintain an active chromatin state (Ng et al., 2003).

In yeast, H3K4 is methylated by the Set1/COMPASS complex. Set1 N-terminal region and COMPASS subunit Swd2 interaction is required and are both needed for the recruitment of the complex to chromatin via RNAPII CTD Ser5 (Bae et al., 2020). PAF/RTF is a multi-subunit, evolutionarily conserved, elongation complex loaded onto the Ser5P form of RNAPII CTD (Qiu et al., 2006). PAF is critical for extending Rad6/Bre1 histone ubiquitin ligase binding to RNAPII into the ORF, where Rad6 performs H2BK123 ubiquitination. H2BK123 ubiquitination is required for di- and trimethylation of H3K4 (Kim et al., 2009; Shahbazian et al., 2005). Therefore, PAF directly regulates both H2B ubiquitination and H3K4 methylation (Krogan et al., 2003a; Wood et al., 2003). PAF dependent H2Bub also facilitates FACT function, a complex involved in the destabilization of nucleosomal H2A/H2B and H3/H4 tetramers, thereby promoting transcription elongation (Fischl et al., 2017; Hou et al., 2019; Pavri et al., 2006).

H3K4 methylation is recognised by PHD domain-containing complexes and can help in their recruitment to activate/repress transcription. H3K4me3 has been shown to stimulate activator-dependent transcription *in vitro*, it increases TFIID occupancy as well as PIC formation and stabilisation (Lauberth et al., 2013). H3K4me3 also recruits the CHD1 remodeler, which in turn maintains H3K4 and H3K36 trimethylation and promotes transcription elongation with RNAPII CTD (Sims et al., 2007; Vermeulen, 2007). H3K4me3 is recognised by the Gcn5 containing HAT complex SAGA, that promote H3K9ac (Bian, 2011). H3K4me3 is also recognised by the Yng1 subunit of NuA3 HAT, that acetylates H3K14 (Taverna et al., 2006).

H3K4me2 is recognised by the Set3C complex via its PHD domain. Set3C contains Hos2 and Hst1 HDACs that deacetylate nucleosomes in the gene body near the 5' end. This was shown to result in promoting efficient elongation of RNAPII as defects in Set1-Set3 pathway results in altered RNAP II levels and the strains showed increased sensitivity to chemical agents (Kim and Buratowski, 2009). Set3C binding also represses cryptic transcription originating closer to the 5' end of yeast ORF (Kim et al., 2012). H3K4 trimethylation was also shown to promote efficient termination by Nrd1-Nab3-Sen1 (NNS) complex (Terzi et al., 2011) (Discussed on page 38).

1.6.2 H3K36me: Closing Chromatin after Polymerase

Set2 is a H3K36 histone methyl transferase (HMT) that preferentially binds to the RNAPII CTD phosphorylated at both Ser5 and Ser2. Set2 travels with RNAPII and therefore mediates H3K36 di- and trimethylation within gene bodies (Kizer et al., 2005; Krogan et al., 2003b). The levels of H3K36me_{2/3} increase towards the 3' end of the genes and the pattern is highly conserved in eukaryotes (Fig. 4) (Weiner et al., 2015).

One role of H3K36me₃ is to suppress histone exchange within the ORF of transcribed genes (Venkatesh et al., 2012). H3K36me₃ reduction or loss of Set2 decreases FACT occupancy on chromatin and FACT-mediated H2B histone exchange during transcription in the gene body (Carvalho et al., 2013). H3K36me₃ also recruits Rpd3S to prevent spurious intragenic transcription in yeast. In humans, H3K36me₃ further promote DNA methylation to restrict intergenic transcription (Carrozza et al., 2005; Neri, 2017).

Loss of Set2, gives rise to improper resetting of the chromatin after transcription, resulting in transcription initiation from within protein coding genes generating non-coding transcripts (Venkatesh et al., 2016). Perturbed levels of H3K36me also result in reduction in life span (Sen et al., 2015). The study supports that H3K36me promotes longevity by suppressing cryptic transcription and that in old yeast cells, upregulated genes lose this mark in the gene bodies. This study further showed that H3K36me₃ also increases lifespan in *C. elegans* (Sen et al., 2015).

H3K36me₃ is repressive towards transcription. Indeed, when Set2 is mistargeted to promoter regions through artificial recruitment, it represses transcription (Landry et al., 2003; Strahl et al., 2002). Upstream overlapping non-coding transcription has been shown to direct Set2-Rpd3S to the promoters of the Set2-repressed genes (Kim et al., 2016). These observations support that Set2 deposits H3K36me co-transcriptionally, which results in the resetting of chromatin to a repressive state after the passage of RNAPII in genes.

1.6.2.1 Rpd3 Histone Deacetylase recognises H3K36me₃

Transcription elongation is promoted by acetylation of multiple histones. After RNAPII passage, deacetylation occurs to re-establish repressed chromatin. Set2-mediated H3K36me₃ promotes the subsequent recruitment of Rpd3S to remove transcription coupled histone acetylation and restore nucleosome positioning after transcription. H3K36me₃ in gene bodies recruits the Rpd3S HDAC complex through a chromodomain in its Eaf3 subunit and a PHD domain in the Rpd3 complex. Increased acetylation in the ORF was observed upon loss of Set2 (Keogh et al., 2005; Li et al., 2007b).

The Rpd3 HDAC exists in two forms: Rpd3S (small) and Rpd3L (Large). Yeast Pho23 and Rxt1 are two components of Rpd3L that recognise H3K4me3 and H3K36me3 respectively via their PHD finger domain and bind the modification present in promoters (Lee et al., 2018a; Shi et al., 2007). Rpd3 and Set3 binding is further enhanced by their interaction with phosphorylated RNAPII CTD, although H3K36me3 is required for the deacetylation activity of Rpd3 (Govind et al., 2010).

Rpd3 is also targeted to the promoters when yeast cells are shifted to glucose depleted medium and when cells enter quiescence (Q). Rpd3 helps maintain a repressive chromatin by deacetylating the promoter chromatin, increasing histone density in the promoter regions of the repressed genes. Rpd3 is essential for Q entry and yeast cell survival (McKnight et al., 2015). Further studies from the lab showed that the chromatin remodeler SWI/SNF activates Q specific genes and is required for Q entry. Snf2 works with the Gis1 TF that is phosphorylated and localised to Q specific upregulated genes. They also showed that Rpd3 binding to the promoters is mediated by Snf2 prior to diauxic shift (DS) (Spain et al., 2018).

1.7 Termination: pushing the break

The RNAPII termination process is highly regulated. It consists of – polyadenylation of the mRNA transcript after cleavage, slowing down of RNAPII, release of the mRNA for nuclear export and eviction of the RNAPII from the DNA. RNAPII density is increased as it reaches the cleavage and polyadenylation sites as observed in nascent RNA sequencing methods - GRO-seq, PRO-seq, mNET-seq (Kwak et al., 2013; Mayer et al., 2015). After processing and releasing the transcript, RNAPII continues transcribing before eventually dissociating from DNA. Two models for RNAPII termination have been proposed – a. allosteric hindrance, in which RNAPII interacts with other factors that destabilise it or b. torpedo model, in which a 5' to 3' RNA exonuclease chases down RNAPII to trigger termination (Proudfoot, 2016).

Knocking down RNA processing and cleavage factors reduces RNAPII accumulation at the polyadenylation site (PAS), which indicates a functional connection between RNAPII pausing at PAS and RNA processing during cleavage. Depletion of cleavage factors and 5'-3' exonuclease also increases RNAPII accumulation near the TSS, suggesting that many transcripts are cleaved at an early stage of transcription (Nojima et al., 2015). Different cleavage factors function in different termination processes; for example the Integrator complex cleaves enhancer RNAs in humans (Lai et al., 2015). In yeast, the cleavage and polyadenylation factor (CPF) performs transcription termination at protein coding genes whereas snoRNAs and non-coding RNA early-termination is mediated by the NNS complex discussed in detail in the non-coding section.

2 Transcription of Non-Coding RNAs

The mechanisms of RNAPII transcription as described above is true for a 'gene'. While reading the literature about the transcription, it is natural to think that it is applicable to protein-coding genes, as most research before the dawn of sequencing has been performed on this set of DNA sequences. Currently, 'Gene' is defined as a basic physical and functional unit of heredity, that *might* code for protein while *most* do not - from the NIH website. A few functional evolutionary studies have proposed that promoters are initially just fortuitous and produce transcripts, which might turn out to be beneficial for the cell and are subsequently selected. The fortuitous promoters acquire canonical promoter architecture after selection (Hughes et al., 2012; Jin et al., 2017). These observations suggest that coding transcription is not the rule; rather, coding RNAs are selected. Thus, in the beginning, both forms of 'genes' are transcribed by RNAPII in a similar fashion.

In yeast, almost the whole genome is transcribed in an interleaved manner (Mellor et al., 2016). Pervasive transcription gives rise to a complex organisation of the transcriptome with many overlapping transcription boundaries on the same or opposite strands of the DNA. These transcripts, coding or not, could act on the non-strand specific component of the DNA i.e. chromatin, thereby influencing neighbouring transcription by modifying nucleosome PTMs, DNA supercoiling and recruiting chromatin associated factors. Thus, pervasive transcription plays an important role in gene regulation.

2.1 Long non-coding RNAs

Long non-coding RNAs are defined as RNAs of ≥ 200 nt in length that are independently transcribed by RNAPII. They resemble mRNAs as they are capped and polyadenylated just as coding RNAs (Quinn and Chang, 2016). Originally, the 200 nt cut-off corresponds to the retention threshold of long RNA purification protocols. These exclude most canonical ncRNAs like small nucleolar RNAs (snoRNAs), small nuclear RNAs (snRNAs) and tRNAs.

In yeast, the first lncRNAs were identified using DNA microarrays to examine total RNA in a mutant lacking the 3'-5' exonuclease Rrp6, a component of the nuclear exosome. They identified polyadenylated RNA species arising from intergenic regions, which are rapidly degraded by the nuclear exosome (Wyers et al., 2005). Transcripts stabilized in the *rrp6* mutant were termed cryptic unstable transcripts (CUTs). Recent methods measuring nascent transcription such as NET-seq or precision run-on sequencing (PRO-seq) identified a large number of unstable lncRNA transcripts.

The number of these transcripts is increasing with the sequencing depth (Churchman and Weissman, 2011; Neil et al., 2009; van Dijk et al., 2011).

Non-coding transcripts have a very short half-life and hence are detectable only after mutating components of the degradation machinery and therefore in yeast, they are classified based on their detection in the specific mutant. Steady state strand specific total RNA analyses identified stable non-coding RNAs that were referred to as stable unannotated transcripts (SUTs). Those in antisense orientation to the coding ORF were termed natural antisense transcripts (NATs) (Castelnuovo and Stutz, 2015; Khorkova et al., 2014; van Dijk et al., 2011; Xu et al., 2009). Finally, the transcripts stabilized when inhibiting the cytoplasmic 5'-3' exonuclease Xrn1 are called Xrn1-sensitive unannotated transcripts (XUTs).

Presently, over 200'000 unique lncRNAs have been annotated in humans and their expression is usually tissue specific (Xu et al., 2017). One type of lncRNA classification is based on the site of function relative to its transcription site. *Cis*-acting lncRNAs are defined as the ones whose activity is based on the loci from where they are transcribed and are generally working or influencing the genome through chromatin-related processes (Gil and Ulitsky, 2020).

Trans-acting lncRNAs depend on the sequence and level of lncRNA produced. In *S. pombe*, *C. elegans*, *D. melanogaster* and mammals, overlapping transcription products have been shown to give rise to dsRNAs that are processed by dicer in the nucleus to produce siRNAs that work with argonaute proteins and histone methyl transferases to convert active chromatin into a heterochromatin state via H3K9 or H3K27 methylation (Castel and Martienssen, 2013; Gullerova and Proudfoot, 2012). *S. cerevisiae* lacks the machinery for RNA-mediated heterochromatin formation. In *A. thaliana*, the COOLAIR antisense transcript mediates the replacement of H3K36me, a mark of active transcription, with H3K27me3 and promotes transient polycomb-mediated heterochromatin silencing (Csorba et al., 2014).

2.2 *Cis*-acting lncRNAs

Cis-acting lncRNAs are known to be of low abundance, usually a few molecules per cell. The sites of lncRNA transcription are more highly conserved than the sequence of the lncRNA itself and they are usually enriched in the chromatin fraction (Pang et al., 2006). Furthermore, the act of transcription itself has been recognised to provide it with regulatory capacity. This supports the view that lncRNAs are evolving to work in a position specific manner. Most commonly, it has been observed that overlapping transcription of ncRNAs results in activating of repressive effect on the chromatin and hence associated transcripts (Kaikkonen and Adelman, 2018; Ulitsky, 2016).

The emerging idea in higher eukaryotes is that in the pre-formed chromatin loops place lncRNA transcription and product in the vicinity of target genes, where it exerts its effects. Apart from transcription itself; mechanism of action of lncRNAs are known to involve sequestering of certain factors, binding to different proteins and repelling binding of specific proteins at a site (Gil and Ulitsky, 2020; Sun et al., 2013).

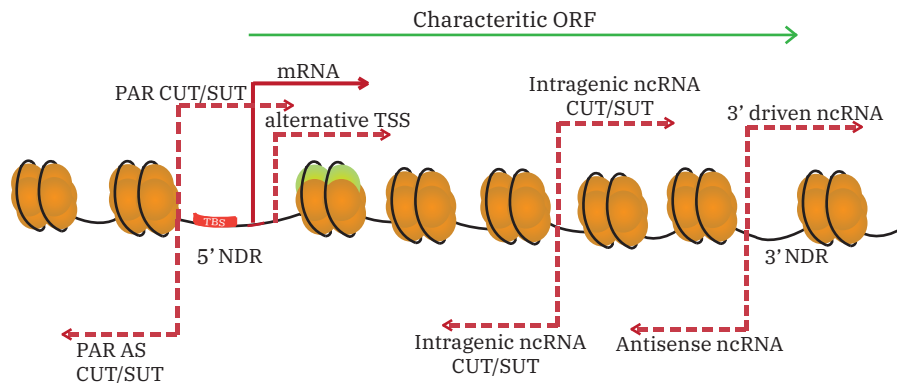


Figure 5 Origins of non-coding RNAs and mRNA relative to an ORF.

Promoter associated RNAs (PAR) originate from the 5' NDR in either direction. Rapidly degraded ncRNAs are termed Cryptic Unstable Transcripts or CUTs and stable ncRNAs are termed Stable Uncharacterized Transcripts or SUTs. A typical mRNA or coding transcript originates from the transcription start site (TSS); there can be more than one TSS, giving rise to different 5' end transcripts. Intragenic cryptic transcripts are usually repressed but originate within coding regions in mutants of Set2, Spt6 or Spt16. ncRNAs originating from 3' end NDRs also give rise to ncRNAs in either direction; the one transcribed towards the Sense promoter and encoded by the opposite strand is termed Antisense ncRNA. Figure adapted from Berretta and Morillon 2009.

2.2.1 Transcription Interference

Transcription interference (TI) can be defined as the direct suppressive effect of RNAPII transcription *in cis* from one transcription passing over another (Shearwin et al., 2005). lncRNA transcription can enter into a transcription unit coming from upstream and running into a downstream promoter region in the case of genes in tandem; alternatively lncRNA transcription could enter from the 3' end direction while transcribing on the antisense strand. This results in interdependent transcriptional units with transcription itself regulating initiation of another transcript (Churchman and Weissman, 2011; Mellor et al., 2016; Nguyen et al., 2014).

The upstream transcription entering into a transcription unit could originate as a non-coding transcript or arise from read-through transcription from an upstream gene in tandem. The initial study that revealed the interference process was in humans where a duplicated second copy of the α -globin gene becomes repressed by transcription from an upstream copy (Proudfoot, 1986).

Transcript isoform sequencing (TIF-seq) in *S. cerevisiae* revealed that about 1/4th of 2747 tandem gene pairs express overlapping long isoforms, that have the potential to regulate the downstream gene. Furthermore, 6.7% of gene products are part of bi-cistronic or tri-cistronic transcripts which could also potentially repress the second or third transcripts (Pelechano et al., 2013).

2.2.2 Chromatin Mediates Transcription Interference

One mechanism of TI mediated chromatin remodelling is the transcribing RNAP II that could produce supercoils in the DNA. RNA transcription generates negative supercoils behind and positive supercoils in front of RNAPII. These supercoils could alter nucleosome occupancy in the region; these combined effects may change chromatin structure and affect gene activation (Naughton, 2013; Teves and Henikoff, 2014).

Negative supercoils favour the transient separation of the DNA strands. These negative supercoils generated behind a transcribing RNAPII could result in the formation of R loops (Roy et al., 2010). R loops are structures formed by annealing of RNA to its genomic template, either during its transcription just behind RNAPII or after maturation. This generates a DNA:RNA hybrid and a displaced single stranded DNA (Costantino and Koshland, 2015). In mammals, R loops are found to associate with Polycomb complexes resulting in the formation of repressive chromatin (Skourti-Stathaki et al., 2014).

Some non-coding transcripts repress the downstream transcripts by increasing the density of nucleosomes in the canonical promoter architecture of the repressed genes. SRG1 lncRNA is located upstream of the *SER3* gene required for serine synthesis. When yeast is grown in rich medium, SRG1 lncRNA is elongated and *SER3* is repressed by FACT complex-mediated nucleosome assembly at the *SER3* promoter (Hainer et al., 2011; Martens et al., 2005).

The act of transcription from upstream of a gene might trigger the displacement of TFs from the compacted promoter region of the downstream gene (Bumgarner et al., 2009). This was observed in Zap1-induced intergenic RNA transcripts that represses *ADH1* and *ADH3* by displacing transcription activators (Bird et al., 2006).

Extension of lncRNAs or transcripts from upstream into ORFs could also result in the deposition of elongation specific PTMs in the downstream promoters that repress transcription initiation. LncRNA expression deposits Set2-mediated H3K36me3 marks co-transcriptionally, which recruit HDACs that repress RNAPII initiation (Ard and Allshire, 2016). Two lncRNAs control *IME1* gene expression in yeast. *IME1* controls mating in yeast. Transcription of the lncRNA IRT1 represses *IME1* expression by inducing methylation and deacetylation. The second lncRNA IRT2, upstream of IRT1,

represses IRT1 and therefore alleviates *IME1* repression (Moretto et al., 2018; van Werven et al., 2012).

Overlapping lncRNAs have been shown to repress downstream transcription via two different mechanisms depending on the distance between the lncRNA and the promoter. Upstream lncRNAs that are close to the downstream promoter deposit Set1-dependent H3K4me2 marks at the promoter which recruit the Set3 HDAC thereby inducing deacetylation of the gene 5'-transcribed regions (Kim et al., 2012). When the distance between lncRNA and promoter is large, lncRNA transcription will preferentially deposit Set2-dependent H3K36me3 at the promoter, which will recruit the Rpd3 HDAC (Kim et al., 2016). Both studies elegantly follow the co-transcriptional PTM deposition by lncRNAs as Set1 is interacting with RNAPII CTD at the beginning of transcription while Set2 is travelling with RNAPII more towards the end of transcription (Fig. 4).

Enhancer RNAs (eRNAs) were also proposed to interact with Mediator to activate transcription (Lai, 2013). The homeobox specific eRNA HOTTIP, transcribed from the HOXA locus, mediates long range interactions and chromosomal looping. It also binds the WDR5/MLL complex that drives H3K4me at close by genes thereby activating transcription (Wang, 2011).

2.3 Antisense LncRNAs act in *Cis*

Antisense (AS) RNAs are transcripts in inverse orientation from the 3' end of coding genes (Pelechano and Steinmetz, 2013). In yeast, many AS transcripts originate from bidirectional promoters, which might be a consequence of genome density (Neil et al., 2009; Xu et al., 2009). AS transcripts are widely expressed in all organisms and current analyses place AS transcripts at 30% of all human annotated transcripts (Ozsolak et al., 2010). AS transcripts mostly localize in the nucleus and associate with chromatin. The expression level of AS transcripts is on average 10-fold less than the coding transcripts (Neil et al., 2009; Xu et al., 2009).

Sense-AS transcript pairs have potential to form self-regulatory circuits in which an equilibrium between their expression exists. Expression of one is mutually inhibitory to the other. This organisation confers interdependent regulatory advantages independent of an action of a TF. Cells can switch faster between an on/off state. This organisation is further known to provide yeast with different transcriptional states within a cell population, that might provide it with survival or evolutionary advantages (Mellor et al., 2016; Pelechano and Steinmetz, 2013; Xu et al., 2011).

AS transcription regulates sense expression through chromatin-based mechanisms. AS transcription has been shown to repress sense transcription at the *PHO84* locus by recruitment of

the HDAC Hda1 (Camblong et al., 2007). Using single-molecule FISH analyses, AS was shown to repress sense transcription upon extension of *PHO84* AS RNA into the promoter of the gene. The study also showed that cell to cell variability exists and *PHO84* mRNA was expressed in only 20% of the cells while the remaining 80% cells exhibit low level of AS expression probably in association with the inactive *PHO84* gene (Castelnuovo et al., 2013).

It has been suggested that AS transcription will deposit histone modifications in the mirror image to the ones deposited by sense transcription. This in turn will lead to promoter closing and repression (Castelnuovo and Stutz, 2015; Castelnuovo et al., 2014; Xue et al., 2014). By contrast, evidence has been presented that AS producing genes have markedly different chromatin states in the ORF and therefore AS transcription is inherently different (Murray et al., 2015)..

Interestingly, AS-mediated repression occurs only when AS transcription reaches the promoter of the sense genes (Castelnuovo et al., 2014; Nevers et al., 2018; Schulz et al., 2013). AS transcription has been further shown to modulate sense transcription by changing the chromatin state over the promoter and gene body, which would then influence sense transcript dynamics and stability. AS results in genes having a bimodal two-state chromatin. This type of chromatin is typical of highly regulated, bursting and noisy genes, that results in transcript variability in a population (Weinberger et al., 2012; Zenklusen et al., 2008). Genes subjected to AS transcription at steady state are characterized by high nucleosome occupancies in the sense promoter (Brown et al., 2018; Murray et al., 2015) and is also associated with increased nucleosome turnover (Murray et al., 2015).

Some studies have proposed that AS transcription can also lead to activation of transcription (Uhler et al., 2007). AS-mediated R-loop formation has been proposed to prevent chromatin compaction and hence support transcription factor recruitment and gene expression (Boque-Sastre et al., 2015). However, a complete mechanism does not exist that could explain AS-mediated Transcription Interference.

2.3.1 Nrd1-Nab3-Sen1 termination

To avoid unintentional transcriptional interference, AS lncRNAs are subjected to early-termination dependent on the Nrd1-Nab3-Sen1 complex (Porrúa and Libri, 2015). In *S. cerevisiae*, the Nrd1-Nab3-Sen1 (NNS) complex is implicated in transcription termination of snRNAs, snoRNAs and cryptic unstable transcripts (CUTs) as well as AS transcripts (Arigo et al., 2006; Schulz et al., 2013; Steinmetz et al., 2001) (Fig. 5). Nrd1 and Nab3 are two RNA-binding proteins and Sen1 is an ATPase dependent 5' to 3' RNA/DNA and DNA helicase. Nrd1 and Nab3 recognise the short sequence motifs GUAA/G and UCUUG on the nascent RNA, respectively (Creamer et al., 2011). This recognition is crucial for

the specific targeting of the NNS complex, however these motifs are abundant and are insufficient to drive NNS binding (Webb et al., 2014). These motifs are more enriched on promoter divergent transcripts or at the 5' end of antisense transcripts starting from the 3' end of coding genes (Porrúa et al., 2012).

Nrd1 is recruited to transcribing genes through its CID domain that interacts with the Ser5P form of RNAPII CTD, which is abundant over the first ~100 bp of transcription (Milligan et al., 2016; Vasiljeva et al., 2008). Termination by NNS is further promoted by interactions with H3K4me3 marks (Terzi et al., 2011). RNAPII CTD Tyr1 has also been shown to be important for NNS recruitment. It promotes efficient termination in its dephosphorylated form, while phosphorylation inhibits Nrd1 binding. Tyr1 was also shown to increase the residence time of RNAPII at the beginning of transcription facilitating the physical interaction and thus recruitment of Nrd1-Nab3 (Collin et al., 2019; Mayer, 2012; Webb et al., 2014).

Once recruited, Nrd1-Nab3 can engage Sen1, a highly conserved ATP-dependent 5' to 3' RNA and DNA helicase belonging to the superfamily 1 of helicases (Han et al., 2017). Sen1 does not exhibit sequence-specific RNA-binding capability (Creamer et al., 2011; Porrúa and Libri, 2013). To perform transcription termination, Sen1 translocates along the nascent RNA towards the transcribing RNAPII. *In vitro*, it has been shown that its central helicase domain is sufficient for transcription termination (Han et al., 2017; Leonaite et al., 2017). Sen1 specificity for transcription termination is provided by its interactions with Nrd1-Nab3 and RNAPII. The Sen1 C-terminal domain is recognised by Nrd1 CID and its N-terminal domain promotes interaction with RNAPII CTD. Interaction with RNAPII is necessary for its termination activity (Han et al., 2020) (Fig. 6). Sen1 also acts to prevent R-loop formation (Mischo et al., 2011). Sen1 is also associated with replication forks and therefore might play a role in coordinating replication and transcription (Alzu et al., 2012).

The NNS complex physically associates with the nuclear RNA exosome and the TRAMP activator complex (Vasiljeva and Buratowski, 2006). This couples NNS dependent termination and degradation of the transcripts. NNS recruits the TRAMP complex through a direct interaction of its Trf4 component with the Nrd1 CID domain (Tudek et al., 2014). The TRAMP complex consists of and got its name from three proteins – a poly(A) polymerase (either Trf4 or Trf5), a zinc knuckle RNA binding protein (Air1 or Air2) and the RNA helicase Mtr4. Trf4/5 adds a short oligo(A) tail to the 3' end of the NNS-terminated RNAs.

The addition of an oligo(A) tail to the 3' end of the RNA primes the transcript for degradation by nuclear exosome. The RNAs are degraded by the nuclear exosome that contains the Rrp6 exonuclease, which catalyses 3' end maturation of snoRNAs or completes degradation of antisense transcripts (LaCava et al., 2005; Vanacova et al., 2005; Wyers et al., 2005). The non-coding RNAs that

escape early termination by NNS are extended and exported to the cytoplasm, where they are targeted by the cytoplasmic surveillance machinery non-sense mediated decay (NMD) pathway (Malabat et al., 2015; Wery et al., 2018).

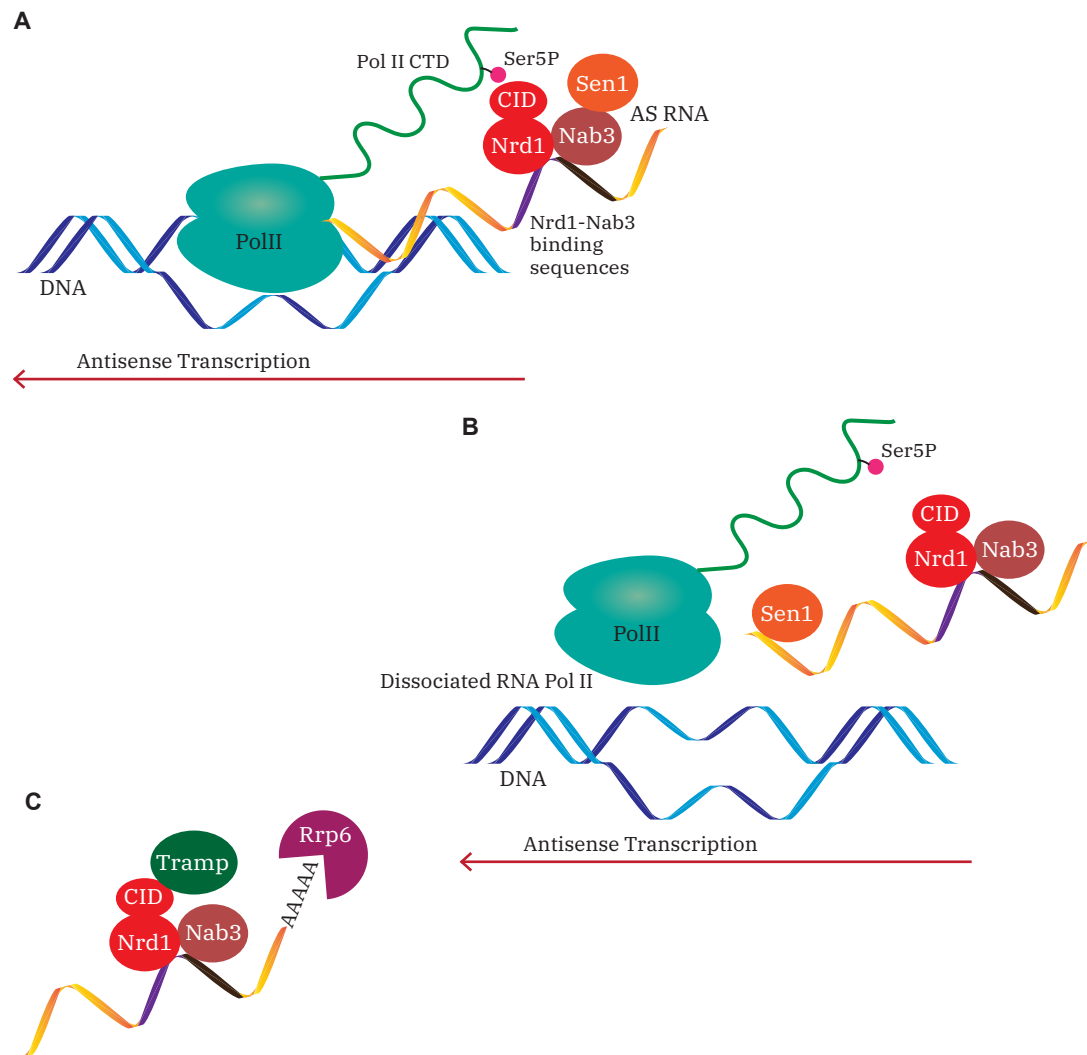


Figure 6. Nrd1/Nab3/Sen1 mediated Antisense early termination

- (A) Recruitment of Nrd1-Nab3 by sequence specific binding motifs on Antisense (AS) RNA and Nrd1 CID interaction with RNA Pol II CTD phosphorylated on Ser5.
 (B) Nrd1-Nab3 mediated recruitment of Sen1 helicase that travels along the RNA to reach RNA Pol II and induce termination.
 (C) AS RNA bound Nrd1-Nab3 interacts with the Tramp complex that adds Poly-A to the RNA promoting its degradation by Rrp6, a component of the nuclear exosome. Figure adapted from Porrua and Libri 2015.

2.3.2 Physiological Antisense Regulation

The individual mutants of the three proteins are known to regulate different but overlapping subsets of AS transcripts. This could be harnessed by the cell to promote rapid remodelling of the transcriptome in response to external stimuli or different physiological conditions. The Nrd1-Nab3 termination pathway has been shown to counteract the Ras signalling pathway and to participate in the response to nutrient depletion (Darby et al., 2012). This study shows that Nrd1 is functional in the rapid suppression of some growth and glycolysis related genes when transferred to the poor growth conditions. Glucose depletion leads to dephosphorylation of Nrd1 that forms nuclear speckles with Nab3 (Darby et al., 2012). Transcription termination in nutrient depletion conditions has been studied using PAR-CLIP. Nrd1-Nab3 have been found to associate with 30% of protein-coding transcripts (Webb et al., 2014).

The glucose depletion response was further characterized by observing the binding of NNS and the nuclear RNA decay machinery on the genome following nutrient depletion. It was shown that Nab3 becomes associated with many downregulated growth related genes, while stress induced genes bypass NNS surveillance (Bresson et al., 2017). The NNS pathway selectively targets mRNAs that code for energy usage or cell growth (Bresson et al., 2017). Nrd1 and Nab3 have also been found to bind snoRNA and tRNA transcripts under glucose deprivation (Jamonnak et al., 2011). The complete understanding of physiological regulation of NNS complex under nutrient stress conditions require further investigation.

The Sen1 helicase protein levels have been shown to vary through the cell cycle. Reduced Sen1 correlates with reduced Sen1-mediated termination, while overexpression of Sen1 leads to excessive termination and reduced cell viability (Mischo et al., 2018). Sen1 levels are regulated, as it is involved in the last step of early-termination after Nrd1-Nab3 binding, and could therefore determine the level of early-termination in the cell. AS transcripts are also observed to be upregulated in quiescence phase (G₀). These changes could either be due to the regulation of one of the three NNS factors, or the consequence of global downregulation of sense transcription leading to an upregulation of AS transcription (Nevers et al., 2018).

3 Objectives

Our lab was one of the first to discover AS-mediated gene regulation (Camblong et al., 2007). We also know that it occurs through a chromatin-related mechanism. However, the precise sequence of molecular events leading to transcription interference is not known. AS and sense transcripts make a co-transcriptional pair: perturbing the expression of an individual AS transcript can affect the level of the sense transcript (Guttman et al., 2011; Xu et al., 2011). Therefore, dissecting the functional properties of AS transcripts using classical approaches of overexpression or systematic knockdown is not possible. To disentangle and study the consequences of AS transcription, dynamic analyses following perturbation have been successful (Castelnuovo et al., 2014; Kim et al., 2012; Schulz et al., 2013). These studies provided a dynamic method to induce AS transcription and were successful in reporting direct effects of AS extension. My thesis work is based on these former studies and can be divided into three parts addressing specific questions:

1. Antisense-Mediated Interference Mechanism. The aim was to perturb the system dynamically and to follow the changes in both sense and antisense transcription. We planned to measure on a genome-wide scale the dynamics of transcription output and occupancy of various factors in response to induction of AS by removing AS early-termination. These studies were complemented by dynamically measuring the transcription output in the absence of a key factor. This work was performed to solve the mechanistic details of AS-mediated repression.

2. Recovery of Antisense-Mediated Repression. The second aim derives from the observations of the first study. AS is able to repress sense through chromatin-related mechanisms and this occurs naturally in the environment when cells encounter harsh conditions, such as limited nutrient (Bresson et al., 2017). The next question was to address the long-term effects of AS mediated repression, by recovering the AS early-termination. This work was performed by dynamically following both transcription and chromatin first when establishing the marks by inducing AS, and then by observing the persistence of transcription and chromatin effects in the absence of AS.

3. Non-coding Transcription Regulate the Replication Program in *Cis*. This study was performed to address the role of non-coding transcription readthrough over autonomously replication sequences (ARS). The hypothesis was that non-coding transcription readthrough may modify and thus close the ARS NDRs. This was performed by measuring dynamically the changes in replication program and chromatin features after inducing non-coding transcription through ARS. The study entitled “Noncoding transcription influences the replication initiation program through chromatin regulation” is published in Genome Research and is part of Appendix B of the thesis (Soudet et al., 2019) (page 154).

Results

1 Antisense-Mediated Interference Mechanism

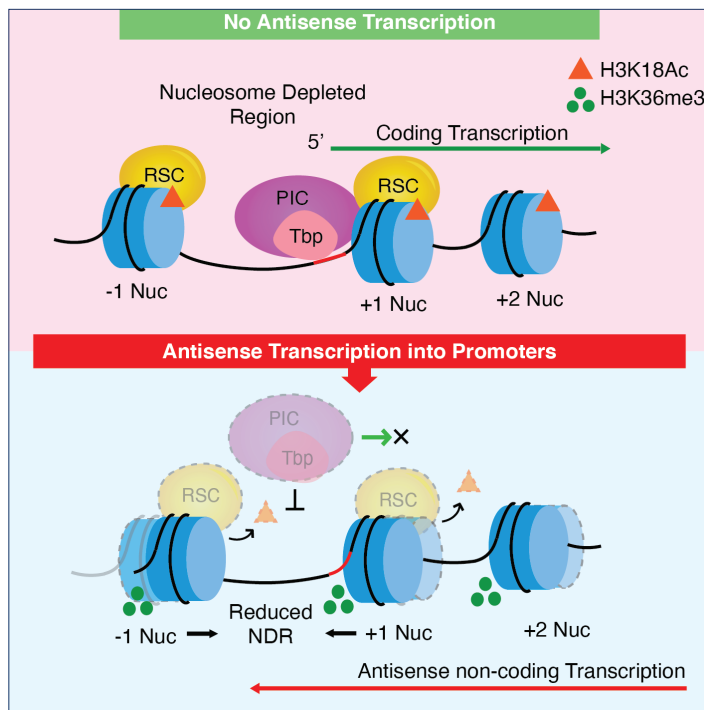
One aim of my thesis was to more precisely define the molecular mechanism by which AS transcription represses sense expression. This question was addressed by dynamically depleting Nrd1 using the anchor away system (Haruki et al., 2008). This leads to rapid AS induction and elongation into the sense promoter, which was followed by performing RNA-seq. We observed 217 genes that were repressed by at least 20% or more after 60 mins of anchoring away of Nrd1. These genes were termed antisense-mediated repressed genes (AMRG). Genes showing an increase in AS but no decrease in sense expression were termed non-responsive genes (NRG). The rest of the non-affected genes were termed Other genes.

AMRG showed reduced TBP occupancy after AS induction, supporting that AS extension represses sense at the PIC formation stage. AMRG were also characterized by an increase in nucleosome occupancy and H3K36me3 at the sense promoters in response to AS induction. AMRG further showed a decrease in H3K18ac and RSC chromatin remodeler occupancy at the promoter regions. This resulted in closing of the sense promoter at these genes with an observed shift in -1 and +1 nucleosomes towards the NDR. Importantly, the AS-mediated transcription interference was observed to occur naturally at 1/5th of yeast genes presenting the highest AS RNA levels at steady state.

The study entitled “Fine Chromatin-Driven Mechanism of Transcription Interference by Antisense Noncoding Transcription” is published in Cell Reports (Gill et al., 2020). My contribution to the work was to perform experiments and analyse data for most figures in the publication.

Fine Chromatin-Driven Mechanism of Transcription Interference by Antisense Noncoding Transcription

Graphical Abstract



Authors

Jatinder Kaur Gill, Andrea Maffioletti, Varinia García-Molinero, Françoise Stutz, Julien Soudet

Correspondence

francoise.stutz@unige.ch (F.S.),
julien.soudet@unige.ch (J.S.)

In Brief

Widespread antisense noncoding transcription often overlaps with coding sense transcription in the compact budding yeast genome. This may lead to transcription interference. Gill et al. propose a comprehensive mechanism of gene repression by antisense transcription occurring through the closing of promoter nucleosome-depleted regions (NDRs).

Highlights

- Antisense transcription leads to -1/+1 nucleosome sliding, reducing sense initiation
- H3K36me3 nucleosomes are differently positioned compared to H3K18ac nucleosomes
- RSC recruitment to -1/+1 nucleosomes is modulated by histone acetylation levels
- 20% of *S. cerevisiae* genes are significantly repressed by the proposed mechanism



Article

Fine Chromatin-Driven Mechanism of Transcription Interference by Antisense Noncoding Transcription

Jatinder Kaur Gill,¹ Andrea Maffioletti,¹ Varinia García-Molinero,^{1,2} Françoise Stutz,^{1,*} and Julien Soudet^{1,3,*}¹Department of Cell Biology, University of Geneva, 1211 Geneva 4, Switzerland²Present address: Institut de Génétique Humaine, CNRS - Université de Montpellier, Montpellier, France³Lead Contact

*Correspondence: francoise.stutz@unige.ch (F.S.), julien.soudet@unige.ch (J.S.)

<https://doi.org/10.1016/j.celrep.2020.107612>

SUMMARY

Eukaryotic genomes are almost entirely transcribed by RNA polymerase II. Consequently, the transcription of long noncoding RNAs often overlaps with coding gene promoters, triggering potential gene repression through a poorly characterized mechanism of transcription interference. Here, we propose a comprehensive model of chromatin-based transcription interference in *Saccharomyces cerevisiae* (*S. cerevisiae*). By using a noncoding transcription-inducible strain, we analyze the relationship between antisense elongation and coding sense repression, nucleosome occupancy, and transcription-associated histone modifications using near-base pair resolution techniques. We show that antisense noncoding transcription leads to the deacetylation of a subpopulation of $-1/+1$ nucleosomes associated with increased H3K36me3. Reduced acetylation results in the decreased binding of the RSC chromatin re-modeler at $-1/+1$ nucleosomes and subsequent sliding into the nucleosome-depleted region hindering pre-initiation complex association. Finally, we extend our model by showing that natural antisense non-coding transcription significantly represses $\sim 20\%$ of *S. cerevisiae* genes through this chromatin-based transcription interference mechanism.

INTRODUCTION

Recent techniques monitoring eukaryotic nascent transcription have revealed that the RNA polymerase II (RNAPII) landscape extends far beyond the sole transcription of mRNA (Churchman and Weissman, 2011; Core et al., 2008; Mayer et al., 2015; Nojima et al., 2015). If 1%–2% of the human genome is devoted to coding genes, >80% is transcribed into >200-nt long noncoding RNAs (lncRNAs) (Djebali et al., 2012). Thus, $\sim 200,000$ lncRNAs originating from nucleosome-depleted regions (NDRs) have been recently annotated across different human tissues and cell types (Kaikkonen and Adelman, 2018). While their function is still under debate, it raises a new concept in which RNAPII transcribes nearly the whole genome as closely interleaved transcription units (Mellor et al., 2016). Consequently, the transcription of many lncRNAs is reaching coding gene promoters, eventually leading to transcription interference (i.e., repression of the coding gene) (Proudfoot, 1986). So far, the precise molecular basis underlying transcription interference remains poorly characterized.

In *Saccharomyces cerevisiae*, noncoding transcription often originates from a NDR, also referred to as bidirectional promoters, transcribing a coding gene in one orientation and a noncoding RNA in the other (Churchman and Weissman, 2011; Jensen et al., 2013; Neil et al., 2009; Xu et al., 2009). Because the yeast genome is compact, a majority of lncRNAs appear as

being antisense to coding genes. To avoid antisense transcription into sense paired promoters and to limit transcription interference, lncRNAs are usually subjected to early termination in a process that is dependent on the Nrd1-Nab3-Sen1 complex, followed by degradation (Porrua and Libri, 2015). Early termination of noncoding transcription is not strict and mostly depends on the number of Nrd1-Nab3 recognition motifs carried by the lncRNA (Castelnuovo et al., 2014; Schulz et al., 2013). This implies that some lncRNAs will be cleared through early termination, while others will naturally extend into sense promoters, followed by export and degradation in the cytoplasm via nonsense-mediated decay (NMD) (Malabat et al., 2015; Wery et al., 2018). The artificial loss of early termination through Nrd1 depletion leads to antisense elongation into paired sense promoters and to a subsequent transcription interference directly correlated with the levels of lncRNA accumulation over the promoters (Schulz et al., 2013). According to this, high steady-state levels of natural antisense transcription into gene promoters may anticorrelate with coding sense expression. However, this question is still open since some analyses have led to opposite conclusions (Brown et al., 2018; Murray et al., 2015; Nevers et al., 2018).

RNAPII transcription has an impact on chromatin structure (Rando and Winston, 2012; Venkatesh and Workman, 2015; Zentner and Henikoff, 2013). First, the mean spacing between nucleosomes correlates with transcription frequency (Chereji

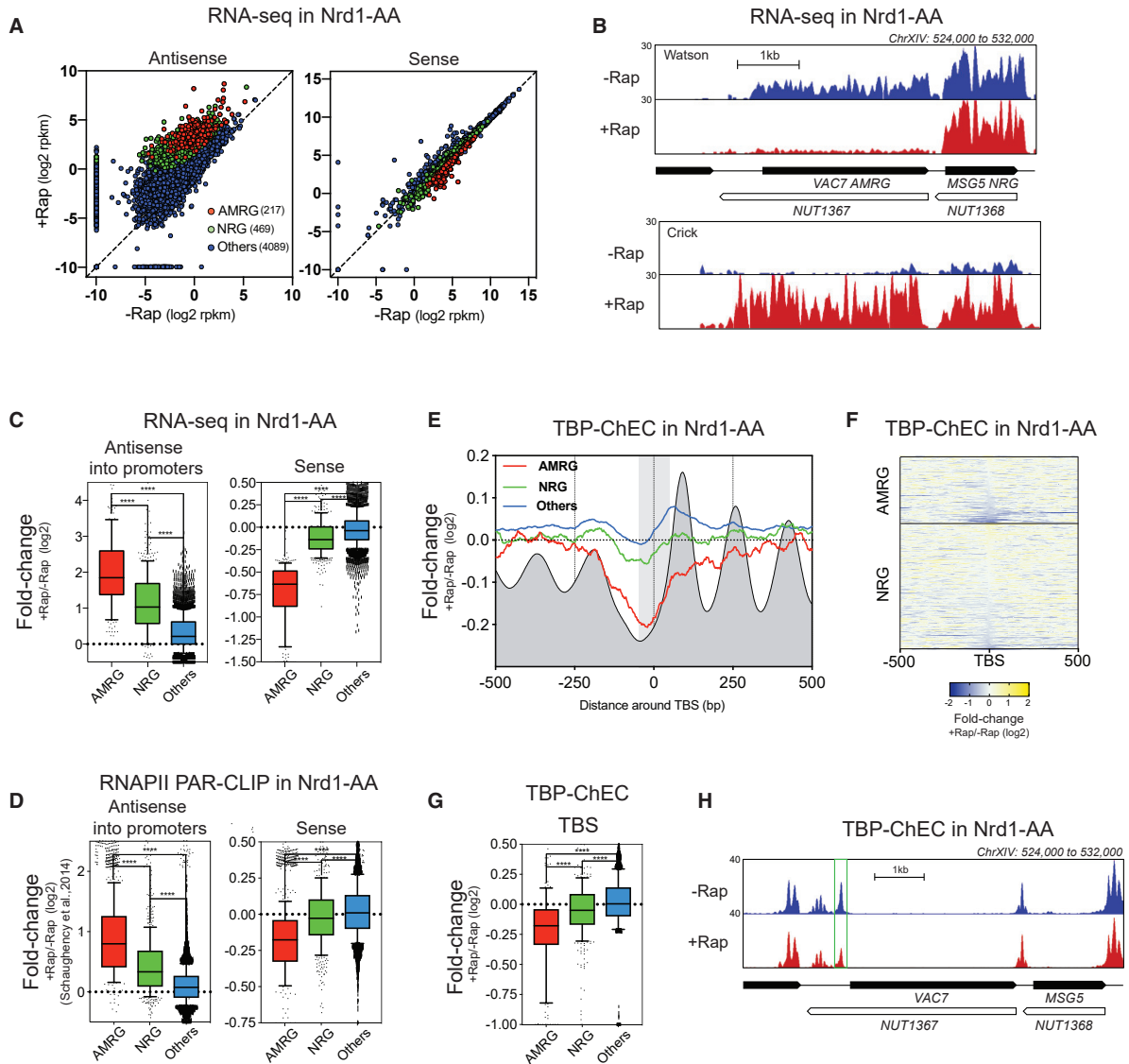


Figure 1. Antisense-Mediated Transcription Interference Decreases PIC Binding

(A) Scatter dot plot of the Nrd1-AA RNA-seq. Nrd1-AA cells were treated or not with rapamycin (Rap) for 1 h before RNA extraction. Results are represented in log₂ of reads per kilobase of transcript per million mapped reads (RPKM) in both antisense and sense orientation. DEseq (Bioconductor) was used to define the different gene classes (see [Method Details](#)).

(B) Snapshot of the Nrd1-AA RNA-seq depicting a locus containing both an AMRG (*VAC7*) and an NRG (*MSG5*). Antisense induction in +Rap leads to the elongation of *NUT1367* noncoding RNA into the *VAC7* promoter and to the subsequent transcription interference of the *VAC7* transcript.

(C) Box-plots showing the (+Rap/–Rap) fold-change for the RNA-seq in the Nrd1-AA strain. Fold-change is calculated based on the coverage in the –100 bp to transcription start site (TSS) region for antisense and over the whole transcript for the sense.

(D) Box plots indicating (+Rap/–Rap) fold-change for the RNAPII PAR-CLIP in an Nrd1-AA strain. Data were adapted from [Schaughency et al. \(2014\)](#). Antisense transcription was measured over the –100 bp to TSS of the paired sense, and sense transcription was examined over 100 bp upstream of the polyA site.

(E) Metagenesis analysis of TBP-ChEC induced for 30 s in an Nrd1-AA strain treated or not with Rap for 1 h. Colored curves represent (+Rap/–Rap) fold-change of the TBP-ChEC for the different classes of genes. The gray profile depicts the position of the nucleosomes as obtained with MNase-seq (see [Figure 2A](#)) for the average gene. The gray box represents the 50-bp area around the TBS over which statistics are generated. The center of the 0- to 120-bp paired-end fragments is represented for the plots and statistical analyses.

(legend continued on next page)

et al., 2018). The more a gene is transcribed, the more the distance between nucleosomes decreases. Second, RNAPII elongation is associated with the concomitant deposition of histone modifications. The carboxy-terminal domain (CTD) of RNAPII interacts with histone methyl transferases (HMTs) catalyzing the transfer of methyl groups to histone H3. Among them, the trimethylation of H3 at lysine 36 (H3K36me3) by Set2 follows a specific pattern over coding genes, being enriched at mid-gene to the end of genes. This modification is a recruitment platform for the Rpd3S histone deacetylase (HDAC) complex, which can deacetylate H3 and H4 histones (Carrozza et al., 2005; Keogh et al., 2005; Rundlett et al., 1996). Accordingly, H3 and H4 acetylations anticorrelate with H3K36me3, being more enriched at -1 and $+1$ nucleosomes flanking the promoter NDRs (Sadeh et al., 2016; Weiner et al., 2015). Deletion of *SET2* or *RPD3* leads to intragenic cryptic transcription, associated with an increase in histone acetylation along gene bodies (Carrozza et al., 2005; Joshi and Struhl, 2005; Kim et al., 2016; Li et al., 2003; Malabat et al., 2015; Venkatesh et al., 2012; Venkatesh and Workman, 2015). Thus, transcription-associated methylation of nucleosomes and subsequent deacetylation can be considered a locking mechanism, limiting spurious transcription initiation events.

Noncoding transcription-mediated transcription interference usually requires RNAPII-dependent nucleosome modifications. The loss of Set2 or HDACs leads to a rescue of coding gene expression when noncoding transcription elongates into promoter NDRs (Camblong et al., 2007; Castelnuovo et al., 2014; du Mee et al., 2018; Kim et al., 2016; Nevers et al., 2018; van Werven et al., 2012). Moreover, the more nascent transcription enters into sense promoters at steady state, the more the NDR becomes narrow (Dai and Dai, 2012; Murray et al., 2015). These data suggest that antisense-mediated transcription interference probably occurs through a nucleosome-based mechanism. Nucleosome positioning at NDRs is crucial for the accessibility of the transcription pre-initiation complex (PIC) to promoters, mainly through the recruitment of the TATA-binding protein (TBP, Spt15 in *S. cerevisiae*) at TATA (or TATA-like)-binding sites (TBSs) (Kubik et al., 2018; Rhee and Pugh, 2012). Genome-wide NDR opening and the subsequent ability to recruit the PIC mainly depends on the RSC (remodeling the structure of chromatin) ATP-dependent chromatin remodeler (Badis et al., 2008; Hartley and Madhani, 2009; Klein-Brill et al., 2019; Kubik et al., 2018).

In this study, we aim at defining a comprehensive mechanism of antisense-mediated transcription interference through a variety of genome-wide approaches. We use a strategy in which antisense noncoding early termination can be turned off, leading to inducible transcription interference of >200 genes. Systematic analyses of transcription initiation, NDR chromatin structure, and transcription-associated histone modifications reveal the choreography of chromatin-related events associated with lncRNA-induced transcription interference. We then validate our model by defining to which extent the *S. cerevisiae* genome is influ-

enced by this chromatin-based transcription interference at steady state.

RESULTS

Induction of Antisense Noncoding Transcription into Paired Sense Promoters Decreases PIC Binding

To investigate the mechanism of transcription interference by antisense noncoding transcription, we defined the list of coding genes that are repressed upon the abrogation of RNAPII early termination. To do so, we performed RNA sequencing (RNA-seq) of the Nrd1-Anchor Away (AA) strain in which Nrd1 can be artificially depleted from the nucleus upon rapamycin (Rap) addition (Figure 1A; Haruki et al., 2008; Schulz et al., 2013). We then classified the genes into 3 categories: (1) the antisense-mediated repressed genes (AMRGs, 217 genes), showing an at least 2-fold increase in antisense and a $>20\%$ sense repression, (2) the nonresponsive genes (NRGs, 469 genes), with a minimum 2-fold increase in antisense but a $<20\%$ decrease in sense expression, and (3) the others (4,089 genes), showing a <2 -fold increase in antisense (Figures 1A and 1B). With these 3 groups, we observed a prominent correlation between the fold increase of antisense levels over the paired sense promoter and the fold decrease in sense transcription, as already described (Figure 1C; Schulz et al., 2013). AMRGs are significantly more repressed than the others, while the NRGs present a mild phenotype. To directly assess nascent transcription, we took advantage of published datasets monitoring RNAPII photoactivatable ribonucleoside-enhanced crosslinking and immunoprecipitation (PAR-CLIP) in an Nrd1-AA strain (Schaughency et al., 2014). The same trend as that obtained with RNA-seq is observed, although with a lower amplitude, supporting the idea that sense repression may occur at the nascent transcription level (Figure 1D; Schaughency et al., 2014). Consistently, we also observed a highly significant overlap between the whole set of genes repressed by $>20\%$ in sense and the genes presenting a >2 -fold increase in antisense upon Nrd1 depletion (Figure S1A), further supporting that the decrease in gene expression may be a direct consequence of paired antisense extension. Of note, the vast majority of antisense lncRNAs extended upon Nrd1-AA appear as full antisense to the paired coding gene (Figure S1B).

Since sense repression may be transcriptional and related to the extension of antisense into the promoters, we investigated whether sense transcription initiation is affected upon antisense induction. To address this question, we performed chromatin-endogenous cleavage (ChEC) of the TBP (Spt15 in *S. cerevisiae*) in the Nrd1-AA strain treated or not with Rap to visualize PIC recruitment (Zentner et al., 2015). With ChEC, we observed the expected distribution of the PIC as peaks around the TBSs (Figure S1C; Rhee and Pugh, 2012). AMRGs present a stronger decrease in PIC binding upon antisense induction as compared to the others, while NRGs again exhibit a milder

(F) Heatmap of (+Rap/−Rap) fold-change of TBP-ChEC for the AMRGs and NRGs from -500 to $+500$ bp around the TBS.

(G) Box plots indicating the (+Rap/−Rap) fold-change of TBP-ChEC in the Nrd1-AA strain as measured 50 bp around the TBS.

(H) Snapshot depicting the AMRG class-coding gene *VAC7* repressed in +Rap by induction of *NUT1367* antisense transcription. The rectangle indicates the PIC involved in *VAC7* transcription.

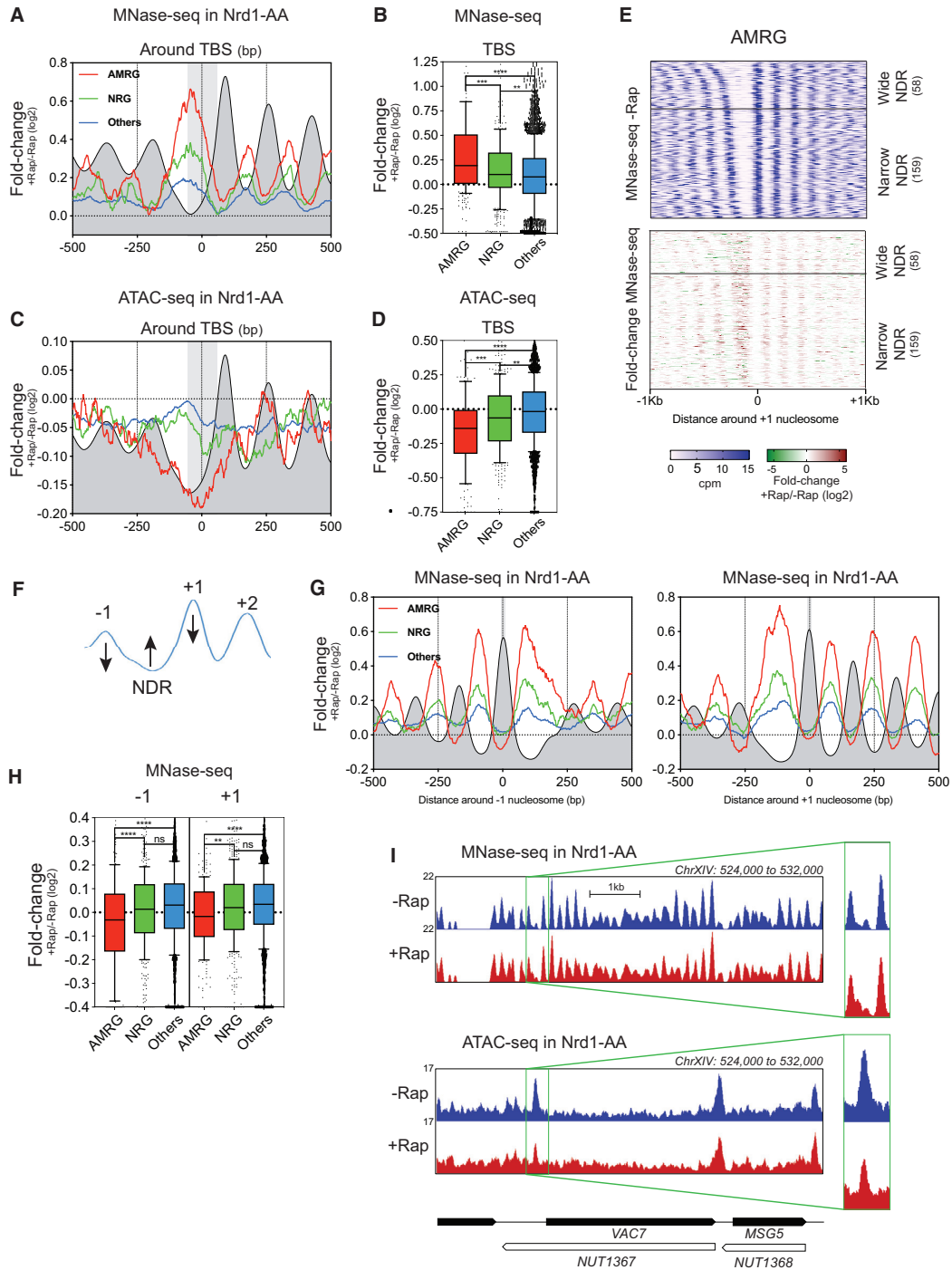


Figure 2. Antisense Induction Leads to Paired Sense Promoter Closing

(A) Metagene analysis of MNase-seq obtained in an Nrd1-AA strain treated or not with Rap for 1 h. Colored curves represent (+Rap/–Rap) fold-change of the MNase-seq for the different classes of genes. The gray profile depicts the position of the nucleosomes as obtained for the average gene. The gray box represents the 50-bp area around the TBS over which statistics are generated. The center of the 120- to 200-bp paired-end fragments is represented for the plots and statistical analyses.

(legend continued on next page)

phenotype (Figures 1E–1H, S1D, and S1E). The almost perfectly overlapping PIC peaks in –Rap/+Rap at the others demonstrate the precision of the measurement and validate the experimental accuracy (Figure S1D).

Hence, as inferred by the lower binding of the PIC at coding gene promoters, sense repression by antisense noncoding transcription occurs at the transcription initiation step.

Antisense Induction into Promoters Increases Nucleosome Occupancy over the TBS through –1/+1 Sliding

As mentioned above, antisense-mediated transcription interference involves a chromatin-based mechanism. An interesting scenario would be that nucleosomes repositioned over promoters upon antisense induction may compete with PIC binding. We investigated this possibility at near-base pair resolution by monitoring nucleosome positioning around TBSs by paired-end micrococcal nuclease sequencing (MNase-seq) upon antisense elongation in +Rap (Figure 2A). To visualize the nucleosomes overlapping with the TBSs, we plotted nucleosome dyads and quantified the occupancy over a 100-bp TBS-centered region. We detected a highly significant increase in nucleosome occupancy at the AMRG TBSs as compared to the NRGs and the others (Figures 2A, 2B, 2I, S2A, and S2B). To rule out the possibility that this measurement may be artifactual due to near-background values, we performed a complementary technique, assay for transposase-accessible chromatin sequencing (ATAC-seq), to convert the “valley” signal into a “peak” signal, making this measurement more accurate. Similar to the MNase-seq, antisense induction into AMRG promoters significantly reduces the accessibility of the NDR (Figures 2C, 2D, and 2I). Even <150-bp NDRs, in which an additional nucleosome cannot fit, demonstrate this increase in nucleosome occupancy, suggesting –1 and/or +1 sliding rather than incorporation of new nucleosomes (Figure 2E).

If –1 and/or +1 nucleosomes were sliding, one would expect a decrease in the occupancy when centering the analysis on their dyads (Figure 2F). This is what we observe for the –1 and +1 of AMRGs upon antisense induction (Figures 2G, 2H, and S2A). This AMRG-specific decrease is subtle in terms of fold-change, but it nicely anticorrelates with the fold increase gained over TBSs. When performing chromatin immunoprecipitation (ChIP) of H3 with sonicated extracts (with ~300-bp resolution) at AMRG promoters, we do not detect any change in H3 content upon antisense induction, justifying the need for near-base pair resolution to visualize antisense-mediated chromatin changes (Figure S2C).

PIC depletion does not lead to –1/+1 sliding at AMRGs (Figures S2D and S2E). This strongly suggests that decreased PIC binding is a consequence of nucleosome repositioning rather than the opposite.

These data show that antisense induction into AMRG promoters leads to the repositioning of a subpopulation of –1/+1 nucleosomes over the TBSs, thereby competing with the recruitment of the PIC. Of note, the increase in nucleosome occupancy at AMRGs is not restricted to the NDRs as it also appears to increase in between +1/+2, +2/+3, and so on (Figures 2G and 2I). Thus, antisense induction leads to not only promoter rearrangement but also phasing changes of the gene body nucleosomal array.

H3K36me3 Absolute Levels Increase over AMRG TBSs upon Antisense Induction

Since H3K36me3 by the Set2 HMT is known to be involved in lncRNA-mediated transcription interference at several individual genes (du Mee et al., 2018; Kim et al., 2016; Nevers et al., 2018; van Werven et al., 2012), we analyzed this modification at nucleosome resolution using MNase-ChIP-seq (Weiner et al., 2015). Upon antisense elongation, we detected an increase in absolute levels of H3K36me3 over TBSs, but not when measuring at –1 and +1 nucleosome dyads (Figures 3A, 3B, 3G, S3A, S3B, and S3E). This increase in H3K36me3 is not biased toward large NDRs, suggesting that this modification corresponds to a *de novo* modification induced by noncoding transcription associated with –1/+1 sliding (Figure 3E). In agreement, H3K36me3 ChIP at individual gene promoters indicates an increase in this modification at AMRGs with longer incubation times in Rap, strengthening the model that antisense elongation into promoters induces *de novo* H3K36me3 deposition (Figure 3F).

Thus, the –1/+1 nucleosome repositioning correlates with the appearance of H3K36me3 over the TBSs induced by antisense transcription, suggesting that newly modified H3K36me3 nucleosomes undergo a sliding event.

H3K18ac Absolute Levels Decrease at –1/+1 AMRG Nucleosomes upon Antisense Induction

HDACs have previously been shown to be involved in antisense-mediated transcription interference (Camblong et al., 2007; Casatenuovo et al., 2013). Hence, we analyzed the H3K18ac modification landscape by MNase-ChIP-seq in the Nrd1-AA strain. In contrast to H3K36me3, H3K18ac absolute levels specifically decrease at –1/+1 nucleosomes but do not change over the TBSs following antisense induction (Figures 3C–3E, 3G, and S3C–S3E).

(B) Box plots indicating the +Rap/–Rap fold-change of dyad occupancy. Statistics are generated in the 50-bp area around the TBS.

(C) Metagene analyses of ATAC-seq in an Nrd1-AA strain treated or not for 1 h with Rap and represented as in (A).

(D) Box plots indicating the +Rap/–Rap fold-change in NDR accessibility as measured with the ATAC-seq. Statistics are generated as in (B).

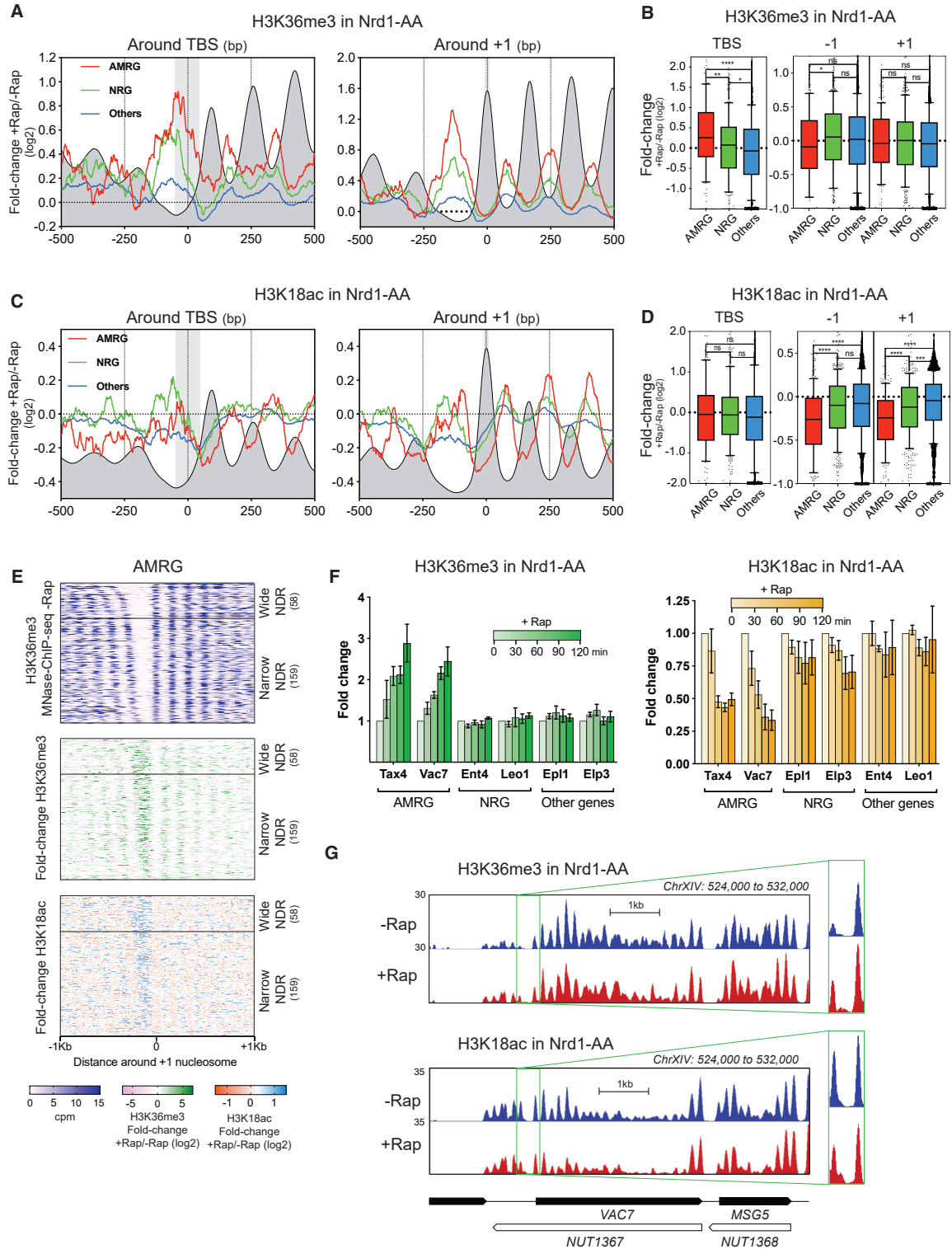
(E) Heatmaps centered on the +1 nucleosome of MNase-seq signal in –Rap (top) and MNase-seq +Rap/–Rap fold-change (bottom) for the AMRG. NDRs were ranked according to their length to discriminate between “wide” NDRs, in which additional nucleosomes can virtually accommodate, and “narrow” NDRs that cannot fit a 150-bp DNA-covered nucleosome.

(F) The gain of nucleosomes around the TBSs through sliding should be accompanied by a –1 and/or +1 decrease in dyad occupancy peaks.

(G) Metagene analysis of MNase-seq as in (A) but centered on the –1 and +1 nucleosomes, respectively. The gray box represents the 10-bp area around –1 and +1 dyad centers in which statistics are generated.

(H) Box plots representing the dyad occupancy (+Rap/–Rap) fold-change in a 10-bp area around the –1 and +1 dyad centers, respectively.

(I) Snapshot of both MNase-seq and ATAC-seq profiles at the AMRG VAC7. The NDR from which VAC7 transcription is initiated is indicated by a rectangle magnified on the right-hand side.



Thus, H3K36me3 and H3K18ac present an opposite pattern of changes. When H3K36me3 levels increase over the TBSs, H3K18ac levels decrease at $-1/+1$ nucleosomes. Since H3K36me3 is a platform to recruit an HDAC and H3K36me3 and H3K18ac are largely anticorrelated, it is tempting to speculate that antisense elongation into promoters may lead to *de novo* H3K36me3 of the $-1/+1$ nucleosomes, triggering deacetylation and subsequent sliding (Carrozza et al., 2005; Keogh et al., 2005; Sadeh et al., 2016; Weiner et al., 2015).

Induced Antisense Transcription Reveals Different Positioning of H3K36me3- and H3K18ac-Containing Nucleosomes

The different behaviors of H3K36me3 and H3K18ac at AMRG NDRs prompt us to propose that H3K36me3- and H3K18ac-containing nucleosomes may be differentially repositioned upon antisense induction and that MNase-seq recapitulates the sum of these changes. We reasoned that since antisense is expressed all along the gene bodies upon Nrd1-AA, the same trend may be observed within the nucleosomal array of gene bodies. We therefore performed a metagene analysis of the nucleosomes $+1$ – $+8$ for the different gene classes using both MNase-seq and H3K36me3 and H3K18ac MNase-ChIP-seq data (Figure 4A). This approach increases the robustness of our measurements since 1,223, 2,981, and 19,899 nucleosomes are taken into account in our analysis for AMRGs, NRGs, and others, respectively. We find that for AMRGs, H3K36me3 levels do not significantly change at the peak but increase upstream and downstream of the peak, while H3K18ac levels decrease at the peak without any change on either side (Figures 4A and 4B). The MNase-seq appears as the sum of these two events since nucleosome occupancy significantly decreases at the peak and increases downstream of the peak.

Thus, our data converge toward a model in which antisense induction leads to *de novo* H3K36me3, associated H3K18 deacetylation, and the subsequent repositioning of nucleosomes (Figure 4C). It implies that H3K18ac-containing nucleosomes may be restricted to the peaks, while H3K36me3-containing nucleosomes may occupy a larger territory by generating several subpopulations: those at the peak that are both H3K36me3

and H3K18ac, and those around the peak that are only H3K36me3. Accordingly, at steady state, H3K36me3 nucleosomes are less well positioned than H3K18ac nucleosomes (Figure 4D).

Decreased RSC Binding at $-1/+1$ AMRG Nucleosomes upon Antisense Induction

Considering the global role of the RSC chromatin remodeler in promoter NDR maintenance (Badis et al., 2008; Hartley and Madhani, 2009; Klein-Brill et al., 2019; Kubik et al., 2018; Yen et al., 2012), we asked whether nucleosome sliding was due to the loss of RSC interaction with the NDR-flanking nucleosomes. This possibility is even more appealing when considering that the RSC complex interacts with acetylated histones *in vitro* through its multiple bromodomains (Chatterjee et al., 2011; Kasten et al., 2004).

Consistently, when the recruitment of the Sth1 catalytic subunit of the RSC complex was examined by ChEC-seq in the Nrd1-AA strain, a specific decrease in RSC interaction with -1 and $+1$ AMRG nucleosomes was detected in the presence of Rap (Figures 5A–5C, S4A, and S4B). RSC recruitment into the NDR of AMRGs shows no significant change when analyses are centered on the TBSs (Figure 5A, left panel). These observations suggest a link between the decreased acetylation of NDR-flanking nucleosomes and the loss of interaction with the essential RSC chromatin remodeler.

Loss of Rpd3 HDAC Partially Rescues Transcription Interference-Associated Phenotypes

If decreased $-1/+1$ acetylation directly affects RSC recruitment, then a mutant in which the deacetylation step is defective may rescue RSC binding. This question was addressed by the deletion of *RPD3* in the Nrd1-AA background. Rpd3 is the HDAC component of the Rpd3S/L complex that maintains H3K18ac levels low in the cell (Rundlett et al., 1996).

We first examined the fold-change in H3K18ac levels by ChIP upon antisense induction at selected AMRG promoters in the presence or absence of Rpd3 (Figure S5A). As expected, upon Rap addition, *RPD3* deletion leads to limited deacetylation of AMRG NDR-flanking nucleosomes as compared to the wild-type (*WT*) strain.

Figure 3. Antisense Elongation into AMRG Promoters Leads to Increased H3K36me3 Absolute Levels around TBS and Decreased H3K18ac Absolute Levels at $-1/+1$ Nucleosomes

- (A) Metagene profiles of H3K36me3 MNase-ChIP-seq centered on TBSs and $+1$ nucleosome dyad centers obtained in an Nrd1-AA strain treated or not for 1 h with Rap. Colored curves represent (+Rap/–Rap) fold-change of the H3K36me3 modification for the different classes of genes. The gray profile depicts the position of H3K36me3 nucleosomes as obtained for the average gene in the absence of Rap. The gray boxes represent the 50-bp area around the TBS and the 10-bp area centered around $+1$ peak over which statistics are generated. The center of the 120- to 200-bp paired-end fragments is represented for the plots and statistical analyses.
- (B) Box plots indicating the +Rap/–Rap fold-change in H3K36me3 levels in the 50-bp area around the TBS and the 10-bp area around $-1/+1$ peaks.
- (C) Metagene profiles as in (A) but for the H3K18ac levels. The gray profile represents the position of H3K18ac nucleosomes for the average gene in the absence of Rap.
- (D) Box plots as in (B) for the H3K18ac modification.
- (E) Heatmaps of H3K36me3 MNase-ChIP-seq signal in –Rap (top) and of H3K36me3 and H3K18ac fold-change centered on the $+1$ nucleosome dyad at AMRG.
- (F) ChIP of H3K36me3 and H3K18ac histone modifications at gene promoters of AMRG, NRG, and other genes. Primers were designed to target each promoter NDR. ChIPs were performed at 0, 30, 60, 90, and 120 min after Rap addition. Immunoprecipitated promoter NDRs were normalized to immunoprecipitated *SPT15* open reading frame (ORF) after qPCR amplification. The fold-change was artificially set to 1 for each gene in the –Rap condition. Error bars represent the standard error of the mean (SEM) for a set of 3 independent experiments.
- (G) Snapshot of H3K36me3 and H3K18ac MNase-ChIP-seq absolute levels at the AMRG *VAC7*. The NDR of *VAC7* is indicated by a rectangle and magnified in the right-hand panels.

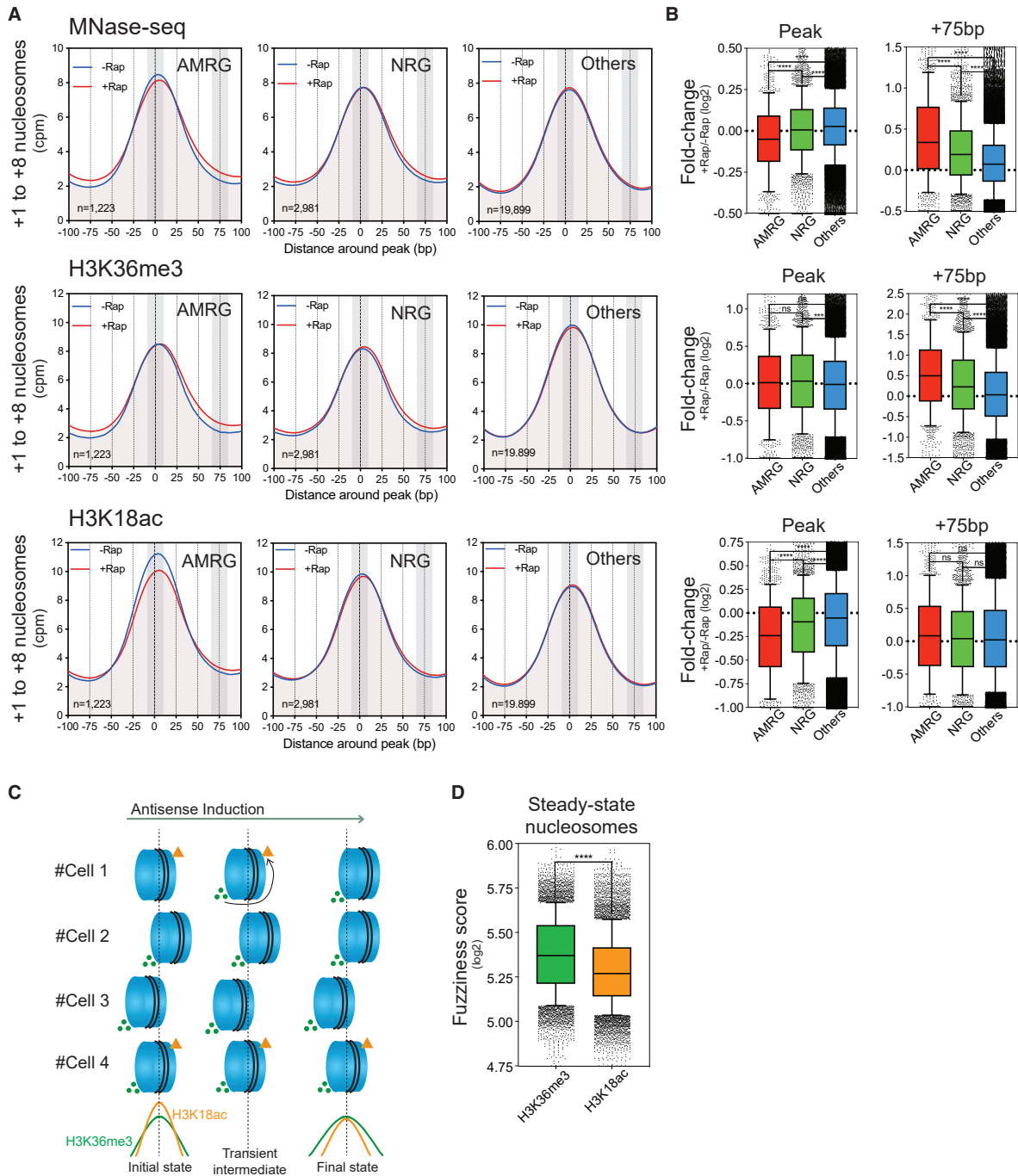


Figure 4. Different Positioning of De Novo H3K36me3- and H3K18ac-Containing Nucleosomes

(A) Metagenes profiles of MNase-seq, H3K36me3, and H3K18ac MNase-ChIP-seq around an average nucleosome peak (+1–+8 nucleosome peaks) upon antisense induction. Nucleosomes were averaged according to the directionality of the sense coding gene. The gray boxes represent the 10-bp area around the nucleosome center and the 10-bp area located at +75 bp, downstream of the nucleosomal peak.

(legend continued on next page)

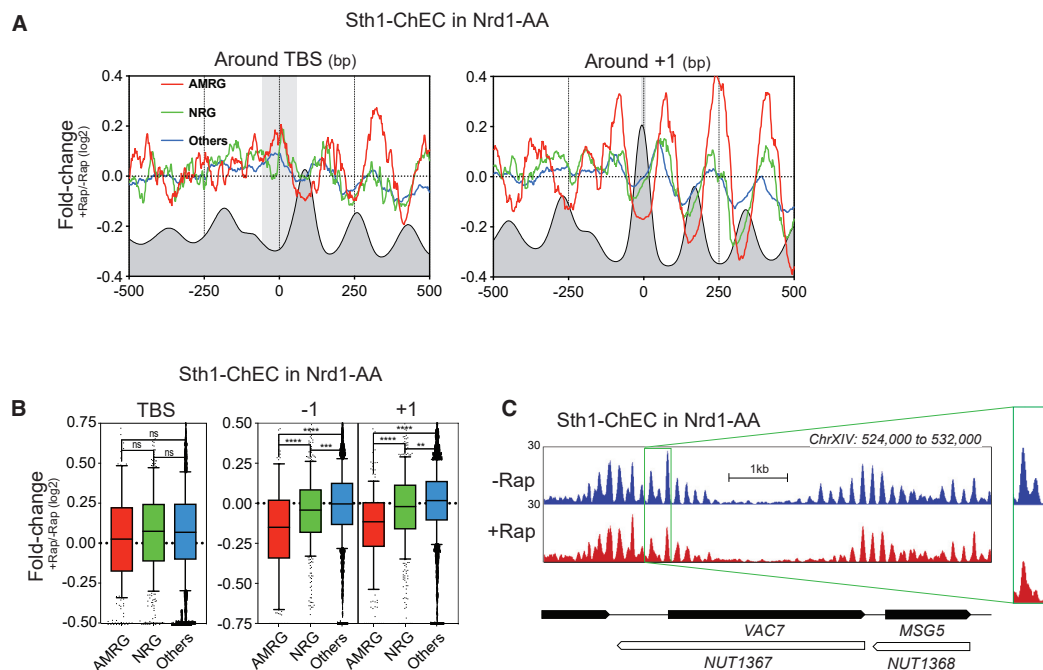


Figure 5. RSC Interaction with $-1/+1$ Nucleosomes Decreases upon Antisense Induction

(A) Metagene profiles of Sth1-ChEC in an Nrd1-AA strain treated or not for 1 h with Rap around the TBS and +1 nucleosome. Colored curves represent (+Rap/ $-$ Rap) fold-change of the Sth1-ChEC for the different classes of genes. The gray profile depicts the position of Sth1-ChEC as obtained for the average gene in the absence of Rap. The gray boxes represent the 50-bp area around the TBS and the 10-bp area around +1 peak area over which statistics are generated. The center of the 120- to 200-bp paired-end fragments is represented for the plots and statistical analyses.

(B) Box plots indicating the (+Rap/ $-$ Rap) fold-change in Sth1-ChEC levels in the 50-bp area around the TBS and the 10-bp area around $-1/+1$ nucleosomal peaks.

(C) Snapshot of Sth1-ChEC levels at the AMRG VAC7. The $-1/+1$ nucleosomes are indicated by a rectangle magnified in the right-hand panel.

We then plotted the +Rap/ $-$ Rap fold-change of RSC binding at the +1 nucleosome, as assayed by Sth1 ChEC-seq (Figures 6A and 6E). When comparing to WT cells, we observed a partial rescue of RSC binding in *rap3Δ* at AMRGs. As RSC is essential for the maintenance of NDR opening (Badis et al., 2008; Hartley and Madhani, 2009; Klein-Brill et al., 2019; Kubik et al., 2018), the increased retention of RSC at AMRG $-1/+1$ nucleosomes in *rap3Δ* may inhibit the nucleosome sliding, as compared to WT cells. As revealed by ATAC-seq, the increase in nucleosome occupancy over the TBS observed in WT cells upon antisense induction is partially abrogated in *rap3Δ* (Figures 6B and 6E). Consequently, the loss of PIC binding and transcription interference at AMRG observed in WT are also alleviated in *rap3Δ* (Figures 6C–6E). The level of antisense accumulation in AMRG is not globally affected in Nrd1-AA *rap3Δ* as compared to Nrd1-AA cells, indicating that the observed rescue is not an indirect effect of decreased antisense transcription (Figure S5B).

Thus, the acetylation level of $-1/+1$ nucleosomes, through its ability to recruit the RSC chromatin remodeler, appears as a cen-

tral regulator of the transcription interference mechanism. Consequently, acetylation influences the accessibility of the PIC to the NDR and hence gene expression.

Model for Antisense-Mediated Transcription Interference in an Inducible System and Its Genome-wide Generalization at Steady-State Condition

Our results suggest the following model (Figure 7A). Under normal conditions ($-$ Rap), noncoding transcription early termination prevents the entry of antisense transcription into the NDRs of promoters, keeping them open and favoring gene expression. When Nrd1 is anchored away, antisense elongation extends into the paired promoter NDR, resulting in H3K36me₃ of the -1 and +1 nucleosomes, which are subsequently deacetylated through a process involving the Rpd3 HDAC. The loss of acetylation leads to decreased RSC recruitment and subsequent sliding of the $-1/+1$ nucleosomes toward the TBSs. These events result in a steric hindrance for PIC binding and, consequently, in gene repression.

(B) Box plots indicating the (+Rap/ $-$ Rap) fold-change in MNase-seq, H3K36me₃, and H3K18ac levels in the 10-bp area around the nucleosomal peak (+1 \rightarrow +8 peaks) and in the 10-bp area located at +75 bp downstream of the nucleosomal peak.

(C) Model recapitulating the observed differences in positioning. Nucleosomes depicted represent the same nucleosome in 4 different cells upon antisense induction.

(D) Fuzziness score of H3K36me₃ and H3K18ac nucleosomes at steady state ($-$ Rap).

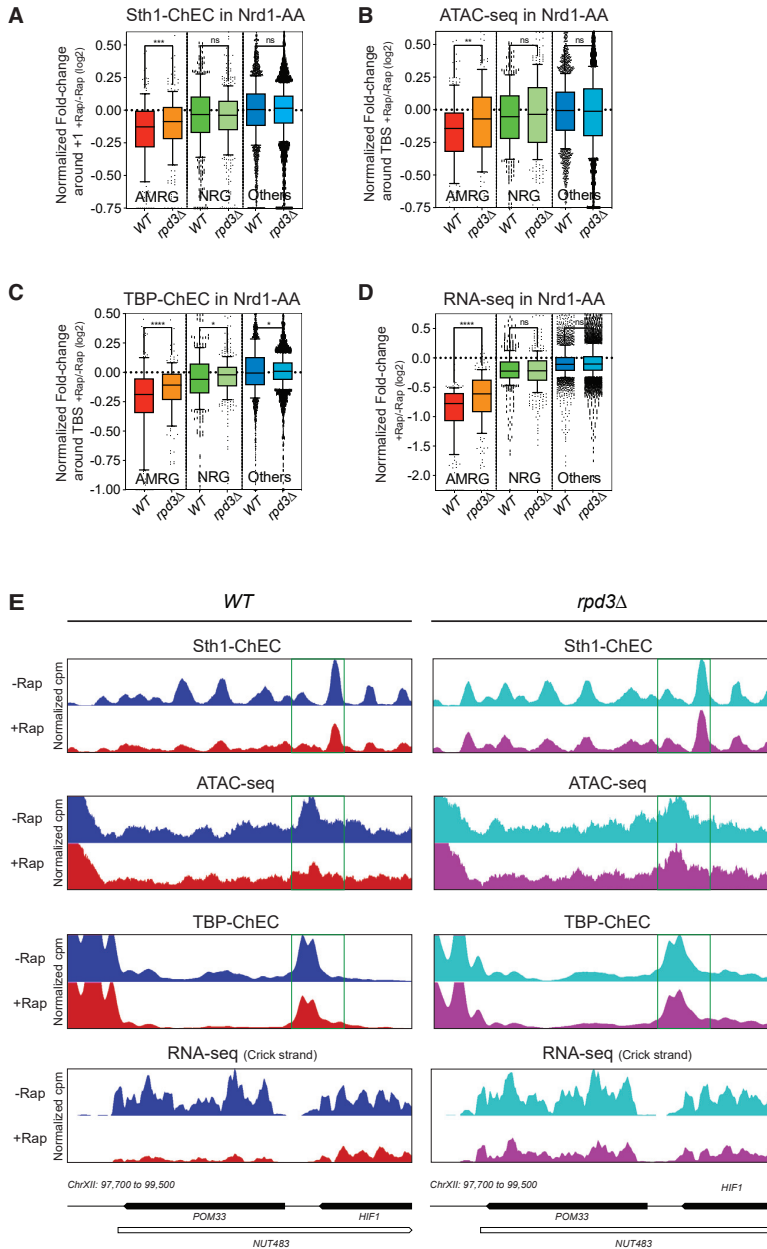


Figure 6. Absence of Rpd3 HDAC Partially Rescues Antisense-Mediated Gene Repression Phenotypes

(A–D) Box plots indicating the normalized (+Rap/–Rap) fold-change for Sth1 ChEC-seq (A), ATAC-seq (B), TBP ChEC-seq (C), and RNA-seq (D) in an Nrd1-AA strain as compared to Nrd1-AA *rpd3Δ* cells. Plots for the Nrd1-AA strain are presented in Figures 1C, 1G, 2D, and 5B, with the exception of the normalized fold-change, the calculation of which is described in Method Details.

(E) Snapshot of Sth1-ChEC, ATAC-seq, TBP-ChEC, and RNA-seq levels at the AMRG *POM33* in the presence or absence of *RPD3*. +Rap condition either in WT or *rpd3Δ* was normalized to the highest value in –Rap within the green rectangles for Sth1-ChEC, ATAC-seq, and TBP-ChEC. RNA-seq levels were normalized to the highest value within the *POM33* transcription unit.

the highest levels of antisense transcription into promoters, are significantly less expressed than the genes of the other quintiles as assessed by RNA-seq and using nascent transcription data (Figures 7B, S6A, and S6B). As predicted by our model, the first quintile shows increased nucleosome occupancy and increased H3K36me3 levels over the TBSs (Figure 7C). Accordingly, the levels of H3K18ac and RSC binding at the +1 nucleosome appear reduced in the first quintile compared to the others (Figure 7D). Consistent with our model, in which H3K36me3-mediated deacetylation of NDR-flanking nucleosomes is involved in natural antisense-mediated transcription interference, the genes upregulated in the absence of Rpd3 HDAC are significantly enriched in the first quintile (Figure 7E). Lastly, we analyzed the sensitivity of the different quintiles to RSC depletion known to induce global NDR shrinkage (Kubik et al., 2018). Analyses of published data show a global increase in nucleosome occupancy over the TBS for all of the quintiles (Figure 7F; Kubik et al., 2018). However, this increase is less important for the genes of the first quintile. Thus, as expected from our model, the genes showing the highest levels of antisense trans-

cription into promoters are less sensitive to RSC depletion because they already present a higher nucleosome occupancy within the NDR at steady-state resulting from the decreased interaction of the NDR-flanking nucleosomes with RSC.

Our model is limited to only 4.5% of the genes in this nonphysiological system to induce antisense elongation. Since antisense transcription can naturally extend into promoter NDRs, depending on the strength of the noncoding transcription early termination process, we investigated whether our chromatin-based transcription interference model could be generalized under steady-state conditions. We ranked the coding genes into five quintiles according to the natural levels of nascent antisense transcription over their promoters (Figure 7B). The genes of the first quintile, presenting

We propose that the chromatin-driven model of antisense-mediated transcription interference defined with a subset of genes in the inducible system can be extended with high significance up to 20% of the genes. These observations support the view that gene regulation through interleaved noncoding

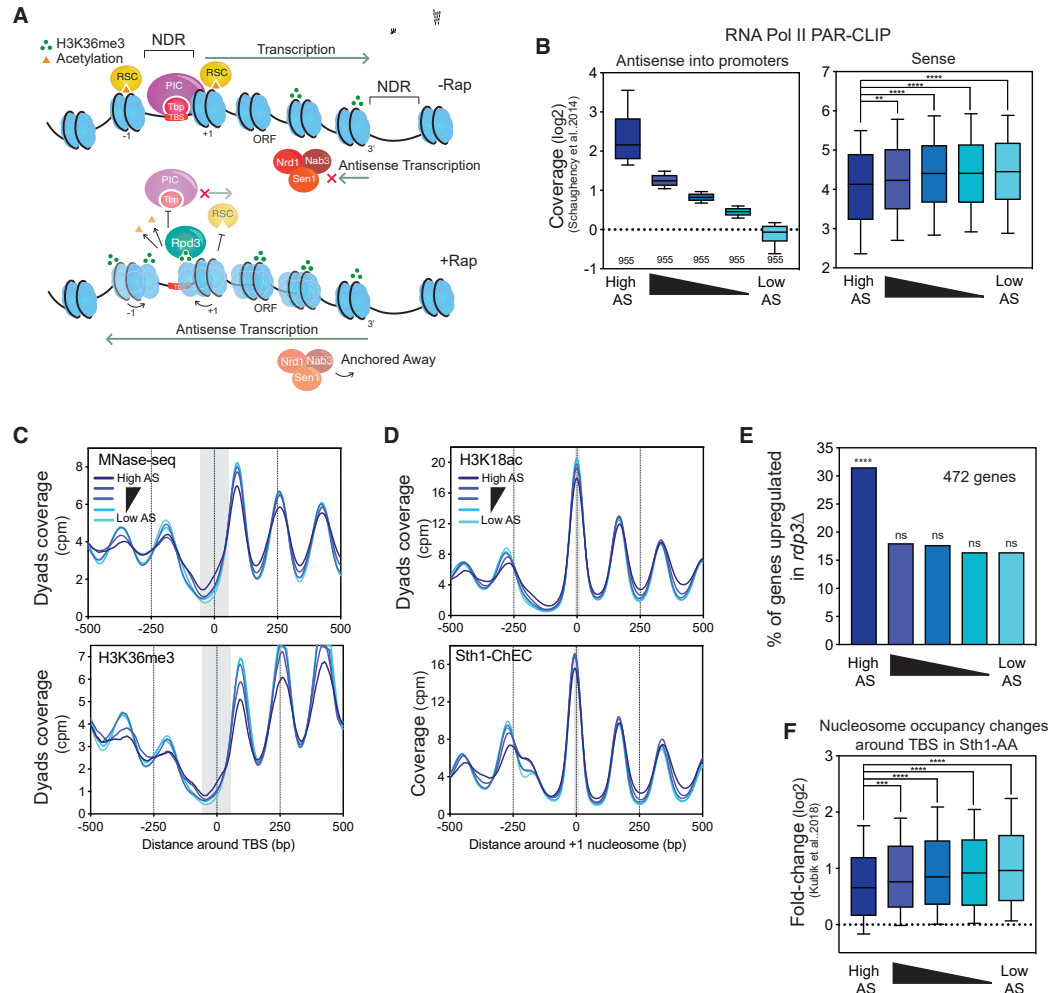


Figure 7. Model of Induced Chromatin-Driven Transcription Interference and Its Generalization in the Steady-State Genome
 (A) Model of antisense-mediated transcription interference through promoter chromatin regulation. For a description of the model, see the Results section.
 (B) Left panel: box plots defining the five quintiles according to their natural level of nascent transcription into gene promoters (–100 bp to TSS area). Each quintile contains 955 genes. RNAPII PAR-CLIP data were taken from Schaughency et al. (2014). Right panel: box plots depicting levels of nascent coding sense transcription in an area of 100 bp upstream of the polyA site.
 (C) Aggregate plot of nucleosome occupancy (top) and H3K36me3 (bottom) levels around the TBS with respect to the different quintiles.
 (D) Metagenome analysis of H3K18ac (top) and RSC binding (bottom) levels around +1 nucleosome according to the different quintiles.
 (E) Percentage of genes from each quintile upregulated in a *rpd3Δ* strain (>2-fold). Significance was defined according to a hypergeometrical test.
 (F) Box plot of nucleosome occupancy fold-change in a 50-bp area around the TBS upon AA of Sth1 for 1 h. Data were retrieved from Kubik et al. (2018).

transcription is a major player in global chromatin shaping of promoters and gene expression in *S. cerevisiae*.

DISCUSSION

A Chromatin-Driven Transcription Interference Model Derived from an Antisense-Inducible System

Based on our results, we propose an antisense-mediated transcription interference mechanism through chromatin regulation (Figure 7A). The rescue of the different molecular phenotypes observed at AMRGs in the absence of the Rpd3 HDAC enables

us to validate such a chromatin-driven model (Figure 6). However, the rescue is only partial and other parameters must be taken into consideration.

Antisense-mediated transcription interference may also implicate other HDACs, as suggested by different earlier reports indicating the involvement of Set3 through recruitment by H3K4me2 or of Hda1 (Camblong et al., 2007; Kim et al., 2016). Another component of transcriptional interference may be the physical eviction of the sense PIC by the RNAPII traveling in antisense direction. However, we believe that this is unlikely since many DNA-binding proteins behave as roadblocking factors in front

of which RNAPII stalls (Candelli et al., 2018; Colin et al., 2014; Mayer et al., 2015). Additional mechanisms such as possible RNAPII collisions (Cinghu et al., 2017; Hobson et al., 2012; Prescott and Proudfoot, 2002) or secondary promoter structures induced by antisense expression such as R-loops (Lim et al., 2017; Mischo et al., 2011; Pefanis et al., 2014) may complete our model of transcription interference and remain to be thoroughly tested.

The fold-change obtained with the antisense inducible system for some of the molecular phenotypes are of low amplitude, albeit highly significant when comparing AMRG to the others. However, we do not expect drastic changes, mainly because AMRGs present relatively high levels of natural antisense transcription into promoters and are consequently already lowly expressed at steady state (Figure S6B). Their chromatin is therefore already partially closed before antisense induction, and Nrd1-AA only results in a subtle additional gain in repressive chromatin or a weak loss of active chromatin (Figures 1, 2, 3, 4, 5, and S6C). If we observe a magnitude of changes from 5%–15% at the chromatin level for the AMRGs (Figures 1, 2, 3, 4, 5), then this ultimately leads to a 40% decrease in mRNA as measured by RNA-seq (Figure 1C). Thus, low-amplitude phenotypes at the chromatin level have important consequences on the cellular RNA content.

Subpopulations of H3K36me3 and H3K18ac Nucleosomes Are Differently Positioned

The induction of antisense into AMRG promoters leads to an increase in nucleosome occupancy over the TBSs, correlating with a loss of occupancy at $-1/+1$ (Figure 2). Concomitantly, a subpopulation of *de novo* H3K36me3 nucleosomes appears over the TBS, while H3K18ac nucleosomes decrease at $-1/+1$ (Figure 3). These considerations are not restricted to AMRG promoters but are applicable to all nucleosomes undergoing forced antisense (Figure 4). These data strongly suggest the existence of subpopulations of H3K36 and H3K18ac nucleosomes that show different positioning.

Based on these observations, we propose a simple model in which the transcription-associated H3K36 methylated nucleosomes prevent transcription initiation while acetylated nucleosomes are pushed aside, allowing PIC binding. Thus, gene expression would depend on the metastable state of the promoter oscillating between a closed and an open conformation. Antisense transcription frequency may promote NDR closing by modulating the *de novo* H3K36me3 levels at NDR-flanking nucleosomes, while histone demethylases, histone exchange, or histone acetyl transferases (HATs) may counteract the shrinkage. Similarly, such nucleosome movements are observed upon gene activation during the metabolic cycle when gene expression is synchronized (Nocetti and Whitehouse, 2016). In agreement with our model, gene expression is maximal when $-1/+1$ nucleosomes are pushed aside in a movement mainly driven by H3K9ac and H3K18ac modifications (Hughes et al., 2012; Nocetti and Whitehouse, 2016; Sánchez-Gaya et al., 2018; Weiner et al., 2010).

We do not detect a shift in the nucleosome peaks themselves upon antisense induction at AMRG (Figure 4A), most likely because we are analyzing regions in which transcription occurs on both strands in the population but is dominated in frequency

by sense transcription. Thus, nucleosome phasing is mainly dictated by sense transcription, and the relative low frequency of antisense production displaces only a subpopulation and not the whole peak. In other words, antisense induction may increase cell-to-cell variability in nucleosome positioning at AMRG promoters and gene bodies within a chromatin structure mainly imposed by sense transcription.

Antisense-Mediated Transcription Interference through Chromatin Regulation as a Widespread Mechanism of Gene Expression Control in *S. cerevisiae*

Our results indicate that the top 20% of the genes showing the highest levels of antisense transcription into promoters are significantly less expressed than the others when taking into account nascent transcription data (Figure 7B). However, in agreement with published observations, the global anticorrelation between sense and antisense transcription is low (Figure S6D; Pearson correlation $r = -0.13$; Brown et al., 2018; Murray et al., 2015). These analyses indicate that noncoding nascent transcription needs to reach a certain absolute level in the promoter NDR to induce transcription interference, as already proposed by Nevers et al. (2018) using RNA-seq data. When this level is reached, transcription into the promoter NDR becomes a dominant parameter, possibly through the chromatin rearrangement mechanism proposed here. Nevertheless, other parameters not considered in our study are likely to be involved, including different promoter sequences or transcription factors, the presence of roadblocking proteins, or the recruitment of chromatin remodelers and histone modifiers.

We show that gene promoters with high levels of natural antisense tend to be more closed as compared to the others, a finding that is in agreement with published data (Dai and Dai, 2012; Murray et al., 2015). However, our results contradict the observation that high levels of antisense into promoters correlate with low levels of H3K36me3 and high levels of histone acetylation at promoters (Brown et al., 2018; Murray et al., 2015). This difference is mainly due to the normalization procedure, as our nucleosome modification data were not normalized to H3 or MNase-seq levels. Considering the shape of the nucleosomal signal along the DNA, normalization in the valley region corresponding to the promoter is more sensitive to the background, increasing the probability of a biased result.

The proposed model mainly considers antisense noncoding transcription; however, a comparable transcription interference mechanism may take place as a result of upstream in tandem noncoding transcription overlapping with a downstream promoter. Based on the described involvement of both nucleosome positioning and H3K36me3 at specific loci (Hainer et al., 2011; Kim et al., 2016; Martens et al., 2004), our model may be relevant to transcription interference by noncoding transcription in a variety of configurations.

Our analyses were performed only in rich medium. Early termination of lncRNA can be regulated in response to growth conditions, leading to different patterns of noncoding transcription elongation (Bresson et al., 2017; van Nues et al., 2017). Thus, a different framework of transcription interference may be expected, depending on external conditions.

It is worth noting that ~100 coding genes are less expressed in mRNA orientation than in lncRNA orientation at the nascent transcription level (data not shown). Thus, in some cases, the mRNA may appear as a spurious transcript undergoing lncRNA-mediated transcription interference. This concept, even if marginal in proportion, perfectly illustrates the plasticity of transcriptional circuits. RNAPII transcription happens all along the genome, and evolution may shape the balance between expression noise and functionality (Struhl, 2007).

A Common Model for All Eukaryotic NDRs?

In *S. cerevisiae*, NDRs are also regions where replication initiates, mainly through the accessibility of the origin recognition complex (ORC) to the autonomously replicating sequence (ARS) consensus sequence (ACS) (Lai and Pugh, 2017). We recently showed that noncoding transcription entering into an ARS NDR is able to influence replication initiation by closing the NDR through increased nucleosome occupancy, as well as elevated H3K36me3 and decreased H3K18ac (Soudet et al., 2018). Replication defects induced by noncoding transcription readthrough into ARS NDR can be partially rescued in the absence of Set2. Although we did not have a precise mechanism in our previous study, the similarity between these earlier observations and the present ones tend to converge in a unique model that may be applicable to all types of NDRs (Soudet and Stutz, 2019).

In higher eukaryotes, several antisense lncRNAs are already described as being regulators of gene expression through chromatin-mediated regulation (Gil and Ulitsky, 2020; Wu et al., 2020). In mammalian cells, replication mainly initiates within gene promoters (Chen et al., 2019; Miotto et al., 2016). Replication initiation efficiency nicely correlates with transcription initiation strength, which itself correlates with the accessibility of the NDR (Brown et al., 2018; Chen et al., 2019). Similar to yeast cells, high levels of antisense lncRNAs over promoter NDRs correlate with a transcription interference phenotype and a closed NDR conformation (Brown et al., 2018; Chen et al., 2016). Together, these observations suggest that noncoding transcription readthrough into NDRs may be a neglected parameter regulating both replication initiation and gene expression in mammalian cells through a chromatin-driven mechanism. It would therefore also be of interest to analyze the consequences of noncoding transcription readthrough on the chromatin structure of enhancers that also correspond to NDRs. High-resolution maps of nucleosomes and histone modifications will reveal whether the proposed chromatin-driven model can be extended to mammalian cells.

STAR★METHODS

Detailed methods are provided in the online version of this paper and include the following:

- KEY RESOURCES TABLE
- RESOURCE AVAILABILITY
 - Lead Contact
 - Materials Availability
 - Data and Code Availability

- EXPERIMENTAL MODEL AND SUBJECT DETAILS
- METHOD DETAILS
 - RNA extraction and RNA-seq
 - MNase(-ChIP)-seq
 - ChEC-seq
 - ATAC-seq
 - ChIP-qPCR
- QUANTIFICATION AND STATISTICAL ANALYSIS
 - List of genes, TBS and nucleosomes
 - RNA-seq analysis
 - MNase(-ChIP)-seq mapping
 - ChEC-seq and ATAC-seq mapping
 - Metagene analyses
 - Statistical analyses

SUPPLEMENTAL INFORMATION

Supplemental Information can be found online at <https://doi.org/10.1016/j.celrep.2020.107612>.

ACKNOWLEDGMENTS

We thank Guillaume Canal, Charlie Rochat, Florian Steiner, Michel Strubin, and all of the members of the Stutz laboratory for critical reading of the manuscript, comments, and discussions. We thank Mylene Docquier and the iGE3 genomics platform of the University of Geneva for performing all of the deep sequencing. This work was supported by funds from the Swiss National Science Foundation (grants 31003A_153331 and 31003A_182344 to F.S.), iGE3, and the Canton of Geneva.

AUTHOR CONTRIBUTIONS

J.K.G., A.M., V.G.-M., and J.S. performed the experiments. J.K.G., F.S., and J.S. analyzed the data and F.S. and J.S. conceived and supervised the study. J.K.G., F.S., and J.S. interpreted the data. J.S. wrote the manuscript with input from all of the authors.

DECLARATION OF INTERESTS

The authors declare no competing interests.

Received: October 29, 2019

Revised: March 12, 2020

Accepted: April 14, 2020

Published: May 5, 2020

REFERENCES

- Afgan, E., Baker, D., Batut, B., van den Beek, M., Bouvier, D., Cech, M., Chilton, J., Clements, D., Coraor, N., Grüning, B.A., et al. (2018). The Galaxy platform for accessible, reproducible and collaborative biomedical analyses: 2018 update. *Nucleic Acids Res.* 46 (W1), W537–W544.
- Badis, G., Chan, E.T., van Bakel, H., Pena-Castillo, L., Tillo, D., Tsui, K., Carlson, C.D., Gossett, A.J., Hasinoff, M.J., Warren, C.L., et al. (2008). A library of yeast transcription factor motifs reveals a widespread function for Rsc3 in targeting nucleosome exclusion at promoters. *Mol. Cell* 32, 878–887.
- Brahma, S., and Henikoff, S. (2019). RSC-Associated Subnucleosomes Define MNase-Sensitive Promoters in Yeast. *Mol. Cell* 73, 238–249.e3.
- Bresson, S., Tuck, A., Staneva, D., and Tollervey, D. (2017). Nuclear RNA Decay Pathways Aid Rapid Remodeling of Gene Expression in Yeast. *Mol. Cell* 65, 787–800.e5.
- Brown, T., Howe, F.S., Murray, S.C., Wouters, M., Lorenz, P., Seward, E., Rata, S., Angel, A., and Mellor, J. (2018). Antisense transcription-dependent

- chromatin signature modulates sense transcript dynamics. *Mol. Syst. Biol.* **14**, e8007.
- Camblong, J., Iglesias, N., Fickentscher, C., Dieppois, G., and Stutz, F. (2007). Antisense RNA stabilization induces transcriptional gene silencing via histone deacetylation in *S. cerevisiae*. *Cell* **131**, 706–717.
- Candelli, T., Challal, D., Briand, J.B., Boulay, J., Porrua, O., Colin, J., and Libri, D. (2018). High-resolution transcription maps reveal the widespread impact of roadblock termination in yeast. *EMBO J.* **37**, e97490.
- Carrozza, M.J., Li, B., Florens, L., Suganuma, T., Swanson, S.K., Lee, K.K., Shia, W.J., Anderson, S., Yates, J., Washburn, M.P., and Workman, J.L. (2005). Histone H3 methylation by Set2 directs deacetylation of coding regions by Rpd3S to suppress spurious intragenic transcription. *Cell* **123**, 581–592.
- Castelnuovo, M., Rahman, S., Guffanti, E., Infantino, V., Stutz, F., and Zenklusen, D. (2013). Bimodal expression of PHO84 is modulated by early termination of antisense transcription. *Nat. Struct. Mol. Biol.* **20**, 851–858.
- Castelnuovo, M., Zaugg, J.B., Guffanti, E., Maffioletti, A., Camblong, J., Xu, Z., Clauder-Münster, S., Steinmetz, L.M., Luscombe, N.M., and Stutz, F. (2014). Role of histone modifications and early termination in pervasive transcription and antisense-mediated gene silencing in yeast. *Nucleic Acids Res.* **42**, 4348–4362.
- Chatterjee, N., Sinha, D., Lemma-Dechassa, M., Tan, S., Shogren-Knaak, M.A., and Bartholomew, B. (2011). Histone H3 tail acetylation modulates ATP-dependent remodeling through multiple mechanisms. *Nucleic Acids Res.* **39**, 8378–8391.
- Chen, K., Xi, Y., Pan, X., Li, Z., Kaestner, K., Tyler, J., Dent, S., He, X., and Li, W. (2013). DANPOS: dynamic analysis of nucleosome position and occupancy by sequencing. *Genome Res.* **23**, 341–351.
- Chen, Y., Pai, A.A., Herudek, J., Lubas, M., Meola, N., Järvelin, A.I., Andersson, R., Pelechano, V., Steinmetz, L.M., Jensen, T.H., and Sandelin, A. (2016). Principles for RNA metabolism and alternative transcription initiation within closely spaced promoters. *Nat. Genet.* **48**, 984–994.
- Chen, Y.H., Keegan, S., Kahli, M., Tonzi, P., Fenyő, D., Huang, T.T., and Smith, D.J. (2019). Transcription shapes DNA replication initiation and termination in human cells. *Nat. Struct. Mol. Biol.* **26**, 67–77.
- Cheraji, R.V., Ramachandran, S., Bryson, T.D., and Henikoff, S. (2018). Precise genome-wide mapping of single nucleosomes and linkers in vivo. *Genome Biol.* **19**, 19.
- Churchman, L.S., and Weissman, J.S. (2011). Nascent transcript sequencing visualizes transcription at nucleotide resolution. *Nature* **469**, 368–373.
- Cinghu, S., Yang, P., Kosak, J.P., Conway, A.E., Kumar, D., Oldfield, A.J., Adelman, K., and Jothi, R. (2017). Intragenic Enhancers Attenuate Host Gene Expression. *Mol. Cell* **68**, 104–117.e6.
- Colin, J., Candelli, T., Porrua, O., Boulay, J., Zhu, C., Lacroute, F., Steinmetz, L.M., and Libri, D. (2014). Roadblock termination by reb1p restricts cryptic and readthrough transcription. *Mol. Cell* **56**, 667–680.
- Core, L.J., Waterfall, J.J., and Lis, J.T. (2008). Nascent RNA sequencing reveals widespread pausing and divergent initiation at human promoters. *Science* **322**, 1845–1848.
- Dai, Z., and Dai, X. (2012). Antisense transcription is coupled to nucleosome occupancy in sense promoters. *Bioinformatics* **28**, 2719–2723.
- Djebali, S., Davis, C.A., Merkel, A., Dobin, A., Lassmann, T., Mortazavi, A., Tanzer, A., Lagarde, J., Lin, W., Schlesinger, F., et al. (2012). Landscape of transcription in human cells. *Nature* **489**, 101–108.
- du Mee, D.J.M., Ivanov, M., Parker, J.P., Buratowski, S., and Marquardt, S. (2018). Efficient termination of nuclear lncRNA transcription promotes mitochondrial genome maintenance. *eLife* **7**, e31989.
- Gil, N., and Ulitsky, I. (2020). Regulation of gene expression by cis-acting long non-coding RNAs. *Nat. Rev. Genet.* **21**, 102–117.
- Hainer, S.J., Pruneski, J.A., Mitchell, R.D., Monteverde, R.M., and Martens, J.A. (2011). Intergenic transcription causes repression by directing nucleosome assembly. *Genes Dev.* **25**, 29–40.
- Hartley, P.D., and Madhani, H.D. (2009). Mechanisms that specify promoter nucleosome location and identity. *Cell* **137**, 445–458.
- Haruki, H., Nishikawa, J., and Laemmli, U.K. (2008). The anchor-away technique: rapid, conditional establishment of yeast mutant phenotypes. *Mol. Cell* **31**, 925–932.
- Hobson, D.J., Wei, W., Steinmetz, L.M., and Svejstrup, J.Q. (2012). RNA polymerase II collision interrupts convergent transcription. *Mol. Cell* **48**, 365–374.
- Hughes, A.L., Jin, Y., Rando, O.J., and Struhl, K. (2012). A functional evolutionary approach to identify determinants of nucleosome positioning: a unifying model for establishing the genome-wide pattern. *Mol. Cell* **48**, 5–15.
- Jensen, T.H., Jacquier, A., and Libri, D. (2013). Dealing with pervasive transcription. *Mol. Cell* **52**, 473–484.
- Joshi, A.A., and Struhl, K. (2005). Eaf3 chromodomain interaction with methylated H3-K36 links histone deacetylation to Pol II elongation. *Mol. Cell* **20**, 971–978.
- Kaikkonen, M.U., and Adelman, K. (2018). Emerging Roles of Non-Coding RNA Transcription. *Trends Biochem. Sci.* **43**, 654–667.
- Kasten, M., Szerlong, H., Erdjument-Bromage, H., Tempst, P., Werner, M., and Cairns, B.R. (2004). Tandem bromodomains in the chromatin remodeler RSC recognize acetylated histone H3 Lys14. *EMBO J.* **23**, 1348–1359.
- Keogh, M.C., Kurdistani, S.K., Morris, S.A., Ahn, S.H., Podolny, V., Collins, S.R., Schuldiner, M., Chin, K., Punna, T., Thompson, N.J., et al. (2005). Cotranscriptional set2 methylation of histone H3 lysine 36 recruits a repressive Rpd3 complex. *Cell* **123**, 593–605.
- Kim, J.H., Lee, B.B., Oh, Y.M., Zhu, C., Steinmetz, L.M., Lee, Y., Kim, W.K., Lee, S.B., Buratowski, S., and Kim, T. (2016). Modulation of mRNA and lncRNA expression dynamics by the Set2-Rpd3S pathway. *Nat. Commun.* **7**, 13534.
- Klein-Brill, A., Joseph-Strauss, D., Appleboim, A., and Friedman, N. (2019). Dynamics of Chromatin and Transcription during Transient Depletion of the RSC Chromatin Remodeling Complex. *Cell Rep.* **26**, 279–292.e5.
- Kubik, S., Bruzzone, M.J., Jacquet, P., Falcone, J.L., Rougemont, J., and Shore, D. (2015). Nucleosome Stability Distinguishes Two Different Promoter Types at All Protein-Coding Genes in Yeast. *Mol. Cell* **60**, 422–434.
- Kubik, S., O'Duibhir, E., de Jonge, W.J., Mattarocci, S., Albert, B., Falcone, J.L., Bruzzone, M.J., Holstege, F.C.P., and Shore, D. (2018). Sequence-Directed Action of RSC Remodeler and General Regulatory Factors Modulates +1 Nucleosome Position to Facilitate Transcription. *Mol. Cell* **71**, 89–102.e5.
- Kuras, L., and Struhl, K. (1999). Binding of TBP to promoters in vivo is stimulated by activators and requires Pol II holoenzyme. *Nature* **399**, 609–613.
- Lai, W.K.M., and Pugh, B.F. (2017). Understanding nucleosome dynamics and their links to gene expression and DNA replication. *Nat. Rev. Mol. Cell Biol.* **18**, 548–562.
- Langmead, B., and Salzberg, S.L. (2012). Fast gapped-read alignment with Bowtie 2. *Nat. Methods* **9**, 357–359.
- Li, B., Howe, L., Anderson, S., Yates, J.R., 3rd, and Workman, J.L. (2003). The Set2 histone methyltransferase functions through the phosphorylated carboxyl-terminal domain of RNA polymerase II. *J. Biol. Chem.* **278**, 8897–8903.
- Lim, J., Giri, P.K., Kazadi, D., Laffleur, B., Zhang, W., Grinstein, V., Pefanis, E., Brown, L.M., Ladewig, E., Martin, O., et al. (2017). Nuclear Proximity of Mtr4 to RNA Exosome Restricts DNA Mutational Asymmetry. *Cell* **169**, 523–537.e15.
- Malabat, C., Feuerbach, F., Ma, L., Saveanu, C., and Jacquier, A. (2015). Quality control of transcription start site selection by nonsense-mediated-mRNA decay. *eLife* **4**. <https://doi.org/10.7554/eLife.06722>.
- Martens, J.A., Laprade, L., and Winston, F. (2004). Intergenic transcription is required to repress the *Saccharomyces cerevisiae* SER3 gene. *Nature* **429**, 571–574.
- Mayer, A., di Iulio, J., Maleri, S., Eser, U., Vierstra, J., Reynolds, A., Sandstrom, R., Stamatoyannopoulos, J.A., and Churchman, L.S. (2015). Native elongating transcript sequencing reveals human transcriptional activity at nucleotide resolution. *Cell* **161**, 541–554.

- Mellor, J., Woloszczuk, R., and Howe, F.S. (2016). The Interleaved Genome. *Trends Genet.* *32*, 57–71.
- Miotto, B., Ji, Z., and Struhl, K. (2016). Selectivity of ORC binding sites and the relation to replication timing, fragile sites, and deletions in cancers. *Proc. Natl. Acad. Sci. USA* *113*, E4810–E4819.
- Mischo, H.E., Gómez-González, B., Grzechnik, P., Rondón, A.G., Wei, W., Steinmetz, L., Aguilera, A., and Proudfoot, N.J. (2011). Yeast Sen1 helicase protects the genome from transcription-associated instability. *Mol. Cell* *41*, 21–32.
- Murray, S.C., Haenni, S., Howe, F.S., Fischl, H., Chocian, K., Nair, A., and Mellor, J. (2015). Sense and antisense transcription are associated with distinct chromatin architectures across genes. *Nucleic Acids Res.* *43*, 7823–7837.
- Neil, H., Malabat, C., d'Aubenton-Carafa, Y., Xu, Z., Steinmetz, L.M., and Jacquier, A. (2009). Widespread bidirectional promoters are the major source of cryptic transcripts in yeast. *Nature* *457*, 1038–1042.
- Nevers, A., Doyen, A., Malabat, C., Néron, B., Kergrohen, T., Jacquier, A., and Badis, G. (2018). Antisense transcriptional interference mediates condition-specific gene repression in budding yeast. *Nucleic Acids Res.* *46*, 6009–6025.
- Nocetti, N., and Whitehouse, I. (2016). Nucleosome repositioning underlies dynamic gene expression. *Genes Dev.* *30*, 660–672.
- Nojima, T., Gomes, T., Grosso, A.R.F., Kimura, H., Dye, M.J., Dhir, S., Carmo-Fonseca, M., and Proudfoot, N.J. (2015). Mammalian NET-Seq Reveals Genome-wide Nascent Transcription Coupled to RNA Processing. *Cell* *161*, 526–540.
- Pefanis, E., Wang, J., Rothschild, G., Lim, J., Chao, J., Rabadan, R., Economides, A.N., and Basu, U. (2014). Noncoding RNA transcription targets AID to divergently transcribed loci in B cells. *Nature* *514*, 389–393.
- Porrua, O., and Libri, D. (2015). Transcription termination and the control of the transcriptome: why, where and how to stop. *Nat. Rev. Mol. Cell Biol.* *16*, 190–202.
- Prescott, E.M., and Proudfoot, N.J. (2002). Transcriptional collision between convergent genes in budding yeast. *Proc. Natl. Acad. Sci. USA* *99*, 8796–8801.
- Proudfoot, N.J. (1986). Transcriptional interference and termination between duplicated alpha-globin gene constructs suggests a novel mechanism for gene regulation. *Nature* *322*, 562–565.
- Ramírez, F., Ryan, D.P., Grüning, B., Bhardwaj, V., Kilpert, F., Richter, A.S., Heyne, S., Dündar, F., and Manke, T. (2016). deepTools2: a next generation web server for deep-sequencing data analysis. *Nucleic Acids Res.* *44* (W1), W160–W165.
- Rando, O.J., and Winston, F. (2012). Chromatin and transcription in yeast. *Genetics* *190*, 351–387.
- Rhee, H.S., and Pugh, B.F. (2012). Genome-wide structure and organization of eukaryotic pre-initiation complexes. *Nature* *483*, 295–301.
- Rundlett, S.E., Carmen, A.A., Kobayashi, R., Bavykin, S., Turner, B.M., and Grunstein, M. (1996). HDA1 and RPD3 are members of distinct yeast histone deacetylase complexes that regulate silencing and transcription. *Proc. Natl. Acad. Sci. USA* *93*, 14503–14508.
- Sadeh, R., Launer-Wachs, R., Wandel, H., Rahat, A., and Friedman, N. (2016). Elucidating Combinatorial Chromatin States at Single-Nucleosome Resolution. *Mol. Cell* *63*, 1080–1088.
- Sánchez-Gaya, V., Casani-Galdón, S., Ugidos, M., Kuang, Z., Mellor, J., Conesa, A., and Tarazona, S. (2018). Elucidating the Role of Chromatin State and Transcription Factors on the Regulation of the Yeast Metabolic Cycle: A Multi-Omic Integrative Approach. *Front. Genet.* *9*, 578.
- Schaughency, P., Merran, J., and Corden, J.L. (2014). Genome-wide mapping of yeast RNA polymerase II termination. *PLoS Genet.* *10*, e1004632.
- Schep, A.N., Buenrostro, J.D., Denny, S.K., Schwartz, K., Sherlock, G., and Greenleaf, W.J. (2015). Structured nucleosome fingerprints enable high-resolution mapping of chromatin architecture within regulatory regions. *Genome Res.* *25*, 1757–1770.
- Schulz, D., Schwalb, B., Kiesel, A., Baejen, C., Torkler, P., Gagneur, J., Soeding, J., and Cramer, P. (2013). Transcriptome surveillance by selective termination of noncoding RNA synthesis. *Cell* *155*, 1075–1087.
- Soudet, J., and Stutz, F. (2019). Regulation of Gene Expression and Replication Initiation by Non-Coding Transcription: A Model Based on Reshaping Nucleosome-Depleted Regions: Influence of Pervasive Transcription on Chromatin Structure. *BioEssays* *41*, e1900043.
- Soudet, J., Gill, J.K., and Stutz, F. (2018). Noncoding transcription influences the replication initiation program through chromatin regulation. *Genome Res.* *28*, 1882–1893.
- Struhl, K. (2007). Transcriptional noise and the fidelity of initiation by RNA polymerase II. *Nat. Struct. Mol. Biol.* *14*, 103–105.
- Tramantano, M., Sun, L., Au, C., Labuz, D., Liu, Z., Chou, M., Shen, C., and Luk, E. (2016). Constitutive turnover of histone H2A.Z at yeast promoters requires the preinitiation complex. *eLife* *5*, e14243.
- van Nues, R., Schweikert, G., de Leau, E., Selega, A., Langford, A., Franklin, R., Iosub, I., Wadsworth, P., Sanguinetti, G., and Granneman, S. (2017). Kinetic CRAC uncovers a role for Nab3 in determining gene expression profiles during stress. *Nat. Commun.* *8*, 12.
- van Werven, F.J., Neuert, G., Hendrick, N., Lardenois, A., Buratowski, S., van Oudenaarden, A., Primig, M., and Amon, A. (2012). Transcription of two long noncoding RNAs mediates mating-type control of gametogenesis in budding yeast. *Cell* *150*, 1170–1181.
- Venkatesh, S., and Workman, J.L. (2015). Histone exchange, chromatin structure and the regulation of transcription. *Nat. Rev. Mol. Cell Biol.* *16*, 178–189.
- Venkatesh, S., Smolle, M., Li, H., Gogol, M.M., Saint, M., Kumar, S., Natarajan, K., and Workman, J.L. (2012). Set2 methylation of histone H3 lysine 36 suppresses histone exchange on transcribed genes. *Nature* *489*, 452–455.
- Weiner, A., Hughes, A., Yassour, M., Rando, O.J., and Friedman, N. (2010). High-resolution nucleosome mapping reveals transcription-dependent promoter packaging. *Genome Res.* *20*, 90–100.
- Weiner, A., Hsieh, T.H., Appleboim, A., Chen, H.V., Rahat, A., Amit, I., Rando, O.J., and Friedman, N. (2015). High-resolution chromatin dynamics during a yeast stress response. *Mol. Cell* *58*, 371–386.
- Wery, M., Gautier, C., Describes, M., Yoda, M., Vennin-Rendos, H., Migeot, V., Gautheret, D., Hermand, D., and Morillon, A. (2018). Native elongating transcript sequencing reveals global anti-correlation between sense and antisense nascent transcription in fission yeast. *RNA* *24*, 196–208.
- Wu, Z., Fang, X., Zhu, D., and Dean, C. (2020). Autonomous Pathway: FLOWERING LOCUS C Repression through an Antisense-Mediated Chromatin-Silencing Mechanism. *Plant Physiol.* *182*, 27–37.
- Xu, Z., Wei, W., Gagneur, J., Perocchi, F., Clauder-Münster, S., Camblong, J., Guffanti, E., Stutz, F., Huber, W., and Steinmetz, L.M. (2009). Bidirectional promoters generate pervasive transcription in yeast. *Nature* *457*, 1033–1037.
- Yen, K., Vinayachandran, V., Batta, K., Koerber, R.T., and Pugh, B.F. (2012). Genome-wide nucleosome specificity and directionality of chromatin remodelers. *Cell* *149*, 1461–1473.
- Zentner, G.E., and Henikoff, S. (2013). Regulation of nucleosome dynamics by histone modifications. *Nat. Struct. Mol. Biol.* *20*, 259–266.
- Zentner, G.E., Kasinathan, S., Xin, B., Rohs, R., and Henikoff, S. (2015). ChEC-seq kinetics discriminates transcription factor binding sites by DNA sequence and shape in vivo. *Nat. Commun.* *6*, 8733.

STAR★METHODS

KEY RESOURCES TABLE

REAGENT or RESOURCE	SOURCE	IDENTIFIER
Antibodies		
Anti-H3K18ac	Abcam	ab1191; RRID:AB_298692
Anti-H4ac	Merck Millipore	06-598; RRID:AB_2295074
Anti-H3K36me3	Abcam	ab9050; RRID:AB_306966
Chemicals, Peptides and Recombinant Proteins		
Micrococcal Nuclease	Thermo Scientific	88216
Critical Commercial Assays		
TD Buffer	Illumina	#15027866
TDE1 enzyme	Illumina	#15027865
Nextera Index Kit	Illumina	#FC-121-1011
NEBnext Ultra II DNA Library preparation kit	NEB	E7645
Deposited Data		
Raw and analyzed data	This paper	GEO: GSE130946
RNAPII PAR-CLIP in Nrd1-AA	(Schaughency et al., 2014)	GEO: GSE56435
MNase-seq in Sth1-AA	(Kubik et al., 2018)	GEO: GSE98260
MNase-seq in TBP-AA	(Tramantano et al., 2016)	BioProject ID: PRJNA271808
Experimental Models: Organisms/Strains		
<i>S. cerevisiae</i> AA (FSY4885)	(Haruki et al., 2008)	<i>MAT</i> α , <i>tor1-1</i> , <i>fpr1</i> Δ :: <i>NAT</i> , <i>RPL13A-2</i> \times <i>FKBP12</i> :: <i>TRP1</i>
<i>S. cerevisiae</i> Nrd1-AA (FSY5065)	(Castelnuovo et al., 2014)	<i>MAT</i> α , <i>tor1-1</i> , <i>fpr1</i> Δ :: <i>NAT</i> , <i>RPL13A-2</i> \times <i>FKBP12</i> :: <i>TRP1</i> , <i>NRD1-FRB</i> :: <i>KanMX6</i>
<i>S. cerevisiae</i> Nrd1-AA <i>rdp3</i> Δ (FSY7015)	This study	<i>MAT</i> α , <i>tor1-1</i> , <i>fpr1</i> :: <i>NAT</i> , <i>RPL13A-2</i> \times <i>FKBP12</i> :: <i>TRP1</i> , <i>NRD1-FRB</i> :: <i>KanMX6</i> , <i>rdp3</i> Δ :: <i>HIS3</i>
<i>S. cerevisiae</i> Nrd1-AA TBP-MNase (FSY8162)	This study	<i>MAT</i> α , <i>tor1-1</i> , <i>fpr1</i> :: <i>NAT</i> , <i>RPL13A-2</i> \times <i>FKBP12</i> :: <i>TRP1</i> , <i>NRD1-FRB</i> :: <i>KanMX6</i> , <i>TBP-3xFLAG-MNase</i> :: <i>HPHMx6</i>
<i>S. cerevisiae</i> Nrd1-AA <i>rdp3</i> Δ TBP-MNase (FSY8164)	This study	<i>MAT</i> α , <i>tor1-1</i> , <i>fpr1</i> :: <i>NAT</i> , <i>RPL13A-2</i> \times <i>FKBP12</i> :: <i>TRP1</i> , <i>NRD1-FRB</i> :: <i>KanMX6</i> , <i>rdp3</i> Δ :: <i>HIS3</i> , <i>TBP-3xFLAG-MNase</i> :: <i>HPHMx6</i>
<i>S. cerevisiae</i> Nrd1-AA STH1-MNase (FSY8254)	This study	<i>MAT</i> α , <i>tor1-1</i> , <i>fpr1</i> :: <i>NAT</i> , <i>RPL13A-2</i> \times <i>FKBP12</i> :: <i>TRP1</i> , <i>NRD1-FRB</i> :: <i>KanMX6</i> , <i>STH1-3xFLAG-MNase</i> :: <i>HPHMx6</i>
<i>S. cerevisiae</i> Nrd1-AA <i>rdp3</i> Δ STH1-MNase (FSY8255)	This study	<i>MAT</i> α , <i>tor1-1</i> , <i>fpr1</i> :: <i>NAT</i> , <i>RPL13A-2</i> \times <i>FKBP12</i> :: <i>TRP1</i> , <i>NRD1-FRB</i> :: <i>KanMX6</i> , <i>rdp3</i> Δ :: <i>HIS3</i> , <i>STH1-3xFLAG-MNase</i> :: <i>HPHMx6</i>
Oligonucleotides		
See Table S2		N/A
Software and Algorithms		
Bowtie	(Langmead and Salzberg, 2012)	http://bowtie-bio.sourceforge.net/bowtie2/index.shtml
deepTools	(Ramírez et al., 2016)	https://deeptools.readthedocs.io/en/develop/index.html
Danpos2	(Chen et al., 2013)	https://sites.google.com/site/danposdoc/
Galaxy	(Afgan et al., 2018)	https://usegalaxy.org/
Prism 8	GraphPad	N/A

RESOURCE AVAILABILITY

Lead Contact

Further information and requests for resources and reagents should be directed to and will be fulfilled by the lead contact, Dr. Julien Soudet (julien.soudet@unige.ch).

Materials Availability

Yeast strains generated in this study are available upon request without restrictions.

Data and Code Availability

The accession number for the data reported in this study is GEO: GSE130946.

EXPERIMENTAL MODEL AND SUBJECT DETAILS

All *Saccharomyces cerevisiae* strains were derived from the Anchor-Away genetic backgrounds (see [Table S1](#)) ([Haruki et al., 2008](#)). Cells were grown in YEPD medium (1% yeast extract, 1% peptone) supplemented with 2% glucose as carbon source. All strains were grown at 30°C and were not affected in growth by the different tags or deletions ([Table S1](#)). Anchor-away of Nrd1-AA was induced by adding 1 μg/ml of rapamycin to the medium.

METHOD DETAILS

RNA extraction and RNA-seq

RNAs were extracted using Glass-beads and TRIzol (Invitrogen). RNA library preparation and single-end stranded sequencing were performed at the IGE3 genomics platform of the University of Geneva.

MNase(-ChIP)-seq

The MNase- and MNase-ChIP-seq experiments were performed mainly as described in [Weiner et al. \(2015\)](#) with the following modifications. Nrd1-AA strain was inoculated overnight and diluted in the morning to $OD_{600} = 0.2$ in YEPD medium. Yeast cell cultures of 100 mL was used per modification. Rapamycin treatment was performed at $OD_{600} = 0.5$ for 60 minutes on half of the culture. The cells were fixed with formaldehyde at a final concentration of 1% for 15 minutes followed by glycine addition at a final concentration of 125 mM for 5 minutes. Cells were washed 2x with ddH₂O, harvested in magnaLyser tubes (Roche) (100 mL cell culture/tube) and frozen at -20°C.

Chromatin extraction was performed by breaking cells in 1 mL of Cell Breaking buffer (0.1 M Tris-HCl, pH 7.9, 20% glycerol, EDTA-free protease inhibitors) and 1 mL of acid-washed glass beads in a magnaLyser (Roche). The cell extract was then centrifuged at 19,000 g at 4°C for 10 minutes to collect chromatin. The chromatin was resuspended in 600 μL of NP buffer (0.5 mM Spermidine, 50 mM NaCl, 1 mM β-mercaptoethanol, 0.075% NP-40, 10 mM Tris-HCl pH 7.4, 5 mM MgCl₂, 1 mM CaCl₂) per tube. The DNA concentration was measured using Qubit dsDNA BR assay kit (Invitrogen). Chromatin was diluted to 20 μg/mL using NP buffer in all conditions for comparable results.

MNase treatment was performed using 0.2 μL of MNase (ThermoScientific 100 units/μL) / 12 μg of chromatin in 600 μL reaction mixture for 14 minutes at 37°C. To perform all the modifications for one replicate from one cell culture the reaction was scaled 10x. The reaction was stopped by adding EDTA (final concentration 20 mM) in the reaction mixture.

For MNase-seq, an equal amount of elution buffer (10 mM Tris-HCl, pH 8.0, 1% SDS, 150 mM NaCl, 5 mM DTT) was added. The further steps for MNase-seq are the same as those performed after MNase-ChIP elution.

For MNase-ChIP, the buffer of the MNase reaction mixture was adjusted to be compatible to FA-lysis buffer (50 mM HEPES-KOH, pH 7.5, 140 mM NaCl, 1 mM EDTA, 1% Triton X-100, 0.1% sodium deoxycholate, EDTA-free protease tablet). The following salts were added to the MNase reaction tube: 80 μL of 0.5 M HEPES-KOH, pH 7.5, 22.4 μL of 5 M NaCl pre-mixed with protease inhibitors. This was followed by the addition of detergents, 6.4 μL of 12.5% sodium deoxycholate and 80 μL of 10% Triton X-100 per 600 μL MNase reaction.

The protein-G dynabeads (ThermoFisher Scientific) were pre-incubated with the antibodies for one hour at 4°C on a rotor, 85 μL beads/reaction. The antibodies used were anti-H3 (Abcam ab1791): 12 μL per reaction; anti-H3K36me3 (Abcam ab9050): 6 μL per reaction; anti-H3K18ac (abcam ab1191): 7 μL per reaction; H4ac (Merck Millipore 06-598): 10 μL per reaction. The beads were washed in FA-lysis buffer twice, followed by incubation with the MNase-treated chromatin for 4 hours at 4°C on a rotor. The beads were sequentially washed with 1 mL of FA-Lysis buffer, 1 mL FA500-lysis Buffer (FA-Lysis Buffer + 500 mM NaCl), 1 mL of Buffer III (10 mM Tris-HCl, pH 8.0, 1 mM EDTA, 250 mM LiCl, 0.5% NP-40, 0.05% sodium deoxycholate), 1 mL of Tris-EDTA pH 8.0. For elution, the beads were incubated in 150 μL of elution buffer at 65°C for 15 minutes.

The crosslinking was reversed by incubation of the eluate at 65°C overnight followed by the addition of 150 μL of TE (10 mM Tris-HCl, pH 8.0, 1 mM EDTA). The eluate was then treated with proteinase K (1 μg/μL final concentration) for 3 hours at 42°C. The DNA was purified using the NucleoSpin Gel and PCR clean-up kit (Macherey-Nagel) using the SDS protocol provided in the manual. The

DNA concentration was measured using Qubit dsDNA HS assay kit (Invitrogen) and the libraries were prepared using NEBnext Ultra DNA library prep kit for Illumina (NEB). Finally, samples were paired-end sequenced at the iGE3 genomics platform of the University of Geneva.

ChEC-seq

The experiment was performed as described in [Zentner et al. \(2015\)](#) with some modifications. The yeast strains were cultured the day before in YEPD medium. They were diluted to $OD_{600} = 0.2$ in YEPD medium in the morning. The 60 min rapamycin treatment was performed at $OD_{600} = 0.4$.

For each condition, 50 mL cell cultures were harvested at room temperature. The cells were washed twice in 1 mL Buffer A (15 mM Tris-HCl pH 7.5, 80 mM KCl, 0.1 mM EGTA, 0.2 mM spermine, 0.5 mM spermidine and protease inhibitor tablet (Sigma-Aldrich)). Cells were resuspended in 594 μ L of buffer A and 6 μ L of 10% digitonin (0.1% final concentration) were added to permeabilize the cells during 5 min at 30°C. $CaCl_2$ was added (final concentration 5 mM) to activate the MNase cleavage. 200 μ L were collected at 30 s for *SPT15-MNase* or 20 s for *STH1-MNase* and were immediately mixed with 200 μ L of 2X Stop solution (400 mM NaCl, 20 mM EDTA, 4 mM EGTA, 1% SDS).

The cells were treated with Proteinase K (0.4 μ g/ μ L final concentration) and incubated at 55°C for 30 minutes. The DNA was extracted using phenol:chloroform:isoamyl extraction, and precipitated by adding 30 μ g glycogen, 500 μ L of 100% ethanol and incubated at -20°C for one hour. RNase treatment was performed by adding 34.5 μ L of Tris, pH 8.0 and 10 μ g of RNase per reaction.

For size selection of DNA fragments, 75 μ L of solid phase reversible immobilization beads (SPRI, AmpureXP Beckman Coulter) were added in 25 μ L of RNase treated DNA and the reaction was mixed by pipetting up and down 10 times. The beads were incubated at room temperature for 5 minutes. The tubes were placed in the magnetic rack and supernatant was transferred to the new tube containing 10 mM Tris and 0.2 M NaCl for each reaction. The DNA was extracted with phenol:chloroform:isoamyl solution and precipitated with 100% ethanol. The pellets were washed with 70% ethanol and resuspended in 29 μ L of Tris, pH 8.0. DNA concentration was measured using Qubit dsDNA HS assay kit (Invitrogen) using 4 μ L sample. The remaining 25 μ L were used to prepare sequencing libraries using NEBnext Ultra DNA library prep kit for Illumina (NEB). The samples were sequenced in the paired-end mode at the iGE3 genomics sequencing platform in Geneva.

ATAC-seq

The experiment was performed after modifying the protocol from [Schep et al. \(2015\)](#). The yeast strains were inoculated the day before in YEPD. Cultures were diluted to $OD_{600} = 0.2$ and allowed to reach $OD_{600} = 0.4$. Half of the culture was then treated with Rapamycin for 1 h at 30°C.

1 mL of the cell culture was harvested from all conditions and strains. Cells were washed twice in 1 mL sorbitol buffer (1.4 M Sorbitol, 40 mM HEPES-KOH, pH 7.5, 0.5 mM $MgCl_2$), resuspended in 190 μ L of sorbitol buffer and 10 μ L of 10 mg/mL Zymolyase (20T Zymolyase, AMSBIO), and incubated at 30°C shaking at 200 rpm for 30 minutes. The cells were washed twice in sorbitol buffer and resuspended in 95 μ L of 1x TD buffer and 5 μ L of the TD enzyme (Illumina). The reaction was incubated at 37°C at 500 rpm for 30 minutes. DNA was then extracted with 3x SPRI beads (AmpureXP Beckman Coulter) and eluted in 28 μ L 10 mM Tris-HCl, pH 8.0.

Initial PCR amplification was performed with 4 μ L of transposed DNA to check the transpositions and cycles required. Final amplification was performed with NEBNext High-Fidelity 2x PCR Master Mix (NEB) using Nextera Primers (Illumina). 12 cycles were performed.

The size selection was performed by sequential SPRI beads precipitation. First, the DNA was mixed by pipetting in 0.5x beads followed by incubation for 5 minutes at room temperature. The supernatant was used for the next DNA precipitation with 2.5x SPRI beads. The supernatant was discarded and the beads were washed with 70% ethanol twice before the DNA was extracted using 28 μ L of 10 mM Tris-HCl, pH 8.0. The DNA concentration was measured and the samples were paired-end sequenced at the iGE3 genomics platform of the University of Geneva.

ChIP-qPCR

The experiments were performed as described in [Kuras and Struhl \(1999\)](#) after some modifications. For both *S. cerevisiae* and *S. pombe* (used here for spike-in), the cultures were grown to exponential phase until $OD_{600} = 0.5$, after which they were treated with Rapamycin for different time points. Cells were fixed and chromatin was extracted as in the MNase(-ChIP)-seq section with the exception of the breaking step performed in FA-lysis buffer (50 mM HEPES-KOH, pH 7.5, 140 mM NaCl, 1 mM EDTA, 1% Triton

X-100, 0.1% sodium deoxycholate, EDTA-free protease table

t). Chromatin was sheared to 300 bp fragments through sonication (Bioruptor, Diagenode).

$2/3^{\text{rd}}$ *S. cerevisiae* chromatin was mixed with $1/3^{\text{rd}}$ of *S. pombe* chromatin. The ChIP was performed with the mixture using on average 200 μ L of the ChIP chromatin at a concentration of 20 μ g/mL. The rest of the experiment was performed as in the MNase(-ChIP)-seq section. After elution and clean-up, DNA fragments were amplified with the different oligos of [Table S2](#) using the SYBR Green PCR Master Mix (Applied Biosystems) and a Real-Time PCR machine (Bio-Rad).

QUANTIFICATION AND STATISTICAL ANALYSIS

List of genes, TBS and nucleosomes

The list of gene coordinates from TSS to poly-A was kindly provided by the Mellor Lab. Among them were picked the ones considered as “Verified” genes in the *Saccharomyces* Genome Database (SGD) giving a complete list of 4,775 coding genes. For the TBS coordinates, our list was crossed with the data from the Pugh lab (Rhee and Pugh, 2012). $-1/+1$ coordinates were extracted from DANPOS2 analysis with default settings (Chen et al., 2013) from our Wig profile of H3K18ac in -Rap. Figure 4A was obtained using the coordinates of the nucleosome atlas from the Friedman lab (Weiner et al., 2015).

RNA-seq analysis

Single-end reads were aligned to *sacCer3* genome assembly using Bowtie2 (Langmead and Salzberg, 2012) with options ‘-k 20–end-to-end–sensitive -X 800’. PCR duplicates were removed from the analysis. BigWig coverage files were generated using Bam2wig function. Differential expression analysis was performed using the R/Bioconductor package DEseq on mRNA annotations Ensembl (*Saccharomyces_cerevisiae*.EF4.65.gtf). Antisense transcripts with a fold-change of at least 2 and multiple testing adjusted p value lower than 0.05 were considered differentially expressed. Among them, AMRG were defined as the genes showing a < 0.8 fold-change with an adjusted p value < 0.05 .

MNase(-ChIP)-seq mapping

Paired-end reads were aligned to *sacCer3* genome assembly using Bowtie2 (Langmead and Salzberg, 2012) with options ‘-k 20–end-to-end–sensitive -X 800’. PCR duplicates were removed from the analysis. Then, deepTools 2.0 (Ramírez et al., 2016) was used through the bamCoverage function with size selection of fragments (120-200bp to visualize only proper nucleosomes and not “fragile nucleosomes” (Brahma and Henikoff, 2019; Kubik et al., 2015)), counting only the 3bp at the center of fragments and cpm normalization.

ChEC-seq and ATAC-seq mapping

Adapters were first removed from the paired-end reads using the TrimGalore! Tool with default options from the Galaxy server (Afgan et al., 2018). Paired-end reads were then aligned to *sacCer3* genome assembly using Bowtie2 (Langmead and Salzberg, 2012). PCR duplicates were removed from the analysis. DeepTools 2.0 (Ramírez et al., 2016) was then used through the bamCoverage function with size selection of fragments (0-120bp for TBP-ChEC and ATAC-seq, and 120-200bp for Sth1-ChEC) and counting of only the 3bp at the center of fragments.

Metagene analyses

Bigwig files of independent duplicates generated via mapping were then averaged in deepTools2.0 using the bigWigCompare command (however, results of each duplicate are shown in Figures S1–S4). Metagene plots were produced using computeMatrix followed by plotProfile commands. +Rap/-Rap fold-changes over TBS or $-1/+1$ nucleosomes were calculated adding no pseudo-count for ATAC-seq, TBP-ChEC and Sth1-ChEC, a pseudo-count of 1 for RNAPII PAR CLIP and a pseudo-count of 0.01 for MNase-seq, H3K36me3 and H3K18ac.

Fuzziness was calculated with DANPOS2 (Chen et al., 2013) using H3K18ac -Rap and H3K36me3 -Rap Wig files. Only peaks showing > 15 cpm were taken into account in the analysis (7’929 and 9’899 peaks for H3K36me3 and H3K18ac, respectively).

Figures 6A–6D were normalized as follows: the mean of +Rap/-Rap fold-change was normalized to 1 in both *WT* and *rdp3Δ* strains giving a normalization factor for each strain. These normalization factors were then applied to the different classes to correct the raw fold-changes.

Statistical analyses

All plots and statistical analyses of this work were performed using Prism 8.0 (Graphpad). All tests are nonpaired tests (with the exception of Figures 6A–6D based on paired tests). t tests or Mann–Whitney *U* tests were used according to the normality of the data analyzed, which was calculated using a d’Agostino–Pearson omnibus normality test. * if p value < 0.05 , ** < 0.01 , *** < 0.001 , **** < 0.0001 .

2 Recovery of Antisense-Mediated Repression

Adaptation to the environment in yeast and cell specialization in multicellular organisms leads to changes in transcription and programming of a specialised transcriptome for the particular cell. This is accomplished by changes in chromatin organisation and transcription by reinforcing signals from TFs, ncRNAs and histone modifications. This complex pattern of transcription has to be passed-on to each successive generation for better survival (Bonasio et al., 2010).

The cells have molecular machineries to generate memory of the past events in the form of epigenetic states, besides changes in the DNA sequence itself. Histone PTMs, prions and DNA methylation form the basis for epigenetic states. Epigenetic inheritance is the transmittance of a specific state of gene expression to the next generation that does not involve a change in DNA sequence, provided the progeny is not exposed to the stimuli that caused the change (Henikoff and Greally, 2016; Ptashne, 2007). The establishment of a modification is then partly dependent on the PTM being copied by enzymes that recognize these pre-existing histone modifications and catalyse the same on newly incorporated neighbouring histones (Moazed, 2011).

We observed that upon induced extension of AS transcripts into the promoters of sense ORFs, the repression was mediated by a change in the chromatin state. The H3K36me3 modification is increasing with an increase in nucleosome occupancy accompanied by a decrease in H3K18ac (Gill et al., 2020). AS transcripts are regulated physiologically as well, when the early-termination is naturally abrogated under nutrient depletion (Bresson et al., 2017; Darby et al., 2012; Webb et al., 2014). Therefore, it is possible that repression by AS transcription might be preserved with the modifications as an epigenetic memory. To study the changes or persistence in PTMs upon abrogation of AS-mediated repression, we first established AS-repressed promoters and then reintroduced AS early-termination followed by the analysis of both transcription and chromatin states over time.

2.1 Introduction

Chromatin state is a key determinant of transcription levels. A specific chromatin state is achieved by the interplay of various chromatin modifying factors, which take input from various signalling pathways, the induction of TFs or a network of feedback loops (Diehl and Muir, 2020). The achieved state should therefore be maintained through cell divisions to have accurate expression but also needs to be plastic enough to respond to programmed cell cycle changes or to the environment. Therefore, molecular mechanisms acting on an epigenetic state could be divided into two classes –

mechanisms that help in maintaining the state and mechanisms involved in erasure of the chromatin state.

2.1.1 Mechanisms of Epigenetic Memory Maintenance

The mechanisms by which an epigenetic process is inherited could be divided into three categories. The first involves certain non-coding RNAs that are described to sequester complexes in order to maintain a chromatin state. The second involves chromatin complexes that bind histone PTMs and deposit the same modification on a new nucleosome, or factors, that copy modified DNA base onto a replicated strand. The third is based on chromosome 3D organization and the observation that the compartments in an active or repressive state influence the epigenetic marks deposited on new histones (Iglesias et al., 2018; Reinberg and Vales, 2018; Yu et al., 2018).

2.1.1.1 Non-coding RNAs Sequester Chromatin Regulators

In fission yeast and higher eukaryotes small RNAs target nascent chromatin-bound ncRNAs and recruit chromatin modifying complexes. RNA interference (RNAi) in *S. pombe* involves an RNA-dependent RNA polymerase (RDRC), Dicer cleaving double stranded RNA (Dcr1), and Argonaute (Ago) that is loaded with small double stranded RNAs to form the RNA-induced transcriptional silencing (RITS) complex. RITS binding to homologous nascent RNAs promotes the recruitment of the H3K9 methyl transferase. Deletion of either of these components results in loss of heterochromatin silencing at pericentromeric DNA repeat regions and H3K9me is reduced (Volpe, 2002). Chp1 was identified as another component of the RITS complex, which has a chromodomain that binds methylated H3K9 stabilizing the complex (Noma et al., 2004; Partridge et al., 2002).

The stabilized RITS complex in turn promotes siRNA amplification as it interacts with RDRC and Dcr1 and act on ncRNAs to generate siRNAs (Motamedi et al., 2004). H3K9me also helps to recruit RDRC via the HP1 homologue Swi6 (Motamedi et al., 2008). In the absence of RDRC, primal heterochromatic RNAs (priRNAs), that are random degradation products of the bidirectional transcription occurring at DNA repeats, associates with Ago1. This triggers siRNA amplification and heterochromatin assembly, suggesting the existence of feedback loops that involve small RNAs and chromatin modifications (Halic and Moazed, 2010; Yu et al., 2014).

The XIST lncRNA represses a whole X chromosome in mammalian females by directing the Polycomb repressive complex 2 (PRC2) to chromatin, to catalyze H3K27me3 (Zhao et al., 2008). LncRNAs such as HOTAIR and HOX can also recruit PRC2 both in *cis* and *trans* (Pandey, 2008; Rinn, 2007). Thus, depending on the interacting protein nascent ncRNAs can reinforce a repressive state.

2.1.1.2 Reader-Modifier Reestablishment of Epigenetic Marks

In *S. cerevisiae*, the presence of H4K16ac functions to establish euchromatin after replication to facilitate transcription (Shogren-Knaak, 2006). Deacetylation of H4K16ac by silent information regulator (Sir2) is necessary for the establishment of condensed chromatin. It is maintained through generations at ribosomal DNA repeat sequences, mating-type loci and telomeres (Allshire and Madhani, 2018; Dodson and Rine, 2015).

In the SIR pathway, the DNA-binding proteins are recruited in a sequence-specific manner. There are four Sir proteins (Sir1-Sir4). Sir2 is a NAD⁺-dependent histone deacetylase (HDAC) that acts on H4K16ac on a neighbouring nucleosome and makes it possible for the complex Sir3-Sir4 to bind that nucleosome and thus the cycle progresses (Armache et al., 2011). In this pathway, Sir3 is defined as the 'reader' protein that recognise the modification, while Sir2 is the 'eraser' that erases the mark. The SIR pathway is restricted to *S. cerevisiae* (Hanson and Wolfe, 2017).

In *S. pombe* and higher eukaryotes, Clr4 performs H3K9me. Clr4 has an N-terminal chromodomain and a C-terminal SET domain, thereby coupling both the reader and modifier in the same protein. It has been shown that once H3K9me is established, it could be maintained through epigenetic mechanisms based on the direct interaction of Clr4 with pre-existing H3K9me in an RNAi independent manner (Ragunathan et al., 2015).

HP1 proteins Swi6 and Chp1 contain both a chromodomain and a chromoshadow domain (CSD) (Brasher, 2000; Cowieson et al., 2000). CSD dimerization forms a binding platform for SHREC (Snf2/HDAC-containing repressor complex) that promotes deacetylation of H3K9 and therefore allowing its methylation (Fischer et al., 2009; Motamedi et al., 2008). The Swi6 dimer binds a modified H3K9me₃ nucleosome and provides the paired Swi6 to bind the neighbouring nucleosome thus bridging two nucleosomes (Canzio, 2013). In higher organisms, feedforward loops also exist with 5mC DNA methyltransferase, which can be recruited to H3K9me sites and the two modifications can therefore promote each other (Hashimshony et al., 2003; Jackson et al., 2002).

In *Drosophila*, methylation of H3K27me₃ is performed by PRC2. PRC2 is composed of four subunits including suppressor of zeste homolog 12 (SUZ12), enhancer of zeste homolog 2 (EZH2) and embrionic ectoderm development (EED). EED binds H3K27me₃ which activates the SET domain of EZH2. PRC2 is required for its epigenetic transmission. PRC2 promotes binding of the PRC1 complex to chromatin (Cao, 2002; Margueron, 2009). PRC1 recruitment acts a restricting mechanism and inhibits remodelling by SWI/SNF, PRC2 requires sequence-specific recruitment to DNA using PRE elements in *Drosophila* for long term inheritance (Laprell et al., 2017). H3K37me₃ is

shown to be inherited at the HOX gene loci in *Drosophila*, and plays a causal role in its repression (Coleman and Struhl, 2017).

H3K20me is another repressive modification that leads to compaction of the chromatin and the methylated K20 is antagonistic towards the activating mark H4K16ac (Kuzmichev et al., 2002; Trojer et al., 2007).

2.1.1.3 Influence of Chromatin Domains on Epigenetics

Chromatin is further packed into a higher order structure in the nucleus which forms 3D domains called topologically associated domains (TADs) which can be several megabase pairs in size (Dixon, 2012). They exist in two types – active A and inactive B domains (Lieberman-Aiden et al., 2009). These domains are largely lost during cell division but are established again after metaphase (Earnshaw and Laemmli, 1983; Gibcus et al., 2018). At a smaller scale, chromatin looping and long-range interactions of genes have been observed (Rao, 2014; Sanyal et al., 2012). In *S. cerevisiae*, self-associating domains exist in smaller configurations that involve on average four genes (Hsieh, 2015). This organisation helps regulate gene expression by maintaining active or repressive states in spatially defined domains.

Presently, there is little information about the role played by the formation of domains in the spreading of H3K9me and H3K27me in *S. pombe* or higher eukaryotes. In *Drosophila*, Chromobox 2 (Cbx2) protein binds to H3K27me₃ and promotes nucleosome compaction, resulting in the formation of domains and Cbx2-mediated compaction is essential for silencing (Lau et al., 2017). Based on the observed changes in H3K27me and H3K36me over generations, a recent study in mESCs computationally showed that domains with different states of these modifications exist, and that the pre-existing state of a domain influences the final state of a modification on a nucleosome (Alabert et al., 2020). Another study showed that PRC1 helps to form chromatin loops that maintain domains containing transcriptionally active genes during development in *Drosophila* (Loubiere et al., 2020).

2.1.2 Mechanisms of Erasure of Epigenetic Marks

If a chromatin state defines the transcriptional level in the cell, it needs to be malleable enough to respond to programmed cell cycle, nutrient conditions or other stimuli. The changes acquired during such a response might be beneficial for survival so that the cell maintains it for longer durations as discussed above. The second scenario is that the chromatin state was transiently achieved for a response and then it needs to be abolished. The most common mechanism deployed for this would be dilution of a chromatin mark during cell division. The active mechanisms include targeted removal of a modification from a histone and active histone replacement.

2.1.2.1 Replication

DNA replication requires dismantling the nucleosome structure from the DNA followed by nucleosome reassembly on the newly replicated DNA (Alabert and Groth, 2012). The newly established nascent chromatin contains both recycled histones from the parent DNA strand and naive histones. Parental histones are mixed with new histones on both strands. New histones have H3K56ac, H4K5ac and H4K12ac (Annunziato, 2015). Each daughter DNA strand receives two-fold diluted parent PTMs (Alabert, 2015). The parental histones preserve their pre-replication PTMs during chromatin assembly (Petryk, 2018; Reverón-Gómez, 2018). Most of the parental H3-H4 histones are recycled as intact tetramers (Xu, 2010; Yu, 2018). They are positioned within 250 bp of their pre-replication site (Reverón-Gómez, 2018). The histone recycling from parent to daughter strands is slightly biased towards the lagging strand in yeast (Yu, 2018). Accurate repositioning of PTMs forms the basis of epigenetic inheritance. If the new histones are not modified post-replication, the PTMs will be lost by successive replication cycles. Accurate recycling per position also defines the template for new histones and restricts the deposition of inhibitory modifications that does not co-occur (Alabert et al., 2020)

The nascent chromatin has half of the total nucleosomes that are modified and different mechanisms exist for different modifications to reach the pre-replication state. H3K9me3, H3K27me3 can recruit enzymes and are potentially self-propagated continuously throughout the cell cycle (Alabert, 2015; Audergon, 2015). The active chromatin marks H3K4me, H3K36me, and H3K79me are shown to be restored completely within a cell cycle both in mouse and in yeast (Petryk, 2018). A possible mechanism might involve active deposition of these marks with transcription (Stewart-Morgan et al., 2019). Passing of a chromatin state could be a selective process based on the presence or absence of specific factors (De and Kassis, 2017; Stewart-Morgan et al., 2020).

2.1.2.2 Replication Independent Histone Exchange

Besides the systematic disruption of chromatin during DNA replication, the chromatin within each cell cycle is very dynamic (Luger et al., 2012). Histone exchange is used by the cell to swap complete or parts of nucleosomes on chromatin with new nucleosomes. This exchange could lead to changes in the stability and thus its residence time on the DNA. This mechanism could also be used to remove nucleosomes containing pre-existing PTMs and thus erase the epigenetic memory. This could be used to reset transcriptional programmes.

Histone exchange is more abundant at open chromatin and nucleosomes flanking NDRs (Dion et al., 2007; Mito et al., 2007). For example, acetylation of H3K56ac and H3K122ac on the nucleosome surface promote nucleosome disassembly (Tropberger, 2013; Williams et al., 2008). Acetylation also enhances nucleosome exchange of H2A with the H2A.Z variant, mediated by the SWR complex (Kusch, 2004), which might enhance RNAPII promoter escape. Transcription elongation also requires removal of one H2A-H2B dimer from the nucleosome *in vitro*. This is facilitated by the presence of H2BK123 ubiquitination and is performed by the FACT histone chaperone complex (Belotserkovskaya, 2003; Kireeva, 2002; Kulaeva, 2009; Pavri et al., 2006).

On the other hand, the Snf2 chromatin remodeler represses histone exchange to stabilize chromatin and promote replication mediated inheritance (Taneja, 2017). Similarly, the H3K36me3 mark restricts histone exchange over coding regions post-transcription (Dion et al., 2007), and the Isw1b complex is proposed to identify H3K36me3 nucleosomes (Maltby, 2012). The chaperone Asf1 was also shown to decrease the accumulation of new, acetylated nucleosomes over the coding regions, suggesting a role in the stabilization of coding regions (Venkatesh, 2012).

2.1.2.3 Active Modification of PTMs

Epigenetic chromatin states are most frequently achieved and characterized by depositing histone methylations and maintaining a repressive state rather than acetylation and active states. Although there are proteins with bromodomains that bind acetylated histones, these marks have never been observed to have a feedback mechanism for their propagation (Reinberg and Vales, 2018). Therefore, epigenetics is currently restricted to repressive states and active demethylation is one of the mechanisms for targeted reversal of this state.

In *S. pombe*, Epe1 has been shown to be the demethylase for H3K9me. After removal of the initial signal to establish heterochromatin, H3K9me is maintained in the Epe1 demethylase mutant cells (Ragunathan et al., 2015). In *S. cerevisiae*, the H3K4me demethylase Jhd2 was shown to genetically inhibit the FACT and NNS complexes. Jhd2 also opposes the Spt6 positioning of nucleosomes near

the TSS (Lee et al., 2018b). In *S. cerevisiae*, H3K36me is removed by Jhd1 and Rph1. Jhd1 demethylates H3K36me1 and H3K36me2, while H3K36me2 and H3K36me3 are removed by Rph1 (Kim and Buratowski, 2007). Rph1-mediated demethylation has been shown to oppose Rpd3S function, consistent with it demethylating H3K36me3 (Lee et al., 2018c).

2.1.3 Antisense Transcription Modifies Chromatin PTMs

Antisense transcription, when extended into the promoters of the sense transcripts, results in the repression of the coding gene promoter. We showed that this repression is mediated by deposition of H3K36me3 marks over sense promoters (Gill et al., 2020). H3K36me3 is deposited co-transcriptionally by the Set2 methyltransferase (Li et al., 2003). H3K36me3 is enriched over coding regions and has one of the longest half-lives in yeast (Weiner et al., 2015). In coding regions, the H3K36me mark restricts histone exchange and helps maintain the old methylated nucleosomes in the gene body thereby preventing intragenic cryptic transcription initiation (Venkatesh et al., 2016; Venkatesh et al., 2012). H3K36me3 was also proposed to recruit the Isw1b chromatin remodelling complex that helps to maintain the chromatin and nucleosome spacing (Smolle, 2012). We showed that H3K36me3 is able to recruit Rpd3 to the promoter regions, inducing chromatin deacetylation and making it repressive. Thus, once deposited on a nucleosome, H3K36me3 is linked to mechanisms that help maintain the repressed state. Based on this, we asked whether the antisense-mediated repression may persist after removal of the cause of repression, i.e. AS transcription readthrough.

2.2 Antisense Mediated Repression primes Sense Transcription for Activation

This study was performed using an auxin-inducible degron system where the Nrd1 is degraded upon addition of auxin (Nishimura et al., 2009). Antisense is first extended to the promoter by degrading Nrd1, so that there is repression. The auxin is then washed away resulting in rapid synthesis of Nrd1 and therefore AS early-termination is resumed. We followed sense and AS nascent transcript expression and chromatin kinetics upon depletion and recovery of Nrd1.

The following work is in preparation with last part of analyses still to be performed. My contribution to the work is to perform experiments, analyse data and make figures for the findings presented. I plan to write the final manuscript with input from both F.S. and J.S.

Antisense-Mediated Repression primes the Sense Transcript Promoter for Activation by Inducing Acetylation

Jatinder Kaur Gill, Jose Manuel Nunez, Françoise Stutz and Julien Soudet

SUMMARY

Eukaryotic genomes are transcribed in an interleaved manner and often on both strands. The complex interlinked transcription programs often involve switches between neighbouring genes on the same or opposite strands that arise from transcription interference (TI). TI is mediated through deposition of histone PTMs. Histone PTMs have the potential to be maintained and inherited after replication. To observe what happens after Antisense-mediated repression (AMR), in the absence of the initial signal, we dynamically induced antisense (AS) non-coding transcription to mediate repression of hundreds of coding genes, followed by reversal to recover AS early-termination. We observed rapid reversal and activation of the sense transcription, the moment AS readthrough is off. Sense transcription recovered in an oscillating manner, with peaks and troughs of expression. H3K18ac was immediately recovered with the first peak of RNA and the nucleosome occupancy in the promoter was reduced within 30 minutes. The recovery is replication dependent, as the nucleosome occupancy in nucleosome depleted region (NDR) decreased slowly in G1-arrested cells. Opening of the NDR was also delayed in the absence of the histone acetyl transferase Esa1, suggesting that NuA4 plays a role in sense transcription recovery. Importantly, this study recapitulates some of the previously observed contradictory consequences of overlapping transcription events, described to have repressive but also activating effects. AS transcription into the sense promoter clearly results in the downregulation of the corresponding gene. However, once readthrough transcription is stopped, a majority of downregulated transcription units are rapidly reactivated, which may explain the different phenotypes observed before.

INTRODUCTION

Advances in nascent transcript analysis and increasing resolution in sequencing technologies have mapped active transcription to >80% of the human genome although only 2% corresponds to protein-coding mRNAs. In *S. cerevisiae*, the RNAPII landscape covers 75% of the genome (Carninci, 2005; Churchman and Weissman, 2011; Djebali, 2012). The current picture of the genome consists of overlapping and co-dependent transcription units (Mellor et al., 2016). One class of non-coding RNAs that are produced are long non-coding RNAs (lncRNAs) >200 nt in length, comprising transcripts from intergenic regions, enhancer RNAs and antisense transcripts (AS) (Derrien, 2012). A transcribing RNAPII running into the promoter of a neighbouring transcription unit results in transcription interference (Camblong et al., 2007; Proudfoot, 1986; Schulz et al., 2013). AS transcription starting at the 3' end of the gene, or transcription from upstream into the NDR of a promoter, results in co-transcriptional deposition of H3K4 and H3K36 histone methylation marks by Set1 or Set2. H3K4 and H3K36 methylation leads to repression by the recruitment of histone deacetylases that makes sense chromatin repressive (Castelnuovo et al., 2014; Gill et al., 2020; Kim et al., 2016; Kim et al., 2012).

Local changes in chromatin environment determine the level of gene expression (Allis and Jenuwein, 2016; Halley-Stott and Gurdon, 2013). Furthermore, expression pattern is inherited across generations as nucleosomes are accurately and symmetrically transmitted to both daughter cells during replication, almost exactly to their pre-replication positions. Thus, the histone post-translational modifications' (PTMs) identity on a DNA sequence is preserved through cell division, which is a form of epigenetic inheritance (Alabert, 2015; Petryk et al., 2018; Reveron-Gomez et al., 2018). Transcriptionally repressive chromatin, that depends on H3K9me3 and H3K27me3 in higher eukaryotes, and Sir complex-mediated repression in yeast, is identified by enzymes on older histones and reproduced on neighbouring new ones by self-propagating read-write and read-erase mechanisms respectively after replication (Reinberg and Vales, 2018).

AS transcription modifies the sense promoter NDR by deposition of the H3K36me3 mark (Gill et al., 2020). H3K36me3 is deposited co-transcriptionally by the Set2 methyltransferase (Li et al., 2003) and has one of the longest half-lives in yeast (Weiner et al., 2015). H3K36me1/2/3 has been shown to be a stable modification in mESCs and in cells lacking H3K27me1/2/3 deposition; H3K36me1/2/3 spreads to the repressive domains that originally had H3K27me and higher H3K36me3 levels are inherited before being diluted by the deposition of naive histones during replication over 3 generations (Alabert et al., 2020). Nucleosome turnover is one way of changing chromatin PTM composition. H3K36me marks restrict histone exchange and help maintain old nucleosomes in the gene body (Venkatesh et al., 2012). H3K36me3 is also known to recruit the Rpd3 HDAC. Consistently,

AS-repressed promoter NDRs present increased Rpd3 occupancy leading to a hypoacetylated chromatin environment (Carrozza et al., 2005; Gill et al., 2020). H3K36me3 could also recruit the Isw1b and Spt6 chromatin remodelling complexes that preserve chromatin by restricting histone exchange; they also maintain nucleosome spacing thereby inhibiting cryptic transcription within gene bodies (Kaplan et al., 2003; Smolle, 2012; Venkatesh et al., 2016).

In contrast, H3/H4 histone exchange is prevalent over promoters and highly transcribed genes (Dion et al., 2007; Thiriet and Hayes, 2005). Rtt109 is a histone acetyl transferase that mediates H3K56ac deposition in the globular core domain of the nucleosome together with Asf1. The H3K56ac modification has been shown to promote chromatin disassembly during transcription (Williams et al., 2008) and is one of the main causes of histone exchange (Rufiange et al., 2007). Esa1 is an essential histone acetyltransferase (HAT) required for cell division and is a component of NuA4 (Allard et al., 1999; Clarke et al., 1999). Esa1 mediates acetylation of nucleosomal H4 and H2A, that promotes the retention of the H2A variant H2A.Z at the +1 nucleosome, facilitating transcription initiation (Watanabe et al., 2013).

AS transcription works opposite to these mechanisms and promotes deacetylation and closing of the NDR by decreasing occupancy of the RSC chromatin remodeler (Gill et al., 2020; Murray et al., 2015). Therefore, the passage of AS transcription results in changes in sense promoter chromatin towards increased H3K36me3, decreased acetylation and possible recruitment of different sets of chromatin factors. Histone modifications are known to co-occur in a limited number of combinations, usually distinct for genic regions and promoters (Kharchenko et al., 2011; Rando, 2012). This is predicted to arise from the modification 'cross-talk' between enzymes that identify one modification and act on another (Suganuma and Workman, 2008). Therefore, after the passage of the AS transcribing RNAPII through an NDR, the induced repressed chromatin state could either be maintained by feed-forward loops or be reconverted to an active promoter.

In this study, we aim to decipher what happens to the AS-induced chromatin state once it has been established. AS ncRNAs are early-terminated by Nrd1/Nab3/Sen1 (NNS) complex followed by degradation (Porrua and Libri, 2015). To address this question, we optimised an auxin inducible degradation protocol for the NNS early termination complex, which allowed us to first rapidly deplete NNS to induce AS extension into sense promoters, followed by rapid recovery of early termination to its initial status. The changes in chromatin states and transcription levels were examined at different time points along these depletion and reactivation steps.

RESULTS

Alleviation of overlapping antisense transcription leads to immediate upregulation of sense transcription

The level of transcription as measured by RNA-seq is the net result of RNA synthesis rate, stability and degradation rate. The cell acclimates to the changes in RNA production by changing the stability and degradation rates (Das et al., 2017). Therefore, to measure the close to real level of RNA transcription at any time in a cell, we used the 4-thiouracil labelling and sequencing approach (Baptista and Devys, 2018). To dynamically modulate antisense (AS) transcription, we tagged the Nrd1 component of the Nrd1/Nab3/Sen1 nuclear RNA surveillance complex with the auxin-inducible degron (AID) system, and the Nrd1 promoter was replaced with the methionine promoter (*pmet*) (Bresson et al., 2017; Morawska and Ulrich, 2013). Nrd1 was rapidly down-regulated and degraded by adding Auxin and Methionine to the medium, leading to AS elongation and ncRNA expression (Figure S1C and S1D). Two hours following depletion, Nrd1 was recovered by washing the cells with normal medium (Figure 1A). Nrd1 decreased by more than 50% in one hour and was undetectable at 120 minutes (Figure S1A). The nascent RNA levels were measured after 4 minutes of 4-tU labelling per time point (Figure 1A).

The levels of AS transcripts increased in the absence of Nrd1. At 120 minutes, we observed 435 genes that were significantly repressed in response to AS elongation (Figure 1B and S1C). AS RNA was reduced to its original levels within the first two time points of recovery. Sense transcription was downregulated during depletion but rapidly upregulated when Nrd1 and AS early termination were restored (Figure 1C, S1B and second panel in Figure 1B). Genes with increase in AS though below cut-off of 1.5 fold also showed repression and recovery behaviour as compared to control genes and untagged strain (Figure S2D).

During recovery, sense transcription was observed to behave in an oscillating manner with peaks and valleys in the levels of expression. The peaks and valleys were not synchronous between the repressed genes, therefore we divided the 435 genes based on the RNA expression pattern during recovery using Kmeans (Figure 1D, see Experimental Procedures). The repressed genes were divided into 5 clusters. RNA expression was significantly upregulated for 3 clusters at the 150 min time point on average, and then repressed at different times, before coming back again. Cluster 1 recovers to initial levels at 150 min. The expression of cluster 5 also oscillated but at a two-fold lower level, and mostly remained repressed at all observed time points. The different recovery response to overlapping AS transcription is partly based on the basal expression levels of the different clusters (Figure 1E). The pattern of RNA expression recovery is not related to the changes in AS levels. Indeed, AS was observed to be decreasing linearly over time for all the clusters (Figure 1F and

S1G). To confirm that the observed fluctuations in RNA levels were not due to the medium changes, we performed the same experiment in an untagged strain and the oscillating patterns of RNA expression recovery were not observed (Figure S1E, S1F and S2C). Also, genes repressing and recovering in expression by TF absence or presence didn't result in this expression pattern either (Figure S2B).

We then compared the levels of nascent RNA expression between the control genes (5081) and all the clusters at each time point to observe the recovery pattern (Figure 1G). While the individual genes can be seen as upregulated at either the 150 min or 180 min time point (Figure 1D, first panel), cluster 1 (111 genes) is on average below the control set of genes at these time points. However it recovers at 240 min and is non-distinguishable from the control genes at 300 min. Cluster 2 genes are well above the control genes at 150 min and stay above the basal expression level until 240 min. Cluster 3 genes were individually upregulated at the 150 min time point (Figure 1D and 1G), but they reached their basal level at 180 min and their expression level reduced again at the last two time points. Cluster 4 consists of only 13 genes, but it shows a very distinct pattern with upregulation at 150 min and then recovery to the mean followed by upregulation again (Figure 1D and Figure 1G). Cluster 5 is expressed at a level below the global average; while the genes are repressed by AS in the same manner, their expression level oscillated 2-fold below their mean expression (Figure 1D, last panel) and never recovered until the last time point of the experiment.

These observations suggest that the recovery pattern in RNA expression is not related to AS transcription *per se*. We also know that AS mediates its effect on sense transcription through changes in H3K36me3 and H3K18ac levels as well as RSC recruitment, and that AS-mediated repression is

Figure 1. Recovery of Antisense Early Termination Leads to Rapid Upregulation of Sense Transcription.

(A) Outline of the experimental scheme. At time 0, Auxin (IAA) and methionine were added to the cells to deplete AID^{*}-Nrd1 for 2 hours, followed by washing of cells to remove Auxin and Methionine. 4tU-seq was performed at the indicated time points.

(B) Scatter plots showing the AS repressed genes in red and others in blue at all time points compared to 0 min.

(C) Line plot showing 4 genes for fold changes in AS (red) and Sense (green) transcription.

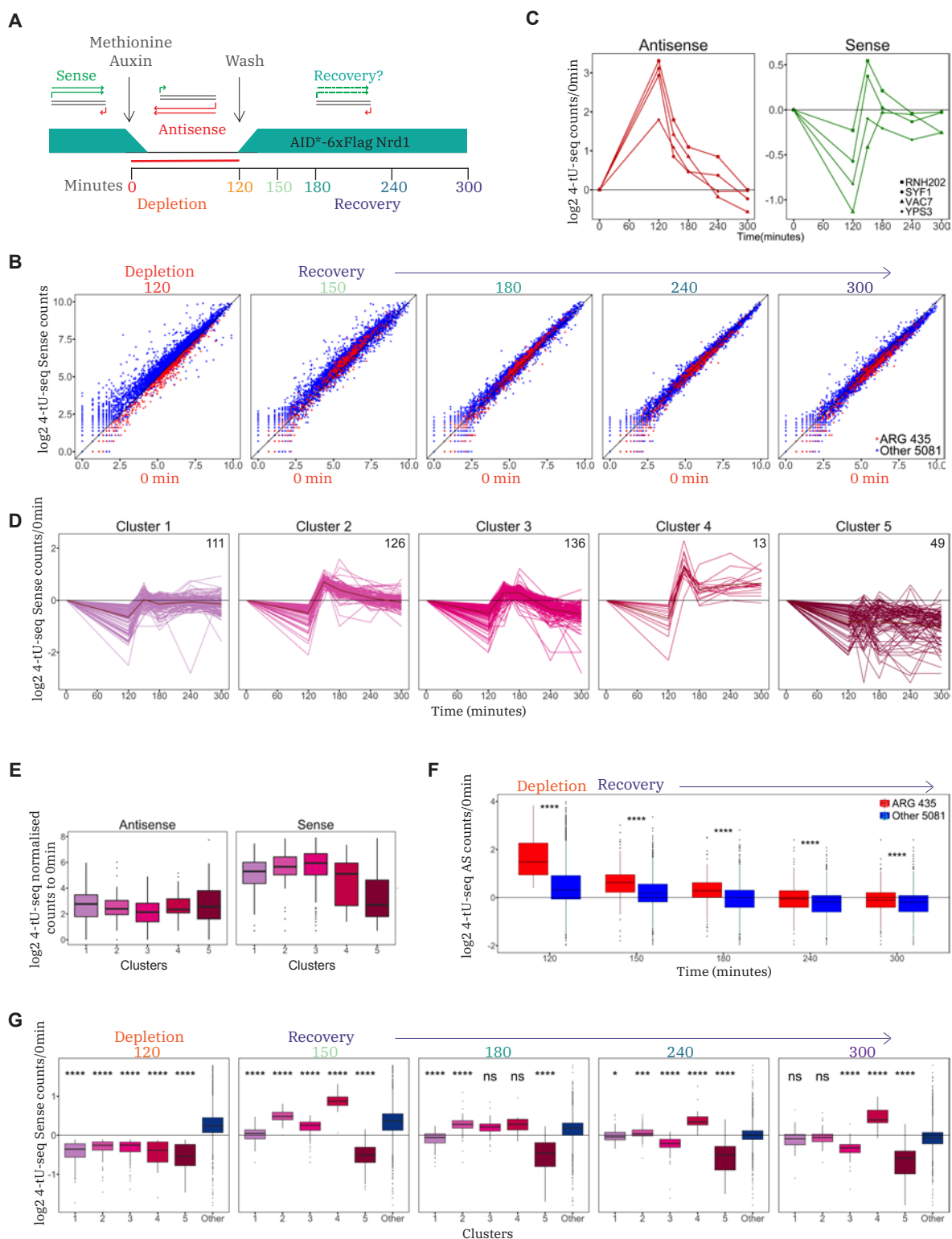
(D) Kmeans divided subclasses of AS repressed genes are shown with the changes in Sense expression during recovery. The number of genes present in each class is shown at the top right.

(E) Log phase expression levels for both AS and Sense at time 0 for the 5 clusters.

(F) Changes in AS expression during recovery for repressed genes (red) and for the rest of the genes (blue). The significance test was performed between repressed and control genes at each time point using Wilcox test and a p-value of <0.0001 is indicated with ****.

(G) Each sub-panel in the figure compares the expression level of repressed genes from each cluster at different time points.

Legend continues on next page.



Legend continued from previous page.

with the control genes for the indicated time points. Significant difference was calculated using Wilcoxon test and the indicated stars corresponds to as follows: * for p-value <0.01, ** for <0.001, *** for <0.0001 and **** for <0.00001.

partially alleviated in the absence of the Rpd3 histone deacetylase (Gill et al., 2020). Expression recovery may therefore be mediated by acetylating the +1 nucleosome after AS early termination is restored. Considering the links between chromatin modifications, nucleosome positioning and AS expression, we also investigated chromatin state changes during the recovery phase.

H3K18ac levels at +1 nucleosome closely mirrors the nascent RNA recovery

To measure the acetylation levels, we performed MNase ChIP-seq of H3K18ac using the same time points as in Figure 1A. The acetylation levels at the +1 nucleosome were reduced at 120 minutes for all the repressed genes in the 5 clusters as compared to control (Figure 2A and Figure S3A). Interestingly, the recovery in H3K18 acetylation at +1 reached levels similar to those observed for the control set of genes (Figure S3A, second panel). At 150 min, the acetylation level was recovered for all the clusters, including cluster 5 (Figure 2B). This might suggest a coherent mechanism of sense recovery by immediate acetylation to promote transcription. These patterns of acetylation were not observed in the untagged control strain (Figures S3B and S3C).

After the initial recovery, the levels of acetylation decreased. At 180 minutes they are below the peak levels observed at 150 min (Figure 2B) and not very different from the control set of genes (Figure S3A). Overall, the acetylation levels of cluster 3 reached a maximum at 150 min, but decreased soon after compared to the control, and were below the global average at all later time points. This is exactly the same pattern as observed for nascent RNA levels. Thus, acetylation might be a major signal for sense transcription recovery.

It is known that AS transcription extension into the promoters leads to deacetylation and results in nucleosome shifting and closing of the promoters (Gill et al., 2020). Our data therefore suggest that the increase in acetylation would result in the opposite and promotes NDR opening during recovery.

Legend continues from previous page.

(C) NDR sizes as measured for all the clusters at time 0 min using -1 and +1 nucleosome dyad centres for every gene from H3K18ac ChIP-seq data.

(D) Nucleosome occupancy as measured by MNase-seq for clusters 1, 4 and 5. Depletion time points are shown with red shades (left) and recovery time points are indicated with green shades (right), as in (A).

(E) The +1 nucleosome distribution as compared to TSS represented at time 0 minute and the changes observed at 120 min depletion and first recovery time point at 150 min.

(F) Fold change in +1 nucleosome distribution as compared to 0 min. Times are indicated at the top of the panel. The P-value is calculated using Wilcox test.

(G) and (H) RNA (AS - red, Sense - green), MNase and H3K18ac normalised profiles for SYF1 and VAC7 respectively

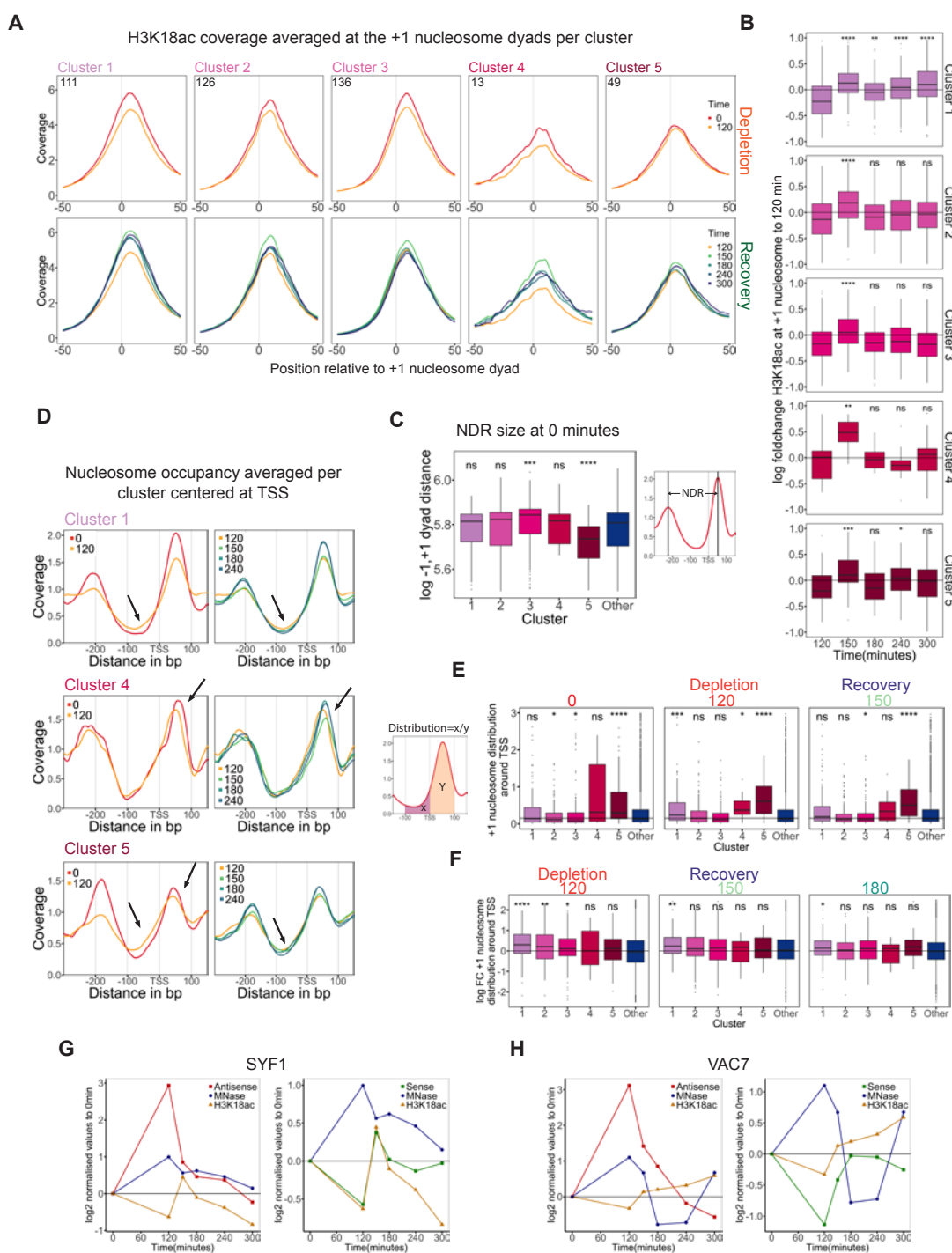


Figure 2. Changes in sense gene expression is closely mirrored in dynamic chromatin changes at the 5' end.

(A) MNase-ChIP-seq of H3K18ac at the same time points as in Figure 1 (A). The top panel shows the changes in coverage at +1 nucleosome for 0 (red) and 120 min (Orange) for depletion. The bottom panel shows the recovery from very light green for 150 min to dark blue for the last time point.

(B) Fold change in the acetylation levels was compared to depleted levels at 120 min. Each panel represents the changes in fold change acetylation per cluster. The indicated p-value is calculated using paired t-test.

Legend continues on next page.

Nucleosome occupancy over promoters is rapidly reduced during reactivation

To measure the changes in nucleosome occupancy over the promoter, we performed MNase-seq using the same time points as in Figure 1. The different clusters were observed to have distinct 5' NDR sizes (Figure 2C). Clusters 1 and 2 are comparable to the average control set, while cluster 3 has a larger NDR size and clusters 4 and 5 have small NDR sizes compared to the control (Figure 2C and 2D). Thus the clusters also correspond to different sets of genes based on promoter features, which are known to possess different gene expression profiles (Tirosh and Barkai, 2008).

Nucleosome occupancy in the NDR was increased upon AS extension into the promoters in all the clusters as compared to control (Figure 2C, 2E and Figure S3D). The clusters 4 and 5 show a shift of the +1 nucleosome peak towards the NDR region during Nrd1 depletion. However, the NDR is open again and the +1 peak fully shifted back at the 150 min time point; the changes we see are measurable but the characteristics of promoters that define specific expression patterns between gene types are not affected (Figure 2D and 2C). This is in accordance with previous study showing that promoter configuration is maintained during expression changes (Zaugg and Luscombe, 2012).

We then examined the changes in the +1 nucleosome distribution at the open (clusters 1, 2 and 3) and closed (clusters 4 and 5) promoters by establishing the ratio of the MNase-seq reads between the -100 to TSS (x) and the TSS to +100 (y) areas (See experimental procedures for calculation) (Figure 2E). The distribution is high if the +1 nucleosome is occupying the closed NDR position before the TSS site. The lower the distribution value, the more open the NDR, as can be seen from the first panel in Figure 2E. The distribution value is quite low for clusters 2 and 3 and very high for clusters 4 and 5, relating to their NDR sizes (Figure 2E). The +1 nucleosome distribution increases upon Nrd1 depletion, although to different extents depending on the cluster, indicating different responses to the overlapping AS based on the type of promoter. The increase is specific to the tagged strain (Figure S3G). The +1 distribution is back to its original level for all clusters at the first recovery time point (150 min). The fold change (FC) in the +1 distribution compared to the 0 min also showed an increased value at 120 min mostly for clusters 1 to 3, which rapidly resets during recovery at 150 min compared to Others (Figure 2F, S3E and S3F).

To define the correlation between nucleosome occupancy, acetylation and expression level, the different values were plotted for two individual genes, SYF1 and VAC7. In the first panel of Figures 2G and 2H, AS is plotted with acetylation and MNase fold change profiles. At 120 min, we can observe that AS is increased during depletion, leading to an increase in nucleosome occupancy and decrease in acetylation. In contrast, at 150 min and during recovery, there is coherent increase in sense transcription and acetylation and the decrease in +1 distribution (Figures 2G and 2H, right panels). Hence, rapid recovery in sense transcription is closely associated with the changes in chromatin.

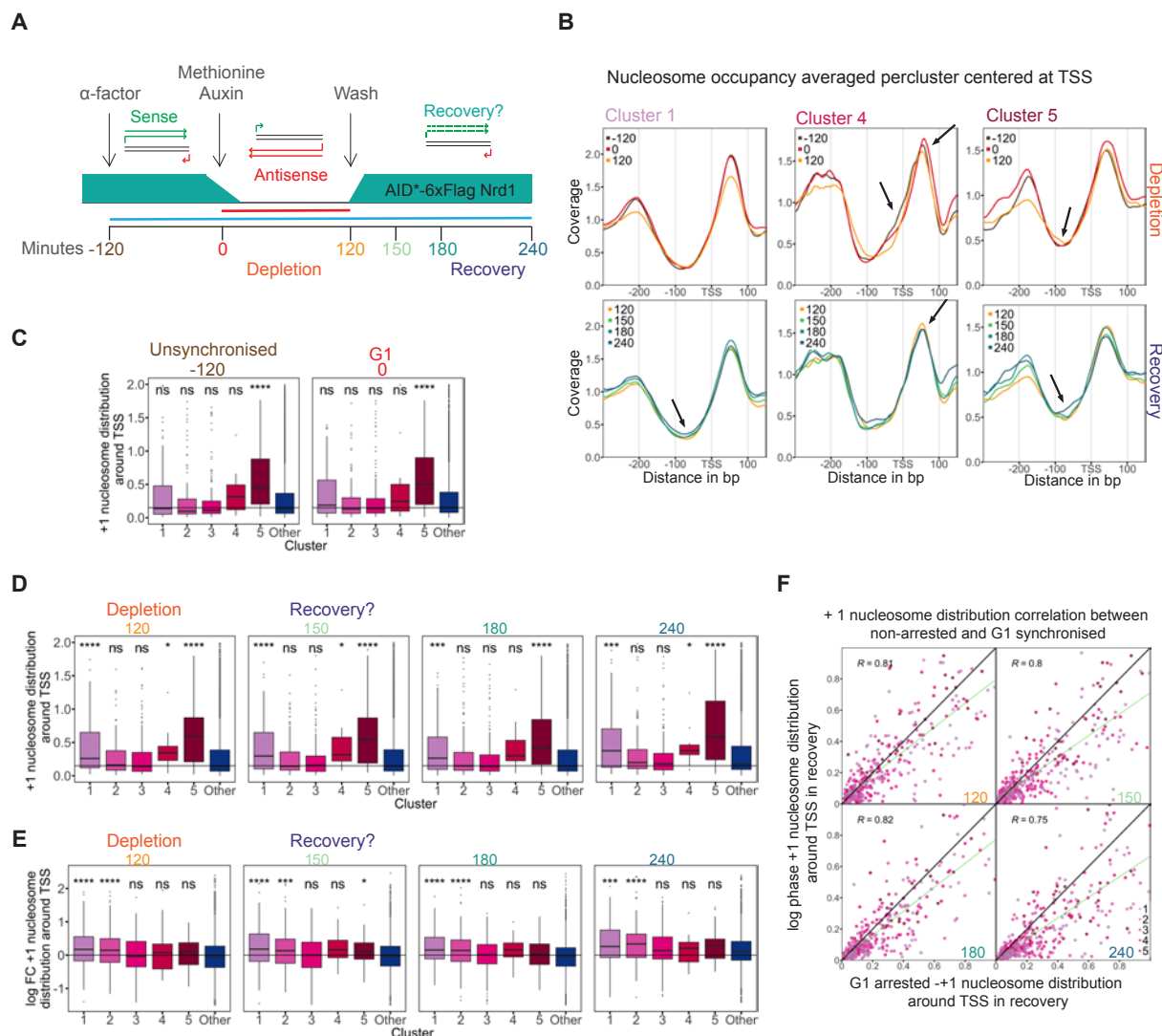


Figure 3. Chromatin recovery from Antisense-repressed state is replication dependent.

(A) Experimental scheme outline. Log phase growing cells were synchronised by adding α -factor at -120 min. Auxin was added at time 0 to deplete Nrd1 and was washed away at 120 min. MNase-seq was performed at the indicated time points.

(B) MNase-seq profile of nucleosome occupancy is shown with the indicated time points for cluster 1, 4 and 5. The coverage was averaged around the TSS.

(C) The +1 nucleosome distribution around the TSS is shown between unsynchronised and synchronised samples in the experiment.

(D) +1 nucleosome distribution profiles & (E) fold change in +1 distribution profiles for the depletion and recovery time points. Each cluster is compared to the non-changing set of Other genes at all time points. P-value is calculated using Wilcox test.

(F) The correlation plot between +1 nucleosome distribution between log phase cells and G1 synchronised cells at the indicated time points.

Changes in acetylation and +1 distribution could be mediated by histone exchange and chromatin factors. Replication is one of the major programs in the cell that might help dilute the deposited methyl marks and it also promotes deposition of new histones that are actually acetylated (Alabert, 2015; Alabert et al., 2017; Petryk et al., 2018; Reveron-Gomez et al., 2018).

Replication promotes recovery from Antisense-mediated repression

To measure the recovery of sense transcription independently of the dilution of chromatin marks by replication, the same experiment was performed in the presence of α -factor (Figure 3A). The cells were synchronised for 2 hours before Nrd1 depletion and washing of auxin was also performed in the presence of the α -factor. Under these conditions, nucleosome occupancy was observed to be increased from 0 min to 120 min of depletion for all the clusters (Figure 3B and S4A). Notably, clusters 4 and 5 show a change in the +1 nucleosome position away from the NDR going from unsynchronised to the synchronised state, in both tagged and untagged strains (Figure 3B and S4B). Nonetheless, these clusters closed upon depletion of Nrd1. The changes in the +1 nucleosome distribution during synchronization were comparably small (Figure 3C).

The +1 nucleosome increased during depletion but in contrast to the recovery observed in log phase, there was no recovery in the nucleosome distribution during G1 (Figure 3D and 3E). The increase in +1 distribution towards the NDR was specific for the tagged strain and was not present in the untagged strain (Figure S4C and S4D). Comparing recovery in the +1 distribution during log phase and in G1 arrested cells, we observed a clear increase in the dots in the lower triangle at the later time points, indicating large values in G1 (Figure 3F). Thus, replication-mediated chromatin resetting plays a role in restoration of sense transcription. The resetting mechanism might increase the naive nucleosomes that are acetylated. Another active mechanism that could mediate the resetting is acetylation by histone acetyl transferases (HATs).

Legend continued for Figure 4.

absence of Rtt109.

(E) +1 nucleosome distribution profile in the 5 clusters compared to the control set (Other), in the Rtt109-FRB strain in the presence of Rapamycin.

(F) Log FC +1 nucleosome distribution compared to 0 min. The profiles are comparing the -Rap and +Rap conditions for each cluster at the indicated time points for Esa1-FRB strain; +Rap is shown with darker shades of the cluster colors.

(G) Log FC +1 nucleosome distribution to 0 min. The boxplots are comparing the distribution in Recovery at 135 min and 150 min to the depletion timepoint of 120 min. The two separate panels show the difference in -Rap and +Rap respectively. The p-value was calculated using Wilcox test in the Figures 4C, 4E, 4F and 4G. All the non-indicated +/-Rap comparison values are non-significant.



Figure 4. Histone acetylation helps to recover from Antisense mediated repression instantly.

(A) Outline of the experiment. *Esa1* or *Rtt109* were tagged with Frb in the *AID**-*Nrd1* strain. *Nrd1* was depleted by adding Auxin at time 0 min. Rapamycin was added at time 110 min just before washing at 120 min. The recovery was observed at indicated time points while *Esa1* or *Rtt109* are anchored away.

(B) Nucleosome occupancy profile is shown for depletion and recovery in both presence and absence of *Esa1-Frb* for clusters 1 and 5.

(C) Changes in the +1 nucleosome distribution in clusters as compared to control (Other) at the indicated time points in *Esa1-Frb* strain in presence of Rapamycin.

(D) Nucleosome coverage profile for clusters 1 and 5; the recovery is shown both in presence or

HAT-mediated acetylation promotes immediate opening of NDR and stimulates transcription

To measure the recovery in the absence of histone acetyltransferase activity, we tagged the HAT encoding genes *ESA1* or *RTT109* with FRB in the *tor1-1* background allowing to anchor away the *Esa1* and *Rtt109* proteins upon addition of Rapamycin (Haruki et al., 2008). These strains were transformed with TIR1 containing construct promoting Auxin uptake and *Nrd1* was tagged with AID* with a *pmet* promoter (see Experimental Procedures). Thus, these strains promote double dynamic depletion of *Nrd1* and HATs when subjected to different treatments. The strains were growing as wild-type in the absence of either treatment (data not shown). *Esa1* was examined in these experiments because it is an essential HAT with widespread functions. *Rtt109* was chosen because loss of this HAT leads to reduced AS and both coding and non-coding transcription more generally (Topal et al., 2019). Moreover, *Rtt109* is also involved in histone turnover.

The experiments were done as shown in Figure 4A and MNase-seq was performed at the indicated time points. *Nrd1* was rapidly depleted in the presence of the HAT. At 110 minutes, Rapamycin was added in half the culture just before the depletion time point of 120 minutes. This was followed by washing of the Auxin in the presence of Rapamycin. Thus, the recovery was followed both in presence and absence of HATs. For both the *Esa1* and *Rtt109* anchor away strains, *Nrd1* depletion from 0 to 120 min led to increases in nucleosome occupancy similar to those observed in the log phase MNase-seq experiments (Figure 4B, 4C, 4D and 4E).

The recovery of the *Esa1*-FRB strain in -Rap conditions was very similar to the log phase MNase-seq experiment (Figure S5A and S5C). However, in the presence of Rapamycin, when *Esa1* was anchored away, the recovery in nucleosome distribution was clearly delayed (Figure 4C and 4F). Being an essential gene and a global H4 acetyltransferase, an effect of *Esa1* anchor away was observed on the control set of genes (Figure S5D). At 120 mins, there is a slight difference in +/-Rap which increases at 135 min. The rapid opening of NDRs in -Rap occurred at the 135 min timepoint (Figure 4F, first panel), just after the washing, but in the tagged strain there was no recovery at 135 min. Although, there is global closing of the promoters (Figure S5D). The clusters 1, 2 and 3 had even higher nucleosome density in the NDRs as compared to others at 135 min (Figure 4C) and had a very high nucleosome density as compared to -Rap condition (Figure 4F).

When comparing the Recovery in -Rap conditions, the +1 distribution decreased significantly when *Esa1* was present, while it didn't in the absence of the HAT (Figure 4G). The significantly opened NDR also implies that the *Esa1*-mediated acetylation helps clearing the NDR, which results in higher recruitment of the PIC machinery and the immediate increase in transcription. These observations indicate that *Esa1*-mediated acetylation is causal in immediate sense recovery. At later time points,

other HATs may intervene and there is compensation for Esa1; alternatively there is closing of NDRs globally and hence we start to measure indirect effects.

In the case of Rtt109, there was no change in the +1 nucleosome distribution between – and + Rap conditions (Figure 4D, 4E and S5B). We cannot measure, but the effect of Rtt109 depletion may be to slow down histone exchange. *The HAT data are very recent and the final conclusions are still under consideration.*

ANALYSES TO DO

Making a Predictive Model

The recovery response to AS was not dependent on the pattern of AS (Figure S1G). But it is more dependent on the inherent characteristics of the promoter. From the data presented here, we could get the information for NDR size, acetylation levels, initial expression levels of both Sense and Antisense and fold change in expression. The steady-state levels of other features of the promoters, for example TF, TBP occupancy could be extracted from (Rhee and Pugh, 2012). Therefore, we could model the pattern of expression observed in recovery based on these characteristics. We could also determine what are the major determinants to define the clusters.

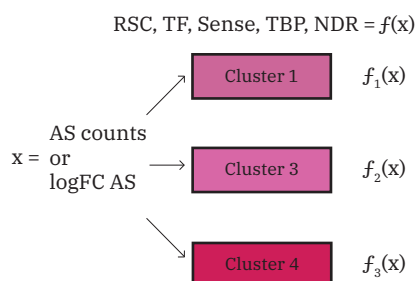


Figure: Scheme of predictive model calculation

Analysing MNase-fragment size changes

MNase-ChIP-seq generates fragments of characteristic sizes, mainly consisting of 147 bp, but also 125 bp, 90 bp etc, which represent remodelling intermediates when DNA has lost contact with proximal or distal parts of a nucleosome in response to transcription dynamics (Ramachandran et al., 2017; Ramani et al., 2019). In our case, reduction in transcription leads to higher NDR nucleosome occupancy. This may also result in changed nucleosome dynamics, which might be captured in changes in the ratio of smaller DNA fragments, especially in MNase-ChIP-seq of H3K18ac, which needs to be reanalysed.

Measure the H3K36me3 and Recovery in Gcn5 HAT

We know that the upregulation in Sense expression is specific of the AS repressed genes. However, the major signal connecting the increase in acetylation to the moment AS readthrough is turned off is still missing. A major hint is provided by the G1-arrest experiment, as there was clearly delayed recovery. It is possible that either acetylation is delayed with reduced histone exchange; alternatively, there may be increased residence time of the H3K36me3 in that state, which somehow inhibits HAT activity.

We performed the recovery in two HAT mutants and observed that Esa1 is associated with a rapid recovery by promoting the opening of the NDR. Of note, we measured an increase in H3K18ac, which is known to be also mediated by Gcn5 and it is therefore likely that both HATs play a role in the recovery by promoting acetylation. It would therefore be informative to measure recovery in a Gcn5 anchor-away strain as well. These possibilities could be addressed in the context of an independent study to solve the complete mechanism.

DISCUSSION

In the discussion section of the thesis.

AUTHOR CONTRIBUTIONS

J.K.G. performed the experiments. J.K.G., J.M.N. and J.S. analysed the data. J.K.G. and F.S. conceived the study. F.S. and J.S. supervised the study. J.K.G., F.S. and J.S. interpreted the data. *Will change, when we actually write it.*

ACKNOWLEDGEMENTS

The AID* Nrd1-tagged strains were kindly shared by the Tollervey lab. I would like to thank Géraldine for her invaluable help in preparing all the media for the experiments. The sequencing was performed at the iGE3 genomics platform of the University of Geneva. The work was supported by the funds from Swiss National Science Foundation, iGE3 and the Canton of Geneva. *Will change, when we actually write it.*

EXPERIMENTAL PROCEDURES

Saccharomyces cerevisiae strains and growth

The *S. cerevisiae* strains used for experiments in Figures 1, 2 and 3 are derived from BY4741 (*MATa*, *his3*, $\Delta 1$ *leu2* $\Delta 0$ *met15* $\Delta 0$ *ura3* $\Delta 0$). The strains used in Figures 1 and 2 were kindly provided by the Tollervey lab and are described in (Bresson et al., 2017). These strains were transformed with *Leu2* with primers flanking *bar1* to synchronise the cells in G1. For HAT anchor away, the strain with an anchor away background (Haruki et al., 2008), was sequentially transformed with the amplified DNA containing the TIR1 construct, followed by transformation with amplified *pmet-AID*-Nrd1* construct from the strain 1. The last was tagging the desired HAT with the FRB with an amplified construct.

The cells were grown in 2% glucose containing Kaiser SC medium, lacking methionine. For *Nrd1* depletion, Auxin was added at a final concentration of 1mM together with 670 μ M of Methionine. The washing was performed with Kaiser SC 2% glucose medium. Anchor-away of the HATs, *Esa1* or *Rtt109*, was induced by adding 1 μ g/mL final concentration of Rapamycin. G1 synchronisation was performed by adding 100 ng/ μ L of α -factor and the repeated addition of half the amount every hour after 2 hours.

Experimental Models: Organisms/Strains

REAGENT OR RESOURCE	SOURCE	IDENTIFIER
<i>S. cerevisiae</i> ySB036	(Bresson et al., 2017)	BY4741 TIR1:his3
<i>S. cerevisiae</i> ySB043	(Bresson et al., 2017)	BY4741 TIR1:his3 <i>Met15 P_{MET25}-AID*-flag-Nrd1</i>
<i>S. cerevisiae</i> (FSY8191)	This study	BY4741 TIR1:his3 <i>bar1:leu2</i>
<i>S. cerevisiae</i> (FSY8192)	This study	BY4741 TIR1:his3 <i>Met15 P_{MET25}-AID*-flag-Nrd1 bar1:leu2</i>
<i>S. cerevisiae</i> (FSY5712)	Strubin Lab (Unige)	<i>MATa</i> , <i>tor1-1</i> , <i>fpr1 :loxP-LEU2-loxP RPL13A-2xFKBP12 :loxP bar1:URA3</i>
<i>S. cerevisiae</i> (FSY8667)	This study	<i>MATa</i> , <i>tor1-1</i> , <i>fpr1 :loxP-LEU2-loxP RPL13A-2xFKBP12 :loxP bar1:URA3 TIR1:his3 P_{MET25}-AID*-flag-Nrd1 Rtt109-FRB:KanMX6</i>
<i>S. cerevisiae</i> (FSY8669)	This study	<i>MATa</i> , <i>tor1-1</i> , <i>fpr1 :loxP-LEU2-loxP RPL13A-2xFKBP12 :loxP bar1:URA3 TIR1:his3 P_{MET25}-AID*-flag-Nrd1 Esa1-FRB:KanMX6</i>

Cell culture and 4-thiouracil labelling and Sequencing

The 4-thiouracil (4-tU) experiment was performed as described in the protocols of (Baptista and Devys, 2018) and (Schmid et al., 2019) with the following modifications. AID*-Nrd1 and untagged control strains were inoculated in the evening and diluted in the morning to $OD_{600}=0.2-0.3$. At each time point, 100 mL of $OD_{600}=0.8$ was labelled with 4-thiouracil at a final concentration of 10 μ M. The labelling was performed for 4 min. The reaction was stopped by adding 100 mL of -20 °C chilled 100% ethanol. The samples were kept in the fridge until collection. Cells were collected by centrifuging at 2000 rpm for 3 min at 4 °C. Cells were washed two times with water and the pellet was collected and stored at -80 °C.

RNA extraction was performed using the ThermoFisher RiboPure RNA purification kit (Cat#AM1926). The purification was performed by following the manufacturer's protocol. RNA concentration was measured using nanodrop and between 300-500 μ g RNA was used for the biotinylation protocol. The total RNA for each time point was diluted to the same final concentration and amount (330 μ g RNA in 140 μ L).

Biotinylation was performed by first heating RNA for 10 min at 65°C followed by cooling for 2 min. An equal volume of biotin-HPDP was then added from a stock of 1 mg/mL biotin-HPDP in DMSO. The mixture was completed with 1/10th volume of Biotinylation buffer prepared in DEPC-treated water (100 mM Tris-HCl, pH 7.5 and 10 mM EDTA). The reaction was incubated for 3 hours at room temperature with gentle agitation. RNA was purified by adding an equal amount of chloroform to the tubes, followed by vigorous mixing. The samples were centrifuged at 13000g for 5 min at 4 °C. The upper phase was transferred to new Eppendorf tubes and 1/10th volume of 5M NaCl and an equal amount of isopropanol were added to the tubes and centrifuged at 13000g for 30 min at 4 °C. The pellet was washed with 75% ethanol and the RNA was resuspended in 100 μ L DEPC-treated water.

Streptavidin purification was started by heat denaturation of RNA at 65 °C for 10 min, followed by cooling on ice for 5 min. 100 μ L of streptavidin coated beads (diluted 6 fold) were added to the biotinylated RNA. The samples were incubated by shaking for 90 min at room temperature. The columns were equilibrated with 900 μ L of washing buffer (100 mM Tris-HCl, pH 7.5, 10mM EDTA, 1M NaCl and 0.1% Tween 20, in DEPC water). The beads RNA mixture was applied to the column and the flowthrough was collected and applied again. The column was washed five times with increasing volumes of washing buffer (600 μ L – 1000 μ L). RNA was eluted twice with 200 μ L of 0.1 M DTT, ending with a 400 μ L eluate. RNA was purified by precipitating with 0.1 volume of 3M NaOAc, pH 5.2 and 3 volumes of 100% ice cold ethanol and 2 μ L of 20 mg/mL glycogen (RNA grade, ThermoFischer) at -20 °C.

RNA was recovered by centrifugation and resuspended in 23 μ L of DEPC-treated water. Ribodepletion was performed with the Ribominus Transcriptome Isolation Kit (Invitrogen), using the manufacturer's protocol. Purified RNA was ethanol precipitated and redissolved in 6.5 μ L of DEPC-treated water. A Stranded library was prepared using NEBNext Ultra II Directional RNA library prep Kit from Illumina. The final library concentration was measured using the Qubit dsDNA High Sensitivity assay kit (Invitrogen). The samples were sequenced at the iGE3 genomics platform of the University of Geneva.

MNase-Seq and MNase-ChIP-Seq

The cells were grown overnight in the Kaiser SC medium and diluted to $OD_{600}=0.2$ on the day of the experiment. The H3K18ac MNase-ChIP-seq experiment and MNase-seq experiments were performed as previously described in (Gill et al., 2020).

List of coordinates and nucleosomes

The data analysis was performed by using the gene list of TSS from the (Pelechano et al., 2013) and the +1 nucleosome position for all the transcripts was taken from (Weiner et al., 2015).

4-tU RNA-seq analysis

Reads were aligned using STAR aligner. Samtools was used to generate the Bam file from aligned reads. HTseq was used to count the number of reads per feature on both the strands. Bedtools was used to generate the coverage profile for 4tU. Fold change analysis and Kmeans were performed in R. Critical parts of the script are included in the appendix A.

MNase and MNase ChIP-seq analysis

Paired-end reads were aligned to the sacCer3 genome using Bowtie2. PCR duplicates were removed. The coverage per feature was calculated using the center of the paired-end fragments and they were filtered based on size in the range of 120-200 bp using GenomicRanges package, and the total reads were normalised per chromosome as in plot2DO created by Chereji and colleagues (Beati and Chereji, 2020). To measure the changes in the level of acetylation, read centers within the 100 bp around the +1 nucleosome were added and the values compared at different timepoints normalised to 0 min. The +1 nucleosome distribution profiles for MNase-Seq experiments were calculated as the ratio between the read dyads observed between -100 bp and TSS and the read dyads observed between TSS and +100 bp for every gene. A representative script is shown in Appendix A.

Figures

All the figures were made using R. The significance of mean difference was calculated using Mann-Whitney Wilcox test.

SUPPLEMENTAL INFORMATION

Supplementary PDF includes 5 figures related to the data presented here. *It is part of the supplementary section of the thesis.*

REFERENCES

- Alabert, C. (2015). Two distinct modes for propagation of histone PTMs across the cell cycle. *Genes Dev.* *29*.
- Alabert, C., Jasencakova, Z., and Groth, A. (2017). Chromatin Replication and Histone Dynamics. *Adv Exp Med Biol* *1042*, 311-333.
- Alabert, C., Loos, C., Voelker-Albert, M., Graziano, S., Forne, I., Reveron-Gomez, N., Schuh, L., Hasenauer, J., Marr, C., Imhof, A., *et al.* (2020). Domain Model Explains Propagation Dynamics and Stability of Histone H3K27 and H3K36 Methylation Landscapes. *Cell Rep* *30*, 1223-1234 e1228.
- Allard, S., Utley, R.T., Savard, J., Clarke, A., Grant, P., Brandl, C.J., Pillus, L., Workman, J.L., and Cote, J. (1999). NuA4, an essential transcription adaptor/histone H4 acetyltransferase complex containing Esa1p and the ATM-related cofactor Tra1p. *EMBO J* *18*, 5108-5119.
- Allis, C.D., and Jenuwein, T. (2016). The molecular hallmarks of epigenetic control. *Nat. Rev. Genet.* *17*.
- Baptista, T., and Devys, D. (2018). *Saccharomyces cerevisiae* Metabolic Labeling with 4-thiouracil and the Quantification of Newly Synthesized mRNA As a Proxy for RNA Polymerase II Activity. *JoVE*, e57982.
- Beati, P., and Chereji, R.V. (2020). Creating 2D Occupancy Plots Using plot2DO. *Methods Mol Biol* *2117*, 93-108.
- Bresson, S., Tuck, A., Staneva, D., and Tollervey, D. (2017). Nuclear RNA Decay Pathways Aid Rapid Remodeling of Gene Expression in Yeast. *Mol Cell* *65*, 787-800 e785.
- Camblong, J., Iglesias, N., Fickentscher, C., Dieppois, G., and Stutz, F. (2007). Antisense RNA stabilization induces transcriptional gene silencing via histone deacetylation in *S. cerevisiae*. *Cell* *131*, 706-717.
- Carninci, P. (2005). The transcriptional landscape of the mammalian genome. *Science* *309*.
- Carrozza, M.J., Li, B., Florens, L., Suganuma, T., Swanson, S.K., Lee, K.K., Shia, W.J., Anderson, S., Yates, J., Washburn, M.P., *et al.* (2005). Histone H3 methylation by Set2 directs deacetylation of coding regions by Rpd3S to suppress spurious intragenic transcription. *Cell* *123*, 581-592.
- Castelnuovo, M., Zaugg, J.B., Guffanti, E., Maffioletti, A., Camblong, J., Xu, Z., Clauder-Munster, S., Steinmetz, L.M., Luscombe, N.M., and Stutz, F. (2014). Role of histone modifications and early termination in pervasive transcription and antisense-mediated gene silencing in yeast. *Nucleic Acids Res* *42*, 4348-4362.
- Churchman, L.S., and Weissman, J.S. (2011). Nascent transcript sequencing visualizes transcription at nucleotide resolution. *Nature* *469*, 368-373.
- Clarke, A.S., Lowell, J.E., Jacobson, S.J., and Pillus, L. (1999). Esa1p is an essential histone acetyltransferase required for cell cycle progression. *Mol. Cell. Biol.* *19*.
- Das, S., Sarkar, D., and Das, B. (2017). The interplay between transcription and mRNA degradation in *Saccharomyces cerevisiae*. *Microb Cell* *4*, 212-228.
- Derrien, T. (2012). The GENCODE v7 catalog of human long noncoding RNAs: analysis of their gene structure, evolution, and expression. *Genome Res.* *22*.
- Dion, M.F., Kaplan, T., Kim, M., Buratowski, S., Friedman, N., and Rando, O.J. (2007). Dynamics of replication-independent histone turnover in budding yeast. *Science* *315*, 1405-1408.
- Djebali, S. (2012). Landscape of transcription in human cells. *Nature* *489*.
- Gill, J.K., Maffioletti, A., Garcia-Moliner, V., Stutz, F., and Soudet, J. (2020). Fine Chromatin-Driven Mechanism of Transcription Interference by Antisense Noncoding Transcription. *Cell Rep* *31*, 107612.

- Halley-Stott, R.P., and Gurdon, J.B. (2013). Epigenetic memory in the context of nuclear reprogramming and cancer. *Brief Funct Genomics* *12*, 164-173.
- Haruki, H., Nishikawa, J., and Laemmli, U.K. (2008). The anchor-away technique: rapid, conditional establishment of yeast mutant phenotypes. *Mol Cell* *31*, 925-932.
- Kaplan, C.D., Laprade, L., and Winston, F. (2003). Transcription elongation factors repress transcription initiation from cryptic sites. *Science* *301*, 1096-1099.
- Kharchenko, P.V., Alekseyenko, A.A., Schwartz, Y.B., Minoda, A., Riddle, N.C., Ernst, J., Sabo, P.J., Larschan, E., Gorchakov, A.A., Gu, T., *et al.* (2011). Comprehensive analysis of the chromatin landscape in *Drosophila melanogaster*. *Nature* *471*, 480-485.
- Kim, J.H., Lee, B.B., Oh, Y.M., Zhu, C., Steinmetz, L.M., Lee, Y., Kim, W.K., Lee, S.B., Buratowski, S., and Kim, T. (2016). Modulation of mRNA and lncRNA expression dynamics by the Set2-Rpd3S pathway. *Nat Commun* *7*, 13534.
- Kim, T., Xu, Z., Clauder-Munster, S., Steinmetz, L.M., and Buratowski, S. (2012). Set3 HDAC mediates effects of overlapping noncoding transcription on gene induction kinetics. *Cell* *150*, 1158-1169.
- Li, B., Howe, L., Anderson, S., Yates, J.R., 3rd, and Workman, J.L. (2003). The Set2 histone methyltransferase functions through the phosphorylated carboxyl-terminal domain of RNA polymerase II. *J Biol Chem* *278*, 8897-8903.
- Mellor, J., Woloszczuk, R., and Howe, F.S. (2016). The Interleaved Genome. *Trends Genet* *32*, 57-71.
- Morawska, M., and Ulrich, H.D. (2013). An expanded tool kit for the auxin-inducible degron system in budding yeast. *Yeast* *30*, 341-351.
- Murray, S.C., Haenni, S., Howe, F.S., Fischl, H., Chocian, K., Nair, A., and Mellor, J. (2015). Sense and antisense transcription are associated with distinct chromatin architectures across genes. *Nucleic Acids Res* *43*, 7823-7837.
- Pelechano, V., Wei, W., and Steinmetz, L.M. (2013). Extensive transcriptional heterogeneity revealed by isoform profiling. *Nature* *497*, 127-131.
- Petryk, N., Dalby, M., Wenger, A., Stromme, C.B., Strandsby, A., Andersson, R., and Groth, A. (2018). MCM2 promotes symmetric inheritance of modified histones during DNA replication. *Science* *361*, 1389-1392.
- Porrua, O., and Libri, D. (2015). Characterization of the mechanisms of transcription termination by the helicase Sen1. *Methods Mol Biol* *1259*, 313-331.
- Proudfoot, N.J. (1986). Transcriptional interference and termination between duplicated alpha-globin gene constructs suggests a novel mechanism for gene regulation. *Nature* *322*, 562-565.
- Ramachandran, S., Ahmad, K., and Henikoff, S. (2017). Transcription and remodeling produce asymmetrically unwrapped nucleosomal intermediates. *Mol. Cell* *68*.
- Ramani, V., Qiu, R., and Shendure, J. (2019). High Sensitivity Profiling of Chromatin Structure by MNase-SSP. *Cell Rep* *26*, 2465-2476 e2464.
- Rando, O.J. (2012). Combinatorial complexity in chromatin structure and function: revisiting the histone code. *Curr Opin Genet Dev* *22*, 148-155.
- Reinberg, D., and Vales, L.D. (2018). Chromatin domains rich in inheritance. *Science* *361*, 33-34.
- Reveron-Gomez, N., Gonzalez-Aguilera, C., Stewart-Morgan, K.R., Petryk, N., Flury, V., Graziano, S., Johansen, J.V., Jakobsen, J.S., Alabert, C., and Groth, A. (2018). Accurate Recycling of Parental Histones Reproduces the Histone Modification Landscape during DNA Replication. *Mol Cell* *72*, 239-249 e235.
- Rhee, H.S., and Pugh, B.F. (2012). Genome-wide structure and organization of eukaryotic pre-initiation complexes. *Nature* *483*, 295-301.
- Rufiange, A., Jacques, P.E., Bhat, W., Robert, F., and Nourani, A. (2007). Genome-wide replication-independent histone H3 exchange occurs predominantly at promoters and implicates H3 K56 acetylation and Asf1. *Molecular cell* *27*, 393-405.
- Schmid, M., Tudek, A., and Jensen, T.H. (2019). Preparation of RNA 3' End Sequencing Libraries of Total and 4-thiouracil Labeled RNA for Simultaneous Measurement of Transcription, RNA Synthesis and Decay in *S. cerevisiae*. *Bio Protoc* *9*.
- Schulz, D., Schwalb, B., Kiesel, A., Baejen, C., Torkler, P., Gagneur, J., Soeding, J., and Cramer, P. (2013). Transcriptome surveillance by selective termination of noncoding RNA synthesis. *Cell* *155*, 1075-1087.
- Smolle, M. (2012). Chromatin remodelers Isw1 and Chd1 maintain chromatin structure during transcription by preventing histone exchange. *Nat. Struct. Mol. Biol.* *19*.
- Suganuma, T., and Workman, J.L. (2008). Crosstalk among Histone Modifications. *Cell* *135*, 604-607.
- Thiriet, C., and Hayes, J.J. (2005). Replication-independent core histone dynamics at transcriptionally active loci in vivo. *Genes & development* *19*, 677-682.

- Tirosh, I., and Barkai, N. (2008). Two strategies for gene regulation by promoter nucleosomes. *Genome research* *18*, 1084-1091.
- Topal, S., Vasseur, P., Radman-Livaja, M., and Peterson, C.L. (2019). Distinct transcriptional roles for Histone H3-K56 acetylation during the cell cycle in Yeast. *Nat Commun* *10*, 4372.
- Venkatesh, S., Li, H., Gogol, M.M., and Workman, J.L. (2016). Selective suppression of antisense transcription by Set2-mediated H3K36 methylation. *Nat Commun* *7*, 13610.
- Venkatesh, S., Smolle, M., Li, H., Gogol, M.M., Saint, M., Kumar, S., Natarajan, K., and Workman, J.L. (2012). Set2 methylation of histone H3 lysine 36 suppresses histone exchange on transcribed genes. *Nature* *489*, 452-455.
- Watanabe, S., Radman-Livaja, M., Rando, O.J., and Peterson, C.L. (2013). A histone acetylation switch regulates H2A. Z deposition by the SWR-C remodeling enzyme. *Science* *340*.
- Weiner, A., Hsieh, T.H., Appleboim, A., Chen, H.V., Rahat, A., Amit, I., Rando, O.J., and Friedman, N. (2015). High-resolution chromatin dynamics during a yeast stress response. *Mol Cell* *58*, 371-386.
- Williams, S.K., Truong, D., and Tyler, J.K. (2008). Acetylation in the globular core of histone H3 on lysine 56 promotes chromatin disassembly during transcriptional activation. *Proc. Natl Acad. Sci. USA* *105*.
- Zaugg, J.B., and Luscombe, N.M. (2012). A genomic model of condition-specific nucleosome behavior explains transcriptional activity in yeast. *Genome research* *22*, 84-94.

Discussion

1 Antisense Mediates Transcription Interference Through Changes in Chromatin at NDR

The first study described in this thesis addresses the mechanism of antisense-induced transcription interference by following the changes in a dynamic rather than steady-state manner. By measuring the dynamic changes, we defined the direct effect of antisense extension into the promoters and therefore avoided to measure the combined effects of molecular feedback and feedforward loops that buffer the final phenotype. We showed that changes in histone modifications and nucleosome positioning are linked to changes in RSC and PIC occupancy at the promoter. These are highly conserved factors.

Nrd1 is not conserved in higher eukaryotes but similar mechanisms have evolved to regulate transcription at a smaller scale in the context of local regulatory systems. For example, antisense transcription into an exon results in its exclusion from the final transcript and AS transcription regulates splicing in humans (Morrissy et al., 2011). In higher eukaryotes, the analysis of lncRNA transcription also suggests that it is the act of transcription rather than the RNA product that is the source of regulatory activity (Engreitz et al., 2016; Kopp and Mendell, 2018). A substantial number of genes in humans also present antisense transcription (Chen et al., 2004; Vallon-Christersson et al., 2007). Hence it would be worth studying whether the chromatin regulators involved at the molecular level act in the same manner as in yeast.

1.1 Precise Positioning of Nucleosomes Regulates Transcription Initiation

Antisense-mediated interference is visible only when antisense transcription extends over the promoter NDR of the sense gene (Gill et al., 2020; Schulz et al., 2013). The NDR is the site of PIC and transcription factor recruitment. This study supports that reduced recruitment and occupancy of PIC and transcription initiation factors as one of the important steps in antisense-mediated regulation. The repositioning of the +1 and -1 nucleosomes leads to increased nucleosome occupancy at the NDR. This repositioning physically hinders TBP binding and/or results in its reduced residence time on DNA.

The TSS is located ~13 bp into the +1 nucleosome. We observed that in response to AS transcription, the newly H3K36 tri-methylated +1 nucleosome shifts towards the NDR and acquires a new translational setting as compared to the acetylated H3K18ac nucleosome at the +1 position at steady state. The difference we observe is not huge as the phenomenon might only be present in a subpopulation or could be very transient, but similar changes have been shown to translate into observable differences during transcription (Chereji et al., 2018). The shifted +1 nucleosome has been shown to be repressive towards transcription initiation (Klein-Brill et al., 2019; Kubik, 2018) as we observe in our studies. Changed +1 position has also been shown to result in usage of an alternative TSS (Klein-Brill et al., 2019). This has also been shown to result in the altered coding potential of the transcript (Malabat et al., 2015; Pelechano et al., 2013).

The same principle might apply to genic regions that are usually constitutively associated with well-spaced nucleosomal arrays and devoid of nucleosome depleted regions. It was shown that in the absence of Set2, there is no co-transcriptional deposition of H3K36me3 and therefore no deacetylation by Rpd3 (Smolle et al., 2013). This gives rise to multiple non-specific TSSs (Malabat et al., 2015), suggesting the generation of opportunistic NDR formation in the middle of coding regions (Wei et al., 2019). Indeed, non-coding intragenic transcripts initiate from these NDRs in the absence of Set2 (Venkatesh et al., 2012). Thus, the H3K36me3 mark might be one important component of the cascade of chromatin regulatory events that distinguishes relatively closed genic regions from promoter regions where this mark is usually absent.

In conclusion, transcription passage indistinctly narrows the distance between nucleosomes, partly through the deposition of histone marks such as H3K36me3 during elongation. Thus, a locus undergoing transcription read-through will show reduced accessibility to *trans-acting* factors, for example PIC components, due to higher occupancy of nucleosomes.

1.2 Binding of Chromatin Regulators to Antisense Modified NDR Chromatin

Upon loss of the Set2/Rpd3 pathway, we did not observe complete abolition of antisense interference, suggesting that more than one pathway might contribute to the final repression we observe in the system. H3K36me3 itself is known to restrict nucleosome dynamics and therefore to hamper transcription (Smolle et al., 2013). The histone chaperones Spt6 and FACT also contribute to the repression or closing of the transcribed region (Jeronimo et al., 2015; Kaplan et al., 2003). Moreover, H3K36me3 can recruit the FACT complex that participates in nucleosome assembly (Carvalho et al., 2013). Thus, these histone chaperones are good candidates for parallel pathways maintaining TI. Another good candidate might be the SET3 HDAC recruited through H3K4me2/me3 and known to be involved in TI (Kim Buratowski, 2012, 2016 publications). It would be of interest to observe TI in the absence of SET3 and histone chaperones or their combinations since we might observe more rescue.

We observed decreased binding of the RSC chromatin remodeler in response to the recruitment of the Rpd3 HDAC. Deacetylation could also promote the binding of INO80 and reduce the association of the SWR1 complex. This would result in lower levels of H2A.Z recruitment and make the promoter repressive. H3K36me3 is also recognised by Eaf3 present in NuA4 and by the PWWP domain in the Pdp3 component of NuA3 (Martin, 2017). Thus, NuA4 and NuA3 are two HAT complexes that could also be recruited to the promoter. NuA4 further shares 4 subunits with the SWR complex (Krogan et al., 2004), and might therefore promote SWR1 binding.

In summary, multiple pathways might either contribute to AS-mediated interference or act against the repression, which could be addressed in future studies.

1.3 Collisions of Transcribing RNA Pol II

We proposed that when transcription from the 3' end of a gene reaches the 5' end, it makes it repressive and the promoter becomes inhibitory for transcription initiation. It is possible that, in a subset of genes or the same gene in a cell population, transcription initiates from both ends at the same time; moreover, yeast has more than 1500 convergent gene pairs, thereby increasing the chance that transcription elongation complexes (ECs) might collide on the gene body.

It has been shown that T3 and T4 bacteriophage RNA polymerases can transcribe past one another (Ma and McAllister, 2009), and the non-transcribed strand has also been shown to be loosely bound to the transcribing polymerase (Kornberg, 2007). However, if there is evidence that the large eukaryotic ECs collide *in vitro* and cannot transcribe past one another. This results in backtracking

and *in vivo* collided RNAPII is removed via ubiquitination and degradation (Hobson et al., 2012). In our system, and also based on smFISH experiments, Sense-AS EC collisions must be rare *in vivo* as there is expression of mostly one type of transcript per cell (Castelnuovo et al., 2013; Gill et al., 2020); nevertheless, since the present study defines a population average, we cannot rule out the possibility that there might be a few.

One possibility to test this hypothesis would be to measure the larger fragments covered by RNAPII using ChIP-exo paired-end sequenced experiments. An increase in the amounts of large fragments that are potentially covered by 2 RNA polymerases when AS is induced, specifically on the genes that show increased AS, might indicate that AS transcription leads to collisions or at least stalling of head-on RNAPII on the DNA.

1.4 Formation of Antisense RNA Secondary Structures

Another mechanism that might contribute to antisense-mediated repression is the formation of RNA secondary structures and recruitment of chromatin regulatory factors through AS RNA. One common form of RNA secondary structure in the nucleus is R-loops, formed when the RNA:DNA hybrid is extended behind transcribing RNAPII. Another interesting possibility would be the formation of Sense-AS RNA dimers, if both could be transcribed simultaneously and remain associated with the transcribing locus. However, these structures are hard to detect and their functional consequences might include downregulation of both transcripts. Such dimers have been observed in higher eukaryotes, and recently also shown in yeast (Wery et al., 2016).

In *S. pombe* and higher eukaryotes, DNA-RNA hybrids or R-loops have been shown to mediate recruitment of repressive factors (Skourti-Stathaki and Proudfoot, 2014). In budding yeast, using an indirect experiment, it was reported that Set1-mediated repression of ribosomal protein genes (RPGs) is alleviated if the intron sequence is removed. The intron is transcribed into a potentially highly structured RNA that might recruit Set1 directly or through an indirect mechanism (Weiner et al., 2012). Furthermore, a study used random mutagenesis to reveal RNA-based silencers and found that many different artificially tethered RNAs are able to repress genes in a Sir-dependent manner (Kehayova and Liu, 2007). This study provides proof of principle that lncRNA-mediated complex sequestration and repression is possible in yeast in the absence of an RNAi machinery. Based on these observations, we can extrapolate that AS lncRNA may be an excellent candidate to mediate effects through this type of mechanism, which needs to be addressed in future.

2 Transcription Interference primes Sense Promoter for Activation

In eukaryotes, transcription initiation is highly controlled by *cis*-acting sequences and chromatin regulators. Even though transcription initiation is regulated and dependent on specific sequences, the genome is pervasively transcribed consisting of many overlapping units. It is relatively well established that a transcription event overlapping the promoter of another transcript results in downregulation of this transcription unit by transcription interference (Kim et al., 2016; Mellor et al., 2016; Proudfoot, 1986). However, once the repression occurs, defining what happens when the overlapping transcription is turned off was still an open question. In this study, we induced extension of AS transcription, resulting in transcription interference at AS-regulated genes (ARGs), followed by restoration of AS early termination. Under these conditions, we observed a rapid upregulation of the repressed transcription units. The mechanism of upregulation or reactivation is dependent on a replication-mediated resetting of the chromatin and on acetylation at the +1 nucleosome. The complete mechanism for the recovery of transcription and the factors that are necessary in this process could be the subject of future investigations.

2.1 Time Series Analysis reveals Transcription and Chromatin Dynamics

We observed a variety of patterns of transcription during recovery. At a certain timepoint of recovery, a subset of genes is upregulated, others are down-regulated and some come back to their original level of expression, all of which changed at the next time point. These dynamic oscillating behaviours in recovery cannot be deduced from a single snapshot that we usually perform during correlation analysis. The interpretation of the results and real direct relations are inferred from a time series analysis (TSA). This approach combined with the dynamic depletion and recovery of the proteins being analysed helps in establishing direct causal links between chromatin changes and expression.

In this study, the transient changes were observed in the presence of all the factors and in the absence of HATs. However, based on our previous studies, we know that AS mediates its affect through deposition of H3K36me3 (Gill et al., 2020). Therefore, changes in chromatin that could be attributed to demethylation need to be confirmed in future studies using time course analysis in the presence or absence of demethylases. The kinetics of recovery might change in the absence of the H3K36me3 demethylases Rph1, Jhd1 and Gis1. These were previously shown to affect the rate of H3K36me3 removal within ORFs, once transcription of the gene is stopped (Sein et al., 2015).

2.2 Transcription Interference Recovery is Promoter Type Dependent

In yeast, promoters have characteristic NDR sizes presenting a bimodal distribution, i.e. small NDRs have an average size of ~30bp and large NDRs close to ~130bp. Three of our gene clusters have large NDRs while clusters 4 and 5 have smaller NDRs. Upon antisense extension, we observe an increase in the +1 distribution towards the NDR for all ARGs, but changes were very different in magnitude for different classes. This might indicate that all 5 clusters respond to both AS induction and recovery, but the change in nucleosome occupancy may depend on promoter type and other characteristics. This has been observed before when NDR sizes were shown to be persistent between different growth conditions and even for genes whose expression changes in response to nutrient alterations (Zaugg and Luscombe, 2012). Thus, the magnitude of differences we observe with MNase-Seq might contribute to the transcription phenotype to varying degrees depending on other features of promoter definition (Results, Section-2, Figures 1 (p. 75) and 2 (p.78)).

For the clusters with large NDRs (mainly clusters 2 and 3), TF binding plays a more prominent role in regulating transcription levels and was previously shown to depend less on chromatin remodelling (Tirosh and Barkai, 2008). Nevertheless, we observed that AS-mediated transcriptional readthrough affects all ARGs and there is a consistent mechanism of recovery - an increase in H3K18 acetylation for all promoters containing different classes of NDRs. The changes in chromatin occur for all genes, however the magnitude of changes and precise oscillating pattern of recovery depend on the promoter type.

So far, promoters have been most commonly grouped based on their NDR size or binding of one major transcription factor (Huisinga and Pugh, 2004; Tirosh and Barkai, 2008). In our analyses, the promoter type needs to be defined based on a few more properties so that we can relate the changes in sense transcription in response to AS and more importantly predict what would happen to a promoter if a transcription overlap occurs. This could be performed by making a model of the extent of changes in AS, Sense, or other factors such as TF and TBP occupancy (Rhee and Pugh, 2012), that could explain the different Sense transcription recovery behaviours.

Transcription is currently viewed as a global phenomenon, covering on average 75% of the genome and giving rise to many transcripts that have at least one overlapping transcription unit at the 3' or 5' end. A transcription unit may downregulate the neighboring unit because it overlaps with its NDR. This can generate many inter-related transcription programs, which may be regulated in a similar manner. Therefore, transcription interference may play a global role as probably many NDRs are subjected to this type of regulation. However, NDRs may respond to overlapping transcription somewhat differently depending on individual characteristics, which may result in numerous

possible combinations of gene expression patterns in a cell. This may contribute significantly to the transcription complexity observed in eukaryotes that cannot be explained just by TF regulation. Although it is probably difficult to assign all the complex phenotypes to changes in transcription (Pelechano, 2017), a certain number of underlying principles can probably be determined.

2.3 Higher Acetylation could Mediate Recovery by Increasing Burst Size

Antisense-mediated TI has been previously shown to be used between the tandem *SUR7* and *GAL80* genes. In this case, Gal4 TF binding to the bidirectional promoter of *GAL80* results in the upregulation of *SUT719*, which is in antisense orientation to the upstream *SUR7* gene and hence results in its repression. Thus, antisense transcription can help in mediating regulatory signals to neighboring chromatin regions (Xu et al., 2011). This type of control has been observed in the regulation of *FLO11*, where two non-coding RNAs regulate toggle switch between expression and repression. This results in the expression of *FLO11* in some cells of a population while it is repressed in the others (Bumgarner et al., 2009). Antisense transcription was further shown to be associated with stress responsive genes or the genes that have to respond in a switch-like manner (Castelnuovo et al., 2014). The changes in expression levels of these genes are known to be regulated through modulation of the bursting frequencies (Larsson et al., 2019).

In our experiments, the recovery from AS-mediated repression is accompanied by a sudden increase in acetylation. The bursting frequency is known to correlate with the acetylation levels of the promoter (Chen et al., 2019). Therefore, the increase in expression during recovery that we observe might result from the increase in bursting frequency. The changes in burst frequency versus burst size are likely to translate into different distributions of RNA in different cells of the population (Liu et al., 2016).

Single molecule FISH analysis or RNA MS2 tagging (Lenstra et al., 2015) could be used to examine the expression of specific transcripts. It would give a better understanding and insight into the changes of expression patterns in individual cells. It could provide a valuable orthogonal dataset to the genome-wide recovery we observe and help in solving the mechanism. If during recovery, transcription is observed in more cells of the population, the recovery is likely due to an increase in bursting frequency; however, detection of more transcripts per cell, but in the same number of cells, would mean that an increase in burst size is responsible for the recovery. One would probably have to measure degradation rates as well to differentiate changes in transcript numbers due to an increase or decrease in RNA stability.

2.4 Histone turnover as the fastest way of changing chromatin around +1

Histone turnover is a mechanism for exchanging one of the older nucleosomes possessing a certain PTM state with naive histones from the soluble pool that are acetylated at H3K56. Since overlapping AS transcription deposits the H3K36me3 mark at +1, promoting acetylation via histone acetyl transferases might make the +1 nucleosome more labile and easy to exchange with the soluble histones lacking H3K36me3. H3K18ac is a known predictor of histone turnover along with H3K56ac (Weiner et al., 2015). The exchanged naive nucleosomes would also result in a weaker barrier for transcription as compared to H3K36me3 nucleosomes at +1 position (Gill et al., 2020; Soudet and Stutz, 2019; Venkatesh and Workman, 2015). Promoting higher histone turnover might itself result in less occupancy of nucleosomes in the promoter and hence more transcription initiation.

During recovery, when we observe a sudden increase in acetylation, the fate of deposited methyl marks should be ascertained in future investigations. It is possible that H3K36me3 is still present as shown in a recent study by Alabert and colleagues. Based on mass spectrometry data, the authors generated a model for the deposition of H3K36me_{1/2/3} and H3K27me_{1/2/3}. Once the H3K36 methyl mark was established at the site of H3K27me in higher eukaryotes, it was inherited for a few generations before being diluted by replication-dependent exchange (Alabert et al., 2020). Of note, the H3K27me₃ domains in higher eukaryotes are usually transcriptionally silent and hence the deposited H3K36me₃ is not subjected to histone exchange. This may be different in our case, since the +1 position is highly active and undergoing rapid histone turnover.

Therefore, it is worth examining how the changes in histone turnover might affect the kinetics of histone PTMs. To assign the observed behaviours to histone turnover, these studies need to be complemented with CAF1, FACT or ASF1 mutants affected in histone exchange (De Koning et al., 2007).

We observed delayed sense recovery during G1-arrest, which results in no replication-dependent histone exchange. In G1-arrested cells, lack of replication might prevent dilution of the H3K36me₃. In a study investigating promoter NDR recovery by restoring RSC, the reopening of the NDR was immediate even in G1-arrested cells (Klein-Brill et al., 2019); however, the +1 was always acetylated in this study, while we know from our previous work that an increase in H3K36me₃ results in deacetylation and reduced occupancy of RSC (Gill et al., 2020).

In summary, by reducing histone turnover during G1-arrest, either the H3K36me₃ is not diluted and therefore Rpd3 is present in the NDR and the deacetylated state is maintained hampering recovery. Alternatively, HATs can acetylate a nucleosome irrespective of H3K36me₃, leading to

histone turnover and promoting immediate recovery, yet their activity is reduced in G1 or has to be stimulated by histone turnover. Additional experiments need to be performed in the future to distinguish between these two possibilities.

2.5 Different Acetylation and Methylation kinetics might play a role in Recovery

We observed a major increase in acetylation at the 30 min timepoint just after the removal of AS readthrough that rapidly went back to the basal levels. This transient increase in acetylation probably resulted in the peak of sense expression that we observed in our 4tu-seq analysis. An earlier study focusing on yeast histone modifications in response to stress revealed transient changes in H4ac (Weiner et al., 2015). These modifications are known to positively correlate with Htz1(H2A.Z) occupancy at the +1 nucleosome, which is further linked to high nucleosome turnover. Therefore, the AS transcription phase might trigger a cascade of changes in modification levels that ultimately result in transcription upregulation during recovery. H4ac, H2A.Z, H3K56ac, H3K18ac, H3K4me3, H3K36me3 and H3K79me are worth investigating during transcriptional changes by individually removing different factors important in the cascade.

Histone methylation and acetylation dynamics differ with respect to cell cycle re-entry (Mews et al., 2014). The ordered waves of changes in PTMs were also observed during transcriptional reprogramming (Weiner et al., 2015). The changes in +1 nucleosome distribution and H3K18ac that we identified in our study finally result in an oscillating gene expression behaviour. It would be worth to know if the changes in different modifications at each step are due to inherently biochemically different reaction kinetics independent of each other, or whether one change acts as a signal for another event in a temporal manner. It would be worth to follow the individual modifications possibly on the same nucleosome with time, and perturb the system to see if these modifications act as an interdependent temporal cascade or as simple linear events, with biochemically different reaction kinetics that result in the observed RNA expression pattern.

It should be addressed whether the commonly observed stable PTM combinatorial complexity consists of all the thermodynamically stable states of chromatin and when overlapping transcription, AS in our case, perturbs the system, it induces a high energy state; during recovery, the oscillating pattern with decreasing amplitude may be the response to the release from the high energy state to go down to one of the stable commonly observed chromatin states.

2.6 Ambivalence of Set1C mediated H3K4me

Deposition of H3K4me3 by Set1 is enriched at +1 nucleosome and is highly correlated with H3K18ac in log phase growing cells. The Set1 methyltransferase performs both H3K4me2 and H3K4me3, which might have contrasting consequences on transcription. Set1-mediated H3K4me2 results in the recruitment of the Set3 histone deacetylase, which deacetylates nucleosomes. Set1 has been shown to work synergistically with Nrd1-mediated termination probably by slowing down transcription initiation kinetics of RNAPII, that might work through H3K4me2-Set3C (Terzi et al., 2011). Set1 was also proposed to promote AS transcription and sense repression by depositing the H3K4me3 active mark at the 3' end of AS-producing genes (Margaritis et al., 2012). Set3C represses genes having H3K4me2 mark especially during transition periods (Kim et al., 2012).

This complex system needs to be better understood by following the dynamic changes of both modifications at both the sense and AS promoters as well as at transcription pairs in the same orientation. Indeed, one conundrum during the transition in expression levels is that to reach H3K4me3 levels one would require to go through H3K4me2 that might result in transient downregulation of expression.

It was shown that at the genes induced during stress response, the +1 nucleosomes are transiently enriched for H3K18ac and lose the H3K4me3 mark (Weiner et al., 2015). We observed the same during recovery since at the 150 min time point, nucleosomes were enriched for H3K18ac. This was followed by depletion of the H3K18ac mark at 180 min, but with the current data we cannot ascertain that H3K18ac is indeed reduced (Results, Section 2, Figure 1B (p. 78)). During the stress response, Weiner and colleagues observed that the decrease in H3K18ac was preceded by an increase in H3K4me3 at the same site (Weiner et al., 2015).

Based on these observations, it will be interesting to define whether changes in H3K4me2/3 mark may be causal for the decrease in acetylation signal to bring both marks to a balanced state. This might be what is happening in the sense recovery oscillations that we observe. Acetylation brings RNAPII and hence Set1; however Set1-mediated H3K4me2 results in Set3C-mediated deacetylation. It would be interesting to know what other mechanisms interfere with this system that finally define whether to remain at the di-methylated level or to reach the tri-methylated state.

2.7 Cell Cycle Regulation of Histone PTMs

Cell-cycle is known to regulate deposition of histone PTMs. It has been shown in higher eukaryotes that deposition of H3K9me3 and H3K27me3 is impeded in cell cycle-blocked cells, although H379me1/2 and H4K20me2/3 can still accumulate in G₀-arrested human fibroblasts (Alabert, 2015). Thus, in our study, it is possible that in the G1-synchronised cells the H3K18 acetylation peak might not occur, or the deposition of this mark by HATs is delayed, and hence we observe a delay in +1 nucleosome distribution recovery. H3K36me3 has been shown to persist for an hour after transcription on the transcribed locus and the removal of the mark was partly dependent on replication-dependent histone exchange (Sein et al., 2015). It would be worth investigating both the acetylation and H3K36me3 levels and their most probably changed dynamics in G1-arrested cells.

2.8 Transcription Interference from Sense or Antisense act in the same manner

We observed that AS extension over the sense promoter results in deacetylation and downregulation of sense expression. During recovery, sense expression is activated and will probably reach its steady state levels after oscillating for a few hours with gene specific amplitude and frequency. Although the AS decreased linearly, we know that AS is regulated post initiation by Nrd1/Nab3/Sen1 pathway. Therefore, one could argue that the AS promoter might still be active while its elongation is stopped, and that sense extension contributes to the down-regulation of the AS promoter, which would result in further repression of AS. However, some studies have concluded that the modifications associated with AS transcription are different as compared to regular transcription (Murray et al., 2015). Since, we observe deposition of H3K36me3 by AS transcription like any other transcription, it is likely that transcription of all kinds and in any orientation would act in the same manner (Gill et al., 2020).

To address this point, it would be worth to examine the acetylation and/or methylation levels at the AS promoter. It would also be interesting to compare the dynamic changes in Ac/Me during overlapping transcription at tandem genes. This would help to conclude whether the different levels of modifications observed on Sense/AS pairs are only due to the fact that the non-strand specific component of Sense/AS, i.e. chromatin, has to exist as a 'hybrid' and incorporate modifications from both polymerases. Or, alternatively, a Sense/AS transcription pair may represent a unique arrangement of *cis*-acting transcriptional regulation. The combination of modifications that exist at the tandem genes could result from addition of co-transcriptional deposition by two polymerases. This would imply that the overlapping transcription coming from either direction with different

RNAPII CTD configurations would deposit different marks on the chromatin and the resulting steady state chromatin would simply be the net average of all the transcription events.

2.9 TI during Physiological Nutrient Stress Response

Nrd1/Nab3/Sen1 early termination has been shown to be downregulated in the presence of nutrient stress (Bresson et al., 2017; Darby et al., 2012). This response results in the upregulation of AS transcripts and downregulation of Sense expression. Furthermore, stress induces Nrd1 dephosphorylation leading to the formation of Nrd1 nuclear speckles. It would be interesting to observe what happens when the stress is relieved. Does it result in the solubilization of those granules or are they maintained in the cell. Another interesting and related analysis would be to examine Nrd1 expression levels through the cell cycle and in arrested cells. Analysing the physiological response to nutrient depletion after different times might result in different outcomes in terms of chromatin modifications and therefore response. It would be interesting to study the recovery from these different stages to define whether it may similarly result in over-acetylation and RNA upregulation. Nab3 expression should also be examined in these scenarios.

2.10 Chromatin Marks Save the Information in Chromatin Combinations

We know that the Histone PTMs occur in a combinatorial pattern at steady state, with promoters enriched in H3K4me3, H3K18ac, H3K56ac and H2A.Z histone variant, while genic regions have higher levels of H3K36me3 and H3K79me (Jenuwein and Allis, 2001). Upon antisense induction, we observed an increase in H3K36me3 around the TBS and a decrease in H3K18 acetylation levels at the +1 and -1 positions. The resulting state is repressive for transcription although the exact PTM state of the promoter is neither genic nor promoter associated. In a different study, Weiner et al. assessed a wide number of modifications in yeast during transcriptional changes in response to diamide stress; they observed transient uncommon PTM states at a small subset of nucleosomes, mostly associated with the promoters (Weiner et al., 2015). Therefore, the exact characterization of the chromatin state at AS-mediated repressed promoters or promoters undergoing transcriptional changes might be more complex than previously thought.

In summary, the commonly observed steady-state correlations between transcription and histone PTMs do not hold true during all types of dynamic changes. Therefore, the exact rules for how or what promotes these modification changes need to be established precisely in order to really understand the dynamics of transcription regulation.

Chromatin marks further act as a memory of time. It is possible that they keep the biological clock with different reaction combinations. If the nucleosome has acquired trimethylation, it has undergone three rounds of methylations, and depending on the biochemical speed of the deposition, it might indicate the time the nucleosome has spent on the DNA. For example, progressive methylation of H3K79me by Dot1 on ageing nucleosomes might signal the cell that it has spent enough time in that particular state (De Vos et al., 2011). In our case, AS-mediated repression deposits certain modifications on the sense promoter, but we only extended AS for 2 hours before measuring the response. Cluster 5 stays repressed after 2 hours of Auxin treatment. It is possible that upon induction of AS for longer durations, this cluster may completely lose its NDR specific marks and these regions may become indistinguishable from a nucleosome array.

It would be interesting to know until which point an NDR could recover from overlapping transcription and when it may lose its identity completely. TF- or GRF- mediated opening of chromatin might be the last resort to express these sense transcripts. We know from individual studies that non-coding transcribing polymerase actually inhibits binding of TFs, and recovery is therefore only possible when transcription readthrough is stopped (Bumgarner, 2012; Bumgarner et al., 2009; Gil and Ulitsky, 2020).

Chromatin acts as a substrate for various metabolic functions that change in response to different physiological signals which recruit factors or TFs that deposit different marks on the chromatin (Diehl and Muir, 2020). It is also becoming clear that the speed and the position of transcription, which are affected by PTMs, also define mRNA stability (Geisberg et al., 2014) and might influence the translatability of the RNA (Lyon et al., 2019). Hence, the final level of marks and overlapping transcription might define the final state of transcription and expression levels. Repression and activation mechanisms during transcription changes underlying all these observations might involve similar chromatin factors and modifications as observed for the overlapping AS-mediated repression and recovery. Our study thus provides hints to which factors need to be examined to precisely solve the mechanisms of overlapping coding and non-coding transcription switches all over the genome.

We are still far from being able to predict RNA expression levels based on the observed types and amounts of deposited marks. With the plethora of overlapping transcriptional programs, it is important to understand how changing the level of expression of one transcript might affect the dynamics of neighbouring genes and those located close in the 3rd-dimension in order to get a more complete picture of gene regulation at the level of transcription.

Supplementary

1 Antisense-Mediated Interference Mechanism

Contains the supplementary information and figures as published with the article presented in the first section of the results.

Cell Reports, Volume 31

Supplemental Information

**Fine Chromatin-Driven Mechanism of Transcription
Interference by Antisense Noncoding Transcription**

Jatinder Kaur Gill, Andrea Maffioletti, Varinia García-Molinero, Françoise Stutz, and Julien Soudet

Figure S1

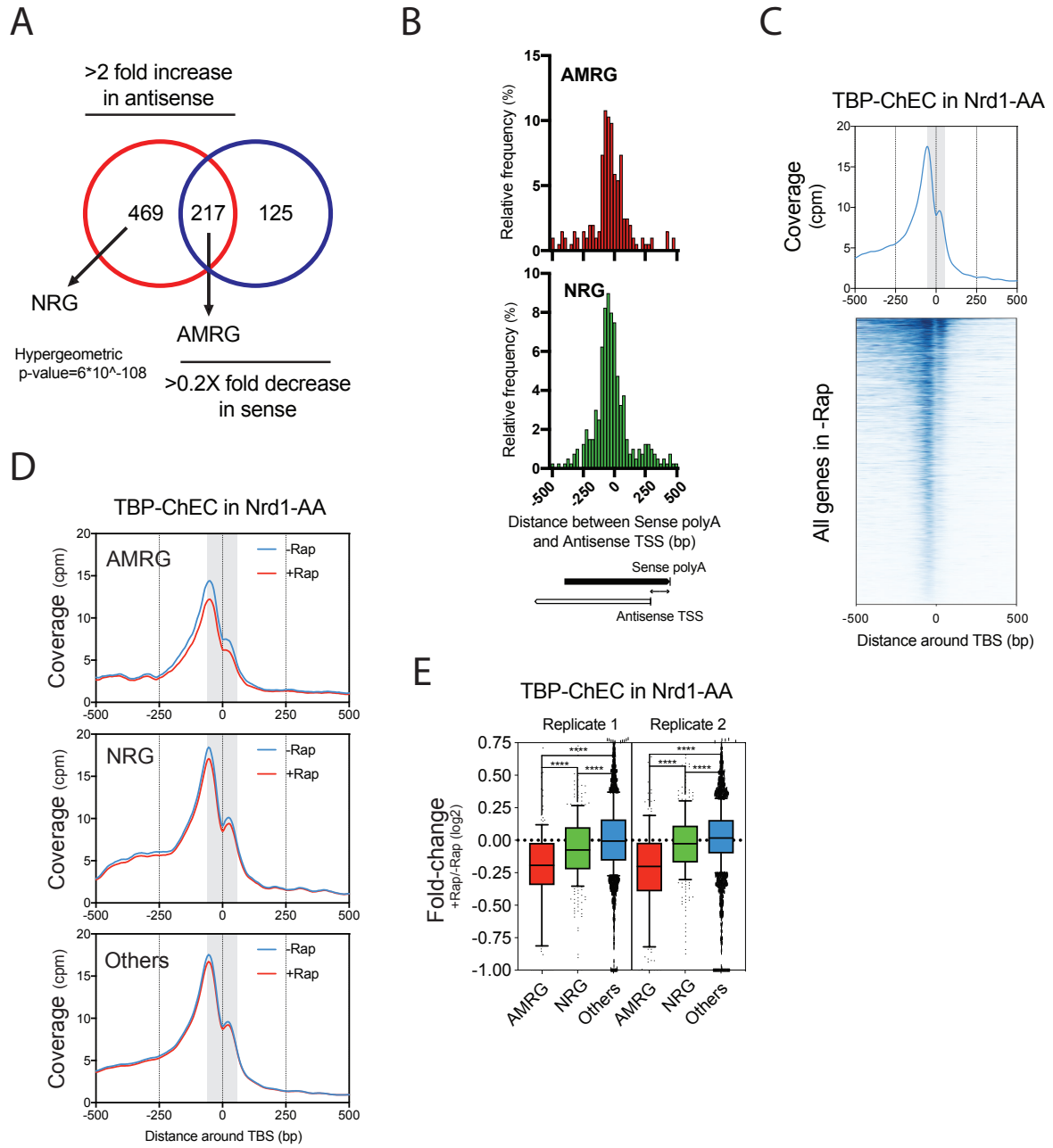


Figure S1: related to Figure 1.

- (A)** Overlap between antisense-containing genes (AMRG + NRG) and repressed genes upon Nrd1 anchor-away.
- (B)** Histogram of distances between Sense polyA and Antisense TSS for AMRG and NRG. LncRNAs (NUTs) coordinates were obtained from (Schulz et al., 2013).
- (C)** Metagene analysis and heatmap depicting the TBP-ChEC profile in the Nrd1-AA in the absence of Rap. Results are centered on the TATA-Binding Site (TBS).
- (D)** Metagene analysis of TBP-ChEC induced for 30sec in an Nrd1-AA strain treated or not with Rap for 1h. The grey box represents the 50bp area around the TBS over which statistics are generated. The center of 0-120bp paired-end fragments is represented for the plots and statistical analyses.
- (E)** Box-plots of the two independent replicates of TBP-ChEC fold-change related to Figure 1G. The fold-change is measured over a 50bp region centered on the TBS.

Figure S2

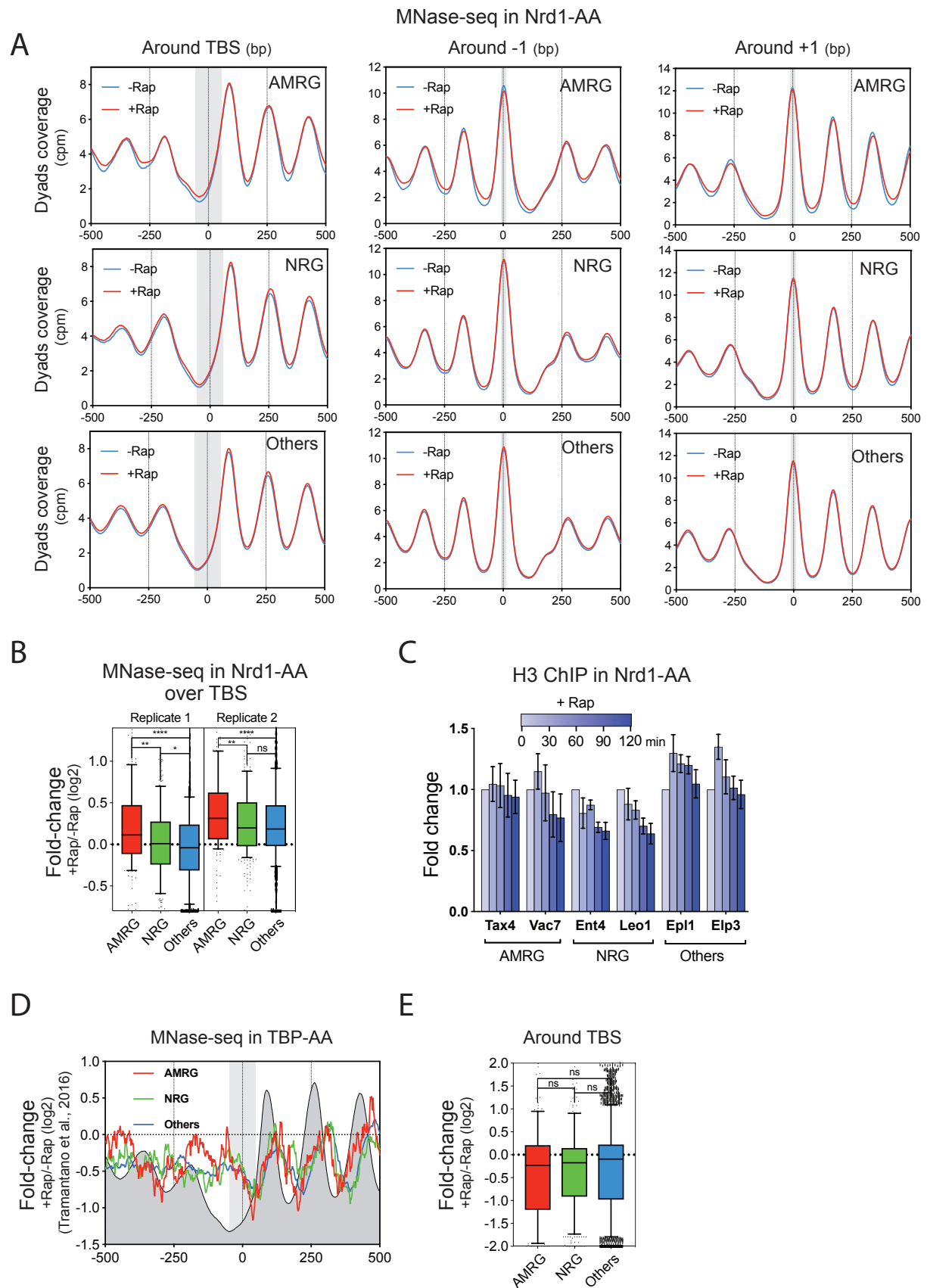


Figure S2: related to Figure 2

(A) Aggregate plots centered on TBSs, -1 and +1 nucleosomes, respectively, of MNase-seq profiles obtained in an Nrd1-AA strain treated or not for 1h with Rap. The centers of 120-200bp paired-end fragments are represented. Grey rectangles represent the 50bp- TBS centered and 10bp- -1/+1 nucleosomes- centered areas.

(B) Box-plots of the two independent replicates of MNase-seq fold-change related to Figure 2B. The fold-change is measured over a 50bp region centered on the TBS.

(C) ChIP of H3 at gene promoters of AMRG, NRG and Other genes. ChIPs were performed at 0, 30, 60, 90 and 120min after rapamycin addition. Immunoprecipitated promoter NDRs were normalized to immunoprecipitated *SPT15* ORF after qPCR amplification. Primers are designed to target promoter NDRs. The fold-change was artificially set to 1 for each gene in the -Rap condition. Error bars represent the Standard Error of the Mean (SEM) for a set of 3 independent experiments.

(D) Metagene plot of MNase-seq performed in a TBP-AA strain treated or not with Rap for 30min. Midpoint of 120-200bp are represented. The grey box represents the 50bp area centered on the TBS. Results were retrieved from (Tramantano et al., 2016).

(E) Box-plots of the dyads occupancy fold-change in +Rap/-Rap in the TBP-AA strain. The fold-change is measured over a 50bp region centered on the TBS.

Figure S3

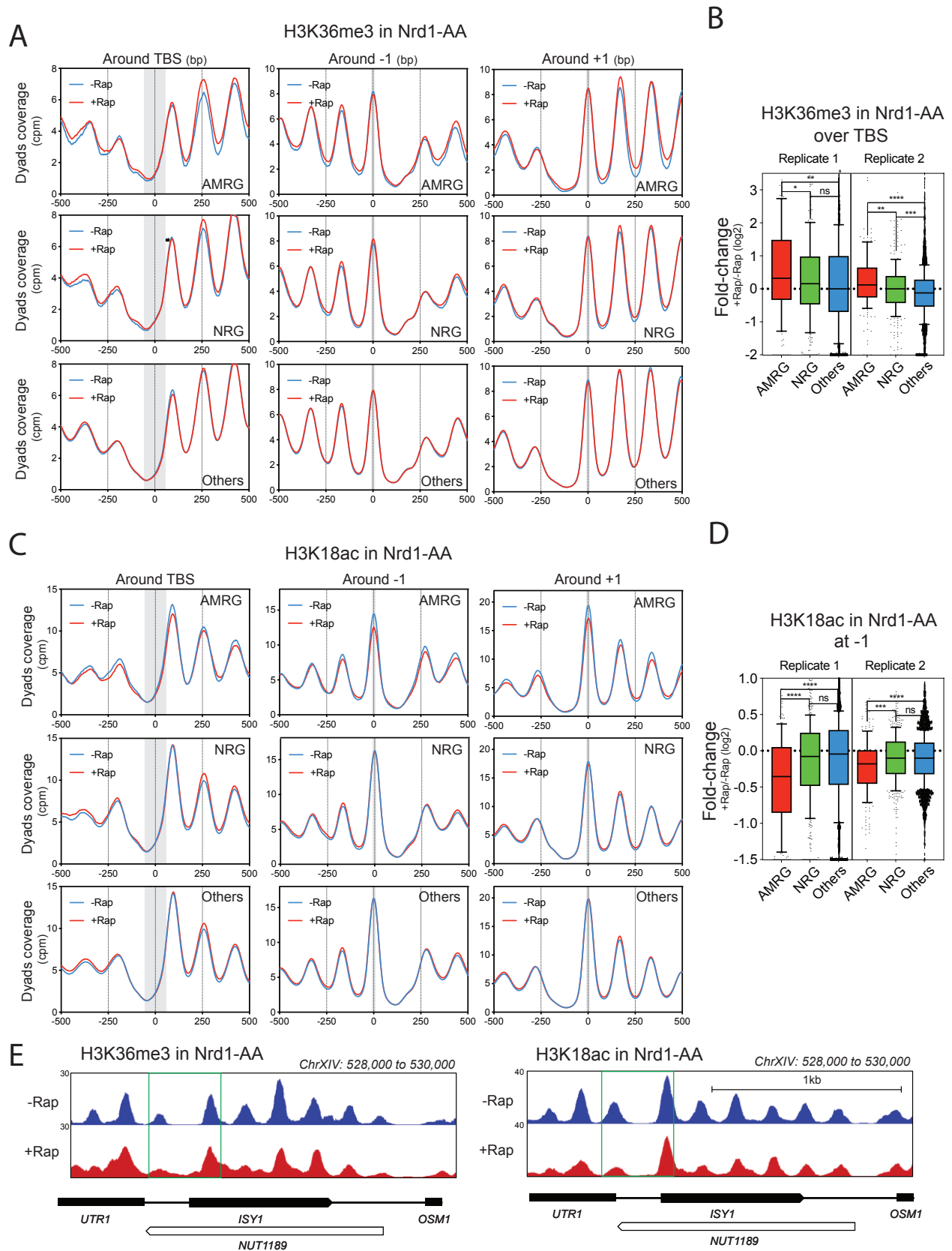
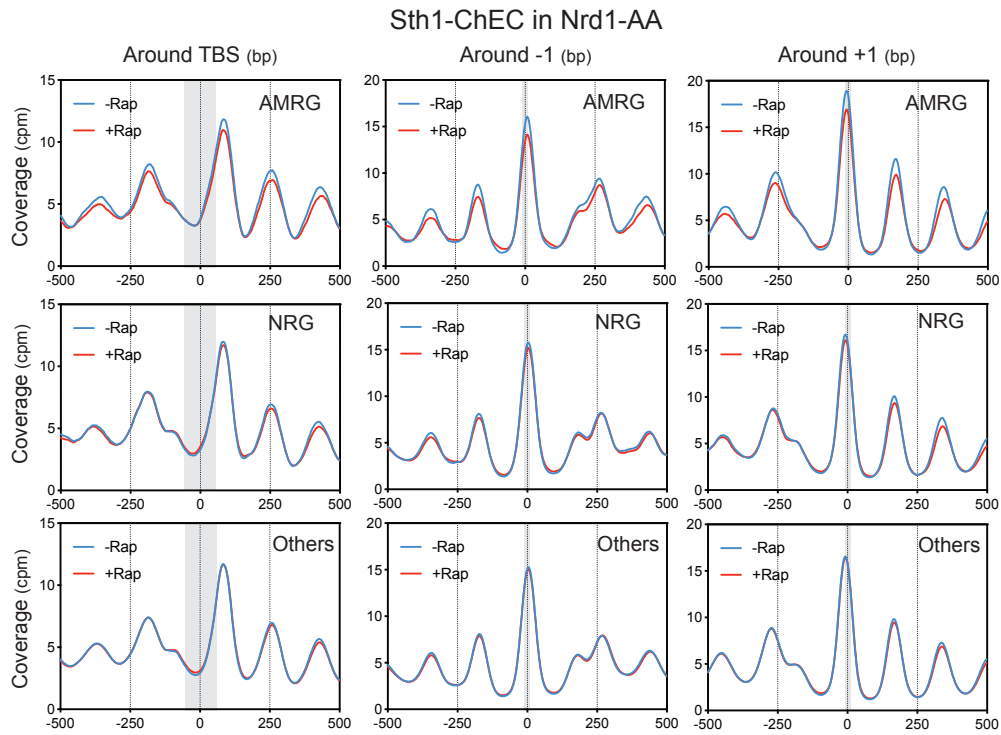


Figure S3: related to Figure 3

- (A)** Metagene plot of H3K36me3 MNase-ChIP-seq related to Figure 3A and centered on the TBS, -1 and +1 nucleosomes, respectively. Midpoint of 120-200bp fragments are represented.
- (B)** Box-plots of the fold-change related to Figure 3B for the two independent replicates of H3K36me3 MNase-ChIP-seq. The fold-change is measured over a 50bp region centered on the TBS.
- (C)** Metagene plot of H3K18ac MNase-ChIP-seq related to Figure 3C and centered on the TBS, -1 and +1 nucleosomes, respectively. Midpoint of 120-200bp fragments are represented.
- (D)** Box-plots of the fold-change related to Figure 3D for the two independent replicates of H3K18ac MNase-ChIP-seq. The fold-change is measured over a 10bp region centered on the -1 nucleosome.
- (E)** Snapshot of H3K36me3 and H3K18ac MNase-ChIP-seq absolute levels at the AMRG *ISY1*. The NDR of *ISY1* is indicated by a rectangle.

Figure S4

A



B

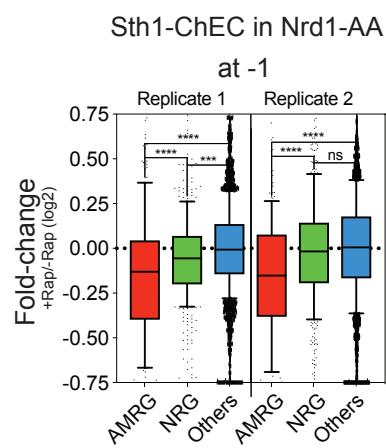


Figure S4: related to Figure 5

(A) Metagene plot of Sth1-ChEC centered on the TBS, -1 and +1 nucleosomes, respectively. Midpoint of 120-200bp fragments are represented.

(B) Box-plots of the (+Rap/-Rap) fold-change related to Figure 5B for the two independent replicates of Sth1-ChEC. The fold-change is measured over a 10bp region centered on the -1 nucleosome.

Figure S5

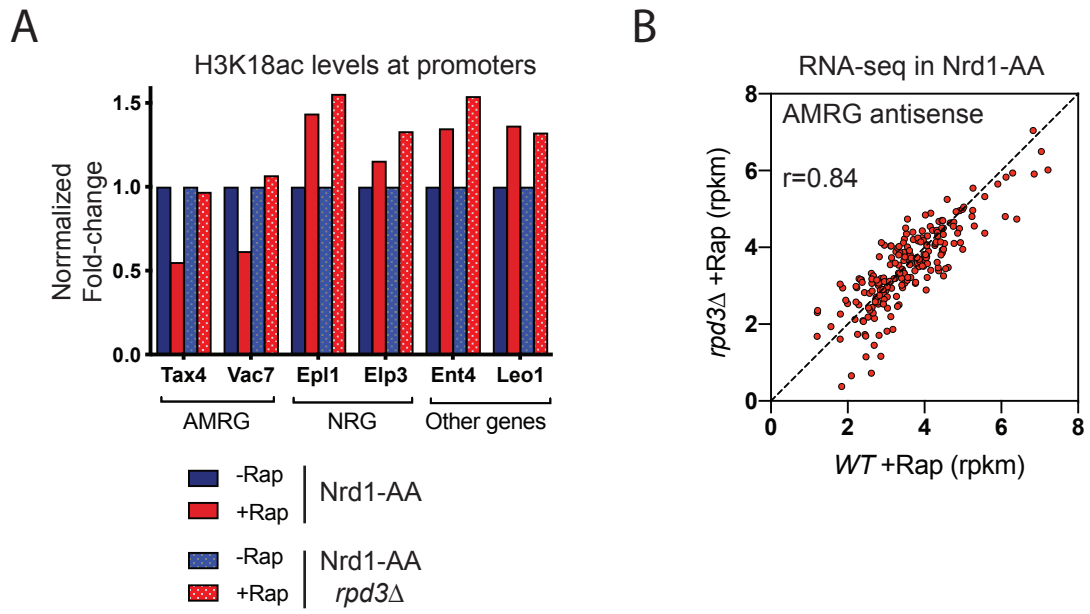


Figure S5: related to Figure 6

(A) ChIP of H3K18ac levels at the promoters of AMRG, NRG and Other genes. *S. pombe* chromatin was used as a spike-in control and mixed with *S. cerevisiae* chromatin before immunoprecipitation. *S. cerevisiae* results are normalized to *S. pombe* *ACT1* ORF. All results are expressed as fold-change with respect to -Rap which value was set to 1.

(B) RNA-seq of AMRG antisense in Nrd1-AA +Rap vs Nrd1-AA *rpd3D* +Rap. Results are depicted in rpkm. The +Rap condition was chosen to have an accurate measurement of antisense production. *r* indicates the Pearson correlation. Even in the absence of Rpd3, antisense RNAs are globally well produced at AMRGs and the rescue of AMRG sense expression (Figure 6) is not a consequence of a lack of antisense production.

Figure S6

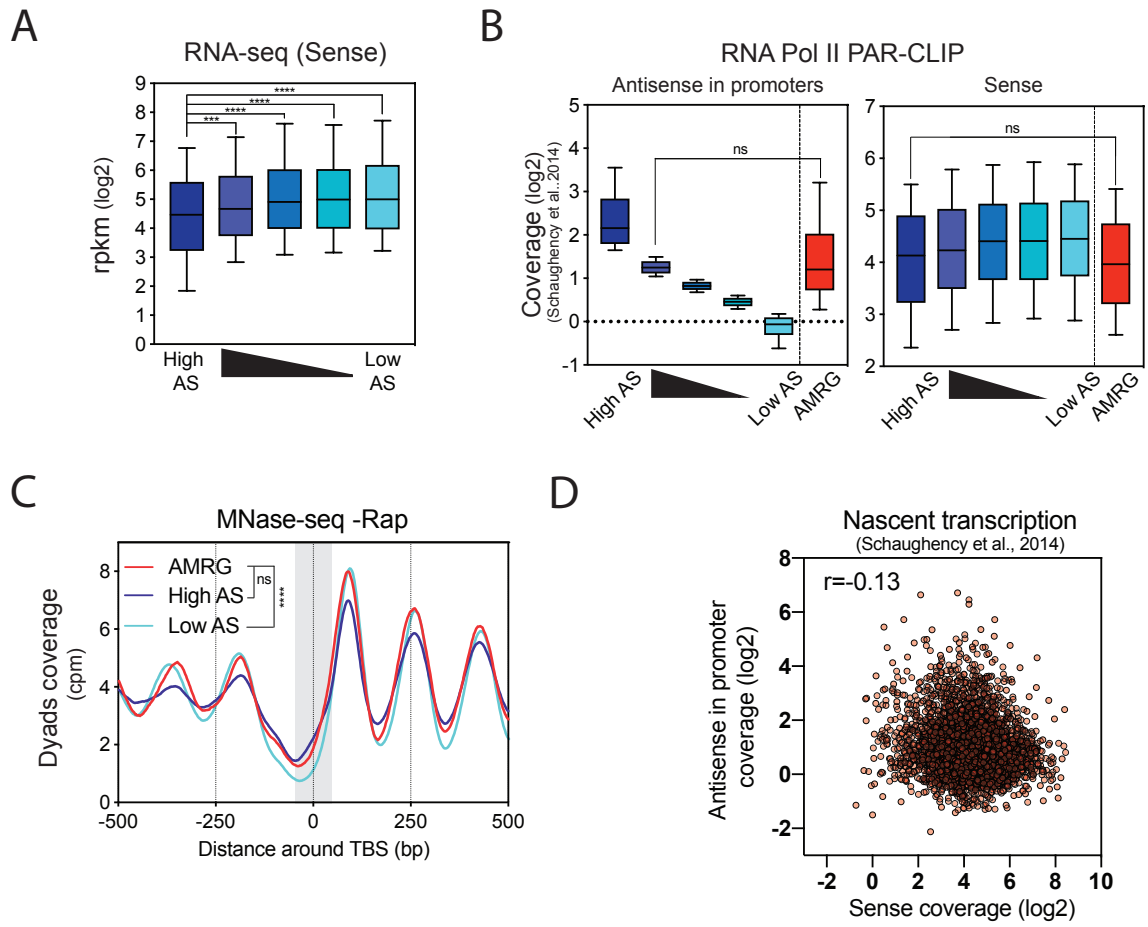


Figure S6: related to Figure 7

- (A) Box-plots of expression by RNA-seq according to the quintiles defined in Figure 7.
- (B) Natural nascent antisense levels in promoters and natural nascent sense levels of AMRG as compared to the quintiles defined in Figure 7.
- (C) Metagene plot of MNase-seq profile at steady state for the AMRG as compared with the high and low antisense quintiles defined in Figure 7. Results are centered on the TBS.
- (D) Global correlation between nascent antisense transcription into promoters (-100bp to TSS area) and nascent sense transcription (100bp area upstream of the polyA site). The correlation coefficient r corresponds to the Pearson correlation.

Table S1. Related to STAR Methods

Experimental Models: Organisms/Strains		
<i>S. cerevisiae</i> AA (FSY4885)	(Haruki et al., 2008)	<i>MAT α, tor1-1, fpr1D::NAT, RPL13A-2 3 FKBP12::TRP1</i>
<i>S. cerevisiae</i> Nrd1-AA (FSY5065)	(Castelnuovo et al., 2014)	<i>MAT α, tor1-1, fpr1D::NAT, RPL13A-2 3 FKBP12::TRP1, NRD1-FRB::KanMX6</i>
<i>S. cerevisiae</i> Nrd1-AA rpd3D (FSY7015)	This study	<i>MAT α, tor1-1, fpr1::NAT, RPL13A-2 3 FKBP12::TRP1, NRD1-FRB::KanMX6, rpd3D::HIS3</i>
<i>S. cerevisiae</i> Nrd1-AA TBP-MNase (FSY8162)	This study	<i>MAT α, tor1-1, fpr1::NAT, RPL13A-2 3 FKBP12::TRP1, NRD1-FRB::KanMX6, TBP-3xFLAG-MNase::HPHMX6</i>
<i>S. cerevisiae</i> Nrd1-AA rpd3D TBP-MNase (FSY8164)	This study	<i>MAT α, tor1-1, fpr1::NAT, RPL13A-2 3 FKBP12::TRP1, NRD1-FRB::KanMX6, rpd3D::HIS3, TBP-3xFLAG- MNase::HPHMX6</i>
<i>S. cerevisiae</i> Nrd1-AA STH1-MNase (FSY8254)	This study	<i>MAT α, tor1-1, fpr1::NAT, RPL13A-2 3 FKBP12::TRP1, NRD1-FRB::KanMX6, STH1-3xFLAG-MNase::HPHMX6</i>
<i>S. cerevisiae</i> Nrd1-AA rpd3D STH1-MNase (FSY8255)	This study	<i>MAT α, tor1-1, fpr1::NAT, RPL13A-2 3 FKBP12::TRP1, NRD1-FRB::KanMX6, rpd3D::HIS3, STH1-3xFLAG- MNase::HPHMX6</i>

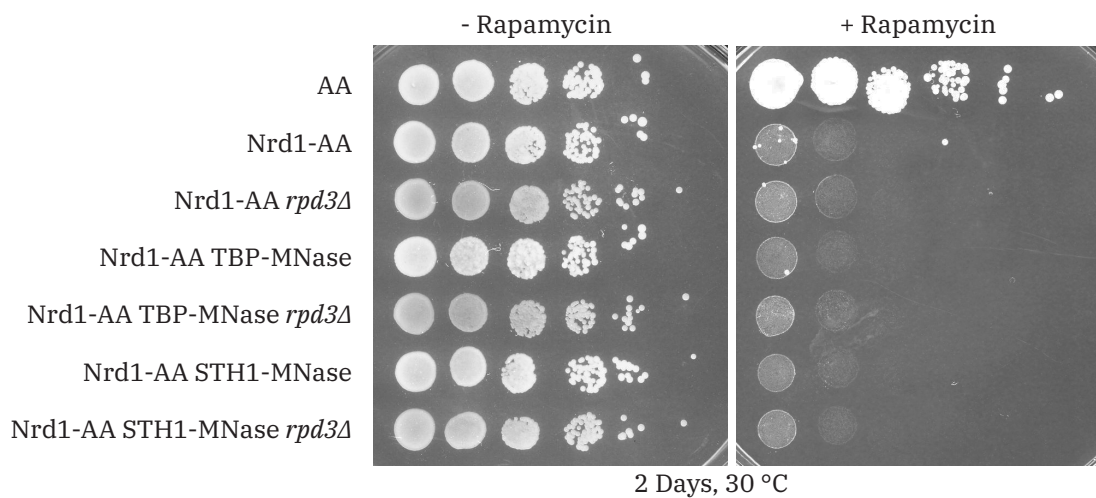


Table S2. Related to STAR Methods

Genes		Oligos
TAX4	Forward	ATAGATGGCGCAAGGGAGTT
	Reverse	AAACGTCAGGGCGTGTATTC
VAC7	Forward	TGTAAGTCTTCCTGGCCACTC
	Reverse	GATCATTATGCAAAATCGAAGG
EPL1	Forward	CACGATCCGACCACAAAAT
	Reverse	GGAACGCGATGTGGTGAAT
ELP3	Forward	TTCAAAAGTCAATACTGCCACTG
	Reverse	CACTGGATAATTTGAGATGAGCTA
LEO1	Forward	AAGCTTTGCCATATTCAATCG
	Reverse	GCTTTCGTATTCACCTTCTATGAGC
ENT4	Forward	CGCTGACACGTTTGTACTTTC
	Reverse	CCTCAATTTTCGTTTTCTCATTC
<i>ACT1 S. pombe</i>	Forward	TCTTTCCATATCATCCAGTTG
	Reverse	CTCAAAGCAAGCGTGGTATTT
SPT15	Forward	TCGGGTTTGCTGCTAAATTC
	Reverse	ACACAATTTTCGGCTTCACC

2 Antisense-Mediated Repression Prime Sense Transcript Promoter for Activation

Contains five supplementary figures for the data presented in the Results section 2 of the thesis.

Figure S1. 4tu-Seq in AID^{*}-Nrd1 tagged and Untagged wt strain. Related to Figure 1.

(A) Western-blot for AID^{*}-Nrd1 at the same time points as shown in Figure 1A .

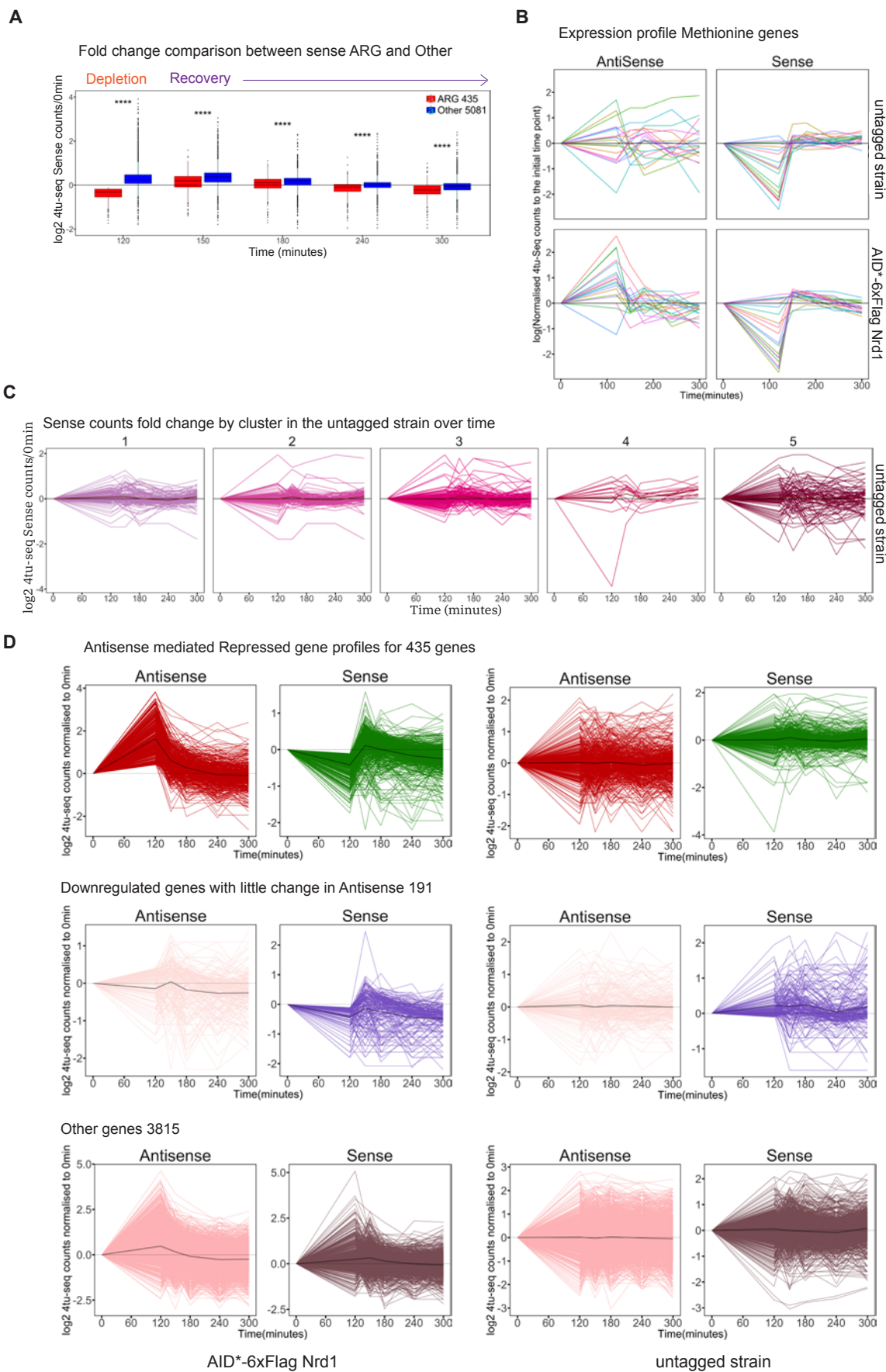
(B) 4tU-Seq coverage profiles for both Sense (dark, top) and Antisense (bottom, light) for each time point during depletion and recovery.

(C) Log normalized 4tU-seq counts for Antisense plotted at each time point compared to 0 min. ARG are represented as red and control genes as blue.

(D) Log normalized 4tU-seq counts for Sense mRNA and the shown classes of ncRNA and snoRNA in the AID^{*}-Nrd1 strain.

(E) and (F) Log of normalized 4tU-seq counts for Antisense and Sense strands respectively in the untagged control strain.

(G) Related to Figure 1D. Antisense fold change values are plotted for each gene cluster at all the time points.



Supplementary Figure 2

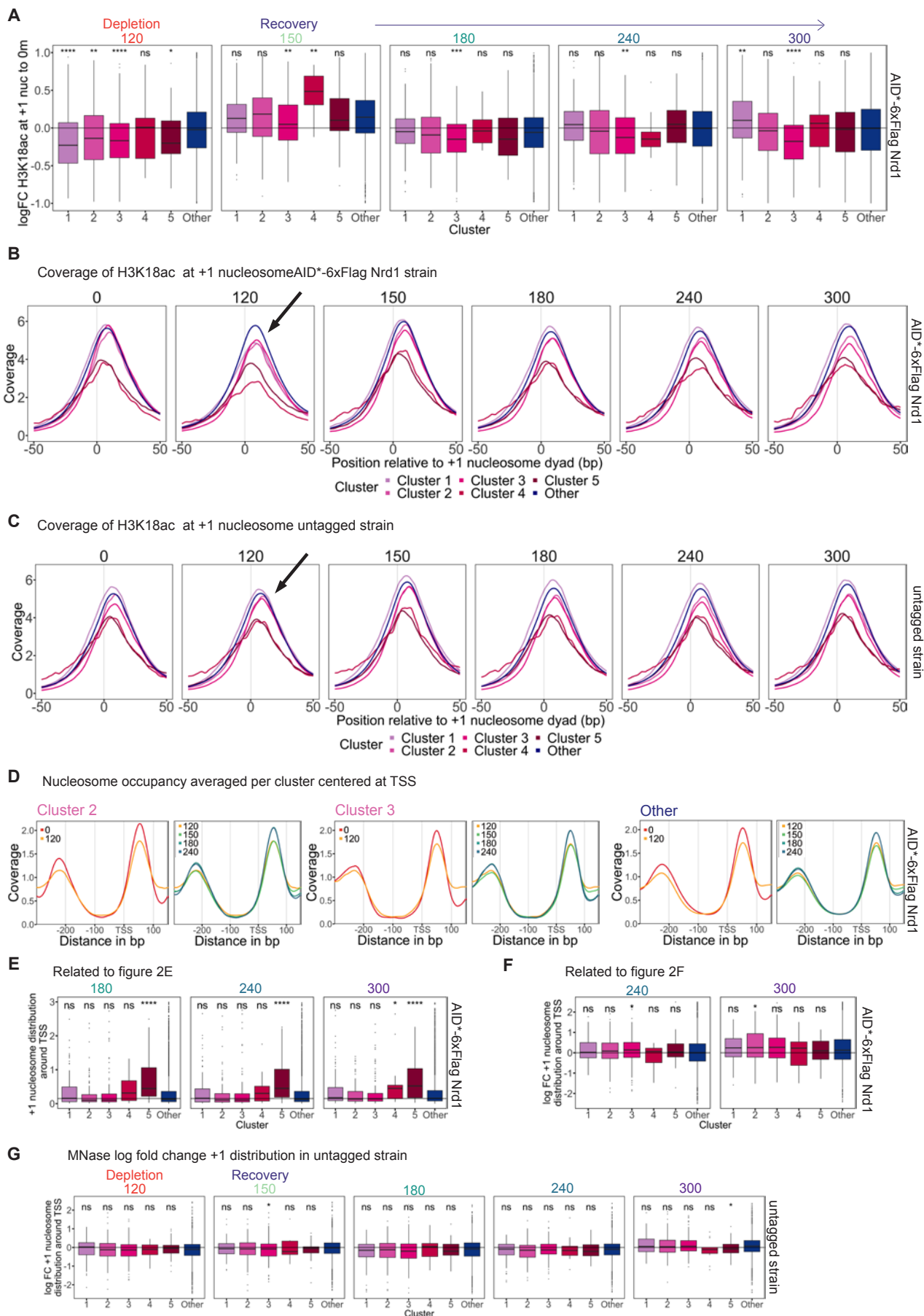
Figure S2. 4tu-seq profiles for all ARG and control genes. Related to Figure 1.

(A) Fold changes in ARG sense expression (all five clusters) vs the control genes. The same is shown for Antisense in Figure 1F.

(B) Expression profile of Methionine genes, for both control and tagged strains on both strands.

(C) Expression profiles of ARG Sense and Antisense transcripts in both AID*-Nrd1 and untagged strains.

(D) Plots showing the Other gene class divided into three. The 2-fold upregulated genes (701) are shown in light and dark blue in both tagged and untagged strains. The downregulated genes (191) are shown in pink and light purple. The last class of non-changing genes (3815) is shown in beige and brown.



Supplementary Figure 3

Figure S3. Related to Figure 2.

(A) Log of normalised fold change acetylation at +1 nucleosome of clusters 1 to 5 compared to Other class of genes. The significance was defined using wilcox test. The panels show all the time points from 120 min of depletion to 300 min of recovery. Related to Figure 2B.

(B) Acetylation profiles at +1 nucleosome and 50 bp on both sides of the peak are shown for each time point. Each plotted line corresponds to a cluster. The blue lines correspond to the Other control genes.

(C) Similar plot as (B) but in the untagged control strain.

(D) Related to Figure 2C. MNase-seq average profiles for clusters 2,5 and Other genes centred at the TSS.

(E) Related to Figure 2E. +1 nucleosome distribution around TSS for different clusters at 180, 240 and 300 min.

(F) Related to Figure 2F. Log FC (fold change) of +1 nucleosome distribution around TSS for time points 240 and 300 min.

(G) Boxplot for MNase in control strain log +1 normalized.

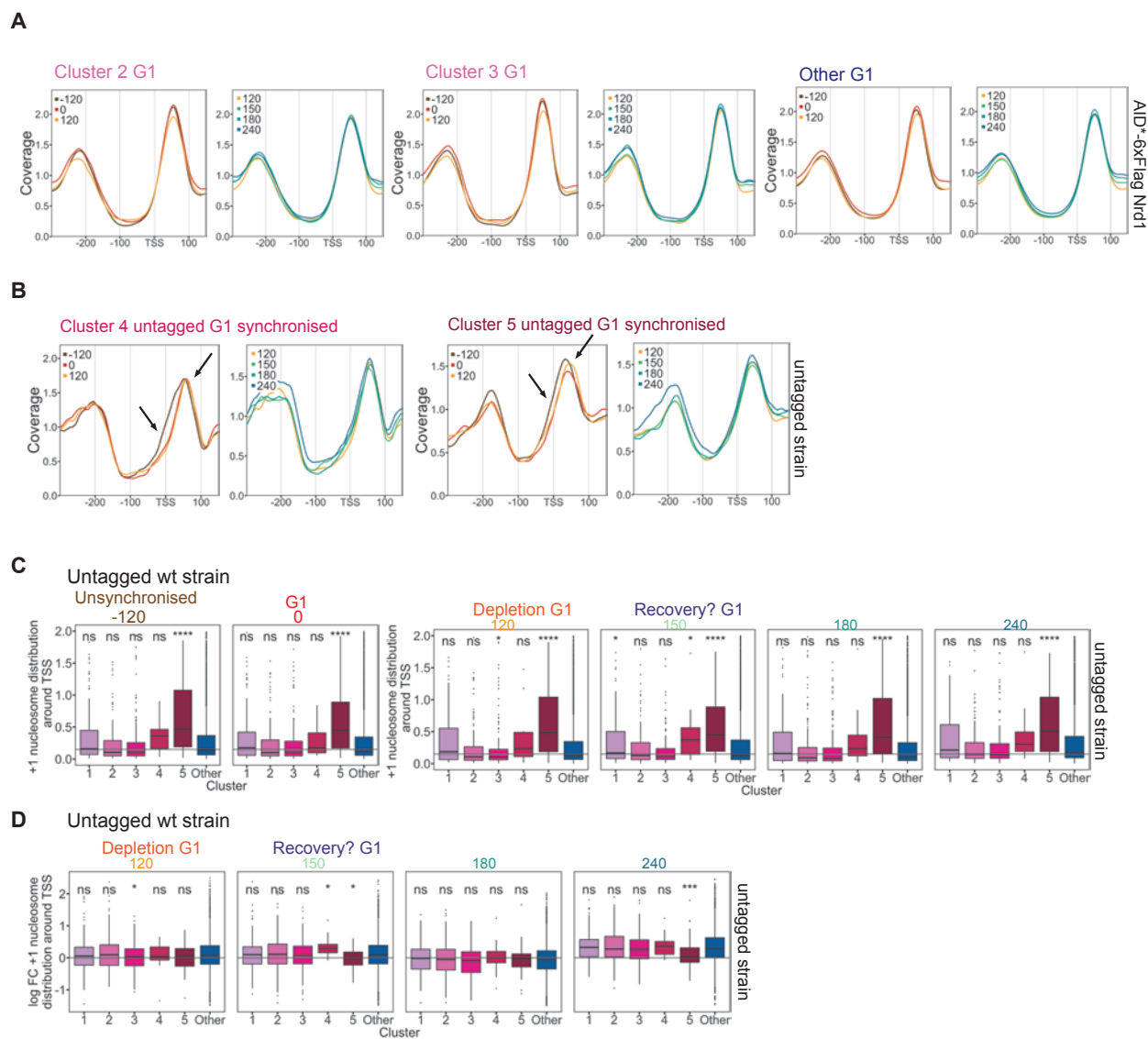


Figure S4. Related to Figure 3

(A) MNase-seq nucleosome occupancy profiles of G1 synchronised cells during depletion and recovery for clusters 2, 3 and Other genes.

(B) MNase-seq nucleosome occupancy profiles for clusters 4 and 5 in the G1 synchronised untagged wt strain.

(C) Related to Figure 3D. Same plot for the untagged wt strain.

(D) Related to Figure 3E. Same plot for the untagged wt strain.

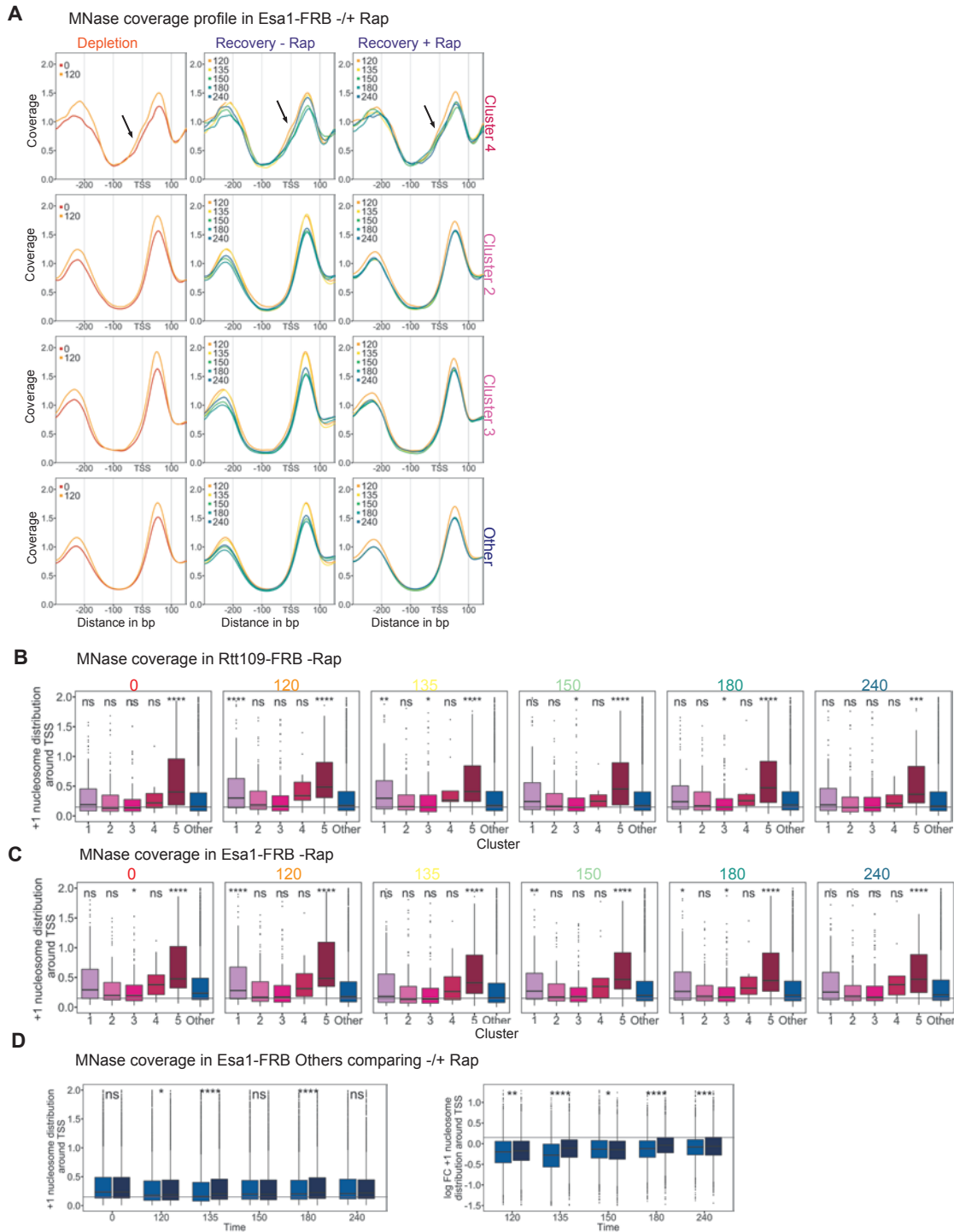


Figure S5. Related to Figure 4

(A) Related to Figure 5B. MNase-seq nucleosome occupancy coverage for clusters 2, 3, 4 and Others in both +Rap and -Rap.

(B) Related to Figures 5D and 5E. +1 nucleosome distribution around TSS at all time points for the *Rtt109-Frb* strain in -Rapamycin.

(C) Related to Figure 5C. +1 nucleosome distribution around TSS at all time points for the *Esa1-Frb* strain in -Rapamycin.

(D) Related to Figures 5D and 5E. +1 distribution and log FC of +1 distribution at all time points for the control set of genes in *Esa1-Frb* comparing between - and + Rap.

References

- Alabert, C. (2015). Two distinct modes for propagation of histone PTMs across the cell cycle. *Genes Dev.* *29*.
- Alabert, C., and Groth, A. (2012). Chromatin replication and epigenome maintenance. *Nat. Rev. Mol. Cell. Biol.* *13*.
- Alabert, C., Loos, C., Voelker-Albert, M., Graziano, S., Forne, I., Reveron-Gomez, N., Schuh, L., Hasenauer, J., Marr, C., Imhof, A., *et al.* (2020). Domain Model Explains Propagation Dynamics and Stability of Histone H3K27 and H3K36 Methylation Landscapes. *Cell Rep* *30*, 1223-1234 e1228.
- Albert, I., Mavrich, T.N., Tomsho, L.P., Qi, J., Zanton, S.J., Schuster, S.C., and Pugh, B.F. (2007). Translational and rotational settings of H2A.Z nucleosomes across the *Saccharomyces cerevisiae* genome. *Nature* *446*, 572-576.
- Allard, S., Utley, R.T., Savard, J., Clarke, A., Grant, P., Brandl, C.J., Pillus, L., Workman, J.L., and Cote, J. (1999). NuA4, an essential transcription adaptor/histone H4 acetyltransferase complex containing Esa1p and the ATM-related cofactor Tra1p. *EMBO J* *18*, 5108-5119.
- Allshire, R.C., and Madhani, H.D. (2018). Ten principles of heterochromatin formation and function. *Nat Rev Mol Cell Biol* *19*, 229-244.
- Alzu, A., Bermejo, R., Begnis, M., Lucca, C., Piccini, D., Carotenuto, W., Saponaro, M., Brambati, A., Cocito, A., Foiani, M., *et al.* (2012). Senataxin associates with replication forks to protect fork integrity across RNA-polymerase-II-transcribed genes. *Cell* *151*, 835-846.
- Angus-Hill, M.L., Schlichter, A., Roberts, D., Erdjument-Bromage, H., Tempst, P., and Cairns, B.R. (2001). A Rsc3/Rsc30 zinc cluster dimer reveals novel roles for the chromatin remodeler RSC in gene expression and cell cycle control. *Mol Cell* *7*, 741-751.
- Annunziato, A.T. (2015). The fork in the road: histone partitioning during DNA replication. *Genes (Basel)* *6*.
- Ard, R., and Allshire, R.C. (2016). Transcription-coupled changes to chromatin underpin gene silencing by transcriptional interference. *Nucleic Acids Res* *44*, 10619-10630.
- Arigo, J.T., Carroll, K.L., Ames, J.M., and Corden, J.L. (2006). Regulation of yeast NRD1 expression by premature transcription termination. *Molecular cell* *21*, 641-651.
- Armache, K.J., Garlick, J.D., Canzio, D., Narlikar, G.J., and Kingston, R.E. (2011). Structural basis of silencing: Sir3 BAH domain in complex with a nucleosome at 3.0 Å resolution. *Science* *334*.
- Audergon, P.N. (2015). Epigenetics. Restricted epigenetic inheritance of H3K9 methylation. *Science* *348*.
- Auger, A. (2008). Eaf1 is the platform for NuA4 molecular assembly that evolutionarily links chromatin acetylation to ATP-dependent exchange of histone H2A variants. *Mol. Cell. Biol.* *28*.
- Badis, G. (2008). A library of yeast transcription factor motifs reveals a widespread function for Rsc3 in targeting nucleosome exclusion at promoters. *Mol. Cell* *32*.
- Badis, G., Chan, E.T., van Bakel, H., Pena-Castillo, L., Tillo, D., Tsui, K., Carlson, C.D., Gossett, A.J., Hasinoff, M.J., Warren, C.L., *et al.* (2008). A library of yeast transcription factor motifs reveals a widespread function for Rsc3 in targeting nucleosome exclusion at promoters. *Mol Cell* *32*, 878-887.
- Bae, H.J., Dubarry, M., Jeon, J., Soares, L.M., Dargemont, C., Kim, J., Geli, V., and Buratowski, S. (2020). The Set1 N-terminal domain and Swd2 interact with RNA polymerase II CTD to recruit COMPASS. *Nat Commun* *11*, 2181.
- Baptista, T., Grunberg, S., Minoungou, N., Koster, M.J.E., Timmers, H.T.M., Hahn, S., Devys, D., and Tora, L. (2017). SAGA Is a General Cofactor for RNA Polymerase II Transcription. *Mol Cell* *68*, 130-143 e135.

- Belotserkovskaya, R. (2003). FACT facilitates transcription-dependent nucleosome alteration. *Science* 301.
- Berndsen, C.E., Tsubota, T., Lindner, S.E., Lee, S., Holton, J.M., Kaufman, P.D., Keck, J.L., and Denu, J.M. (2008). Molecular functions of the histone acetyltransferase chaperone complex Rtt109-Vps75. *Nat Struct Mol Biol* 15, 948-956.
- Bian, C. (2011). Sgf29 binds histone H3K4me2/3 and is required for SAGA complex recruitment and histone H3 acetylation. *EMBO J* 30.
- Bird, A.J., Gordon, M., Eide, D.J., and Winge, D.R. (2006). Repression of ADH1 and ADH3 during zinc deficiency by Zap1-induced intergenic RNA transcripts. *EMBO J* 25, 5726-5734.
- Blair, R.H., Goodrich, J.A., and Kugel, J.F. (2012). Single-molecule fluorescence resonance energy transfer shows uniformity in TATA binding protein-induced DNA bending and heterogeneity in bending kinetics. *Biochemistry* 51.
- Bonasio, R., Tu, S., and Reinberg, D. (2010). Molecular signals of epigenetic states. *Science* 330, 612-616.
- Bonnet, J., Wang, C.Y., Baptista, T., Vincent, S.D., Hsiao, W.C., Stierle, M., Kao, C.F., Tora, L., and Devys, D. (2014). The SAGA coactivator complex acts on the whole transcribed genome and is required for RNA polymerase II transcription. *Genes Dev* 28, 1999-2012.
- Boque-Sastre, R., Soler, M., Oliveira-Mateos, C., Portela, A., Moutinho, C., Sayols, S., Villanueva, A., Esteller, M., and Guil, S. (2015). Head-to-head antisense transcription and R-loop formation promotes transcriptional activation. *Proc Natl Acad Sci U S A* 112, 5785-5790.
- Boudreault, A.A., Cronier, D., Selleck, W., Lacoste, N., Utley, R.T., Allard, S., Savard, J., Lane, W.S., Tan, S., and Cote, J. (2003). Yeast enhancer of polycomb defines global Esa1-dependent acetylation of chromatin. *Genes Dev* 17, 1415-1428.
- Bowman, G.D. (2010). Mechanisms of ATP-dependent nucleosome sliding. *Curr Opin Struct Biol* 20, 73-81.
- Brahma, S. (2017). INO80 exchanges H2A. Z for H2A by translocating on DNA proximal to histone dimers. *Nat. Commun.* 8.
- Brahma, S., and Henikoff, S. (2019). RSC-associated subnucleosomes define MNase-sensitive promoters in yeast. *Mol. Cell* 73.
- Brasher, S.V. (2000). The structure of mouse HP1 suggests a unique mode of single peptide recognition by the shadow chromo domain dimer. *EMBO J* 19.
- Brenner, S., Jacob, F., and Meselson, M. (1961). An unstable intermediate carrying information from genes to ribosomes for protein synthesis. *Nature* 190.
- Bresson, S., Tuck, A., Staneva, D., and Tollervey, D. (2017). Nuclear RNA Decay Pathways Aid Rapid Remodeling of Gene Expression in Yeast. *Mol Cell* 65, 787-800 e785.
- Brodsky, S., Jana, T., Mittelman, K., Chapal, M., Kumar, D.K., Carmi, M., and Barkai, N. (2020). Intrinsically Disordered Regions Direct Transcription Factor In Vivo Binding Specificity. *Molecular Cell* 79, 459-471.e454.
- Brown, C.E. (2001). Recruitment of HAT complexes by direct activator interactions with the ATM-related Tra1 subunit. *Science* 292.
- Brown, T., Howe, F.S., Murray, S.C., Wouters, M., Lorenz, P., Seward, E., Rata, S., Angel, A., and Mellor, J. (2018). Antisense transcription-dependent chromatin signature modulates sense transcript dynamics. *Mol Syst Biol* 14, e8007.
- Bruzzo, M.J., Grunberg, S., Kubik, S., Zentner, G.E., and Shore, D. (2018). Distinct patterns of histone acetyltransferase and Mediator deployment at yeast protein-coding genes. *Genes Dev* 32, 1252-1265.
- Bumgarner, S.L. (2012). Single-cell analysis reveals that noncoding RNAs contribute to clonal heterogeneity by modulating transcription factor recruitment. *Mol. Cell* 45.
- Bumgarner, S.L., Dowell, R.D., Grisafi, P., Gifford, D.K., and Fink, G.R. (2009). Toggle involving cis-interfering noncoding RNAs controls variegated gene expression in yeast. *Proc Natl Acad Sci U S A* 106, 18321-18326.
- Buratowski, S. (2009). Progression through the RNA polymerase II CTD cycle. *Mol. Cell* 36.
- Cairns, B.R. (2005). Chromatin remodeling complexes: strength in diversity, precision through specialization. *Curr Opin Genet Dev* 15, 185-190.
- Cairns, B.R., Lorch, Y., Li, Y., Zhang, M., Lacomis, L., Erdjument-Bromage, H., Tempst, P., Du, J., Laurent, B., and Kornberg, R.D. (1996). RSC, an essential, abundant chromatin-remodeling complex. *Cell* 87, 1249-1260.
- Cakiroglu, A., Clapier, C.R., Ehrensberger, A.H., Darbo, E., Cairns, B.R., Luscombe, N.M., and Svejstrup, J.Q. (2019). Genome-wide reconstitution of chromatin transactions reveals that RSC preferentially disrupts H2AZ-containing nucleosomes. *Genome Res* 29, 988-998.
- Camblong, J., Iglesias, N., Fickentscher, C., Dieppo, G., and Stutz, F. (2007). Antisense RNA stabilization induces transcriptional gene silencing via histone deacetylation in *S. cerevisiae*. *Cell* 131, 706-717.
- Candelli, T., Challal, D., Briand, J.B., Boulay, J., Porrua, O., Colin, J., and Libri, D. (2018). High-resolution transcription maps reveal the widespread impact of roadblock termination in yeast. *EMBO J* 37.

- Canzio, D. (2013). A conformational switch in HP1 releases auto-inhibition to drive heterochromatin assembly. *Nature* *496*.
- Cao, R. (2002). Role of histone H3 lysine 27 methylation in polycomb-group silencing. *Science* *298*.
- Carey, M., Li, B., and Workman, J.L. (2006). RSC Exploits Histone Acetylation to Abrogate the Nucleosomal Block to RNA Polymerase II Elongation. *Molecular Cell* *24*, 481-487.
- Carninci, P. (2005). The transcriptional landscape of the mammalian genome. *Science* *309*.
- Carrozza, M.J., Li, B., Florens, L., Sukanuma, T., Swanson, S.K., Lee, K.K., Shia, W.J., Anderson, S., Yates, J., Washburn, M.P., *et al.* (2005). Histone H3 methylation by Set2 directs deacetylation of coding regions by Rpd3S to suppress spurious intragenic transcription. *Cell* *123*, 581-592.
- Carvalho, S., Raposo, A.C., Martins, F.B., Grosso, A.R., Sridhara, S.C., Rino, J., Carmo-Fonseca, M., and de Almeida, S.F. (2013). Histone methyltransferase SETD2 coordinates FACT recruitment with nucleosome dynamics during transcription. *Nucleic Acids Res* *41*, 2881-2893.
- Castel, S.E., and Martienssen, R.A. (2013). RNA interference in the nucleus: roles for small RNAs in transcription, epigenetics and beyond. *Nature reviews. Genetics* *14*, 100-112.
- Castelnuovo, M., Rahman, S., Guffanti, E., Infantino, V., Stutz, F., and Zenklusen, D. (2013). Bimodal expression of PHO84 is modulated by early termination of antisense transcription. *Nat Struct Mol Biol* *20*, 851-858.
- Castelnuovo, M., and Stutz, F. (2015). Role of chromatin, environmental changes and single cell heterogeneity in non-coding transcription and gene regulation. *Curr Opin Cell Biol* *34*, 16-22.
- Castelnuovo, M., Zaugg, J.B., Guffanti, E., Maffioletti, A., Camblong, J., Xu, Z., Clauder-Munster, S., Steinmetz, L.M., Luscombe, N.M., and Stutz, F. (2014). Role of histone modifications and early termination in pervasive transcription and antisense-mediated gene silencing in yeast. *Nucleic Acids Res* *42*, 4348-4362.
- Cavallini, B. (1988). A yeast activity can substitute for the HeLa cell TATA box factor. *Nature* *334*.
- Challal, D., Barucco, M., Kubik, S., Feuerbach, F., Candelli, T., Geoffroy, H., Benaksas, C., Shore, D., and Libri, D. (2018). General Regulatory Factors Control the Fidelity of Transcription by Restricting Non-coding and Ectopic Initiation. *Mol Cell* *72*, 955-969 e957.
- Chambers, A.L., Pearl, L.H., Oliver, A.W., and Downs, J.A. (2013). The BAH domain of Rsc2 is a histone H3 binding domain. *Nucleic Acids Res* *41*, 9168-9182.
- Chapman, R.D., Heidemann, M., Hintermair, C., and Eick, D. (2008). Molecular evolution of the RNA polymerase II CTD. *Trends Genet* *24*, 289-296.
- Chen, G. (2013). LncRNADisease: a database for long-non-coding RNA-associated diseases. *Nucleic Acids Res.* *41*.
- Chen, J., Sun, M., Kent, W.J., Huang, X., Xie, H., Wang, W., Zhou, G., Shi, R.Z., and Rowley, J.D. (2004). Over 20% of human transcripts might form sense-antisense pairs. *Nucleic Acids Res* *32*, 4812-4820.
- Chen, L.F., Lin, Y.T., Gallegos, D.A., Hazlett, M.F., Gomez-Schiavon, M., Yang, M.G., Kalmeta, B., Zhou, A.S., Holtzman, L., Gersbach, C.A., *et al.* (2019). Enhancer Histone Acetylation Modulates Transcriptional Bursting Dynamics of Neuronal Activity-Inducible Genes. *Cell Rep* *26*, 1174-1188 e1175.
- Cheng, X., and Cote, J. (2014). A new companion of elongating RNA Polymerase II: TINTIN, an independent sub-module of NuA4/TIP60 for nucleosome transactions. *Transcription* *5*.
- Chereji, R.V., Ocampo, J., and Clark, D.J. (2017). MNase-Sensitive Complexes in Yeast: Nucleosomes and Non-histone Barriers. *Mol Cell* *65*, 565-577 e563.
- Chereji, R.V., Ramachandran, S., Bryson, T.D., and Henikoff, S. (2018). Precise genome-wide mapping of single nucleosomes and linkers in vivo. *Genome Biol* *19*, 19.
- Chubb, J.R., Trcek, T., Shenoy, S.M., and Singer, R.H. (2006). Transcriptional pulsing of a developmental gene. *Curr Biol* *16*, 1018-1025.
- Churchman, L.S., and Weissman, J.S. (2011). Nascent transcript sequencing visualizes transcription at nucleotide resolution. *Nature* *469*, 368-373.
- Cirillo, L.A. (2002). Opening of compacted chromatin by early developmental transcription factors HNF3 (FoxA) and GATA-4. *Mol. Cell* *9*.
- Clapier, C.R., and Cairns, B.R. (2009). The biology of chromatin remodeling complexes. *Annu Rev Biochem* *78*, 273-304.
- Clapier, C.R., Iwasa, J., Cairns, B.R., and Peterson, C.L. (2017). Mechanisms of action and regulation of ATP-dependent chromatin-remodelling complexes. *Nat. Rev. Mol. Cell Biol.* *18*.
- Clarke, A.S., Lowell, J.E., Jacobson, S.J., and Pillus, L. (1999). Esa1p is an essential histone acetyltransferase required for cell cycle progression. *Mol. Cell. Biol.* *19*.
- Coleman, R.T., and Struhl, G. (2017). Causal role for inheritance of H3K27me3 in maintaining the OFF state of a *Drosophila* HOX gene. *Science* *356*, eaai8236.

- Colin, J., Candelli, T., Porrua, O., Boulay, J., Zhu, C., Lacroute, F., Steinmetz, Lars M., and Libri, D. (2014). Roadblock Termination by Reb1p Restricts Cryptic and Readthrough Transcription. *Molecular Cell* *56*, 667-680.
- Collin, P., Jeronimo, C., Poitras, C., and Robert, F. (2019). RNA Polymerase II CTD Tyrosine 1 Is Required for Efficient Termination by the Nrd1-Nab3-Sen1 Pathway. *Mol Cell* *73*, 655-669 e657.
- Conaway, R.C., and Conaway, J.W. (2009). The INO80 chromatin remodeling complex in transcription, replication and repair. *Trends Biochem Sci* *34*, 71-77.
- Core, L.J., Waterfall, J.J., and Lis, J.T. (2008). Nascent RNA sequencing reveals widespread pausing and divergent initiation at human promoters. *Science* *322*, 1845-1848.
- Costantino, L., and Koshland, D. (2015). The Yin and Yang of R-loop biology. *Curr Opin Cell Biol* *34*, 39-45.
- Cowieson, N.P., Partridge, J.F., Allshire, R.C., and McLaughlin, P.J. (2000). Dimerisation of a chromo shadow domain and distinctions from the chromodomain as revealed by structural analysis. *Curr. Biol.* *10*.
- Creamer, T.J., Darby, M.M., Jamonnak, N., Schaughency, P., Hao, H., Wheelan, S.J., and Corden, J.L. (2011). Transcriptome-wide binding sites for components of the *Saccharomyces cerevisiae* non-poly(A) termination pathway: Nrd1, Nab3, and Sen1. *PLoS Genet* *7*, e1002329.
- Crick, F.H. (1958). On protein synthesis. *Symp Soc Exp Biol* *12*, 138-163.
- Crump, N.T. (2011). Dynamic acetylation of all lysine-4 trimethylated histone H3 is evolutionarily conserved and mediated by p300/CBP. *Proc. Natl Acad. Sci. USA* *108*.
- Csorba, T., Questa, J.I., Sun, Q., and Dean, C. (2014). Antisense COOLAIR mediates the coordinated switching of chromatin states at FLC during vernalization. *Proc Natl Acad Sci U S A* *111*, 16160-16165.
- Darby, M.M., Serebreni, L., Pan, X., Boeke, J.D., and Corden, J.L. (2012). The *Saccharomyces cerevisiae* Nrd1-Nab3 transcription termination pathway acts in opposition to Ras signaling and mediates response to nutrient depletion. *Mol Cell Biol* *32*, 1762-1775.
- De Koning, L., Corpet, A., Haber, J.E., and Almouzni, G. (2007). Histone chaperones: an escort network regulating histone traffic. *Nature Struct. Mol. Biol.* *14*.
- De, S., and Kassis, J.A. (2017). Passing epigenetic silence to the next generation. *Science* *356*, 28-29.
- De Vos, D., Frederiks, F., Terweij, M., van Welsem, T., Verzijlbergen, K.F., Iachina, E., de Graaf, E.L., Altelaar, A.F.M., Oudgenoeg, G., Heck, A.J.R., *et al.* (2011). Progressive methylation of ageing histones by Dot1 functions as a timer. *EMBO Rep* *12*, 956-962.
- Diehl, K.L., and Muir, T.W. (2020). Chromatin as a key consumer in the metabolite economy. *Nat Chem Biol* *16*, 620-629.
- Ding, Q., and MacAlpine, D.M. (2011). Defining the replication program through the chromatin landscape. *Crit Rev Biochem Mol Biol* *46*, 165-179.
- Dinger, M.E. (2008). Long noncoding RNAs in mouse embryonic stem cell pluripotency and differentiation. *Genome Res.* *18*.
- Dion, M.F., Altschuler, S.J., Wu, L.F., and Rando, O.J. (2005). Genomic characterization reveals a simple histone H4 acetylation code. *Proceedings of the National Academy of Sciences of the United States of America* *102*, 5501-5506.
- Dion, M.F., Kaplan, T., Kim, M., Buratowski, S., Friedman, N., and Rando, O.J. (2007). Dynamics of replication-independent histone turnover in budding yeast. *Science* *315*, 1405-1408.
- Dixon, J.R. (2012). Topological domains in mammalian genomes identified by analysis of chromatin interactions. *Nature* *485*.
- Djebali, S. (2012). Landscape of transcription in human cells. *Nature* *489*.
- Dodson, A.E., and Rine, J. (2015). Heritable capture of heterochromatin dynamics in *Saccharomyces cerevisiae*. *eLife* *4*, e05007.
- Downey, M. (2015). Acetylome profiling reveals overlap in the regulation of diverse processes by sirtuins, *gcn5*, and *esa1*. *Mol. Cell. Proteom.* *14*.
- Doyon, Y., and Cote, J. (2004). The highly conserved and multifunctional NuA4 HAT complex. *Curr. Opin. Genet. Dev.* *14*.
- Durand, A., Bonnet, J., Fournier, M., Chavant, V., and Schultz, P. (2014). Mapping the deubiquitination module within the SAGA complex. *Structure* *22*.
- Durant, M., and Pugh, B.F. (2007). NuA4-directed chromatin transactions throughout the *Saccharomyces cerevisiae* genome. *Mol Cell Biol* *27*, 5327-5335.
- Earnshaw, W.C., and Laemmli, U.K. (1983). Architecture of metaphase chromosomes and chromosome scaffolds. *J Cell Biol* *96*, 84-93.
- Eaton, M.L., Galani, K., Kang, S., Bell, S.P., and MacAlpine, D.M. (2010). Conserved nucleosome positioning defines replication origins. *Genes Dev.* *24*.

- Engelholm, M., de Jager, M., Flaus, A., Brenk, R., van Noort, J., and Owen-Hughes, T. (2009). Nucleosomes can invade DNA territories occupied by their neighbors. *Nat Struct Mol Biol* *16*, 151-158.
- Engel, C., Sainsbury, S., Cheung, A.C., Kostrewa, D., and Cramer, P. (2013). RNA polymerase I structure and transcription regulation. *Nature* *502*.
- Engreitz, J.M., Ollikainen, N., and Guttman, M. (2016). Long non-coding RNAs: spatial amplifiers that control nuclear structure and gene expression. *Nat Rev Mol Cell Biol* *17*, 756-770.
- Fan, X. (2010). Nucleosome depletion in yeast terminator regions is not intrinsic and can occur by a transcriptional mechanism linked to 3' end formation. *Proc. Natl. Acad. Sci. USA* *107*.
- Fang, S. (2018). NONCODEV5: a comprehensive annotation database for long non-coding RNAs. *Nucleic Acids Res.* *46*.
- Fazio, T.G., and Tsukiyama, T. (2003). Chromatin remodeling in vivo: evidence for a nucleosome sliding mechanism. *Mol. Cell* *12*.
- Ferreira, H., Flaus, A., and Owen-Hughes, T. (2007). Histone modifications influence the action of Snf2 family remodelling enzymes by different mechanisms. *J Mol Biol* *374*, 563-579.
- Filippakopoulos, P. (2012). Histone recognition and large-scale structural analysis of the human bromodomain family. *Cell* *149*.
- Fischer, T., Cui, B., Dhakshnamoorthy, J., Zhou, M., Rubin, C., Zofall, M., Veenstra, T.D., and Grewal, S.I. (2009). Diverse roles of HP1 proteins in heterochromatin assembly and functions in fission yeast. *Proc Natl Acad Sci U S A* *106*, 8998-9003.
- Fischl, H., Howe, F.S., Furger, A., and Mellor, J. (2017). Paf1 Has Distinct Roles in Transcription Elongation and Differential Transcript Fate. *Molecular cell* *65*, 685-698.e688.
- Ford, J., Odeyale, O., and Shen, C.H. (2008). Activator-dependent recruitment of SWI/SNF and INO80 during INO1 activation. *Biochem Biophys Res Commun* *373*, 602-606.
- Friis, R.M. (2009). A glycolytic burst drives glucose induction of global histone acetylation by picNuA4 and SAGA. *Nucleic Acids Res.* *37*.
- Fujisawa, T., and Filippakopoulos, P. (2017). Functions of bromodomain-containing proteins and their roles in homeostasis and cancer. *Nat. Rev. Mol. Cell Biol.* *18*.
- Gates, L.A., Foulds, C.E., and O'Malley, B.W. (2017). Histone Marks in the 'Driver's Seat': Functional Roles in Steering the Transcription Cycle. *Trends Biochem Sci* *42*, 977-989.
- Geisberg, J.V., Moqtaderi, Z., Fan, X., Oszolak, F., and Struhl, K. (2014). Global analysis of mRNA isoform half-lives reveals stabilizing and destabilizing elements in yeast. *Cell* *156*, 812-824.
- Gibcus, J.H., Samejima, K., Goloborodko, A., Samejima, I., Naumova, N., Nuebler, J., Kanemaki, M.T., Xie, L., Paulson, J.R., Earnshaw, W.C., *et al.* (2018). A pathway for mitotic chromosome formation. *Science* *359*.
- Gil, N., and Ulitsky, I. (2020). Regulation of gene expression by cis-acting long non-coding RNAs. *Nature reviews. Genetics* *21*, 102-117.
- Gilbert, W., and Muller-Hill, B. (1966). Isolation of the lac repressor. *Proc. Natl Acad. Sci. USA* *56*.
- Gill, J.K., Maffioletti, A., Garcia-Molinero, V., Stutz, F., and Soudet, J. (2020). Fine Chromatin-Driven Mechanism of Transcription Interference by Antisense Noncoding Transcription. *Cell Rep* *31*, 107612.
- Gkikopoulos, T. (2011). A role for Snf2-related nucleosome-spacing enzymes in genome-wide nucleosome organization. *Science* *333*.
- Govind, C.K., Qiu, H., Ginsburg, D.S., Ruan, C., Hofmeyer, K., Hu, C., Swaminathan, V., Workman, J.L., Li, B., and Hinnebusch, A.G. (2010). Phosphorylated Pol II CTD recruits multiple HDACs, including Rpd3C(S), for methylation-dependent deacetylation of ORF nucleosomes. *Molecular cell* *39*, 234-246.
- Grant, P.A. (1997). Yeast Gcn5 functions in two multisubunit complexes to acetylate nucleosomal histones: characterization of an Ada complex and the SAGA (Spt/Ada) complex. *Genes Dev.* *11*.
- Grant, P.A., Schieltz, D., Pray-Grant, M.G., Yates, J.R., and Workman, J.L. (1998). The ATM-related cofactor Tra1 is a component of the purified SAGA complex. *Mol. Cell* *2*.
- Grünberg, S., Warfield, L., and Hahn, S. (2012). Architecture of the RNA polymerase II preinitiation complex and mechanism of ATP-dependent promoter opening. *Nat. Struct. Mol. Biol.* *19*.
- Gullerova, M., and Proudfoot, N.J. (2012). Convergent transcription induces transcriptional gene silencing in fission yeast and mammalian cells. *Nat Struct Mol Biol* *19*, 1193-1201.
- Guttman, M., Donaghey, J., Carey, B.W., Garber, M., Grenier, J.K., Munson, G., Young, G., Lucas, A.B., Ach, R., Bruhn, L., *et al.* (2011). lincRNAs act in the circuitry controlling pluripotency and differentiation. *Nature* *477*, 295-300.
- Haberle, V., and Stark, A. (2018). Eukaryotic core promoters and the functional basis of transcription initiation. *Nat. Rev. Mol. Cell Biol.* *19*.

- Hainer, S.J., Pruneski, J.A., Mitchell, R.D., Monteverde, R.M., and Martens, J.A. (2011). Intergenic transcription causes repression by directing nucleosome assembly. *Genes Dev* 25, 29-40.
- Halic, M., and Moazed, D. (2010). Dicer-independent primal RNAs trigger RNAi and heterochromatin formation. *Cell* 140, 504-516.
- Han, M., and Grunstein, M. (1988). Nucleosome loss activates yeast downstream promoters in vivo. *Cell* 55, 1137-1145.
- Han, Z., Jasnovidova, O., Haidara, N., Tudek, A., Kubicek, K., Libri, D., Stefl, R., and Porrua, O. (2020). Termination of non-coding transcription in yeast relies on both an RNA Pol II CTD interaction domain and a CTD-mimicking region in Sen1. *EMBO J* 39, e101548.
- Han, Z., Libri, D., and Porrua, O. (2017). Biochemical characterization of the helicase Sen1 provides new insights into the mechanisms of non-coding transcription termination. *Nucleic Acids Res* 45, 1355-1370.
- Hanson, S.J., and Wolfe, K.H. (2017). An evolutionary perspective on yeast mating-type switching. *Genetics* 206.
- Harlen, K.M., and Churchman, L.S. (2017). The code and beyond: transcription regulation by the RNA polymerase II carboxy-terminal domain. *Nat Rev Mol Cell Biol* 18, 263-273.
- Harlen, K.M., Trotta, K.L., Smith, E.E., Mosaheb, M.M., Fuchs, S.M., and Churchman, L.S. (2016). Comprehensive RNA Polymerase II Interactomes Reveal Distinct and Varied Roles for Each Phospho-CTD Residue. *Cell Rep* 15, 2147-2158.
- Hartley, P.D., and Madhani, H.D. (2009). Mechanisms that specify promoter nucleosome location and identity. *Cell* 137, 445-458.
- Haruki, H., Nishikawa, J., and Laemmli, U.K. (2008). The anchor-away technique: rapid, conditional establishment of yeast mutant phenotypes. *Mol Cell* 31, 925-932.
- Hashimshony, T., Zhang, J., Keshet, I., Bustin, M., and Cedar, H. (2003). The role of DNA methylation in setting up chromatin structure during development. *Nat. Genet.* 34.
- Hassan, A.H., Prochasson, P., Neely, K.E., Galasinski, S.C., Chandy, M., Carrozza, M.J., and Workman, J.L. (2002). Function and Selectivity of Bromodomains in Anchoring Chromatin-Modifying Complexes to Promoter Nucleosomes. *Cell* 111, 369-379.
- Henikoff, S., and Gready, J.M. (2016). Epigenetics, cellular memory and gene regulation. *Curr Biol* 26, R644-648.
- Henikoff, S., Ramachandran, S., Krassovsky, K., Bryson, T.D., Codomo, C.A., Brogaard, K., Widom, J., Wang, J.P., and Henikoff, J.G. (2014). The budding yeast Centromere DNA Element II wraps a stable Cse4 hemisome in either orientation in vivo. *Elife* 3, e01861.
- Henriques, T. (2013). Stable pausing by RNA polymerase II provides an opportunity to target and integrate regulatory signals. *Mol. Cell* 52.
- Henry, K.W., Wyce, A., Lo, W.S., Duggan, L.J., Emre, N.C., Kao, C.F., Pillus, L., Shilatfard, A., Osley, M.A., and Berger, S.L. (2003). Transcriptional activation via sequential histone H2B ubiquitylation and deubiquitylation, mediated by SAGA-associated Ubp8. *Genes & development* 17, 2648-2663.
- Hirota, K., Miyoshi, T., Kugou, K., Hoffman, C.S., Shibata, T., and Ohta, K. (2008). Stepwise chromatin remodelling by a cascade of transcription initiation of non-coding RNAs. *Nature* 456, 130-134.
- Hoagland, M.B., Stephenson, M.L., Scott, J.F., Hecht, L.I., and Zamecnik, P.C. (1958). A soluble ribonucleic acid intermediate in protein synthesis. *J. Biol. Chem.* 231.
- Hobson, D.J., Wei, W., Steinmetz, L.M., and Svejstrup, J.Q. (2012). RNA polymerase II collision interrupts convergent transcription. *Mol Cell* 48, 365-374.
- Hong, L., Schroth, G.P., Matthews, H.R., Yau, P., and Bradbury, E.M. (1993). Studies of the DNA binding properties of histone H4 amino terminus – thermal denaturation studies reveal that acetylation markedly reduces the binding constant of the H4 “tail” to DNA. *J. Biol. Chem.* 268.
- Hornung, G. (2012). Noise-mean relationship in mutated promoters. *Genome Res.* 22.
- Hou, L., Wang, Y., Liu, Y., Zhang, N., Shamovsky, I., Nudler, E., Tian, B., and Dynlacht, B.D. (2019). Paf1C regulates RNA polymerase II progression by modulating elongation rate. *Proceedings of the National Academy of Sciences* 116, 14583-14592.
- Hsieh, T.H. (2015). Mapping nucleosome resolution chromosome folding in yeast by Micro-C. *Cell* 162.
- Hsu, C.C. (2018). Recognition of histone acetylation by the GAS41 YEATS domain promotes H2A.Z deposition in non-small cell lung cancer. *Genes Dev.* 32.
- Hudson, B.P., Martinez-Yamout, M.A., Dyson, H.J., and Wright, P.E. (2000). Solution structure and acetyl-lysine binding activity of the GCN5 bromodomain. *J Mol Biol* 304, 355-370.
- Hughes, A.L., Jin, Y., Rando, O.J., and Struhl, K. (2012). A functional evolutionary approach to identify determinants of nucleosome positioning: a unifying model for establishing the genome-wide pattern. *Mol Cell* 48, 5-15.

- Huisinga, K.L., and Pugh, B.F. (2004). A genome-wide housekeeping role for TFIID and a highly regulated stress-related role for SAGA in *Saccharomyces cerevisiae*. *Mol. Cell* *13*.
- Iglesias, N., Currie, M.A., Jih, G., Paulo, J.A., Siuti, N., Kalocsay, M., Gygi, S.P., and Moazed, D. (2018). Automethylation-induced conformational switch in Clr4 (Suv39h) maintains epigenetic stability. *Nature* *560*, 504-508.
- Jackson, J.P., Lindroth, A.M., Cao, X., and Jacobsen, S.E. (2002). Control of CpNpG DNA methylation by the KRYPTONITE histone H3 methyltransferase. *Nature* *416*.
- Jacob, F., and Monod, J. (1961). Genetic regulatory mechanisms in the synthesis of proteins. *J. Mol. Biol.* *3*.
- Jamonnak, N., Creamer, T.J., Darby, M.M., Schaughency, P., Wheelan, S.J., and Corden, J.L. (2011). Yeast Nrd1, Nab3, and Sen1 transcriptome-wide binding maps suggest multiple roles in post-transcriptional RNA processing. *RNA* *17*, 2011-2025.
- Jenuwein, T., and Allis, C.D. (2001). Translating the histone code. *Science* *293*.
- Jeronimo, C. (2016). Tail and kinase modules differently regulate core Mediator recruitment and function in vivo. *Mol. Cell* *64*.
- Jeronimo, C., Bataille, A.R., and Robert, F. (2013). The writers, readers, and functions of the RNA polymerase II C-terminal domain code. *Chem Rev* *113*, 8491-8522.
- Jeronimo, C., Watanabe, S., Kaplan, C.D., Peterson, C.L., and Robert, F. (2015). The Histone Chaperones FACT and Spt6 Restrict H2A.Z from Intragenic Locations. *Mol Cell* *58*, 1113-1123.
- Jin, Y., Eser, U., Struhl, K., and Churchman, L.S. (2017). The ground state and evolution of promoter region directionality. *Cell* *170*.
- Kaikkonen, M.U., and Adelman, K. (2018). Emerging Roles of Non-Coding RNA Transcription. *Trends Biochem Sci* *43*, 654-667.
- Kanno, T. (2004). Selective recognition of acetylated histones by bromodomain proteins visualized in living cells. *Mol. Cell* *13*.
- Kaplan, C.D., Laprade, L., and Winston, F. (2003). Transcription elongation factors repress transcription initiation from cryptic sites. *Science* *301*, 1096-1099.
- Kaplan, N. (2009). The DNA-encoded nucleosome organization of a eukaryotic genome. *Nature* *458*.
- Kasten, M., Szerlong, H., Erdjument-Bromage, H., Tempst, P., Werner, M., and Cairns, B.R. (2004). Tandem bromodomains in the chromatin remodeler RSC recognize acetylated histone H3 Lys14. *EMBO J* *23*, 1348-1359.
- Kato, D., Osakabe, A., Arimura, Y., Mizukami, Y., Horikoshi, N., Saikusa, K., Akashi, S., Nishimura, Y., Park, S.Y., Nogami, J., *et al.* (2017). Crystal structure of the overlapping dinucleosome composed of hexasome and octasome. *Science* *356*, 205-208.
- Kehayova, P.D., and Liu, D.R. (2007). In vivo evolution of an RNA-based transcriptional silencing domain in *S. cerevisiae*. *Chem Biol* *14*, 65-74.
- Keogh, M.C., Kim, J.A., Downey, M., Fillingham, J., Chowdhury, D., Harrison, J.C., Onishi, M., Datta, N., Galicia, S., Emili, A., *et al.* (2006). A phosphatase complex that dephosphorylates gammaH2AX regulates DNA damage checkpoint recovery. *Nature* *439*, 497-501.
- Keogh, M.C., Kurdistani, S.K., Morris, S.A., Ahn, S.H., Podolny, V., Collins, S.R., Schuldiner, M., Chin, K., Punna, T., Thompson, N.J., *et al.* (2005). Cotranscriptional set2 methylation of histone H3 lysine 36 recruits a repressive Rpd3 complex. *Cell* *123*, 593-605.
- Khapersky, D.A., Ammerman, M.L., Majovski, R.C., and Ponticelli, A.S. (2008). Functions of *Saccharomyces cerevisiae* TFIIF during transcription start site utilization. *Mol. Cell. Biol.* *28*.
- Khorkova, O., Myers, A.J., Hsiao, J., and Wahlestedt, C. (2014). Natural antisense transcripts. *Hum Mol Genet* *23*, R54-63.
- Kim, J., Guermah, M., McGinty, R.K., Lee, J.S., Tang, Z., Milne, T.A., Shilatifard, A., Muir, T.W., and Roeder, R.G. (2009). RAD6-Mediated transcription-coupled H2B ubiquitylation directly stimulates H3K4 methylation in human cells. *Cell* *137*, 459-471.
- Kim, J.H., Lee, B.B., Oh, Y.M., Zhu, C., Steinmetz, L.M., Lee, Y., Kim, W.K., Lee, S.B., Buratowski, S., and Kim, T. (2016). Modulation of mRNA and lncRNA expression dynamics by the Set2-Rpd3S pathway. *Nat Commun* *7*, 13534.
- Kim, T., and Buratowski, S. (2007). Two *Saccharomyces cerevisiae* JmjC domain proteins demethylate histone H3 Lys36 in transcribed regions to promote elongation. *J Biol Chem* *282*, 20827-20835.
- Kim, T., and Buratowski, S. (2009). Dimethylation of H3K4 by Set1 recruits the Set3 histone deacetylase complex to 5' transcribed regions. *Cell* *137*, 259-272.
- Kim, T., Xu, Z., Clauder-Munster, S., Steinmetz, L.M., and Buratowski, S. (2012). Set3 HDAC mediates effects of overlapping noncoding transcription on gene induction kinetics. *Cell* *150*, 1158-1169.

- Kim, T.K., Ebright, R.H., and Reinberg, D. (2000). Mechanism of ATP-dependent promoter melting by transcription factor IIH. *Science* *288*.
- Kim, Y.J., Bjorklund, S., Li, Y., Sayre, M.H., and Kornberg, R.D. (1994). A multiprotein mediator of transcriptional activation and its interaction with the C-terminal repeat domain of RNA polymerase II. *Cell* *77*.
- Kireeva, M.L. (2002). Nucleosome remodeling induced by RNA polymerase II: loss of the H2A/H2B dimer during transcription. *Mol. Cell* *9*.
- Kizer, K.O., Phatnani, H.P., Shibata, Y., Hall, H., Greenleaf, A.L., and Strahl, B.D. (2005). A novel domain in Set2 mediates RNA polymerase II interaction and couples histone H3 K36 methylation with transcript elongation. *Mol Cell Biol* *25*, 3305-3316.
- Kleff, S., Andrulis, E.D., Anderson, C.W., and Sternglanz, R. (1995). Identification of a gene encoding a yeast histone H4 acetyltransferase. *J. Biol. Chem.* *270*.
- Klein-Brill, A., Joseph-Strauss, D., Appleboim, A., and Friedman, N. (2019). Dynamics of Chromatin and Transcription during Transient Depletion of the RSC Chromatin Remodeling Complex. *Cell Rep* *26*, 279-292 e275.
- Knutson, B.A., and Hahn, S. (2011). Domains of Tra1 important for activator recruitment and transcription coactivator functions of SAGA and NuA4 complexes. *Mol. Cell. Biol.* *31*.
- Kobor, M.S., Venkatasubrahmanyam, S., Meneghini, M.D., Gin, J.W., Jennings, J.L., Link, A.J., Madhani, H.D., and Rine, J. (2004). A protein complex containing the conserved Swi2/Snf2-related ATPase Swr1p deposits histone variant H2A.Z into euchromatin. *PLoS Biol* *2*, E131.
- Köhler, A., Schneider, M., Cabal, G.G., Nehrbass, U., and Hurt, E. (2008). Yeast Ataxin-7 links histone deubiquitination with gene gating and mRNA export. *Nat Cell Biol* *10*, 707-715.
- Köhler, A., Zimmerman, E., Schneider, M., Hurt, E., and Zheng, N. (2010). Structural basis for assembly and activation of the heterotetrameric SAGA histone H2B deubiquitinase module. *Cell* *141*, 606-617.
- Kolonko, E.M., Albaugh, B.N., Lindner, S.E., Chen, Y., Satyshur, K.A., Arnold, K.M., Kaufman, P.D., Keck, J.L., and Denu, J.M. (2010). Catalytic activation of histone acetyltransferase Rtt109 by a histone chaperone. *Proc Natl Acad Sci U S A* *107*, 20275-20280.
- Kopp, F., and Mendell, J.T. (2018). Functional Classification and Experimental Dissection of Long Noncoding RNAs. *Cell* *172*, 393-407.
- Kornberg, R.D. (1977). Structure of chromatin. *Annu Rev Biochem* *46*, 931-954.
- Kornberg, R.D. (2007). The molecular basis of eukaryotic transcription. *Proc. Natl Acad. Sci. USA* *104*.
- Kornberg, R.D., and Lorch, Y. (2020). Primary Role of the Nucleosome. *Molecular Cell* *79*, 371-375.
- Kornberg, R.D., and Thomas, J.O. (1974). Chromatin structure; oligomers of the histones. *Science* *184*.
- Kos, M., and Tollervey, D. (2010). Yeast pre-rRNA processing and modification occur cotranscriptionally. *Mol Cell* *37*, 809-820.
- Kostreva, D. (2009). RNA polymerase II-TFIIB structure and mechanism of transcription initiation. *Nature* *462*.
- Koutelou, E., Hirsch, C.L., and Dent, S.Y. (2010). Multiple faces of the SAGA complex. *Curr Opin Cell Biol* *22*, 374-382.
- Kouzarides, T. (2007). Chromatin modifications and their function. *Cell* *128*.
- Krogan, N.J., Baetz, K., Keogh, M.C., Datta, N., Sawa, C., Kwok, T.C., Thompson, N.J., Davey, M.G., Pootoolal, J., Hughes, T.R., *et al.* (2004). Regulation of chromosome stability by the histone H2A variant Htz1, the Swr1 chromatin remodeling complex, and the histone acetyltransferase NuA4. *Proc Natl Acad Sci U S A* *101*, 13513-13518.
- Krogan, N.J., Dover, J., Wood, A., Schneider, J., Heidt, J., Boateng, M.A., Dean, K., Ryan, O.W., Golshani, A., Johnston, M., *et al.* (2003a). The Paf1 complex is required for histone H3 methylation by COMPASS and Dot1p: linking transcriptional elongation to histone methylation. *Molecular cell* *11*, 721-729.
- Krogan, N.J., Kim, M., Tong, A., Golshani, A., Cagney, G., Canadien, V., Richards, D.P., Beattie, B.K., Emili, A., Boone, C., *et al.* (2003b). Methylation of histone H3 by Set2 in *Saccharomyces cerevisiae* is linked to transcriptional elongation by RNA polymerase II. *Molecular and cellular biology* *23*, 4207-4218.
- Kuang, Z., Cai, L., Zhang, X., Ji, H., Tu, B.P., and Boeke, J.D. (2014). High-temporal-resolution view of transcription and chromatin states across distinct metabolic states in budding yeast. *Nat Struct Mol Biol* *21*, 854-863.
- Kubik, S. (2018). Sequence-directed action of RSC remodeler and general regulatory factors modulates +1 nucleosome position to facilitate transcription. *Mol. Cell* *71*.
- Kubik, S. (2019). Opposing chromatin remodelers control transcription initiation frequency and start site selection. *Nat. Struct. Mol. Biol.* *26*.
- Kubik, S., Bruzzone, M.J., Albert, B., and Shore, D. (2017). A Reply to "MNase-Sensitive Complexes in Yeast: Nucleosomes and Non-histone Barriers," by Chereji *et al.* *Mol Cell* *65*, 578-580.

- Kubik, S., Bruzzone, M.J., Jacquet, P., Falcone, J.L., Rougemont, J., and Shore, D. (2015). Nucleosome Stability Distinguishes Two Different Promoter Types at All Protein-Coding Genes in Yeast. *Mol Cell* *60*, 422-434.
- Kuehner, J.N., and Brow, D.A. (2006). Quantitative analysis of in vivo initiator selection by yeast RNA polymerase II supports a scanning model. *J. Biol. Chem.* *281*.
- Kulaeva, O.I. (2009). Mechanism of chromatin remodeling and recovery during passage of RNA polymerase II. *Nature Struct. Mol. Biol.* *16*.
- Kuo, M.H. (1996). Transcription-linked acetylation by Gcn5p of histones H3 and H4 at specific lysines. *Nature* *383*.
- Kusch, T. (2004). Acetylation by Tip60 is required for selective histone variant exchange at DNA lesions. *Science* *306*.
- Kuzmichev, A., Nishioka, K., Erdjument-Bromage, H., Tempst, P., and Reinberg, D. (2002). Histone methyltransferase activity associated with a human multiprotein complex containing the enhancer of zeste protein. *Genes Dev.* *16*.
- Kwak, H., Fuda, N.J., Core, L.J., and Lis, J.T. (2013). Precise maps of RNA polymerase reveal how promoters direct initiation and pausing. *Science* *339*, 950-953.
- LaCava, J., Houseley, J., Saveanu, C., Petfalski, E., Thompson, E., Jacquier, A., and Tollervey, D. (2005). RNA degradation by the exosome is promoted by a nuclear polyadenylation complex. *Cell* *121*, 713-724.
- Lai, F. (2013). Activating RNAs associate with Mediator to enhance chromatin architecture and transcription. *Nature* *494*.
- Lai, F., Gardini, A., Zhang, A., and Shiekhattar, R. (2015). Integrator mediates the biogenesis of enhancer RNAs. *Nature* *525*, 399-403.
- Lai, W.K.M., and Pugh, B.F. (2017). Understanding nucleosome dynamics and their links to gene expression and DNA replication. *Nature Reviews Molecular Cell Biology* *18*, 548.
- Landry, J., Sutton, A., Hesman, T., Min, J., Xu, R.M., Johnston, M., and Sternglanz, R. (2003). Set2-catalyzed methylation of histone H3 represses basal expression of GAL4 in *Saccharomyces cerevisiae*. *Mol Cell Biol* *23*, 5972-5978.
- Laprell, F., Finkl, K., and Muller, J. (2017). Propagation of Polycomb-repressed chromatin requires sequence-specific recruitment to DNA. *Science* *356*, 85-88.
- Larsson, A.J.M., Johnsson, P., Hagemann-Jensen, M., Hartmanis, L., Faridani, O.R., Reinius, B., Segerstolpe, A., Rivera, C.M., Ren, B., and Sandberg, R. (2019). Genomic encoding of transcriptional burst kinetics. *Nature* *565*, 251-254.
- Lau, M.S., Schwartz, M.G., Kundu, S., Savol, A.J., Wang, P.I., Marr, S.K., Grau, D.J., Schorderet, P., Sadreyev, R.I., Tabin, C.J., *et al.* (2017). Mutation of a nucleosome compaction region disrupts Polycomb-mediated axial patterning. *Science* *355*, 1081-1084.
- Lauberth, S.M., Nakayama, T., Wu, X., Ferris, A.L., Tang, Z., Hughes, S.H., and Roeder, R.G. (2013). H3K4me3 interactions with TAF3 regulate preinitiation complex assembly and selective gene activation. *Cell* *152*, 1021-1036.
- Lee, B.B., Choi, A., Kim, J.H., Jun, Y., Woo, H., Ha, S.D., Yoon, C.Y., Hwang, J.T., Steinmetz, L., Buratowski, S., *et al.* (2018a). Rpd3L HDAC links H3K4me3 to transcriptional repression memory. *Nucleic Acids Res* *46*, 8261-8274.
- Lee, K.Y., Chen, Z., Jiang, R., and Meneghini, M.D. (2018b). H3K4 Methylation Dependent and Independent Chromatin Regulation by JHD2 and SET1 in Budding Yeast. *G3 (Bethesda)* *8*, 1829-1839.
- Lee, K.Y., Ranger, M., and Meneghini, M.D. (2018c). Combinatorial Genetic Control of Rpd3S Through Histone H3K4 and H3K36 Methylation in Budding Yeast. *G3 (Bethesda)* *8*, 3411-3420.
- Lee, W. (2007). A high-resolution atlas of nucleosome occupancy in yeast. *Nat. Genet.* *39*.
- Lemon, B., Inouye, C., King, D.S., and Tjian, R. (2001). Selectivity of chromatin-remodelling cofactors for ligand-activated transcription. *Nature* *414*, 924-928.
- Lenstra, T.L., Benschop, J.J., Kim, T., Schulze, J.M., Brabers, N.A., Margaritis, T., van de Pasch, L.A., van Heesch, S.A., Brok, M.O., Groot Koerkamp, M.J., *et al.* (2011). The specificity and topology of chromatin interaction pathways in yeast. *Molecular cell* *42*, 536-549.
- Lenstra, T.L., Coulon, A., Chow, C.C., and Larson, D.R. (2015). Single-Molecule Imaging Reveals a Switch between Spurious and Functional ncRNA Transcription. *Molecular cell* *60*, 597-610.
- Leonaite, B., Han, Z., Basquin, J., Bonneau, F., Libri, D., Porrua, O., and Conti, E. (2017). Sen1 has unique structural features grafted on the architecture of the Upf1-like helicase family. *EMBO J* *36*, 1590-1604.
- LeRoy, G., Orphanides, G., Lane, W.S., and Reinberg, D. (1998). Requirement of RSF and FACT for Transcription of Chromatin Templates in Vitro. *Science* *282*, 1900-1904.
- Levine, M., and Tjian, R. (2003). Transcription regulation and animal diversity. *Nature* *424*.
- Li, B., Carey, M., and Workman, J.L. (2007a). The role of chromatin during transcription. *Cell* *128*.

- Li, B., Gogol, M., Carey, M., Lee, D., Seidel, C., and Workman, J.L. (2007b). Combined action of PHD and chromo domains directs the Rpd3S HDAC to transcribed chromatin. *Science* *316*, 1050-1054.
- Li, B., Howe, L., Anderson, S., Yates, J.R., 3rd, and Workman, J.L. (2003). The Set2 histone methyltransferase functions through the phosphorylated carboxyl-terminal domain of RNA polymerase II. *J Biol Chem* *278*, 8897-8903.
- Li, B., Pattenden, S.G., Lee, D., Gutierrez, J., Chen, J., Seidel, C., Gerton, J., and Workman, J.L. (2005). Preferential occupancy of histone variant H2AZ at inactive promoters influences local histone modifications and chromatin remodeling. *Proc Natl Acad Sci U S A* *102*, 18385-18390.
- Li, W., Chen, P., Yu, J., Dong, L., Liang, D., Feng, J., Yan, J., Wang, P.-Y., Li, Q., Zhang, Z., *et al.* (2016). FACT Remodels the Tetranucleosomal Unit of Chromatin Fibers for Gene Transcription. *Molecular Cell* *64*, 120-133.
- Li, Y. (2014). AF9 YEATS domain links histone acetylation to DOT1L-mediated H3K79 methylation. *Cell* *159*.
- Lieberman-Aiden, E., van Berkum, N.L., Williams, L., Imakaev, M., Ragooczy, T., Telling, A., Amit, I., Lajoie, B.R., Sabo, P.J., Dorschner, M.O., *et al.* (2009). Comprehensive mapping of long-range interactions reveals folding principles of the human genome. *Science* *326*, 289-293.
- Lin, J.M., Collins, P.J., Trinklein, N.D., Fu, Y., Xi, H., Myers, R.M., and Weng, Z. (2007). Transcription factor binding and modified histones in human bidirectional promoters. *Genome Res* *17*, 818-827.
- Liu, G., Mattick, J., and Taft, R.J. (2013). A meta-analysis of the genomic and transcriptomic composition of complex life. *Cell Cycle* *12*.
- Liu, J., Francois, J.M., and Capp, J.P. (2016). Use of noise in gene expression as an experimental parameter to test phenotypic effects. *Yeast* *33*, 209-216.
- Lorch, Y., LaPointe, J.W., and Kornberg, R.D. (1987). Nucleosomes inhibit the initiation of transcription but allow chain elongation with the displacement of histones. *Cell* *49*.
- Lorch, Y., Maier-Davis, B., and Kornberg, R.D. (2006). Chromatin remodeling by nucleosome disassembly in vitro. *Proc Natl Acad Sci U S A* *103*, 3090-3093.
- Lorch, Y., Maier-Davis, B., and Kornberg, R.D. (2014). Role of DNA sequence in chromatin remodeling and the formation of nucleosome-free regions. *Genes Dev.* *28*.
- Loubiere, V., Papadopoulos, G.L., Szabo, Q., Martinez, A.M., and Cavalli, G. (2020). Widespread activation of developmental gene expression characterized by PRC1-dependent chromatin looping. *Sci Adv* *6*, eaax4001.
- Luger, K., Dechassa, M.L., and Tremethick, D.J. (2012). New insights into nucleosome and chromatin structure: an ordered state or a disordered affair? *Nat. Rev. Mol. Cell Biol.* *13*.
- Luger, K., Mäder, A.W., Richmond, R.K., Sargent, D.F., and Richmond, T.J. (1997). Crystal structure of the nucleosome core particle at 2.8Å resolution. *Nature* *389*.
- Luk, E., Ranjan, A., Fitzgerald, P.C., Mizuguchi, G., Huang, Y., Wei, D., and Wu, C. (2010). Stepwise histone replacement by SWR1 requires dual activation with histone H2A.Z and canonical nucleosome. *Cell* *143*, 725-736.
- Luk, E., Vu, N.D., Patteson, K., Mizuguchi, G., Wu, W.H., Ranjan, A., Backus, J., Sen, S., Lewis, M., Bai, Y., *et al.* (2007). Chz1, a nuclear chaperone for histone H2AZ. *Mol Cell* *25*, 357-368.
- Lyon, K., Aguilera, L.U., Morisaki, T., Munsky, B., and Stasevich, T.J. (2019). Live-Cell Single RNA Imaging Reveals Bursts of Translational Frameshifting. *Molecular Cell* *75*, 172-183.e179.
- Ma, N., and McAllister, W.T. (2009). In a head-on collision, two RNA polymerases approaching one another on the same DNA may pass by one another. *J Mol Biol* *391*, 808-812.
- Malabat, C., Feuerbach, F., Ma, L., Saveanu, C., and Jacquier, A. (2015). Quality control of transcription start site selection by nonsense-mediated-mRNA decay. *Elife* *4*.
- Malik, S., Molina, H., and Xue, Z. (2017). PIC Activation through Functional Interplay between Mediator and TFIIF. *J Mol Biol* *429*, 48-63.
- Malik, S., and Roeder, R.G. (2016). Mediator: A Drawbridge across the Enhancer-Promoter Divide. *Mol Cell* *64*, 433-434.
- Maltby, V.E. (2012). Histone H3 lysine 36 methylation targets the Isw1b remodeling complex to chromatin. *Mol. Cell Biol.* *32*.
- Margaritis, T., Oreal, V., Brabers, N., Maestroni, L., Vitaliano-Prunier, A., Benschop, J.J., van Hooff, S., van Leenen, D., Dargemont, C., Geli, V., *et al.* (2012). Two distinct repressive mechanisms for histone 3 lysine 4 methylation through promoting 3'-end antisense transcription. *PLoS genetics* *8*, e1002952.
- Margueron, R. (2009). Role of the polycomb protein EED in the propagation of repressive histone marks. *Nature* *461*.
- Marquardt, S., Escalante-Chong, R., Pho, N., Wang, J., Churchman, L.S., Springer, M., and Buratowski, S. (2014). A Chromatin-Based Mechanism for Limiting Divergent Noncoding Transcription. *Cell* *158*, 462.
- Marques, M., Laflamme, L., Gervais, A.L., and Gaudreau, L. (2010). Reconciling the positive and negative roles of histone H2AZ in gene transcription. *Epigenetics* *5*, 267-272.

- Martens, J.A., Wu, P.Y., and Winston, F. (2005). Regulation of an intergenic transcript controls adjacent gene transcription in *Saccharomyces cerevisiae*. *Genes & development* *19*, 2695-2704.
- Martin, B.J. (2017). Histone H3K4 and H3K36 methylation independently recruit the NuA3 histone acetyltransferase in *Saccharomyces cerevisiae*. *Genetics* *205*.
- Martin, B.J.E., Brind'Amour, J., Jensen, K.N., Kuzmin, A., Liu, Z.C., Lorincz, M., and Howe, L.J. (2019). The majority of histone acetylation is a consequence of transcription. *bioRxiv*, 785998.
- Matangkasombut, O., Buratowski, R.M., Swilling, N.W., and Buratowski, S. (2000). Bromodomain factor 1 corresponds to a missing piece of yeast TFIID. *Genes Dev* *14*, 951-962.
- Matangkasombut, O., and Buratowski, S. (2003). Different sensitivities of bromodomain factors 1 and 2 to histone H4 acetylation. *Mol Cell* *11*, 353-363.
- Mattick, J.S., and Gagen, M.J. (2005). Accelerating networks. *Science* *307*.
- Mavrich, T.N. (2008). Nucleosome organization in the *Drosophila* genome. *Nature* *453*.
- Mayer, A. (2012). CTD tyrosine phosphorylation impairs termination factor recruitment to RNA polymerase II. *Science* *336*.
- Mayer, A., di Iulio, J., Maleri, S., Eser, U., Vierstra, J., Reynolds, A., Sandstrom, R., Stamatoyannopoulos, J.A., and Churchman, L.S. (2015). Native elongating transcript sequencing reveals human transcriptional activity at nucleotide resolution. *Cell* *161*, 541-554.
- McCracken, S., Fong, N., Rosonina, E., Yankulov, K., Brothers, G., Siderovski, D., Hessel, A., Foster, S., Shuman, S., and Bentley, D.L. (1997). 5'-Capping enzymes are targeted to pre-mRNA by binding to the phosphorylated carboxy-terminal domain of RNA polymerase II. *Genes Dev* *11*, 3306-3318.
- McKnight, J.N., Boerma, J.W., Breeden, L.L., and Tsukiyama, T. (2015). Global Promoter Targeting of a Conserved Lysine Deacetylase for Transcriptional Shutoff during Quiescence Entry. *Mol Cell* *59*, 732-743.
- Mechali, M., Yoshida, K., Coulombe, P., and Pasero, P. (2013). Genetic and epigenetic determinants of DNA replication origins, position and activation. *Curr Opin Genet Dev* *23*, 124-131.
- Meers, M.P., Janssens, D.H., and Henikoff, S. (2019). Pioneer Factor-Nucleosome Binding Events during Differentiation Are Motif Encoded. *Molecular Cell* *75*, 562-575.e565.
- Mellor, J., Woloszczuk, R., and Howe, F.S. (2016). The Interleaved Genome. *Trends Genet* *32*, 57-71.
- Meluh, P.B., Yang, P., Glowczewski, L., Koshland, D., and Smith, M.M. (1998). Cse4p is a component of the core centromere of *Saccharomyces cerevisiae*. *Cell* *94*, 607-613.
- Mercer, T.R., Dinger, M.E., Sunkin, S.M., Mehler, M.F., and Mattick, J.S. (2008). Specific expression of long noncoding RNAs in the mouse brain. *Proc. Natl Acad. Sci. USA* *105*.
- Mews, P., Zee, B.M., Liu, S., Donahue, G., Garcia, B.A., and Berger, S.L. (2014). Histone methylation has dynamics distinct from those of histone acetylation in cell cycle reentry from quiescence. *Mol Cell Biol* *34*, 3968-3980.
- Miller, C. (2012). Mediator phosphorylation prevents stress response transcription during non-stress conditions. *J. Biol. Chem.* *287*.
- Miller, G., and Hahn, S.A. (2006). DNA-tethered cleavage probe reveals the path for promoter DNA in the yeast preinitiation complex. *Nature Struct. Mol. Biol.* *13*.
- Milligan, L., Huynh-Thu, V.A., Delan-Forino, C., Tuck, A., Petfalski, E., Lombrana, R., Sanguinetti, G., Kudla, G., and Tollervey, D. (2016). Strand-specific, high-resolution mapping of modified RNA polymerase II. *Mol Syst Biol* *12*, 874.
- Mirny, L.A. (2010). Nucleosome-mediated cooperativity between transcription factors. *Proc. Natl Acad. Sci. USA* *107*.
- Mischo, H.E., Chun, Y., Harlen, K.M., Smalec, B.M., Dhir, S., Churchman, L.S., and Buratowski, S. (2018). Cell-Cycle Modulation of Transcription Termination Factor Sen1. *Mol Cell* *70*, 312-326.e317.
- Mischo, H.E., Gomez-Gonzalez, B., Grzechnik, P., Rondon, A.G., Wei, W., Steinmetz, L., Aguilera, A., and Proudfoot, N.J. (2011). Yeast Sen1 helicase protects the genome from transcription-associated instability. *Mol Cell* *41*, 21-32.
- Mitchell, L. (2008). Functional dissection of the NuA4 histone acetyltransferase reveals its role as a genetic hub and that Eaf1 is essential for complex integrity. *Mol. Cell. Biol.* *28*.
- Mito, Y., Henikoff, J.G., and Henikoff, S. (2007). Histone replacement marks the boundaries of cis-regulatory domains. *Science* *315*, 1408-1411.
- Mitra, D., Parnell, E.J., Landon, J.W., Yu, Y., and Stillman, D.J. (2006). SWI/SNF binding to the HO promoter requires histone acetylation and stimulates TATA-binding protein recruitment. *Mol Cell Biol* *26*, 4095-4110.
- Mivelaz, M., Cao, A.-M., Kubik, S., Zencir, S., Hovius, R., Boichenko, I., Stachowicz, A.M., Kurat, C.F., Shore, D., and Fierz, B. (2020). Chromatin Fiber Invasion and Nucleosome Displacement by the Rap1 Transcription Factor. *Molecular Cell* *77*, 488-500.e489.

- Mizuguchi, G., Shen, X., Landry, J., Wu, W.H., Sen, S., and Wu, C. (2004). ATP-driven exchange of histone H2AZ variant catalyzed by SWR1 chromatin remodeling complex. *Science* *303*, 343-348.
- Moazed, D. (2011). Mechanisms for the inheritance of chromatin states. *Cell* *146*, 510-518.
- Mohibullah, N., and Hahn, S. (2008). Site-specific cross-linking of TBP in vivo and in vitro reveals a direct functional interaction with the SAGA subunit Spt3. *Genes Dev* *22*, 2994-3006.
- Moretto, F., Wood, N.E., Kelly, G., Doncic, A., and van Werven, F.J. (2018). A regulatory circuit of two lncRNAs and a master regulator directs cell fate in yeast. *Nat Commun* *9*, 780.
- Morrissy, A.S., Griffith, M., and Marra, M.A. (2011). Extensive relationship between antisense transcription and alternative splicing in the human genome. *Genome Res* *21*.
- Motamedi, M.R., Hong, E.J., Li, X., Gerber, S., Denison, C., Gygi, S., and Moazed, D. (2008). HP1 proteins form distinct complexes and mediate heterochromatic gene silencing by nonoverlapping mechanisms. *Mol Cell* *32*, 778-790.
- Motamedi, M.R., Verdel, A., Colmenares, S.U., Gerber, S.A., Gygi, S.P., and Moazed, D. (2004). Two RNAi complexes, RITS and RDRC, physically interact and localize to noncoding centromeric RNAs. *Cell* *119*, 789-802.
- Murray, S.C., Haenni, S., Howe, F.S., Fischl, H., Chocian, K., Nair, A., and Mellor, J. (2015). Sense and antisense transcription are associated with distinct chromatin architectures across genes. *Nucleic Acids Res* *43*, 7823-7837.
- Nagai, S., Davis, R.E., Mattei, P.J., Eagen, K.P., and Kornberg, R.D. (2017). Chromatin potentiates transcription. *Proceedings of the National Academy of Sciences* *114*, 1536-1541.
- Narita, T., Weinert, B.T., and Choudhary, C. (2018). Functions and mechanisms of non-histone protein acetylation. *Nat. Rev. Mol. Cell Biol.*
- Naughton, C. (2013). Transcription forms and remodels supercoiling domains unfolding large-scale chromatin structures. *Nat. Struct. Mol. Biol.* *20*.
- Neil, H., Malabat, C., d'Aubenton-Carafa, Y., Xu, Z., Steinmetz, L.M., and Jacquier, A. (2009). Widespread bidirectional promoters are the major source of cryptic transcripts in yeast. *Nature* *457*, 1038-1042.
- Neri, F. (2017). Intragenic DNA methylation prevents spurious transcription initiation. *Nature* *543*.
- Nevers, A., Doyen, A., Malabat, C., Neron, B., Kergrohen, T., Jacquier, A., and Badis, G. (2018). Antisense transcriptional interference mediates condition-specific gene repression in budding yeast. *Nucleic Acids Res* *46*, 6009-6025.
- Ng, H.H., Robert, F., Young, R.A., and Struhl, K. (2003). Targeted recruitment of Set1 histone methylase by elongating Pol II provides a localized mark and memory of recent transcriptional activity. *Molecular cell* *11*, 709-719.
- Nguyen, T., Fischl, H., Howe, F.S., Woloszczuk, R., Serra Barros, A., Xu, Z., Brown, D., Murray, S.C., Haenni, S., Halstead, J.M., *et al.* (2014). Transcription mediated insulation and interference direct gene cluster expression switches. *Elife* *3*, e03635.
- Nishimura, K., Fukagawa, T., Takisawa, H., Kakimoto, T., and Kanemaki, M. (2009). An auxin-based degron system for the rapid depletion of proteins in nonplant cells. *Nature methods* *6*, 917-922.
- Nocetti, N., and Whitehouse, I. (2016). Nucleosome repositioning underlies dynamic gene expression. *Genes Dev* *30*, 660-672.
- Nojima, T., Gomes, T., Grosso, A.R.F., Kimura, H., Dye, M.J., Dhir, S., Carmo-Fonseca, M., and Proudfoot, N.J. (2015). Mammalian NET-Seq Reveals Genome-wide Nascent Transcription Coupled to RNA Processing. *Cell* *161*, 526-540.
- Noma, K., Sugiyama, T., Cam, H., Verdel, A., Zofall, M., Jia, S., Moazed, D., and Grewal, S.I. (2004). RITS acts in cis to promote RNA interference-mediated transcriptional and post-transcriptional silencing. *Nat Genet* *36*, 1174-1180.
- North, J.A. (2012). Regulation of the nucleosome unwrapping rate controls DNA accessibility. *Nucleic Acids Res.* *40*.
- Oberbeckmann, E. (2019). Absolute nucleosome occupancy for the *Saccharomyces cerevisiae* genome. *Genome Biol.* *29*.
- Ocampo, J., Chereji, R.V., Eriksson, P.R., and Clark, D.J. (2016). The ISW1 and CHD1 ATP-dependent chromatin remodelers compete to set nucleosome spacing in vivo. *Nucleic Acids Res.* *44*.
- Ocampo, J., Chereji, R.V., Eriksson, P.R., and Clark, D.J. (2019). Contrasting roles of the RSC and ISW1/CHD1 chromatin remodelers in RNA polymerase II elongation and termination. *Genome Res* *29*, 407-417.
- Oesterreich, F.C., Herzel, L., Straube, K., Hujer, K., Howard, J., and Neugebauer, K.M. (2016). Splicing of Nascent RNA Coincides with Intron Exit from RNA Polymerase II. *Cell* *165*, 372-381.
- Ozsolak, F., Kapranov, P., Foissac, S., Kim, S.W., Fishilevich, E., Monaghan, A.P., John, B., and Milos, P.M. (2010). Comprehensive polyadenylation site maps in yeast and human reveal pervasive alternative polyadenylation. *Cell* *143*, 1018-1029.
- Palade, G.E. (1955). A small particulate component of the cytoplasm. *J. Biophys. Biochem. Cytol.* *1*.

- Pandey, R.R. (2008). Kcnq1ot1 antisense noncoding RNA mediates lineage-specific transcriptional silencing through chromatin-level regulation. *Mol. Cell* 32.
- Pang, K.C., Frith, M.C., and Mattick, J.S. (2006). Rapid evolution of noncoding RNAs: lack of conservation does not mean lack of function. *Trends Genet.* 22.
- Papamichos-Chronakis, M., Watanabe, S., Rando, O.J., and Peterson, C.L. (2011). Global regulation of H2A.Z localization by the INO80 chromatin-remodeling enzyme is essential for genome integrity. *Cell* 144, 200-213.
- Parnell, T.J., Huff, J.T., and Cairns, B.R. (2008). RSC regulates nucleosome positioning at Pol II genes and density at Pol III genes. *EMBO J.* 27.
- Partridge, J.F., Scott, K.S., Bannister, A.J., Kouzarides, T., and Allshire, R.C. (2002). Cis-acting DNA from fission yeast centromeres mediates histone H3 methylation and recruitment of silencing factors and cohesin to an ectopic site. *Curr. Biol.* 12.
- Paule, M.R., and White, R.J. (2000). Survey and summary: transcription by RNA polymerases I and III. *Nucleic acids research* 28, 1283-1298.
- Pavri, R., Zhu, B., Li, G., Trojer, P., Mandal, S., Shilatifard, A., and Reinberg, D. (2006). Histone H2B Monoubiquitination Functions Cooperatively with FACT to Regulate Elongation by RNA Polymerase II. *Cell* 125, 703-717.
- Pelechano, V. (2017). From transcriptional complexity to cellular phenotypes: Lessons from yeast. *Yeast* 34, 475-482.
- Pelechano, V., and Steinmetz, L.M. (2013). Gene regulation by antisense transcription. *Nature reviews. Genetics* 14, 880-893.
- Pelechano, V., Wei, W., and Steinmetz, L.M. (2013). Extensive transcriptional heterogeneity revealed by isoform profiling. *Nature* 497, 127-131.
- Petrenko, N., Jin, Y., Wong, K.H., and Struhl, K. (2016). Mediator undergoes a compositional change during transcriptional activation. *Mol. Cell* 64.
- Petryk, N. (2018). MCM2 promotes symmetric inheritance of modified histones during DNA replication. *Science* 361.
- Plaschka, C. (2015). Architecture of the RNA polymerase II–Mediator core initiation complex. *Nature* 518.
- Poirier, M.G., Bussiek, M., Langowski, J., and Widom, J. (2008). Spontaneous access to DNA target sites in folded chromatin fibers. *J. Mol. Biol.* 379.
- Pokholok, D.K., Harbison, C.T., Levine, S., Cole, M., Hannett, N.M., Lee, T.I., Bell, G.W., Walker, K., Rolfe, P.A., Herbolsheimer, E., *et al.* (2005). Genome-wide map of nucleosome acetylation and methylation in yeast. *Cell* 122, 517-527.
- Porrua, O., Hobor, F., Boulay, J., Kubicek, K., D'Aubenton-Carafa, Y., Gudipati, R.K., Stefl, R., and Libri, D. (2012). In vivo SELEX reveals novel sequence and structural determinants of Nrd1-Nab3-Sen1-dependent transcription termination. *The EMBO journal* 31, 3935-3948.
- Porrua, O., and Libri, D. (2013). A bacterial-like mechanism for transcription termination by the Sen1p helicase in budding yeast. *Nature Struct. Mol. Biol.* 20.
- Porrua, O., and Libri, D. (2015). Transcription termination and the control of the transcriptome: why, where and how to stop. *Nat Rev Mol Cell Biol* 16, 190-202.
- Poss, Z.C., Ebmeier, C.C., and Taatjes, D.J. (2013). The Mediator complex and transcription regulation. *Crit. Rev. Biochem. Mol. Biol.* 48.
- Protacio, R.U., Li, G., Lowary, P.T., and Widom, J. (2000). Effects of histone tail domains on the rate of transcriptional elongation through a nucleosome. *Mol. Cell. Biol.* 20.
- Proudfoot, N.J. (1986). Transcriptional interference and termination between duplicated alpha-globin gene constructs suggests a novel mechanism for gene regulation. *Nature* 322, 562-565.
- Proudfoot, N.J. (2016). Transcriptional termination in mammals: stopping the RNA polymerase II juggernaut. *Science* 352.
- Ptashne, M. (2007). On the use of the word 'epigenetic'. *Curr Biol* 17, R233-236.
- Qiu, H., Hu, C., Wong, C.M., and Hinnebusch, A.G. (2006). The Spt4p subunit of yeast DSIF stimulates association of the Paf1 complex with elongating RNA polymerase II. *Mol Cell Biol* 26, 3135-3148.
- Quan, T.K., and Hartzog, G.A. (2010). Histone H3K4 and K36 methylation, Chd1 and Rpd3S oppose the functions of *Saccharomyces cerevisiae* Spt4-Spt5 in transcription. *Genetics* 184, 321-334.
- Quinn, J.J., and Chang, H.Y. (2016). Unique features of long non-coding RNA biogenesis and function. *Nature reviews. Genetics* 17, 47-62.
- Ragunathan, K., Jih, G., and Moazed, D. (2015). Epigenetic inheritance uncoupled from sequence-specific recruitment. *Science* 348.

- Ramachandran, S., Ahmad, K., and Henikoff, S. (2017). Transcription and remodeling produce asymmetrically unwrapped nucleosomal intermediates. *Mol. Cell* *68*.
- Ramachandran, S., Zentner, G.E., and Henikoff, S. (2015). Asymmetric nucleosomes flank promoters in the budding yeast genome. *Genome Res* *25*.
- Ramani, V., Qiu, R., and Shendure, J. (2019). High Sensitivity Profiling of Chromatin Structure by MNase-SSP. *Cell Rep* *26*, 2465-2476 e2464.
- Rando, O.J., and Winston, F. (2012). Chromatin and transcription in yeast. *Genetics* *190*, 351-387.
- Rao, S.S. (2014). A 3D map of the human genome at kilobase resolution reveals principles of chromatin looping. *Cell* *159*.
- Raveh-Sadka, T. (2012). Manipulating nucleosome disfavoring sequences allows fine-tune regulation of gene expression in yeast. *Nat. Genet.* *44*.
- Rawal, Y. (2018). SWI/SNF and RSC cooperate to reposition and evict promoter nucleosomes at highly expressed genes in yeast. *Genes Dev.* *32*.
- Reinberg, D., and Vales, L.D. (2018). Chromatin domains rich in inheritance. *Science* *361*, 33-34.
- Reverón-Gómez, N. (2018). Accurate recycling of parental histones reproduces the histone modification landscape during DNA replication. *Mol. Cell* *72*.
- Rhee, H.S., and Pugh, B.F. (2012). Genome-wide structure and organization of eukaryotic pre-initiation complexes. *Nature* *483*, 295-301.
- Rinn, J.L. (2007). Functional demarcation of active and silent chromatin domains in human HOX loci by noncoding RNAs. *Cell* *129*.
- Robinson, P.J. (2016). Structure of a complete Mediator–RNA polymerase II pre-initiation complex. *Cell* *166*.
- Roeder, R.G., and Rutter, W.J. (1969). Multiple forms of DNA-dependent RNA polymerase in eukaryotic organisms. *Nature* *224*.
- Roy, D., Zhang, Z., Lu, Z., Hsieh, C.L., and Lieber, M.R. (2010). Competition between the RNA transcript and the nontemplate DNA strand during R-loop formation in vitro: a nick can serve as a strong R-loop initiation site. *Mol Cell Biol* *30*, 146-159.
- Rufiange, A., Jacques, P.E., Bhat, W., Robert, F., and Nourani, A. (2007). Genome-wide replication-independent histone H3 exchange occurs predominantly at promoters and implicates H3 K56 acetylation and Asf1. *Molecular cell* *27*, 393-405.
- Saha, A., Wittmeyer, J., and Cairns, B.R. (2002). Chromatin remodeling by RSC involves ATP-dependent DNA translocation. *Genes Dev.* *16*.
- Sainsbury, S., Bernecky, C., and Cramer, P. (2015). Structural basis of transcription initiation by RNA polymerase II. *Nat. Rev. Mol. Cell Biol.* *16*.
- Santisteban, M.S., Kalashnikova, T., and Smith, M.M. (2000). Histone H2A.Z regulates transcription and is partially redundant with nucleosome remodeling complexes. *Cell* *103*, 411-422.
- Sanyal, A., Lajoie, B.R., Jain, G., and Dekker, J. (2012). The long-range interaction landscape of gene promoters. *Nature* *489*.
- Schafer, G., McEvoy, C.R., and Patterton, H.G. (2008). The *Saccharomyces cerevisiae* linker histone Hho1p is essential for chromatin compaction in stationary phase and is displaced by transcription. *Proc Natl Acad Sci U S A* *105*, 14838-14843.
- Schalch, T., Duda, S., Sargent, D.F., and Richmond, T.J. (2005). X-ray structure of a tetranucleosome and its implications for the chromatin fibre. *Nature* *436*.
- Schlichter, A., Kasten, M.M., Parnell, T.J., and Cairns, B.R. (2019). Specialization of the Chromatin Remodeler RSC to Mobilize Partially-Unwrapped Nucleosomes. *bioRxiv*, 799361.
- Schneider, J., Bajwa, P., Johnson, F.C., Bhaumik, S.R., and Shilatifard, A. (2006). Rtt109 is required for proper H3K56 acetylation: a chromatin mark associated with the elongating RNA polymerase II. *J Biol Chem* *281*, 37270-37274.
- Schulz, D., Schwab, B., Kiesel, A., Baejen, C., Torkler, P., Gagneur, J., Soeding, J., and Cramer, P. (2013). Transcriptome surveillance by selective termination of noncoding RNA synthesis. *Cell* *155*, 1075-1087.
- Segal, E., Fondufe-Mittendorf, Y., Chen, L., Thastrom, A., Field, Y., Moore, I.K., Wang, J.P., and Widom, J. (2006). A genomic code for nucleosome positioning. *Nature* *442*, 772-778.
- Sein, H., Värsv, S., and Kristjuhan, A. (2015). Distribution and Maintenance of Histone H3 Lysine 36 Trimethylation in Transcribed Locus. *PLOS ONE* *10*, e0120200.
- Sen, P., Dang, W., Donahue, G., Dai, J., Dorsey, J., Cao, X., Liu, W., Cao, K., Perry, R., Lee, J.Y., *et al.* (2015). H3K36 methylation promotes longevity by enhancing transcriptional fidelity. *Genes Dev* *29*, 1362-1376.

- Sentenac, A. (1985). Eukaryotic RNA polymerases. *CRC Crit. Rev. Biochem.* *18*.
- Shahbazian, M.D., Zhang, K., and Grunstein, M. (2005). Histone H2B ubiquitylation controls processive methylation but not monomethylation by Dot1 and Set1. *Molecular cell* *19*, 271-277.
- Shearwin, K.E., Callen, B.P., and Egan, J.B. (2005). Transcriptional interference--a crash course. *Trends Genet* *21*, 339-345.
- Sheikh, B.N., and Akhtar, A. (2019). The many lives of KATs - detectors, integrators and modulators of the cellular environment. *Nature reviews. Genetics* *20*, 7-23.
- Shen, X., Mizuguchi, G., Hamiche, A., and Wu, C. (2000). A chromatin remodelling complex involved in transcription and DNA processing. *Nature* *406*.
- Shi, X., Kachirskaja, I., Walter, K.L., Kuo, J.H., Lake, A., Davrazou, F., Chan, S.M., Martin, D.G., Fingerman, I.M., Briggs, S.D., *et al.* (2007). Proteome-wide analysis in *Saccharomyces cerevisiae* identifies several PHD fingers as novel direct and selective binding modules of histone H3 methylated at either lysine 4 or lysine 36. *The Journal of biological chemistry* *282*, 2450-2455.
- Shogren-Knaak, M. (2006). Histone H4-K16 acetylation controls chromatin structure and protein interactions. *Science* *311*.
- Shukla, M.S., Syed, S.H., Montel, F., Faivre-Moskalenko, C., Bednar, J., Travers, A., Angelov, D., and Dimitrov, S. (2010). Remosomes: RSC generated non-mobilized particles with approximately 180 bp DNA loosely associated with the histone octamer. *Proc Natl Acad Sci U S A* *107*, 1936-1941.
- Sims, R.J., 3rd, Millhouse, S., Chen, C.F., Lewis, B.A., Erdjument-Bromage, H., Tempst, P., Manley, J.L., and Reinberg, D. (2007). Recognition of trimethylated histone H3 lysine 4 facilitates the recruitment of transcription postinitiation factors and pre-mRNA splicing. *Mol Cell* *28*, 665-676.
- Skourti-Stathaki, K., Kamieniarz-Gdula, K., and Proudfoot, N.J. (2014). R-loops induce repressive chromatin marks over mammalian gene terminators. *Nature* *516*, 436-439.
- Skourti-Stathaki, K., and Proudfoot, N.J. (2014). A double-edged sword: R loops as threats to genome integrity and powerful regulators of gene expression. *Genes Dev* *28*, 1384-1396.
- Smale, S.T., and Kadonaga, J.T. (2003). The RNA polymerase II core promoter. *Annu Rev Biochem* *72*, 449-479.
- Smith, E.R. (1998). ESA1 is a histone acetyltransferase that is essential for growth in yeast. *Proc. Natl Acad. Sci. USA* *95*.
- Smolle, M. (2012). Chromatin remodelers Isw1 and Chd1 maintain chromatin structure during transcription by preventing histone exchange. *Nat. Struct. Mol. Biol.* *19*.
- Smolle, M., Workman, J.L., and Venkatesh, S. (2013). reSETting chromatin during transcription elongation. *Epigenetics* *8*, 10-15.
- Soares, L.M., He, P.C., Chun, Y., Suh, H., Kim, T., and Buratowski, S. (2017). Determinants of Histone H3K4 Methylation Patterns. *Mol Cell* *68*, 773-785 e776.
- Somers, J., and Owen-Hughes, T. (2009). Mutations to the histone H3 alpha N region selectively alter the outcome of ATP-dependent nucleosome-remodelling reactions. *Nucleic Acids Res* *37*, 2504-2513.
- Soudet, J., and Stutz, F. (2019). Regulation of Gene Expression and Replication Initiation by Non-Coding Transcription: A Model Based on Reshaping Nucleosome-Depleted Regions: Influence of Pervasive Transcription on Chromatin Structure. *Bioessays* *41*, e1900043.
- Soufi, A. (2015). Pioneer transcription factors target partial DNA motifs on nucleosomes to initiate reprogramming. *Cell* *161*.
- Soutourina, J. (2018). Transcription regulation by the Mediator complex. *Nat Rev Mol Cell Biol* *19*, 262-274.
- Soutourina, J., Wydau, S., Ambroise, Y., Boschiero, C., and Werner, M. (2011). Direct interaction of RNA polymerase II and mediator required for transcription in vivo. *Science* *331*, 1451-1454.
- Spain, M.M., Bracerros, K.C.A., and Tsukiyama, T. (2018). SWI/SNF coordinates transcriptional activation through Rpd3-mediated histone hypoacetylation during quiescence entry. *bioRxiv*, 426288.
- Squatrito, M., Gorrini, C., and Amati, B. (2006). Tip60 in DNA damage response and growth control: many tricks in one HAT. *Trends Cell. Biol.* *16*.
- Stasevich, T.J. (2014). Regulation of RNA polymerase II activation by histone acetylation in single living cells. *Nature* *516*.
- Steensel, B., and Furlong, E.E.M. (2019). The role of transcription in shaping the spatial organization of the genome. *Nat. Rev. Mol. Cell Biol.* *20*.
- Steinmetz, E.J., Conrad, N.K., Brow, D.A., and Corden, J.L. (2001). RNA-binding protein Nrd1 directs poly(A)-independent 3'-end formation of RNA polymerase II transcripts. *Nature* *413*, 327-331.
- Steunou, A.L. (2016). Combined action of histone reader modules regulates NuA4 local acetyltransferase function but not its recruitment on the genome. *Mol. Cell. Biol.* *36*.

- Stewart-Morgan, K.R., Petryk, N., and Groth, A. (2020). Chromatin replication and epigenetic cell memory. *Nat Cell Biol* 22, 361-371.
- Stewart-Morgan, K.R., Reverón-Gómez, N., and Groth, A. (2019). Transcription restart establishes chromatin accessibility after DNA replication. *Mol. Cell* 75.
- Strahl, B.D., Grant, P.A., Briggs, S.D., Sun, Z.W., Bone, J.R., Caldwell, J.A., Mollah, S., Cook, R.G., Shabanowitz, J., Hunt, D.F., *et al.* (2002). Set2 is a nucleosomal histone H3-selective methyltransferase that mediates transcriptional repression. *Mol Cell Biol* 22, 1298-1306.
- Struhl, K. (1985). Naturally occurring poly(dA-dT) sequences are upstream promoter elements for constitutive transcription in yeast. *Proc. Natl. Acad. Sci. USA* 82.
- Struhl, K. (1999). Fundamentally different logic of gene regulation in eukaryotes and prokaryotes. *Cell* 98.
- Struhl, K. (2007). Transcriptional noise and the fidelity of initiation by RNA polymerase II. *Nat Struct Mol Biol* 14, 103-105.
- Suka, N., Suka, Y., Carmen, A.A., Wu, J., and Grunstein, M. (2001). Highly specific antibodies determine histone acetylation site usage in yeast heterochromatin and euchromatin. *Mol Cell* 8, 473-479.
- Sun, S., Del Rosario, B.C., Szanto, A., Ogawa, Y., Jeon, Y., and Lee, J.T. (2013). Jpx RNA activates Xist by evicting CTCF. *Cell* 153, 1537-1551.
- Suter, B., Schnappauf, G., and Thoma, F. (2000). Poly(dA-dT) sequences exist as rigid DNA structures in nucleosome-free yeast promoters in vivo. *Nucleic Acids Res.* 28.
- Talbert, P.B., and Henikoff, S. (2017). Histone variants on the move: substrates for chromatin dynamics. *Nat. Rev. Mol. Cell Biol.* 18.
- Taneja, N. (2017). SNF2 family protein Fft3 suppresses nucleosome turnover to promote epigenetic inheritance and proper replication. *Mol. Cell* 66.
- Tang, Y., Holbert, M.A., Wurtele, H., Meeth, K., Rocha, W., Gharib, M., Jiang, E., Thibault, P., Verreault, A., Cole, P.A., *et al.* (2008). Fungal Rtt109 histone acetyltransferase is an unexpected structural homolog of metazoan p300/CBP. *Nat Struct Mol Biol* 15, 738-745.
- Tantale, K. (2016). A single-molecule view of transcription reveals convoys of RNA polymerases and multi-scale bursting. *Nat. Commun.* 7.
- Taverna, S.D., Ilin, S., Rogers, R.S., Tanny, J.C., Lavender, H., Li, H., Baker, L., Boyle, J., Blair, L.P., Chait, B.T., *et al.* (2006). Yng1 PHD finger binding to H3 trimethylated at K4 promotes NuA3 HAT activity at K14 of H3 and transcription at a subset of targeted ORFs. *Mol Cell* 24, 785-796.
- Teif, V.B. (2012). Genome-wide nucleosome positioning during embryonic stem cell development. *Nat. Struct. Mol. Biol.* 19.
- Terzi, N., Churchman, L.S., Vasiljeva, L., Weissman, J., and Buratowski, S. (2011). H3K4 trimethylation by Set1 promotes efficient termination by the Nrd1-Nab3-Sen1 pathway. *Mol Cell Biol* 31, 3569-3583.
- Teves, S.S., and Henikoff, S. (2014). Transcription-generated torsional stress destabilizes nucleosomes. *Nat. Struct. Mol. Biol.* 21.
- Tirosh, I., and Barkai, N. (2008). Two strategies for gene regulation by promoter nucleosomes. *Genome research* 18, 1084-1091.
- Tirosh, I., Weinberger, A., Carmi, M., and Barkai, N. (2006). A genetic signature of interspecies variations in gene expression. *Nature genetics* 38, 830-834.
- Tome, J.M., Tippens, N.D., and Lis, J.T. (2018). Single-molecule nascent RNA sequencing identifies regulatory domain architecture at promoters and enhancers. *Nat. Genet.* 50.
- Topal, S., Vasseur, P., Radman-Livaja, M., and Peterson, C.L. (2019). Distinct transcriptional roles for Histone H3-K56 acetylation during the cell cycle in Yeast. *Nat Commun* 10, 4372.
- Tramantano, M., Sun, L., Au, C., Labuz, D., Liu, Z., Chou, M., Shen, C., and Luk, E. (2016). Constitutive turnover of histone H2A.Z at yeast promoters requires the preinitiation complex. *Elife* 5.
- Trojer, P., Li, G., Sims, R.J., 3rd, Vaquero, A., Kalakonda, N., Boccuni, P., Lee, D., Erdjument-Bromage, H., Tempst, P., Nimer, S.D., *et al.* (2007). L3MBTL1, a histone-methylation-dependent chromatin lock. *Cell* 129, 915-928.
- Tropberger, P. (2013). Regulation of transcription through acetylation of H3K122 on the lateral surface of the histone octamer. *Cell* 152.
- Truong, D.M., and Boeke, J.D. (2017). Resetting the Yeast Epigenome with Human Nucleosomes. *Cell* 171, 1508-1519 e1513.
- Tsai, K.L. (2017). Mediator structure and rearrangements required for holoenzyme formation. *Nature* 544.
- Tsankov, A.M., Thompson, D.A., Socha, A., Regev, A., and Rando, O.J. (2010). The role of nucleosome positioning in the evolution of gene regulation. *PLoS Biol.* 8.

- Tsubota, T., Berndsen, C.E., Erkmann, J.A., Smith, C.L., Yang, L., Freitas, M.A., Denu, J.M., and Kaufman, P.D. (2007). Histone H3-K56 acetylation is catalyzed by histone chaperone-dependent complexes. *Molecular cell* *25*, 703-712.
- Tudek, A., Porrua, O., Kabzinski, T., Lidschreiber, M., Kubicek, K., Fortova, A., Lacroute, F., Vanacova, S., Cramer, P., Stefl, R., *et al.* (2014). Molecular basis for coordinating transcription termination with noncoding RNA degradation. *Molecular cell* *55*, 467-481.
- Udugama, M., Sabri, A., and Bartholomew, B. (2011). The INO80 ATP-dependent chromatin remodeling complex is a nucleosome spacing factor. *Mol Cell Biol* *31*, 662-673.
- Uhler, J.P., Hertel, C., and Svejstrup, J.Q. (2007). A role for noncoding transcription in activation of the yeast PHO5 gene. *Proceedings of the National Academy of Sciences of the United States of America* *104*, 8011-8016.
- Ulitsky, I. (2016). Evolution to the rescue: using comparative genomics to understand long non-coding RNAs. *Nature reviews. Genetics* *17*, 601-614.
- Vallon-Christersson, J., Staaf, J., Kvist, A., Medstrand, P., Borg, A., and Rovira, C. (2007). Non-coding antisense transcription detected by conventional and single-stranded cDNA microarray. *BMC Genomics* *8*, 295.
- Valouev, A. (2011). Determinants of nucleosome organization in primary human cells. *Nature* *474*.
- van Dijk, E.L., Chen, C.L., d'Aubenton-Carafa, Y., Gourvenec, S., Kwapisz, M., Roche, V., Bertrand, C., Silvain, M., Legoix-Ne, P., Loeillet, S., *et al.* (2011). XUTs are a class of Xrn1-sensitive antisense regulatory non-coding RNA in yeast. *Nature* *475*, 114-117.
- van Werven, F.J., Neuert, G., Hendrick, N., Lardenois, A., Buratowski, S., van Oudenaarden, A., Primig, M., and Amon, A. (2012). Transcription of two long noncoding RNAs mediates mating-type control of gametogenesis in budding yeast. *Cell* *150*, 1170-1181.
- Vanacova, S., Wolf, J., Martin, G., Blank, D., Dettwiler, S., Friedlein, A., Langen, H., Keith, G., and Keller, W. (2005). A new yeast poly(A) polymerase complex involved in RNA quality control. *PLoS Biol* *3*, e189.
- VanDemark, A.P., Kasten, M.M., Ferris, E., Heroux, A., Hill, C.P., and Cairns, B.R. (2007). Autoregulation of the *rsc4* tandem bromodomain by *gcn5* acetylation. *Mol Cell* *27*, 817-828.
- Vannini, A., and Cramer, P. (2012). Conservation between the RNA polymerase I, II, and III transcription initiation machineries. *Mol. Cell* *45*.
- Vary, J.C., Jr., Gangaraju, V.K., Qin, J., Landel, C.C., Kooperberg, C., Bartholomew, B., and Tsukiyama, T. (2003). Yeast *Isw1p* forms two separable complexes in vivo. *Mol Cell Biol* *23*, 80-91.
- Vasiljeva, L., and Buratowski, S. (2006). *Nrd1* interacts with the nuclear exosome for 3' processing of RNA polymerase II transcripts. *Mol Cell* *21*, 239-248.
- Vasiljeva, L., Kim, M., Mutschler, H., Buratowski, S., and Meinhart, A. (2008). The *Nrd1-Nab3-Sen1* termination complex interacts with the Ser5-phosphorylated RNA polymerase II C-terminal domain. *Nat Struct Mol Biol* *15*, 795-804.
- Venkatesh, S. (2012). *Set2* methylation of histone H3 lysine 36 suppresses histone exchange on transcribed genes. *Nature* *489*.
- Venkatesh, S., Li, H., Gogol, M.M., and Workman, J.L. (2016). Selective suppression of antisense transcription by *Set2*-mediated H3K36 methylation. *Nat Commun* *7*, 13610.
- Venkatesh, S., Smolle, M., Li, H., Gogol, M.M., Saint, M., Kumar, S., Natarajan, K., and Workman, J.L. (2012). *Set2* methylation of histone H3 lysine 36 suppresses histone exchange on transcribed genes. *Nature* *489*, 452-455.
- Venkatesh, S., and Workman, J.L. (2015). Histone exchange, chromatin structure and the regulation of transcription. *Nat Rev Mol Cell Biol* *16*, 178-189.
- Vermeulen, M. (2007). Selective anchoring of TFIID to nucleosomes by trimethylation of histone H3 lysine 4. *Cell* *131*.
- Vermeulen, M., Eberl, H.C., Matarese, F., Marks, H., Denissov, S., Butter, F., Lee, K.K., Olsen, J.V., Hyman, A.A., Stunnenberg, H.G., *et al.* (2010). Quantitative Interaction Proteomics and Genome-wide Profiling of Epigenetic Histone Marks and Their Readers. *Cell* *142*, 967-980.
- Vinayachandran, V., Reja, R., Rossi, M.J., Park, B., Rieber, L., Mittal, C., Mahony, S., and Pugh, B.F. (2018). Widespread and precise reprogramming of yeast protein-genome interactions in response to heat shock. *Genome Res*.
- Volpe, T.A. (2002). Regulation of heterochromatic silencing and histone H3 lysine-9 methylation by RNAi. *Science* *297*.
- Wan, Y., Saleem, R.A., Ratushny, A.V., Roda, O., Smith, J.J., Lin, C.H., Chiang, J.H., and Aitchison, J.D. (2009). Role of the histone variant H2A.Z/Htz1p in TBP recruitment, chromatin dynamics, and regulated expression of oleate-responsive genes. *Mol Cell Biol* *29*, 2346-2358.
- Wang, A.Y. (2009a). Asf1-like structure of the conserved Yaf9 YEATS domain and role in H2A. Z deposition and acetylation. *Proc. Natl Acad. Sci. USA* *106*.

- Wang, K.C. (2011). A long noncoding RNA maintains active chromatin to coordinate homeotic gene expression. *Nature* *472*.
- Wang, Z. (2008). Combinatorial patterns of histone acetylations and methylations in the human genome. *Nat. Genet.* *40*.
- Wang, Z. (2009b). Genome-wide mapping of HATs and HDACs reveals distinct functions in active and inactive genes. *Cell* *138*.
- Watanabe, S., Radman-Livaja, M., Rando, O.J., and Peterson, C.L. (2013). A histone acetylation switch regulates H2A. Z deposition by the SWR-C remodeling enzyme. *Science* *340*.
- Webb, S., Hector, R.D., Kudla, G., and Granneman, S. (2014). PAR-CLIP data indicate that Nrd1-Nab3-dependent transcription termination regulates expression of hundreds of protein coding genes in yeast. *Genome Biol* *15*, R8.
- Wei, W., Hennig, B.P., Wang, J., Zhang, Y., Piazza, I., Pareja Sanchez, Y., Chabbert, C.D., Adjalley, S.H., Steinmetz, L.M., and Pelechano, V. (2019). Chromatin-sensitive cryptic promoters putatively drive expression of alternative protein isoforms in yeast. *Genome Res* *29*, 1974-1984.
- Weinberger, L., Voickek, Y., Tirosh, I., Hornung, G., Amit, I., and Barkai, N. (2012). Expression noise and acetylation profiles distinguish HDAC functions. *Mol Cell* *47*, 193-202.
- Weiner, A., Chen, H.V., Liu, C.L., Rahat, A., Klien, A., Soares, L., Gudipati, M., Pfeffner, J., Regev, A., Buratowski, S., *et al.* (2012). Systematic dissection of roles for chromatin regulators in a yeast stress response. *PLoS Biol* *10*, e1001369.
- Weiner, A., Hsieh, T.H., Appleboim, A., Chen, H.V., Rahat, A., Amit, I., Rando, O.J., and Friedman, N. (2015). High-resolution chromatin dynamics during a yeast stress response. *Mol Cell* *58*, 371-386.
- Weiner, A., Hughes, A., Yassour, M., Rando, O.J., and Friedman, N. (2010). High-resolution nucleosome mapping reveals transcription-dependent promoter packaging. *Genome Res* *20*, 90-100.
- Wery, M., Descrimes, M., Vogt, N., Dallongeville, A.S., Gautheret, D., and Morillon, A. (2016). Nonsense-Mediated Decay Restricts LncRNA Levels in Yeast Unless Blocked by Double-Stranded RNA Structure. *Molecular cell* *61*, 379-392.
- Wery, M., Gautier, C., Descrimes, M., Yoda, M., Vennin-Rendos, H., Migeot, V., Gautheret, D., Hermand, D., and Morillon, A. (2018). Native elongating transcript sequencing reveals global anti-correlation between sense and antisense nascent transcription in fission yeast. *RNA* *24*, 196-208.
- Whitehouse, I., Rando, O.J., Delrow, J., and Tsukiyama, T. (2007). Chromatin remodelling at promoters suppresses antisense transcription. *Nature* *450*.
- Williams, S.K., Truong, D., and Tyler, J.K. (2008). Acetylation in the globular core of histone H3 on lysine 56 promotes chromatin disassembly during transcriptional activation. *Proc. Natl Acad. Sci. USA* *105*.
- Wood, A., Schneider, J., Dover, J., Johnston, M., and Shilatifard, A. (2003). The Paf1 complex is essential for histone monoubiquitination by the Rad6-Bre1 complex, which signals for histone methylation by COMPASS and Dot1p. *J Biol Chem* *278*, 34739-34742.
- Wu, A.C.K., Patel, H., Chia, M., Moretto, F., Frith, D., Snijders, A.P., and van Werven, F.J. (2018). Repression of Divergent Noncoding Transcription by a Sequence-Specific Transcription Factor. *Molecular Cell* *72*, 942-954.e947.
- Wu, W.H., Alami, S., Luk, E., Wu, C.H., Sen, S., Mizuguchi, G., Wei, D., and Wu, C. (2005). Swc2 is a widely conserved H2AZ-binding module essential for ATP-dependent histone exchange. *Nat Struct Mol Biol* *12*, 1064-1071.
- Wu, W.H., Wu, C.H., Ladurner, A., Mizuguchi, G., Wei, D., Xiao, H., Luk, E., Ranjan, A., and Wu, C. (2009). N terminus of Swr1 binds to histone H2AZ and provides a platform for subunit assembly in the chromatin remodeling complex. *J Biol Chem* *284*, 6200-6207.
- Wu, Z., Fang, X., Zhu, D., and Dean, C. (2020). Autonomous Pathway: FLOWERING LOCUS C Repression through an Antisense-Mediated Chromatin-Silencing Mechanism. *Plant Physiol* *182*, 27-37.
- Wyce, A., Xiao, T., Whelan, K.A., Kosman, C., Walter, W., Eick, D., Hughes, T.R., Krogan, N.J., Strahl, B.D., and Berger, S.L. (2007). H2B ubiquitylation acts as a barrier to Ctk1 nucleosomal recruitment prior to removal by Ubp8 within a SAGA-related complex. *Mol Cell* *27*, 275-288.
- Wyers, F., Rougemaille, M., Badis, G., Rousselle, J.C., Dufour, M.E., Boulay, J., Regnault, B., Devaux, F., Namane, A., Seraphin, B., *et al.* (2005). Cryptic pol II transcripts are degraded by a nuclear quality control pathway involving a new poly(A) polymerase. *Cell* *121*, 725-737.
- Xu, J., Bai, J., Zhang, X., Lv, Y., Gong, Y., Liu, L., Zhao, H., Yu, F., Ping, Y., Zhang, G., *et al.* (2017). A comprehensive overview of lncRNA annotation resources. *Brief Bioinform* *18*, 236-249.
- Xu, M. (2010). Partitioning of histone H3-H4 tetramers during DNA replication-dependent chromatin assembly. *Science* *328*.
- Xu, Z., Wei, W., Gagneur, J., Clauder-Munster, S., Smolik, M., Huber, W., and Steinmetz, L.M. (2011). Antisense expression increases gene expression variability and locus interdependency. *Mol Syst Biol* *7*, 468.

- Xu, Z., Wei, W., Gagneur, J., Perocchi, F., Clauder-Munster, S., Camblong, J., Guffanti, E., Stutz, F., Huber, W., and Steinmetz, L.M. (2009). Bidirectional promoters generate pervasive transcription in yeast. *Nature* *457*, 1033-1037.
- Xue, Y., Van, C., Pradhan, S.K., Su, T., Gehrke, J., Kuryan, B.G., Kitada, T., Vashisht, A., Tran, N., Wohlschlegel, J., *et al.* (2015). The Ino80 complex prevents invasion of euchromatin into silent chromatin. *Genes Dev* *29*, 350-355.
- Xue, Z., Ye, Q., Anson, S.R., Yang, J., Xiao, G., Kowbel, D., Glass, N.L., Crosthwaite, S.K., and Liu, Y. (2014). Transcriptional interference by antisense RNA is required for circadian clock function. *Nature* *514*, 650-653.
- Yan, C., Chen, H., and Bai, L. (2018). Systematic Study of Nucleosome-Displacing Factors in Budding Yeast. *Mol Cell* *71*, 294-305 e294.
- Yarragudi, A., Parfrey, L.W., and Morse, R.H. (2007). Genome-wide analysis of transcriptional dependence and probable target sites for Abf1 and Rap1 in *Saccharomyces cerevisiae*. *Nucleic Acids Res* *35*, 193-202.
- Yu, C. (2018). A mechanism for preventing asymmetric histone segregation onto replicating DNA strands. *Science* *361*.
- Yu, R., Jih, G., Iglesias, N., and Moazed, D. (2014). Determinants of heterochromatic siRNA biogenesis and function. *Mol Cell* *53*, 262-276.
- Yu, R., Wang, X., and Moazed, D. (2018). Epigenetic inheritance mediated by coupling of RNAi and histone H3K9 methylation. *Nature* *558*, 615-619.
- Yuan, G.C., Liu, Y.J., Dion, M.F., Slack, M.D., Wu, L.F., Altschuler, S.J., and Rando, O.J. (2005). Genome-scale identification of nucleosome positions in *S. cerevisiae*. *Science* *309*, 626-630.
- Yudkovsky, N., Ranish, J.A., and Hahn, S. (2000). A transcription reinitiation intermediate that is stabilized by activator. *Nature* *408*.
- Zaret, K.S., Lerner, J., and Iwafuchi-Doi, M. (2016). Chromatin scanning by dynamic binding of pioneer factors. *Mol. Cell* *62*.
- Zaugg, J.B., and Luscombe, N.M. (2012). A genomic model of condition-specific nucleosome behavior explains transcriptional activity in yeast. *Genome research* *22*, 84-94.
- Zenkhusen, D., Larson, D.R., and Singer, R.H. (2008). Single-RNA counting reveals alternative modes of gene expression in yeast. *Nature structural & molecular biology* *15*, 1263-1271.
- Zentner, G.E., and Henikoff, S. (2013). Regulation of nucleosome dynamics by histone modifications. *Nat Struct Mol Biol* *20*, 259-266.
- Zhang, H., Roberts, D.N., and Cairns, B.R. (2005). Genome-wide dynamics of Htz1, a histone H2A variant that poises repressed/basal promoters for activation through histone loss. *Cell* *123*, 219-231.
- Zhang, R., Erler, J., and Langowski, J. (2017). Histone acetylation regulates chromatin accessibility: role of H4K16 in inter-nucleosome interaction. *Biophys. J.* *112*.
- Zhang, T., Cooper, S., and Brockdorff, N. (2015). The interplay of histone modifications - writers that read. *EMBO Rep.* *16*.
- Zhang, X., Wang, X., Zhang, Z., and Cai, G. (2019). Structure and functional interactions of INO80 actin/Arp module. *J Mol Cell Biol* *11*, 345-355.
- Zhang, Z. (2011). A packing mechanism for nucleosome organization reconstituted across a eukaryotic genome. *Science* *332*.
- Zhao, J., Sun, B.K., Erwin, J.A., Song, J.J., and Lee, J.T. (2008). Polycomb proteins targeted by a short repeat RNA to the mouse X chromosome. *Science* *322*.

Appendix

A R scripts

The following are the annotated R scripts representing key parts of the analyses performed in Results section-2.

A.1 Calculating Antisense Repressed Genes and Defining Clusters

The following script was used to calculate most of the values plotted in Result part-2 Figure1 page 75. The script reads the htseq count files.

```
##### Making a function to read the files #####
make_df <- function(f1_file){
  df1 <- read.table(f1_file, sep = "\t")
  colgene <- paste(substr(f1_file,20, 25), substr(f1_file, 33, 37), sep = "-")
  colnames(df1) <- c("ID", colgene)
  return(df1)
}
#### Reading HT-seq count files and making the dataframe
path1="ht-seq_counts-file"
flist <- list.files(path = path1)
all_counts <- paste(path1, flist, sep = "/")
c1 <- Map(make_df, all_counts)
df <- join_all(c1, by = "ID")

##### removing the last row with unaligned counts #####
n<- dim(df)
df <- df[1:(n-5),]
##### making DF for the model #####
dfmod <- reshape2::melt(df,id.var=1)
dfmod <- dfmod %>% tidyr::separate(variable, c("strain_tp", "strand"))
dfmod$exp <- substr(dfmod$strain_tp, 1,3)
dfmod$strain <- substr(dfmod$strain_tp, 4,5)
dfmod$time <- substr(dfmod$strain_tp, 6,6)
```

```

dfmod$strain_tp <- NULL
colnames(dfmod)[3] <- "counts"
convert_timepoint <- function(x) {
  switch(x, '0'=0, '2'=120, '3'=150, '4'=180, '5'=240, '6'=300)
}

dfmod$time <- unlist(lapply(dfmod$time, convert_timepoint))

##### converting all zeros to 1 and normalizing #####

dfref <- dfmod[dfmod$time == 0, ]
dfnorm <- merge(dfmod, dfref, by=c(1,2,4,5), all=TRUE)
colnames(dfnorm)[c(5,6,7)] <- c("counts", "time", "refcounts")
dfnorm$time.y <- NULL
dfnorm$normcounts <- (dfnorm$counts+1)/(dfnorm$refcounts+1)
summary(log(dfnorm$normcounts))

##### to remove MET genes #####
IDtogenes <- read.csv(file = "SGDtogenes.csv", header = FALSE, sep = ";")
IDtogenes$V3 <- NULL
colnames(IDtogenes) <- c("ID", "genes")
m1 <- merge(IDtogenes, dfnorm, by = "ID")
dfnorm <- dfnorm[!(dfnorm$ID %in% dfmet$ID),]

##### removing Nrd1 #####
dfnorm <- dfnorm[!(dfnorm$ID == "YNL251C"),]

##### writing dataframe of normalised counts for further analysis #####
#####write.csv(dfnorm, file = "dfnorm.csv", row.names = FALSE)
##### to get the changing genes in the experiment #####

dfdif1 <- dataframe[dataframe$time == 120,]
b1<- reshape2::dcast(dfdif1, value.var = "normcounts", formula = ID+strain~strand)
str(b1)
summary(log(dfdif1$normcounts))
dfdif1 <- b1
rm(b1)

##### Calculating ARG genes #####

nrg43 <- as.character(with(dfdif1, dfdif1$ID[strain=="43" & (Sense < 0.9 & AntiS > 1.5)]))
nrg36 <- as.character(with(dfdif1, dfdif1$ID[strain=="36" & (Sense < 0.9 & AntiS > 1.5)]))
nrgoi <- setdiff(nrg43,nrg36)
rm(nrg36,nrg43)
dfnrgoi <- dataframe[dataframe$ID %in% nrgoi & dataframe$strain == "43",]
rm(dfdif1)

##### Calculating Kmeans for dividing ARG into Clusters #####

dfgoikmeans <- reshape2::dcast(dfnrgoi, value.var = "normcounts", formula = ID+strain+strand~time)
dfgoikmeans1 <- dfgoikmeans[dfgoikmeans$strand=="Sense",]
dfgoikmeans1 <- dfgoikmeans1[,c(2,3,4)]

set.seed(123)
k.max=8
wss <- sapply(1:k.max, function(k){kmeans(dfgoikmeans1[,c(1)], k,nstart = 25)$tot.withinss})
wss

plot(1:k.max, wss, type="b", pch = 19, frame = FALSE, xlab="Number of clusters K", ylab="Total within-clusters
sum of squares")

```

```

goiclusterv <- kmeans(dfgoikmeans1[,c(1)], 5, nstart = 30)
goiclusterv
dfgoikmeans1$clusterv <- goiclusterv$clusterv

write.csv(dfgoikmeans1, file = "4tU-cluster.csv", sep = "\t", quote = FALSE, row.names = FALSE)
write.csv(dfnrngoi, file="dfnrngoi_444.csv", sep = "\t", quote = FALSE, row.names = FALSE)

rm(dfgoikmeans1,dfnrngoi)
#####

```

A.2 Calculating Acetylation for H3K18ac MNase-ChIP-seq

The dataframe with per bp values was generated using modified script from Chereji Plot2DO. The coverage values range from -1000 bp to +1000 bp around a +1 peak per gene. This data was generated for every time point in the experiment and was used as an input for the following script.

```

#50 bp around +1 analysis
make_df <- function(f1_file){
  df1 <- read.table(f1_file, sep = "\t")
  df2 <- df1[,c(1,2,seq(478,528))]
  df2$mean1 <- rowMeans(df2[,c(3,53)])
  df3 <- data.matrix(df2[,c(seq(3,53))], rownames.force = NA)
  df2$area <- rowMaxs(df3,value=FALSE)-df2$mean1
  df2$area <- df2$area*25
  df4 <- df2[,c(1,2,55)]
  colgene <- paste(substr(f1_file,52,52), substr(f1_file, 53, 54),substr(f1_file,55,55), sep = "-")
  colnames(df4) <- c("ID", "clusterv", colgene)
  return(df4)
}

get_files <- function(path,func){
  flist <- list.files(path = path)
  all_occ <- paste(path, flist, sep = "/")
  c1 <- Map(func, all_occ)
  df <- join_all(c1)
  dfR <- reshape2::melt(df,id.var=c(1,2))
  dfR <- dfR %>% tidyr::separate(variable, c("exp", "strain", "time"))
  return(dfR)
}

convert_timepoint <- function(x) {
  switch(x, '1'=0, '2'=120, '3'=150, '4'=180, '5'=240, '6'=300)
}

path1="output/2D_dyads_Plus1_R"
func="make_df"
dfR <- get_files(path1,func)

dfR$time <- unlist(lapply(dfR$time, convert_timepoint))
colnames(dfR)[6] <- "occ"

write.table(dfR, file="Per_gene_analysis/H3K18ac_plus1_per-gene.txt", sep="\t", row.names = FALSE,
col.names = TRUE, quote = FALSE)

```

The data generated was used to make figures on Result part-2, Figure 2 and Figure S3, page 78 and page 125.

A.3 NDR Size Calculation

The coverage data generated for H3K18ac MNase ChIP-seq was used for the NDR size calculation.

```
cal_nuc_dyad <- function(x){
  c1 <- which.min(abs(x-quantile(x,probs = c(1),names = TRUE,warn=TRUE )))
  return(c1)
}

make_df_ndr <- function(f1_file){
  df1 <- read.table(f1_file, sep = "\t")
  df2 <- df1[,c(1,2,seq(253,403))]
  df3 <- as.data.frame(t(df2[,c(seq(3,153))]))
  nucm <- unlist(lapply(df3, cal_nuc_dyad))
  names(nucm) <- NULL
  df4 <- df1[,c(1,2,seq(428,578))]
  df5 <- as.data.frame(t(df4[,c(seq(3,153))]))
  nucp <- unlist(lapply(df5, cal_nuc_dyad))
  names(nucp) <- NULL
  df6 <- cbind(df2[,c(1,2)], nucm, nucp)
  df6$ndr <- df6$nucp+275-df6$nucm
  df6$nucm <- NULL
  df6$nucp <- NULL
  colgene <- paste(substr(f1_file,52,52), substr(f1_file, 53, 54),substr(f1_file,55,55), sep = "-")
  colnames(df6) <- c("ID","cluster", colgene)
  return(df6)
}

path1="output/2D_dyads_Plus1_R"
func="make_df_ndr"

dfRndr <- get_files(path1,func)

dfRndr$time <- unlist(lapply(dfRndr$time, convert_timepoint))
colnames(dfRndr)[6] <- "dyaddistance"

write.table(dfRndr, file="Per_gene_analysis/H3K18ac_dyad_dist_per-gene.txt", sep="\t", row.names = FALSE,
col.names = TRUE, quote = FALSE)
```

A.4 +1 Nucleosome Distribution Calculation

The data for per bp coverage was calculated using the modified script of Plot2DO.

```
make_df3 <- function(f1_file){
  df1 <- read.table(f1_file, sep = "\t")
  df2 <- df1[,c(1,2,seq(403,603))]
  t1 <- rowSums(df2[,c(seq(3,102))])
  t2 <- rowSums(df2[,c(seq(104,203))])
```

```
nucdist <- t1/t2
nucdist <- nucdist
df4 <- cbind(df2[,c(1,2)],nucdist)
colgene <- paste("mn", substr(f1_file, 63, 64),substr(f1_file,65,65), sep = "-")
colnames(df4) <- c("ID","cluster", colgene)
return(df4)
}

make_mnasedf <- function(path) {
  flist <- list.files(path = path)
  all_occ <- paste(path, flist, sep = "/")
  c1 <- Map(make_df3, all_occ)
  df <- join_all(c1)
  dfmnase <- reshape2::melt(df,id.var=c(1,2))
  dfmnase <- dfmnase %>% tidyr::separate(variable, c("exp", "strain", "time"))
  dfmnase$time <- unlist(lapply(dfmnase$time, convert_timepoint))
  colnames(dfmnase)[6] <- "nucdist"
  return(dfmnase)
}
```

B Non-coding Transcription Regulates Replication Program in *Cis*

DNA replication initiates at autonomously replicating sequences (ARS) distributed all over the genome. Efficient genome duplication requires coordinated firing of all the DNA replication origins. In yeast, there are 200-300 ARSs in the genome that are usually nucleosome depleted. Origin function is significantly affected by the context of local chromatin (Ding and MacAlpine, 2011; Mechali et al., 2013). ARSs were originally described to be intergenic and were thought to be shielded from transcription. With the development of nascent RNA sequencing techniques, we know that almost the whole yeast genome is pervasively transcribed (Churchman and Weissman, 2011). The aim of this study was to define the effect of non-coding transcription readthrough at ARSs NDRs on the replication program.

We selected 234 ARSs for our study and first analysed the distribution of non-coding transcripts around the ARSs NDRs. We found that early and efficient ARSs present robust transcription termination in the vicinity of the origin. To investigate the effect of non-coding transcription readthrough, we used the Nrd1 anchor away strain. After induction of non-coding transcription, we observed closing of ARSs NDRs using MNase sequencing. Using BrdU-seq, we also observed that the ARSs affected by transcription readthrough are usually late and inefficient. Importantly, ARSs that are relatively highly transcribed at steady state are associated with higher MNase density and H3K36me3, as well as lower acetylation. Thus, non-coding transcription-mediated chromatin modifications negatively affect the replication program.

This study entitled “Noncoding transcription influences the replication initiation program through chromatin regulation” has been published in *Genome Research* (Soudet et al., 2019).

My contribution to this work was to perform the experiment for Figure 2 and supplementary Figure 2C.

Noncoding transcription influences the replication initiation program through chromatin regulation

Julien Soudet, Jatinder Kaur Gill, and Françoise Stutz

Department of Cell Biology, University of Geneva, 1211 Genève 4, Switzerland

In eukaryotic organisms, replication initiation follows a temporal program. Among the parameters that regulate this program in *Saccharomyces cerevisiae*, chromatin structure has been at the center of attention without considering the contribution of transcription. Here, we revisit the replication initiation program in the light of widespread genomic noncoding transcription. We find that noncoding RNA transcription termination in the vicinity of autonomously replicating sequences (ARSs) shields replication initiation from transcriptional readthrough. Consistently, high natural nascent transcription correlates with low ARS efficiency and late replication timing. High readthrough transcription is also linked to increased nucleosome occupancy and high levels of H3K36me₃. Moreover, forcing ARS readthrough transcription promotes these chromatin features. Finally, replication initiation defects induced by increased transcriptional readthrough are partially rescued in the absence of H3K36 methylation. Altogether, these observations indicate that natural noncoding transcription into ARSs influences replication initiation through chromatin regulation.

[Supplemental material is available for this article.]

DNA replication is a fundamental process occurring in all living organisms and ensuring accurate duplication of the genome. Eukaryotic replication initiation takes place at several dispersed locations termed replication origins. Origins are defined by a specific chromatin structure consisting of a nucleosome-depleted region (NDR) and the binding of specific replication initiation factors. In *Saccharomyces cerevisiae*, replication origins or ARSs (autonomously replicating sequences) are specified by an 11bp T-rich ARS consensus sequence (ACS) (Stinchcomb et al. 1979; Nieduszynski et al. 2006). ARSs also contain more degenerate A-rich B elements proposed to contribute to origin function by excluding nucleosomes (Bell 1995; Segal and Widom 2009; Eaton et al. 2010). Despite the occurrence of thousands of ACSs in the genome, only 200–300 are efficient for the recruitment of the AAA + ATPase origin recognition complex (ORC) (Raghuraman et al. 2001; Hawkins et al. 2013; McGuffee et al. 2013). During the G1-phase, the ORC in conjunction with Cdt1 and Cdc6 promotes the binding of the MCM2-7 double hexamer helicase complex giving rise to the prereplication complex (pre-RC) (Deegan and Diffley 2016). The resulting ORC/MCM2-7-bound ARSs are said to be licensed for replication initiation and have the ability to initiate replication during the subsequent S-phase (Aparicio 2013).

Replication follows a temporal program of activation during S-phase. ARSs are defined by an activation timing based on the observation that some ARSs replicate earlier than others (Raghuraman et al. 2001; Hawkins et al. 2013). Moreover, using DNA combing, it appears that the fraction of cells in a population initiating replication at a given ARS is variable, defining a firing efficiency probability for each ARS (Czajkowsky et al. 2008; Hawkins et al. 2013; McGuffee et al. 2013). Timing and efficiency are linked, as inefficient origins tend to fire late during S-phase or to be replicated passively through the use of a neighboring origin (Yang et al. 2010). These two interdependent measurements of timing and ef-

iciency are usually used to describe the replication initiation properties of ARSs.

In *S. cerevisiae*, many parameters affect ARS activity including limiting *trans*-acting factors, different chromosomal location, and/or subnuclear localization (Yoshida et al. 2013). ARS activity also depends on the chromatin context and histone modifications. First, early origins have a wider NDR than late ARSs and adjacent nucleosomes are more precisely positioned (Soriano et al. 2014; Rodriguez et al. 2017). Moreover, the strength of ORC recruitment correlates with ARS activity and is itself important for NDR establishment (Eaton et al. 2010; Belsky et al. 2015). Second, early ARS activation during S-phase depends on histone acetylation (Vogelauer et al. 2002; Unnikrishnan et al. 2010). Indeed, the Class I Histone Deacetylase (HDAC) Rpd3 delays initiation of a huge number of replication origins (Vogelauer et al. 2002; Aparicio et al. 2004; Knott et al. 2009) and narrows their nucleosome-depleted regions (Soriano et al. 2014).

Numerous studies attempting to consider transcription as another parameter to define replication initiation led to conflicting results. On one hand, transcription revealed some positive links with replication initiation, as highly transcribed genes were proposed to replicate earlier than lowly expressed genes (Fraser 2013). Furthermore, stalled RNA polymerase II (RNA Pol II) was involved in the recruitment of the ORC at the rDNA locus, and the activity of many replication origins depends on the presence of specific transcription factor binding sites (Knott et al. 2012; Mayan 2013). On the other hand, active ARSs are excluded from annotated ORFs and tend to localize after 3'-transcription terminators, suggesting that transcription and replication initiation do not coexist (Nieduszynski et al. 2006). Furthermore, natural or artificial induction of transcription through origins leads to replication defects via dissociation or sliding of the pre-RC and MCMs, respectively (Snyder et al. 1988; Nieduszynski et al. 2005; Mori and Shirahige 2007; Blitzblau et al. 2012; Gros et al. 2015). In this study, we aimed at clarifying the role of transcription in

Corresponding authors: julien.soudet@unige.ch, francoise.stutz@unige.ch

Article published online before print. Article, supplemental material, and publication date are at <http://www.genome.org/cgi/doi/10.1101/gr.239582.118>. Freely available online through the *Genome Research* Open Access option.

© 2018 Soudet et al. This article, published in *Genome Research*, is available under a Creative Commons License (Attribution-NonCommercial 4.0 International), as described at <http://creativecommons.org/licenses/by-nc/4.0/>.

replication initiation considering the widespread genomic noncoding transcription.

The analysis of appropriate mutants and the development of new tools to examine nascent transcription have revealed that RNA Pol II occurs pervasively and that the transcriptional landscape in eukaryotic genomes extends far beyond mRNAs and stable noncoding RNAs (Churchman and Weissman 2011; Schaughency et al. 2014). One source of noncoding transcription stems from initiation at NDRs, an event controlled through early termination by the Nrd1-Nab3-Sen1 (NNS) complex recruited at the 5' end of all RNA Pol II transcription units via interaction with the RNA Pol II C-terminal domain (CTD) (Steinmetz et al. 2001; Arigo et al. 2006). Recognition by Nrd1/Nab3 of specific motifs on the nascent RNA induces RNA Pol II termination usually within the first kilobase of transcription in a process coupled to degradation by the nuclear exosome component Rrp6 (Tudek et al. 2014). These cryptic unstable transcripts (CUTs) are revealed in the absence of Rrp6 (Wyers et al. 2005; Neil et al. 2009; Xu et al. 2009; van Dijk et al. 2011; Jensen et al. 2013). Depletion of Nrd1 results in transcriptional readthrough and accumulation of Nrd1 unterminated transcripts (NUTs), most of which correspond to extended CUTs (Schulz et al. 2013; Schaughency et al. 2014). In the presence of inefficient early termination signals, loss of Rrp6 can also favor readthrough transcription and elongation of CUTs (Castelnuovo et al. 2013). Another source of noncoding transcription is linked to mRNA 3' end formation. The cleavage and polyadenylation (CPF) and cleavage factor (CF) complexes cleave the nascent mRNA just upstream of RNA Pol II. RNA Pol II release depends on a CPF-induced allosteric modification of the elongation complex as well as on the digestion of the generated 3' fragment by the 5'-3' exonuclease Rat1 (for a recent review, see Porrua et al. 2016). Thus, before being caught up by the so-called "torpedo," RNA Pol II continues transcription, leading to an average 160-bp termination window after the polyadenylation site. Inefficient cleavage and polyadenylation can increase the level of this natural source of pervasive transcription (Kim et al. 2004; Luo et al. 2006; Baejen et al. 2017).

Using nascent transcription and replication analyses in strains depleted for early termination activities, we delineate how noncoding transcription negatively influences replication initiation by shaping the chromatin structure of ARS. Our study clearly defines genome-wide noncoding transcription as a new parameter regulating replication initiation.

Results

CUTs and NUTs are enriched at early and efficient ARSs

To determine the overlap of NUTs and CUTs with replication origins, we defined a list of 234 ARSs (Supplemental Table S1) with previously annotated ACSs (Nieduszynski et al. 2006; Soriano et al. 2014) and for which replication timing and efficiency had been established (Hawkins et al. 2013). Among the 234 well-defined ARSs used in this analysis, 52 (22%) overlap with a CUT (as already observed in Looke et al. 2010), a NUT, or both (Fig. 1A; Supplemental Fig. S1A; Xu et al. 2009; Schulz et al. 2013). CUTs and NUTs are defined in a mutant context when early termination is compromised. The presence of CUTs and NUTs over 52 replication origins indicates that termination of noncoding transcription through the NNS pathway is robust around these ARSs. Notably, the 52 ARSs overlapping with NUTs and/or CUTs (ncARSs) tend to be replicated earlier and more efficiently, on average, than the

remaining 182 ARSs (Other ARSs) (Fig. 1B). These observations suggest that noncoding transcription termination may be a determinant of ARS replication timing and efficiency.

Noncoding transcription readthrough affects replication initiation

One hypothesis is that NNS termination in the vicinity of a subset of ARSs may shield them from pervasive transcription potentially deleterious for replication initiation. To investigate the effect of noncoding transcription readthrough on replication, early termination of noncoding RNAs was abrogated by rapid nuclear depletion of Nrd1 through anchor away (AA) (Haruki et al. 2008). Nrd1 depletion, induced by addition of rapamycin (Rap) to the engineered Nrd1-AA strain, is accompanied by transcription elongation and accumulation of NUTs (Schulz et al. 2013). To examine the effect on replication, the Nrd1-AA strain was treated with alpha factor to synchronize the cells in G1-phase and incubated an additional hour $-/+$ Rap to induce noncoding transcription. Cells were then released from G1 arrest in the presence of BrdU (Fig. 1C). FACS analyses indicate a slight cell cycle delay at 80 min in cells depleted for Nrd1, with an increased number of cells in G1 in +Rap compared to $-$ Rap (Supplemental Fig. S1B). Samples were harvested for BrdU-seq at 70 min after G1-phase release. Visualization of the data revealed a number of well-defined peaks centered on specific ARSs (Fig. 1D; Supplemental Fig. S1C,D). Global analysis of the BrdU-seq showed that, out of the 178 selected early ARSs, 36 (20.2%) present a reproducible, more than 35% decrease in BrdU incorporation in +Rap versus $-$ Rap (17 show $>50\%$ decrease and 19 between 35%–50% decrease) (Fig. 1E). Consistently, metagene analysis from -10 to $+10$ Kb around the ACS of the $>50\%$ affected ARSs revealed a substantial reduction in the BrdU-seq profile in +Rap, while the curves including the $<35\%$ affected ARSs presented only a slight change in +Rap versus $-$ Rap (Fig. 1F). Affected ARSs showed a nice overlap with the NUTs-containing ARSs defined in Figure 1A (Supplemental Fig. S1E). To define whether the decreased BrdU-seq signal of affected ARSs upon Nrd1 depletion was linked to transcription, RNA Pol II PAR-CLIP data from the Corden lab (Schaughency et al. 2014) were used to examine the level of nascent transcription over ARS when depleting Nrd1. The ARSs with the strongest decrease in BrdU incorporation in +Rap versus $-$ Rap also showed the highest increase in nascent RNA Pol II transcription into the ACSs to $+100$ bp ORC-footprinting area (Fig. 1E–G; Belsky et al. 2015). Thus, the replication defect observed following Nrd1 depletion is not due to the slightly slower cell cycle progression in +Rap but is directly linked to increased nascent transcription through the affected ARS.

RNA and BrdU analyses were also performed with the Rrp6-AA strain. Anchor away of Rrp6 has already been described by our lab to result in CUT elongation (Castelnuovo et al. 2014). Depletion of Rrp6 resulted in similar effects on ncRNA accumulation and replication initiation (Supplemental Fig. S2).

Overall, these data suggest that replication initiation may be hindered by noncoding readthrough transcription.

High noncoding readthrough transcription leads to ARS chromatin regulation

Given the links between replication initiation and chromatin structure, we then analyzed the effects of the Nrd1 depletion-induced transcription readthrough into replication origins on nucleosome positioning. Chromatin was extracted from Nrd1-AA cells either untreated or treated for 1 h with rapamycin and digested

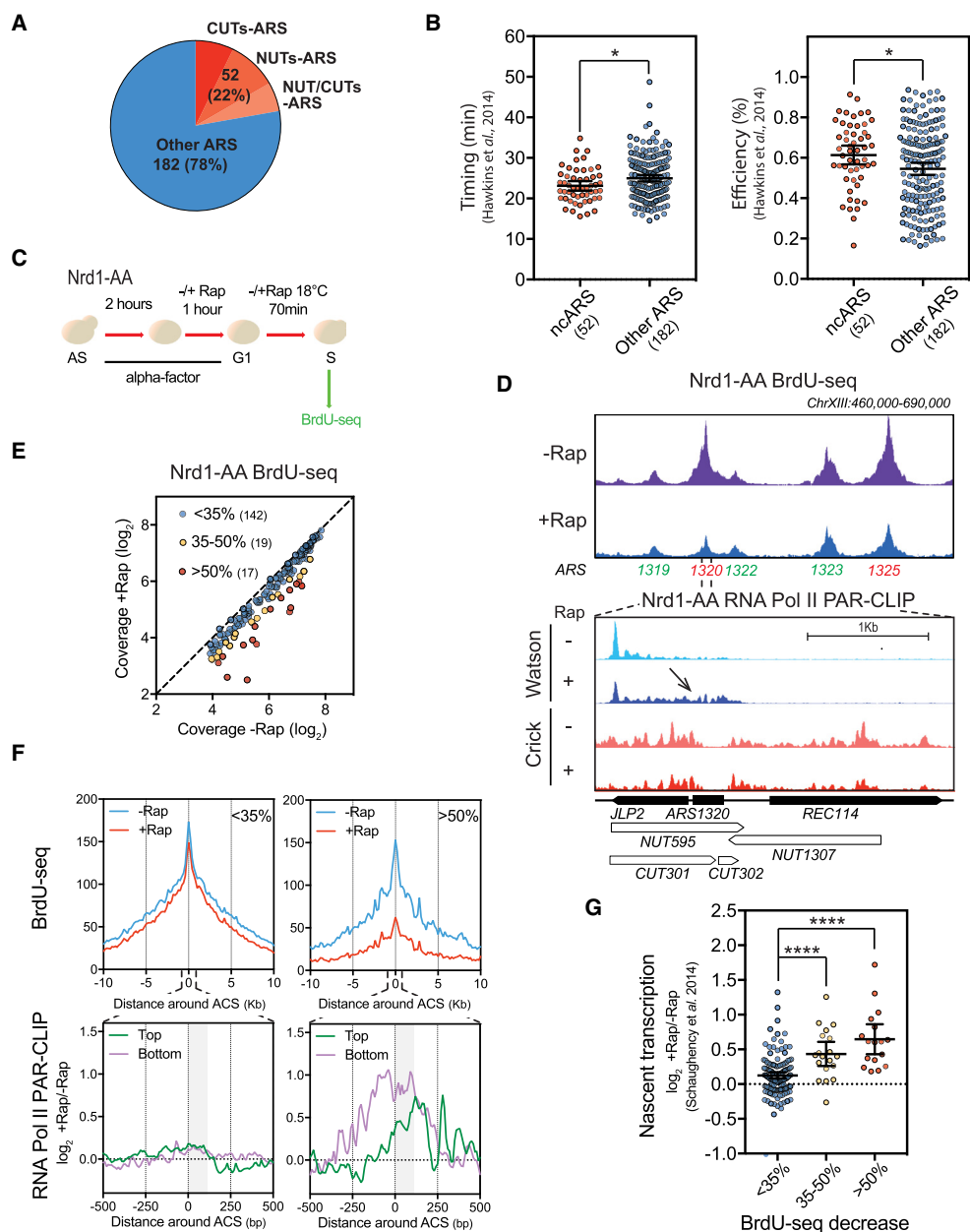


Figure 1. NUTS- and CUTs-containing ARSs are down-regulated when early termination of noncoding RNAs is abrogated. (A) Numbers and proportions of ARSs overlapping with CUTs only (red), NUTs only (orange), or both CUTs and NUTs (pink). ARS annotations used in this study are listed in Supplemental Table S1. CUTs and NUTs were considered as overlapping when showing 50 bp of overlap in the ACS to +100 bp area according to the ACS T-rich sequence. (B) Scatter dot-plot indicating the timing and efficiency of the noncoding RNA-containing ARSs (ncARSs) compared to replication origins devoid of overlapping CUTs and NUTs (Other ARSs). Timing and efficiency data were retrieved from Hawkins et al. (2013). The mean and the 95% confidence interval are indicated. (C) Nrd1-AA cells were synchronized in G1-phase with alpha-factor for 3 h at 30°C. During the last hour, rapamycin (Rap) was added or not in the medium. Cells were then washed and released into the cell cycle at 18°C in the presence of BrdU and +/-Rap. After 70 min, cells were collected for DNA extraction and BrdU-seq. (D) Snapshot depicting a part of Chromosome XIII for the BrdU-seq. Affected ARSs are indicated in red and nonaffected in green. *Bottom* panel shows a zoom around ARS1320 of the RNA Pol II PAR-CLIP in the Nrd1-AA strain (Schaughency et al. 2014). Transcriptional read-through is indicated by an arrow. (E) Plot depicting the mean coverage of BrdU nascent DNA in a 5-kb window around ACS in -Rap versus +Rap. The 17 red dots and 19 yellow dots represent the ARSs showing at least 50% and 35%–50% decrease in BrdU incorporation in +Rap, respectively. Blue dots represent the ARSs defined as nonaffected in BrdU incorporation. (F) *Top*: Metagenesis of the BrdU-seq for the 142 nonaffected ARSs (<35%) and the 17 most affected ARSs (>50%). Profiles represent the mean coverage smoothed by a 200-bp moving window. ARSs were oriented according to their ACS T-rich sequence. *Bottom*: Metagenesis profiles of the ratio $\log_2 +\text{Rap}/-\text{Rap}$ of the RNA Pol II PAR-CLIP signal 500 bp around the oriented ACS of the least and most affected ARS (Schaughency et al. 2014). Plots were smoothed by a 10-bp moving window. Since ARSs are oriented, nascent transcription going toward replication origins is defined as Top and Bottom. The gray box represents the window in which transcriptional read-through was analyzed in G. (G) Scatter dot-plots representing the ratio $\log_2 +\text{Rap}/-\text{Rap}$ of the RNA Pol II PAR-CLIP signal over the three classes of ARSs defined in E. Total nascent transcription in +Rap and -Rap was defined on oriented ARSs by adding the RNA Pol II PAR-CLIP mean densities between the ACS to +100 bp on the top strand to the signal over the same region on the bottom strand in each condition using the data from Schaughency et al. (2014). Each 100-bp segment was considered as 1 bin (see Methods). (*) P -value < 0.05; (****) P -value < 0.0001.

with micrococcal nuclease (MNase). First, sequencing of the 120- to 200-bp fragments protected by nucleosomes revealed the typical NDR around the ACS as previously described (Fig. 2A; Eaton et al. 2010). Second, analysis of nucleosome positioning at the classes of ARS defined in Figure 1E revealed a statistically significant increased density of nucleosome dyads in the NDRs of the ARSs that are the most affected for replication initiation and present a higher increase in readthrough transcription (Figs. 1G, 2A–C). Additional analyses reveal that the >50% class is significantly different from the <35% group not only when taking the mean of two replicates but also when considering each individual experiment (Fig. 2B; Supplemental Fig. S3). These results suggest that high levels of noncoding transcription into replication origins leads to chromatin closing, which may in turn perturb replication initiation. However, additional parameters are likely to influence replication since the mildly affected ARSs (35%–50%) do not show significant nucleosome shifting although they are affected in replication initiation.

ARSs with a high basal level of readthrough transcription are late and inefficient

Recent data show that noncoding transcription occurs all over eukaryotic genomes (Jensen et al. 2013), and our results indicate that this transcription is detrimental for replication initiation. These observations led to the hypothesis that differences in nascent transcription between ARSs may influence both their activity and

chromatin structure at steady-state. First, we confirmed that the production of stable transcripts, defined by RNA-seq, strongly drops in the vicinity of the 234 replication origins (including both early and late origins), while profiles of nascent transcription indicate that RNA Pol II density stays relatively constant through these ARSs (Fig. 3A,B). These observations establish that noncoding transcription through replication origins is a frequent event. The same set of ARS was then analysed for the level of natural basal readthrough transcription over a 100-bp segment between the ACS and the B elements using published RNA Pol II PAR-CLIP data (Schaughency et al. 2014). ARSs were subdivided into three groups according to their natural readthrough transcription levels into this region using a nonbiased *k*-means clustering approach (Fig. 3C). The highly transcribed ARSs were significantly enriched in ARS lying between two convergent genes (Supplemental Fig. S4A). Importantly, nascent transcription toward the ARSs measured upstream of and downstream from the oriented ACS was also significantly different for the three groups (Supplemental Fig. S4B), indicating that high ARS readthrough mainly stems from higher levels of nascent transcription from the adjacent convergent genes. Running these three groups of ARSs through replication timing and efficiency data (Hawkins et al. 2013) revealed that the 72 ARSs with high readthrough transcription have a significantly delayed replication timing and reduced replication efficiency compared to the ARSs with lower transcriptional readthrough (Fig. 3D), although the global correlation was low (Supplemental Fig. S4C). This suggests that once a certain threshold of pervasive

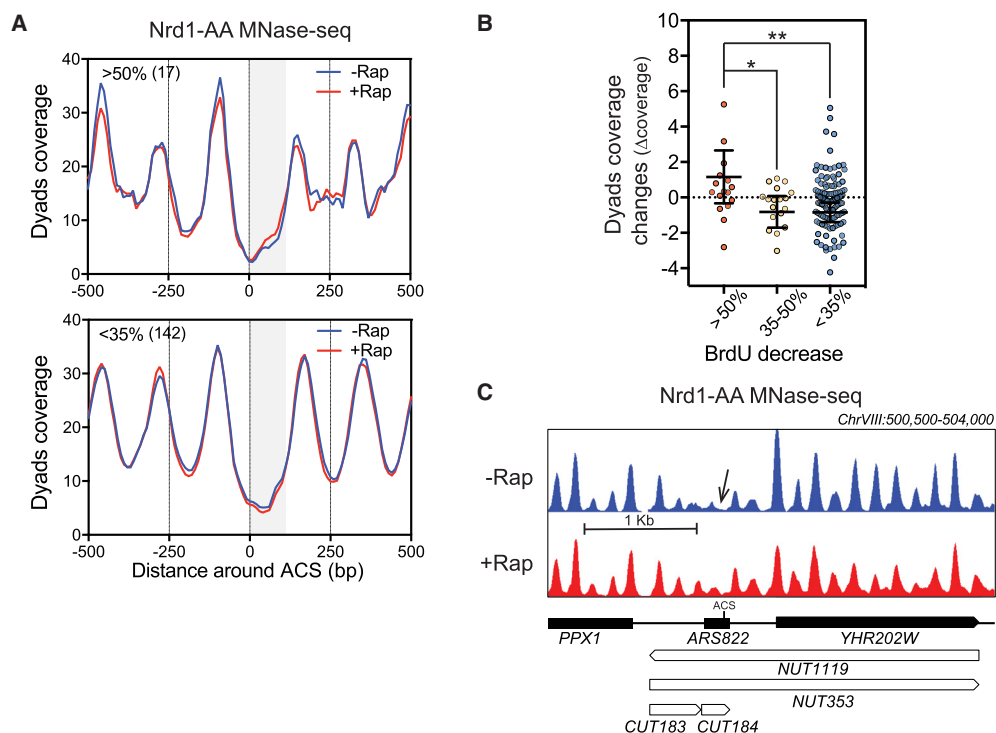


Figure 2. Noncoding transcription readthrough into replication origins alters nucleosome occupancy. (A) Metagenome analysis of MNase-seq from Nrd1-AA cells treated or not with rapamycin for 1 h at the three classes of ARSs defined in Figure 1. Only paired-end reads from 120 to 200 bp length were considered to define nucleosome dyad coverage. The gray box represents the window in which transcriptional readthrough was analyzed. (B) Scatter dot-plot representing the difference of dyads coverage (Δ coverage = coverage [+Rap] – coverage [–Rap]) between the ACS to +100 of oriented ARSs when comparing +Rap and –Rap conditions. (C) Snapshot of the MNase-seq around ARS822 belonging to the class of most affected ARSs. (*) *P*-value < 0.05; (**) *P*-value < 0.01.

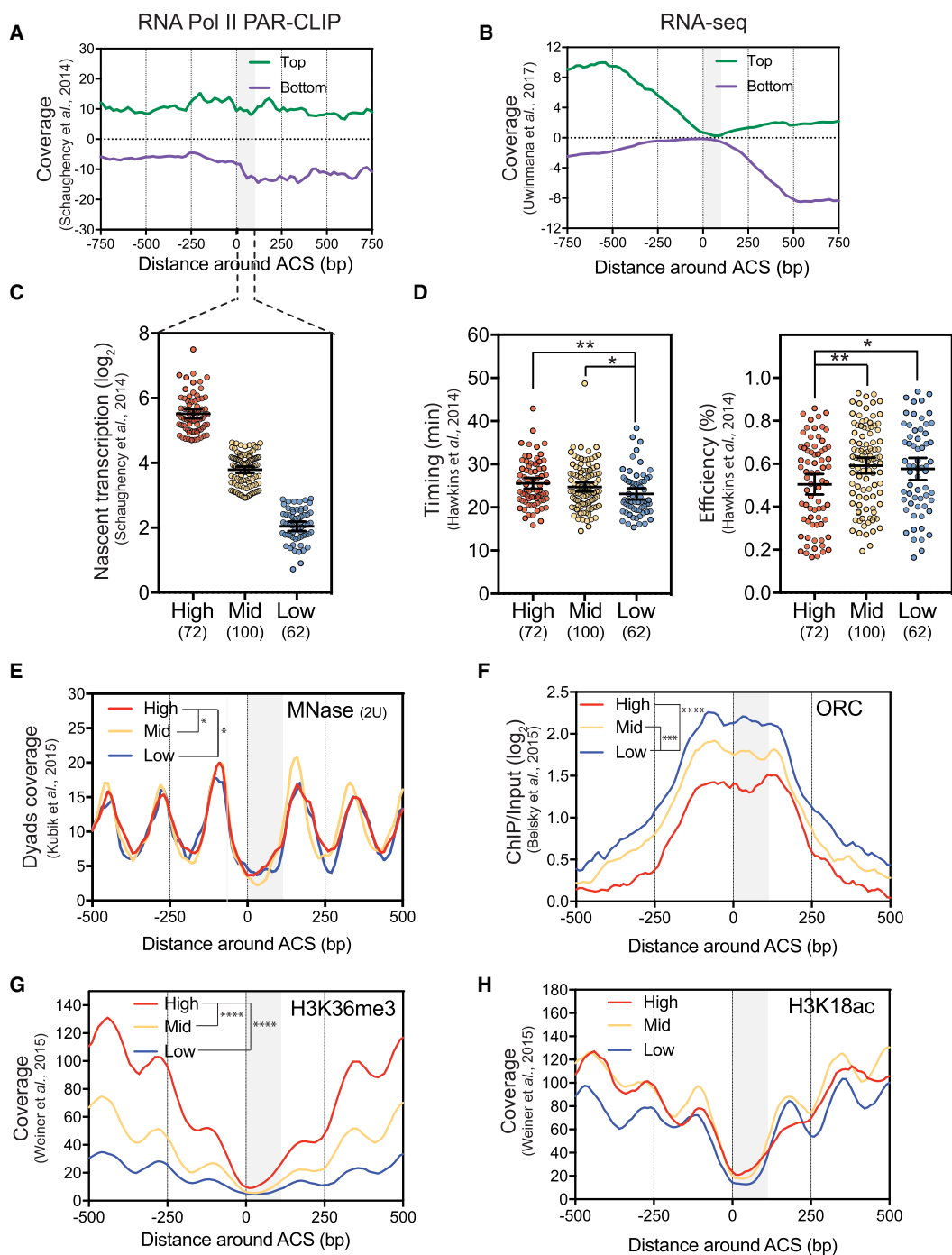


Figure 3. Natural pervasive transcription correlates with timing/efficiency and specific chromatin features of replication origins. (A) Metagene analysis of Top and Bottom RNA Pol II PAR-CLIP (Schaughency et al. 2014) and (B) RNA-seq (Uwimana et al. 2017) data in the vicinity of 234 oriented replication origins. Data were smoothed by a 20-bp moving window. The gray box represents the window in which transcriptional readthrough was analyzed. (C) The 234 replication origins were divided into three classes (High, Mid, or Low) according to their level of total natural readthrough transcription using a nonbiased *k*-means clustering approach. This basal nascent transcription was calculated on oriented ARSs by adding the RNA Pol II PAR-CLIP mean densities between the ACS and +100 bp on the top strand to the signal over the same region on the bottom strand. Each 100-bp segment was considered as 1 bin. Natural nascent transcription data were taken from Schaughency et al. (2014). (D) Replication timing and efficiency of the three classes of ARSs defined as in C. (E–H) Nucleosome positioning, ORC, H3K36me3, and H3K18ac levels considering the three classes of replication origins. Data for nucleosome positioning, ORC recruitment, and histone marks were retrieved from Kubik et al. (2015), Belsky et al. (2015), and Weiner et al. (2015), respectively. For these plots, ARSs were oriented and aligned according to their ACS T-rich sequence. The significance of differences between the three classes was calculated over the ACS to +100 bp region considered as 1 bin and is indicated in the *top left* of each panel. No annotation is considered as nonsignificant. (*) *P*-value < 0.05; (**) *P*-value < 0.01; (***) *P*-value < 0.001; (****) *P*-value < 0.0001.

transcription readthrough is reached, ARS activity is significantly reduced. Notably, the 52 NUTs/CUTs-containing ARSs present significantly lower natural readthrough transcription than the highly transcribed ARSs and appear more similar to the mildly transcribed ARSs, further supporting that NNS-mediated termination positively contributes to replication timing and efficiency by shielding ARSs from pervasive transcription (Supplemental Fig. S4D). Consistent with these results, earlier-defined ORC-bound ARSs (ORC-ARS) exhibit significantly less readthrough transcription compared to non-ORC-bound and nonreplicated ARSs (nr-ARSs) (Supplemental Fig. S4E; Eaton et al. 2010).

Thus, natural pervasive transcription into the ORC-binding area appears to be anti-correlated with ARS function as defined by its timing and efficiency as well as its ability to bind the ORC complex.

Steady-state highly transcribed ARSs present distinctive chromatin features

Using recently published nucleosome occupancy data (Kubik et al. 2015; Weiner et al. 2015), the 72 ARSs with high pervasive transcription levels appear to be associated with significantly increased nucleosome dyad density over the ORC-binding area compared to the 162 with lower transcription levels (Fig. 3E). This observation appears to be independent of the MNase sensitivity of the replication origins NDRs since less digested chromatin leads to a similar conclusion (Supplemental Fig. S5A; Kubik et al. 2015). Thus, high levels of nascent transcription into the ACS to +100 bp area correlate with higher nucleosome occupancy and are, as expected, also associated with lower ORC binding (Fig. 3F; Hoggard et al. 2013; Looke et al. 2013; Belsky et al. 2015; Das et al. 2015; Peace et al. 2016).

We also analyzed the correlations between natural pervasive transcription into ARSs and histone modifications (Weiner et al. 2015). We found that H3K36me3 levels over the ACS-100-bp area positively correlate with the levels of nascent transcription (Fig. 3G). We did not detect a significant correlation between nascent transcription and H3K18, H3K14, H4K12, and H4K5 acetylation over the ORC-binding region (Fig. 3H; Supplemental Fig. S5B–D). However, we detected a significant lack of these acetylation marks at the downstream nucleosome of the highly transcribed class (Supplemental Fig. S5F).

H3K36me3 is deposited by the Set2 histone methyltransferase and leads to the recruitment of the Rpd3 HDAC known to de-acetylate the lysines cited above and described as being involved in replication control (Rundlett et al. 1996; Knott et al. 2009). In contrast, the three groups of ARSs present no difference in H3K4me2, another mark promoting de-acetylation of the chromatin via binding of the Set3 HDAC (Supplemental Fig. S5E; Woo et al. 2017).

Together these observations support the view that noncoding transcription through an ARS promotes the formation of a closed chromatin structure reducing its ability to interact with an ORC, thereby decreasing its efficiency and/or delaying its replication timing.

Noncoding and mRNA readthrough transcription over ARSs induce H3K36 methylation, histone deacetylation, and increased nucleosome occupancy

To strengthen the causal relationship between nascent transcription, changes in chromatin organization and ARS activity, we examined the effect of induced transcription on ARS chromatin

changes. We first ranked the replication origins according to their increase in transcriptional readthrough levels in the Nrd1-AA strain and to their decrease in BrdU incorporation during early S-phase. We picked three ARSs belonging to the most affected ARSs in BrdU incorporation and presenting high levels of induced transcriptional readthrough (Fig. 4A). As a control, we took two replication origins belonging to the least affected ARSs in replication and showing no or weak induced readthrough. To relate the replication defect induced by noncoding readthrough transcription to changes in chromatin structure, chromatin immunoprecipitation was used to compare histone H3 occupancy, H3K36 methylation, and H3K18 acetylation in $-/+$ Rap. Primers for qPCR were designed to target the NDR of the ARSs. At the three affected ARSs, rapamycin treatment resulted in increased H3 occupancy and H3K36 methylation as well as a decrease in H3K18 acetylation, while no changes were observed at the nonaffected ARSs (Fig. 4B).

Since 86% of replication origins are located in the vicinity of a convergent coding gene, we decided to anchor away the essential mRNA 3' cleavage and polyadenylation factor (CPF/CF) endonuclease Ysh1. As expected, nuclear depletion of Ysh1 has a major impact on replication progression and more specifically on replication initiation, as most of the 178 considered ARSs showed reduced BrdU incorporation in the presence of rapamycin, with 31 ARSs presenting more than an 80% decrease (Supplemental Fig. S6A–D). Combining BrdU-Seq in Ysh1-AA $-/+$ Rap with published RNA Pol II PAR-CLIP data of this strain (Schaughency et al. 2014) revealed that the 31 ARSs with the strongest replication defect also present the highest increase in readthrough transcription, suggesting a direct involvement of nascent transcription readthrough in this massive replication defect (Supplemental Fig. S6D,E). However, due to the general role of Ysh1 as an mRNA termination factor, we cannot fully rule out an indirect effect of its depletion on completion of replication. Replication origins were then ranked according to their induced levels of readthrough and defects in early replication as performed for the Nrd1-AA strain (Fig. 4A). Chromatin immunoprecipitation revealed increased H3 occupancy for the ARSs showing high levels of mRNA readthrough (with the exception of ARS507), while H3K36me3 levels increased and H3K18ac levels decreased (Fig. 4C).

Taken together, these experiments demonstrate that increased noncoding and mRNA readthrough transcription causes increased nucleosome occupancy and histone deacetylation at the downstream ARSs, two parameters described to interfere with the efficiency of ORC binding and ARS licensing (Vogelauer et al. 2002; Aparicio et al. 2004; Knott et al. 2009; Soriano et al. 2014).

Replication defects induced by noncoding readthrough transcription are partially rescued in the absence of H3K36 methylation

To decipher the molecular cascade of events, we analyzed the effects of noncoding transcription readthrough on replication initiation in a Nrd1-AA *set2Δ* strain (Fig. 5A). Global analysis of replication by flow cytometry indicates that replication is still delayed in the absence of H3K36 methylation in the Nrd1-AA background (Supplemental Fig. S7A). However, by taking the same classes of defective ARSs as defined in Figure 1, we observed a partial rescue of BrdU incorporation (Fig. 5B–D), although noncoding RNAs were still produced in the absence of Set2 (Supplemental Fig. S7B). These observations support the view that

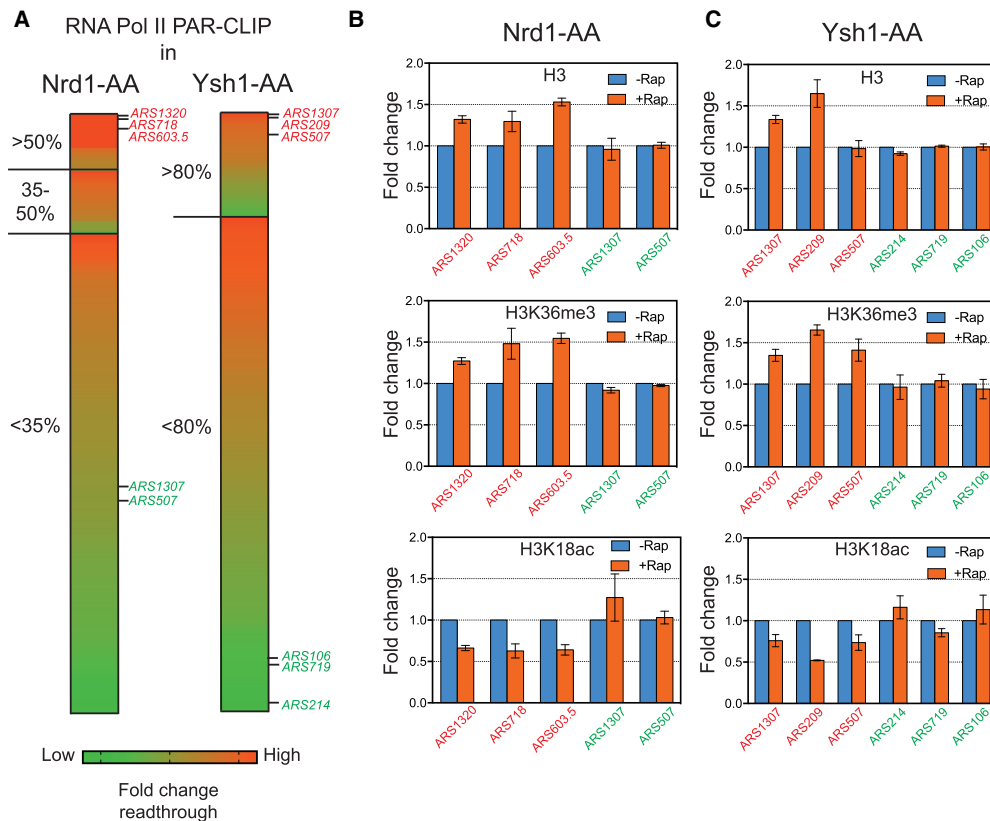


Figure 4. Noncoding and mRNA transcription readthrough at replication origins leads to chromatin changes. (A) Heat map representing the fold change of transcriptional readthrough at replication origins in Nrd1-AA and Ysh1-AA mutants. The 178 ARSs were classified according to their BrdU incorporation defects and ranked by their total readthrough increase over the ACS to +100 bp region. The three ARSs indicated in red for each mutant present a high increase in total readthrough. The ARSs depicted in green show mid or low total readthrough and have been used as controls for the following experiments. (B, C) Chromatin immunoprecipitation (ChIP) of H3, H3K36me3, or H3K18ac at ARSs with high (red) and low (green) readthrough transcription. Asynchronous cells were treated 1 h or 30 min with rapamycin to induce Nrd1 and Ysh1 depletion from the nucleus, respectively. ChIP was performed as described in Methods. Immunoprecipitated ARS loci were normalized to immunoprecipitated *SPT15* ORF after qPCR amplification. Fold enrichment was artificially set to 1 for the -Rap condition ($n = 3$). Error bars represent the standard error of the mean (SEM).

nascent transcription drives chromatin regulation of replication origins, which in turn defines, at least in part, ARS activity.

Rapamycin treatment of the Nrd1-AA *set2Δ* strain led to the appearance of small BrdU incorporation peaks all over the genome (Fig. 5D), suggesting that replication initiation loses its specificity when both noncoding transcription termination and H3K36 methylation are abrogated. Moreover, analysis of BrdU incorporation around non-ORC-bound and non-replicated ACSs (Eaton et al. 2010) revealed an increase of replication initiation at non-canonical sites when noncoding transcription readthrough is induced in the absence of Set2 (Fig. 5E,F). Thus, while noncoding transcription interferes with replication in the presence of Set2 by favoring a closed chromatin structure, transcription over dormant ARSs in the absence of Set2 activates replication, probably as a result of nucleosome instability.

Discussion

We have shown that ncRNA early termination by the Nrd1-dependent pathway in the vicinity of a subset of ARSs protects these origins from transcription and replication initiation defects. These observations suggest that inefficient noncoding transcription ter-

mination may influence replication origin activity. Consistently, our analyses reveal that natural readthrough transcription correlates with reduced ARS activity and a specific replication origin chromatin structure. Moreover, using mRNA or cryptic transcription termination mutants, we have established that nascent transcription is the causal link defining chromatin organization at a number of ARSs. Finally, we have presented evidence that transcription-induced chromatin modifications and not only nascent transcription per se control ARS activity. Thus, we propose widespread noncoding transcription as a novel primordial parameter defining replication initiation features (Fig. 6).

Nrd1-dependent transcription termination protects a subset of early/efficient replication origins from noncoding transcription

Previous studies on the relationship between transcription and replication have led to conflicting observations. Our analyses of pervasive transcription lead to the conclusion that transcriptional readthrough at ARSs is detrimental for replication initiation as already proposed by some reports (Snyder et al. 1988; Mori and Shirahige 2007; Blitzblau et al. 2012; Gros et al. 2015). Importantly, we show that natural nascent transcription per se is

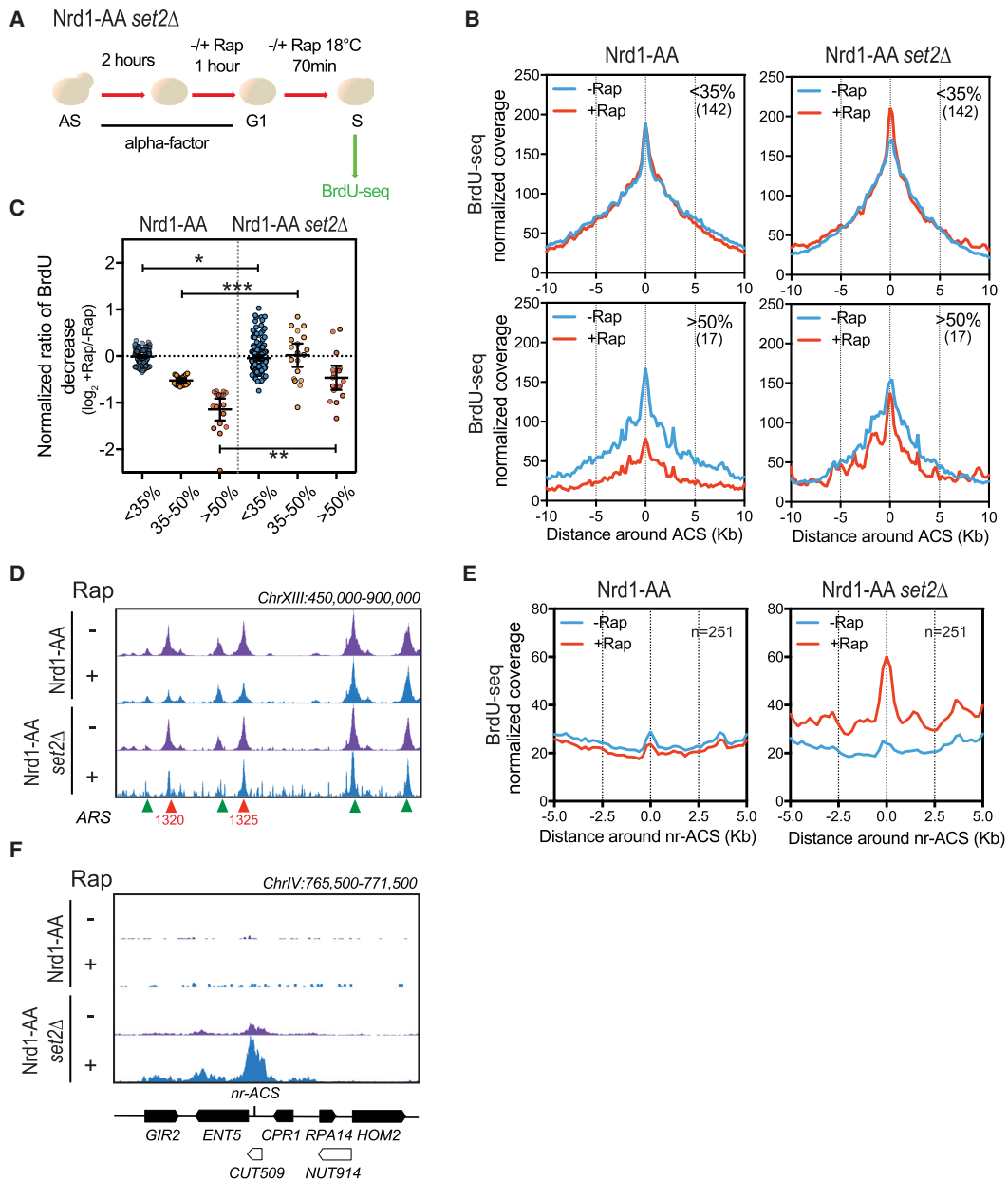


Figure 5. Absence of Set2 H3K36 methyltransferase partially rescues replication defects due to noncoding transcription readthrough. (A) Experimental scheme as described in Figure 1C. (B) Metagene analysis of the BrdU-seq for the 142 nonaffected ARSs (<35%) and the 17 most affected ARSs (>50%) for the Nrd1-AA and Nrd1-AA *set2Δ* strains. Plots for the Nrd1-AA strain were already presented in Figure 1F, with the exception of the normalized coverage, for which calculation is detailed in Methods. Profiles represent the mean coverage smoothed by a 200-bp moving window. ARSs were oriented according to their ACS T-rich sequence. (C) Scatter dot-plot presenting the normalized BrdU ratio for the different classes of ARS affected in BrdU incorporation in an Nrd1-AA strain and for the same classes of ARSs in the Nrd1-AA *set2Δ* strain. (D) Snapshot depicting the BrdU-seq reads for a part of Chromosome XIII. ARSs that are rescued in BrdU incorporation in the Nrd1-AA *set2Δ* +Rap condition are depicted in red, while nonaffected ARSs are in green. (E) Metagene analysis of BrdU incorporation 5 kb around nonreplicating ACSs (nr-ACS) in the indicated strains grown in -/+Rap. The representation is smoothed over a 200-bp moving window. (F) Snapshot illustrating the activation of a dormant nr-ACS in the Nrd1-AA *set2Δ* +Rap condition. (*) *P*-value < 0.05; (**) *P*-value < 0.01; (***) *P*-value < 0.001.

a criterion defining ARS activity genome-wide. Thus, the strategy for a replication origin to increase its activity would be to limit pervasive transcription. Accordingly, a subset of early and efficient ARSs are protected from pervasive transcription thanks to surrounding noncoding transcription termination by the Nrd1-de-

pendent pathway (Figs. 1, 3; Supplemental Fig. S4D). Thus, we propose that Nrd1-dependent termination in the vicinity of a replication origin is an efficient way to decrease transcriptional readthrough. Since Nrd1-dependent termination is regulated under stress conditions, it is tempting to speculate that this might also

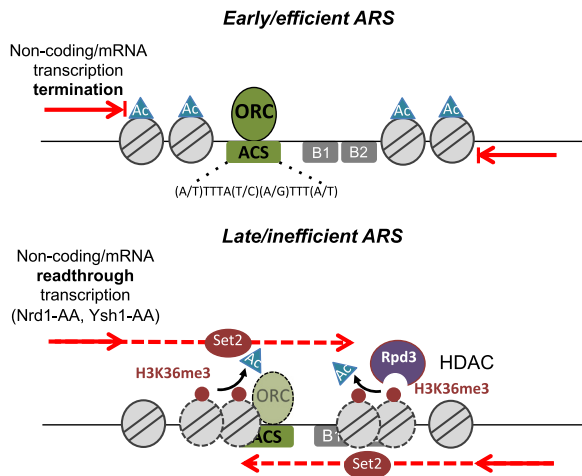


Figure 6. Noncoding transcription influences replication timing/efficiency by modulating ARS chromatin structure and ORC binding. The chromatin structure of replication origins is defined, at least in part, by the level of pervasive readthrough transcription. In the presence of efficient noncoding (Nrd1/Nab3/Sen1-dependent) or mRNA (CPF/CF-dependent) transcription termination, ARSs present low H3K36 trimethylation, high downstream nucleosome acetylation (Ac), a wide NDR, and more ORC binding at the ACS, favoring early and efficient replication. If transcription termination is deficient, H3K36me3 by Set2 increases and histone acetylation decreases, likely through the recruitment of the Rpd3 histone deacetylase; these modifications increase nucleosome stability and occupancy over the ARS, lowering the level of ORC recruitment and resulting in late and inefficient ARS replication.

affect replication origins usage (Bresson et al. 2017; van Nues et al. 2017). This scenario would define a novel role for noncoding transcription in the regulation of genome maintenance.

No mechanism similar to Nrd1-dependent termination has been described in other eukaryotes yet (Wittmann et al. 2017). In *S. cerevisiae*, Nrd1-protected origins reach a median firing efficiency peaking at 58%, while firing efficiency is around 30% in *Schizosaccharomyces pombe* (Heichinger et al. 2006). An attractive view is that Nrd1-dependent transcription termination represents an evolutionary pathway maximizing replication initiation efficiency.

Our results indicate that there is no significant linear correlation between nascent transcription and ARS activity. This connection appears when ARSs are divided into subsets (Fig. 3). Similar data were described in a recent paper (Candelli et al. 2018). These observations indicate that nascent transcription influences ARS activity only beyond a certain threshold and that other parameters contribute to origin function. Accordingly, a variety of molecular events have been involved in regulating ARS activity, which include MCM levels bound to ARSs, cell cycle regulated binding, and affinity of the ORC for the ACS, or the presence of Fkh1/2 proteins (Hoggard et al. 2013; Looke et al. 2013; Belsky et al. 2015; Das et al. 2015; Peace et al. 2016).

Replication origin chromatin structure is influenced by noncoding readthrough transcription

Previous work has involved the chromatin structure at replication origins as a parameter defining replication initiation. Early ARSs tend to show an open chromatin, low H3K36me3, and high histone acetylation levels (Pryde et al. 2009; Soriano et al.

2014). Our results indicate that these features may be directly related to the level of natural nascent transcription. Indeed, when compared to highly transcribed ARSs, origins with a low level of readthrough transcription present lower nucleosome occupancy, lower H3K36me3, and higher histone acetylation levels (Fig. 3). Of note, H3K36me3 is deposited by Set2, a histone methyltransferase (HMT) recruited through interaction with the elongating RNA Pol II CTD. H3K36me3 serves as a platform for the binding of Rpd3S, a histone deacetylase complex described to deacetylate and stabilize reassembled nucleosomes in the wake of the transcription machinery, suppressing initiation from cryptic sites within ORFs (Carrozza et al. 2005; for a recent review, see Woo et al. 2017). This molecular mechanism may represent the connection between pervasive transcription and chromatin structure of replication origins. Indeed, increasing transcriptional readthrough into replication origins is accompanied by higher levels of H3K36me3, lower levels of H3K18ac, increased nucleosome occupancy, and replication defects (Figs. 1, 2, 4; Supplemental Fig. S6). Importantly, BrdU-seq experiments cannot discriminate between timing and efficiency defects. However, since nucleosome methylations are relatively stable modifications, it would be appealing to propose that even rare events of noncoding transcription may stably inactivate replication origins until the subsequent S-phase dilutes or a histone de-methylase erases these methylation marks. In such a model, pervasive transcription may shape replication origin chromatin for inefficient usage.

These observations shed new light on earlier published results. First, loss of Rpd3 leads to a global increase in acetylation around ARSs and early firing of many late origins (Vogelauer et al. 2002; Knott et al. 2009). It was proposed that the “accelerated” replication in *rpd3Δ* is mainly due to a reduced titration of replication initiation factors by the rDNA origins (Yoshida et al. 2014); however, loss of Rpd3 also has a global impact on increasing the size of replication origins NDR (Soriano et al. 2014). Of note, loss of Rpd3 abrogates the function of both Rpd3S and Rpd3L, another histone deacetylase complex involved in gene repression following recruitment to promoters via a Set2/H3K36me3-independent pathway (Woo et al. 2017). While loss of Rpd3L subunits was shown to result in increased BrdU incorporation at a number of ARSs, especially those adjacent to up-regulated genes, loss of Rpd3S subunits or Set2 led to a weaker but more generalized increase in ARS replication initiation (Knott et al. 2009). This difference could reflect a primary specific effect of loss of Rpd3L on rDNA replication and increased availability of replication factors in the absence of this HDAC. Although the replication phenotype was less pronounced when deleting Rpd3S, the data support the view that pervasive transcription promotes Set2/H3K36me3-mediated histone de-acetylation by Rpd3S and globally contributes to negatively regulate replication origin activity.

Our results further indicate that high readthrough transcription correlates with decreased ORC binding (Fig. 3; Supplemental Fig. S4E). It was proposed that replication initiation timing depends more on the surrounding chromatin than on the ORC-ACS in vitro affinity by itself (Hoggard et al. 2013). It would be interesting to further dissect the molecular events at origins and to define whether nascent transcription per se evicts the ORC, leading to nucleosome deposition and histone modifications, or whether RNA Pol II readthrough and nucleosome incorporation outcompete ORC turnover (Fig. 6).

We observe genome-wide appearance of BrdU peaks when *SET2* is deleted in conjunction with the anchor away of Nrd1. These peaks are not detected in the *set2Δ* mutant alone, indicating

that activation of dormant origins is not only related to the absence of the histone mark. Deletion of *SET2* is known to drastically increase the level of intra-genic transcription initiation (Malabat et al. 2015). A fraction of this novel nascent transcription may be cleared by the Nrd1-dependent termination pathway. We propose that, in the absence of Nrd1, transcription may hit dormant origins, which, in the absence of H3K36 methylation, will promote replication initiation due to nucleosome instability and chromatin opening. Thus, when not associated with H3K36 methylation, transcription may have a positive effect on replication initiation.

Implications for a pervasive transcription-dependent replication initiation model in metazoans

Identification of replication origins in mouse embryonic stem cells showed that nearly half of them are contained in promoters (Sequeira-Mendes et al. 2009), and recent ORC binding data in human cells led to the same conclusion (Dellino et al. 2013; Miotto et al. 2016). In contrast, replication initiation in *S. cerevisiae* more frequently occurs next to gene terminators (Nieduszynski et al. 2006). Human promoters are bidirectional and lead to the production of highly unstable promoter upstream transcripts (PROMPTs), suggesting that pervasive transcription could also play a role in metazoan replication initiation (Preker et al. 2008; Mayer et al. 2015; Nojima et al. 2015). It has recently been shown that replication initiation in human cells occurs within broad, over-30-kb regions, flanked by ORC binding at one of the two ends (Petryk et al. 2016). Considering that MCM helicases can slide along the chromosome with the help of transcription (Gros et al. 2015), it is appealing to propose that promoter-associated noncoding transcription redistributes the MCM helicases from their ORC binding initial site of loading. Since we have established widespread noncoding transcription as a novel primordial parameter regulating replication initiation in *S. cerevisiae*, its importance for the metazoan replication program warrants future study.

Methods

Yeast strains

All strains were derived from W303 and Anchor-Away genetic backgrounds (see Supplemental Table S2; Haruki et al. 2008). Cells were cultivated as described in Supplemental Material.

G1-phase synchronization and BrdU labeling

Cells were grown as described in Soudet et al. (2014) with some modifications, indicated in Supplemental Material.

BrdU immunoprecipitation and sequencing

BrdU immunoprecipitation was mainly performed as described in Soudet et al. (2014) with some modifications, indicated in the Supplemental Material. Libraries of immunoprecipitated BrdU-containing DNA were constructed using the iDeal Library Preparation kit (Diagenode). Sequencing was performed on the HiSeq 4000 sequencer (Illumina). For specific loci analyses by quantitative PCR, BrdU-containing DNA was amplified using the SYBR Select Master Mix for CFX (Applied Biosciences) on a CFX96 real-time detection system (Bio-Rad).

MNase-seq

MNase treatment was performed as described in Weiner et al. (2015). Chromatin was extracted by breaking cells with bead beating in a magnalyser (Roche). Chromatin was then collected by centrifugation and resuspended in NP-buffer (0.5 mM spermidine, 1 mM β -ME, 0.075% NP-40, 50 mM NaCl, 10 mM Tris at pH 7.4, 5 mM $MgCl_2$, 1 mM $CaCl_2$). MNase (Thermo Fisher Scientific) treatment was performed at a previously optimized concentration to have comparable intensity of both mono- and di-nucleosomes within and between the samples. MNase treatment was followed by de-crosslinking and protease treatment, and DNA was extracted using NucleoSpin gel and PCR extraction columns (Macherey-Nagel). An iDeal Library Preparation kit (Diagenode) was then used for library construction. Sequencing was performed on the HiSeq 4000 sequencer (Illumina).

BrdU-seq and MNase-seq bioinformatic analyses

Fifty-base pair paired-end reads were aligned to sacCer3 genome assembly using HTSstation (David et al. 2014). PCR duplicates were removed from the analysis. For the MNase-seq, 120- to 200-bp fragments were filtered to detect molecules with nucleosome size using HTS Bioscript (David et al. 2014). BrdU-seq and MNase-seq density files (bigWig) were averaged for the two replicates of each condition. All subsequent analyses were performed using HTS Bioscript including metagene analyses. To assign one value of BrdU incorporation to each ARS, BrdU incorporation was measured 5 kb around ACSs considering this area as 1 bin. For the MNase-seq, nucleosome occupancy was quantified over the ACS to +100 bp area of oriented ARSs.

Since no spike-in was used in our experiments and since Nrd1-AA *set2 Δ* +Rap substantially changes the density profile because of dormant origins firing, Figure 5 was normalized as follows: The <35% affected ARS class for BrdU incorporation was considered as equal in +Rap and -Rap in an average 5 kb around the ACS in both Nrd1-AA and Nrd1-AA *set2 Δ* . This gave a normalization factor for each strain, which was then used to quantify the other classes.

Chromatin immunoprecipitation (ChIP)

ChIP experiments were performed as described previously with some modifications (Camblong et al. 2007), described in the Supplemental Material. ChIPs were repeated three times with different chromatin extracts from independent cultures. Immunoprecipitated DNA was then purified and quantified by qPCR. Immunoprecipitated ARS loci were normalized to immunoprecipitated *SPT15* ORF after qPCR amplification.

List of noncoding RNAs and replication origins

The list of CUTs was obtained from Xu et al. (2009), while the list of NUTs was kindly provided by the Cramer lab (Schulz et al. 2013). Among the NUTs, only those showing at least a twofold increase in +Rap/-Rap were taken into account to unify the threshold of ncRNA definition between CUTs and NUTs. The list of ARS (Supplemental Table S1) consists of the 234 ACS taken from Soriano et al. (2014) that overlap with the replication origins described in Hawkins et al. (2013), for which replication timing and efficiency have been defined. Replication origins with an efficiency <15% were not taken into account.

Statistical analysis

All statistical analyses of this work were performed using Prism 7.0 (Graphpad). All tests are nonpaired tests (with the exception of Fig.

5C). *t*-tests or Mann–Whitney *U* tests were used according to the normality of the data analyzed, which was calculated using a d'Agostino–Pearson omnibus normality test.

Downloaded data sets

For RNA Pol II PAR-CLIP, RNA-seq, chromatin and ORC profiles, data were retrieved from Schaughency et al. (2014) (GEO: GSE56435), Uwimana et al. (2017) (GEO: GSE89601), Kubik et al. (2015) (GEO: GSE73337), Weiner et al. (2015) (GEO: GSE61888), and Belsky et al. (2015) (SRA: SRP041314).

Data access

All sequencing data from this study have been submitted to the NCBI Gene Expression Omnibus (GEO; <https://www.ncbi.nlm.nih.gov/geo/>) under accession number GSE111058.

Acknowledgments

We thank O. Aparicio, D. MacAlpine, and P. Cramer for sharing data and reagents and M. Strubin, F. Steiner, M. Shyian, G. Canal, T. Halazonetis, and all members from the Stutz lab for comments on the manuscript. We also thank D. Libri for communication of unpublished results. This work was funded by the Swiss National Science Foundation (31003A 153331), iGE3, and the Canton of Geneva, as well as a Polish Swiss Research Programme (PSRP NoCore 183/2010).

Author contributions: J.S. and F.S. conceived the study. J.S. performed most experiments and analyzed the results together with F.S.; J.K.G. performed the MNase-seq; J.S. and F.S. wrote the manuscript.

References

- Aparicio OM. 2013. Location, location, location: it's all in the timing for replication origins. *Genes Dev* **27**: 117–128. doi:10.1101/gad.209999.112
- Aparicio JG, Viggiani CJ, Gibson DG, Aparicio OM. 2004. The Rpd3-Sin3 histone deacetylase regulates replication timing and enables intra-S origin control in *Saccharomyces cerevisiae*. *Mol Cell Biol* **24**: 4769–4780. doi:10.1128/MCB.24.11.4769-4780.2004
- Arigo JT, Eyler DE, Carroll KL, Corden JL. 2006. Termination of cryptic unstable transcripts is directed by yeast RNA-binding proteins Nrd1 and Nab3. *Mol Cell* **23**: 841–851. doi:10.1016/j.molcel.2006.07.024
- Baejen C, Andreani J, Torkler P, Battaglia S, Schwalb B, Lidschreiber M, Maier KC, Boltendahl A, Rus P, Esslinger S, et al. 2017. Genome-wide analysis of RNA polymerase II termination at protein-coding genes. *Mol Cell* **66**: 38–49.e6. doi:10.1016/j.molcel.2017.02.009.
- Bell SP. 1995. Eukaryotic replicators and associated protein complexes. *Curr Opin Genet Dev* **5**: 162–167. doi:10.1016/0959-437X(95)80003-4
- Belsky JA, MacAlpine HK, Lubelsky Y, Hartemink AJ, MacAlpine DM. 2015. Genome-wide chromatin footprinting reveals changes in replication origin architecture induced by pre-RC assembly. *Genes Dev* **29**: 212–224. doi:10.1101/gad.247924.114
- Blitzblau HG, Chan CS, Hochwagen A, Bell SP. 2012. Separation of DNA replication from the assembly of break-competent meiotic chromosomes. *PLoS Genet* **8**: e1002643. doi:10.1371/journal.pgen.1002643
- Bresson S, Tuck A, Staneva D, Tollervey D. 2017. Nuclear RNA decay pathways aid rapid remodeling of gene expression in yeast. *Mol Cell* **65**: 787–800.e5. doi:10.1016/j.molcel.2017.01.005
- Camblong J, Iglesias N, Fickentscher C, Dieppois G, Stutz F. 2007. Antisense RNA stabilization induces transcriptional gene silencing via histone deacetylation in *S. cerevisiae*. *Cell* **131**: 706–717. doi:10.1016/j.cell.2007.09.014
- Candelli T, Gros J, Libri D. 2018. Pervasive transcription fine-tunes replication origin activity. *bioRxiv* doi:10.1101/384859
- Carrozza MJ, Li B, Florens L, Suganuma T, Swanson SK, Lee KK, Shia WJ, Anderson S, Yates J, Washburn MP, et al. 2005. Histone H3 methylation by Set2 directs deacetylation of coding regions by Rpd3S to suppress spurious intragenic transcription. *Cell* **123**: 581–592. doi:10.1016/j.cell.2005.10.023

- Castelnuovo M, Rahman S, Guffanti E, Infantino V, Stutz F, Zenklusen D. 2013. Bimodal expression of *PHO84* is modulated by early termination of antisense transcription. *Nat Struct Mol Biol* **20**: 851–858. doi:10.1038/nsmb.2598
- Castelnuovo M, Zaugg JB, Guffanti E, Maffioletti A, Camblong J, Xu Z, Clauder-Münster S, Steinmetz LM, Luscombe NM, Stutz F. 2014. Role of histone modifications and early termination in pervasive transcription and antisense-mediated gene silencing in yeast. *Nucleic Acids Res* **42**: 4348–4362. doi:10.1093/nar/gku100
- Churchman LS, Weissman JS. 2011. Nascent transcript sequencing visualizes transcription at nucleotide resolution. *Nature* **469**: 368–373. doi:10.1038/nature09652
- Czajkowsky DM, Liu J, Hamlin JL, Shao Z. 2008. DNA combing reveals intrinsic temporal disorder in the replication of yeast chromosome VI. *J Mol Biol* **375**: 12–19. doi:10.1016/j.jmb.2007.10.046
- Das SP, Borrmann T, Liu VW, Yang SC, Bechhoefer J, Rhind N. 2015. Replication timing is regulated by the number of MCMs loaded at origins. *Genome Res* **25**: 1886–1892. doi:10.1101/gr.195305.115
- David FP, Delafontaine J, Carat S, Ross FJ, Lefebvre G, Jarosz Y, Sinclair L, Noordermeer D, Rougemont J, Leleu M. 2014. HTSstation: a web application and open-access libraries for high-throughput sequencing data analysis. *PLoS One* **9**: e85879. doi:10.1371/journal.pone.0085879
- Deegan TD, Diffley JF. 2016. MCM: one ring to rule them all. *Curr Opin Struct Biol* **37**: 145–151. doi:10.1016/j.sbi.2016.01.014
- Dellino GI, Cittaro D, Piccioni R, Luzi L, Banfi S, Segalla S, Cesaroni M, Mendoza-Maldonado R, Giacca M, Pelicci PG. 2013. Genome-wide mapping of human DNA-replication origins: Levels of transcription at ORC1 sites regulate origin selection and replication timing. *Genome Res* **23**: 1–11. doi:10.1101/gr.142331.112
- Eaton ML, Galani K, Kang S, Bell SP, MacAlpine DM. 2010. Conserved nucleosome positioning defines replication origins. *Genes Dev* **24**: 748–753. doi:10.1101/gad.1913210
- Fraser HB. 2013. Cell-cycle regulated transcription associates with DNA replication timing in yeast and human. *Genome Biol* **14**: R111. doi:10.1186/gb-2013-14-10-r111
- Gros J, Kumar C, Lynch G, Yadav T, Whitehouse I, Remus D. 2015. Post-licensing specification of eukaryotic replication origins by facilitated Mcm2-7 sliding along DNA. *Mol Cell* **60**: 797–807. doi:10.1016/j.molcel.2015.10.022
- Haruki H, Nishikawa J, Laemmli UK. 2008. The anchor-away technique: rapid, conditional establishment of yeast mutant phenotypes. *Mol Cell* **31**: 925–932. doi:10.1016/j.molcel.2008.07.020
- Hawkins M, Retkute R, Muller CA, Saner N, Tanaka TU, de Moura AP, Nieduszynski CA. 2013. High-resolution replication profiles define the stochastic nature of genome replication initiation and termination. *Cell Rep* **5**: 1132–1141. doi:10.1016/j.celrep.2013.10.014
- Heichinger C, Penkett CJ, Bähler J, Nurse P. 2006. Genome-wide characterization of fission yeast DNA replication origins. *EMBO J* **25**: 5171–5179. doi:10.1038/sj.emboj.7601390
- Hoggart T, Shor E, Muller CA, Nieduszynski CA, Fox CA. 2013. A link between ORC-origin binding mechanisms and origin activation time revealed in budding yeast. *PLoS Genet* **9**: e1003798. doi:10.1371/journal.pgen.1003798
- Jensen TH, Jacquier A, Libri D. 2013. Dealing with pervasive transcription. *Mol Cell* **52**: 473–484. doi:10.1016/j.molcel.2013.10.032
- Kim M, Krogan NJ, Vasiljeva L, Rando OJ, Nedea E, Greenblatt JF, Buratowski S. 2004. The yeast Rat1 exonuclease promotes transcription termination by RNA polymerase II. *Nature* **432**: 517–522. doi:10.1038/nature03041
- Knott SR, Viggiani CJ, Tavaré S, Aparicio OM. 2009. Genome-wide replication profiles indicate an expansive role for Rpd3L in regulating replication initiation timing or efficiency, and reveal genomic loci of Rpd3 function in *Saccharomyces cerevisiae*. *Genes Dev* **23**: 1077–1090. doi:10.1101/gad.1784309
- Knott SR, Peace JM, Ostrow AZ, Gan Y, Rex AE, Viggiani CJ, Tavaré S, Aparicio OM. 2012. Forkhead transcription factors establish origin timing and long-range clustering in *S. cerevisiae*. *Cell* **148**: 99–111. doi:10.1016/j.cell.2011.12.012
- Kubik S, Bruzzone MJ, Jacquet P, Falcone JL, Rougemont J, Shore D. 2015. Nucleosome stability distinguishes two different promoter types at all protein-coding genes in yeast. *Mol Cell* **60**: 422–434. doi:10.1016/j.molcel.2015.10.002
- Looke M, Reimand J, Sedman T, Sedman J, Jarvinen L, Varv S, Peil K, Kristjuhan K, Vilo J, Kristjuhan A. 2010. Relicensing of transcriptionally inactivated replication origins in budding yeast. *J Biol Chem* **285**: 40004–40011. doi:10.1074/jbc.M110.148924
- Looke M, Kristjuhan K, Varv S, Kristjuhan A. 2013. Chromatin-dependent and -independent regulation of DNA replication origin activation in budding yeast. *EMBO Rep* **14**: 191–198. doi:10.1038/embor.2012.196
- Luo W, Johnson AW, Bentley DL. 2006. The role of Rat1 in coupling mRNA 3'-end processing to transcription termination: implications for a

- unified allosteric–torpedo model. *Genes Dev* **20**: 954–965. doi:10.1101/gad.1409106
- Malabat C, Feuerbach F, Ma L, Saveanu C, Jacquier A. 2015. Quality control of transcription start site selection by nonsense-mediated-mRNA decay. *eLife* **4**: e06722. doi:10.7554/eLife.06722
- Mayan MD. 2013. RNAP-II molecules participate in the anchoring of the ORC to rDNA replication origins. *PLoS One* **8**: e53405. doi:10.1371/journal.pone.0053405
- Mayer A, di Iulio J, Maleri S, Eser U, Vierstra J, Reynolds A, Sandstrom R, Stamatoyannopoulos JA, Churchman LS. 2015. Native elongating transcript sequencing reveals human transcriptional activity at nucleotide resolution. *Cell* **161**: 541–554. doi:10.1016/j.cell.2015.03.010
- McGuffee SR, Smith DJ, Whitehouse I. 2013. Quantitative, genome-wide analysis of eukaryotic replication initiation and termination. *Mol Cell* **50**: 123–135. doi:10.1016/j.molcel.2013.03.004
- Miotto B, Ji Z, Struhl K. 2016. Selectivity of ORC binding sites and the relation to replication timing, fragile sites, and deletions in cancers. *Proc Natl Acad Sci* **113**: E4810–E4819. doi:10.1073/pnas.1609060113
- Mori S, Shirahige K. 2007. Perturbation of the activity of replication origin by meiosis-specific transcription. *J Biol Chem* **282**: 4447–4452. doi:10.1074/jbc.M609671200
- Neil H, Malabat C, d'Aubenton-Carafa Y, Xu Z, Steinmetz LM, Jacquier A. 2009. Widespread bidirectional promoters are the major source of cryptic transcripts in yeast. *Nature* **457**: 1038–1042. doi:10.1038/nature07747
- Nieduszynski CA, Blow JJ, Donaldson AD. 2005. The requirement of yeast replication origins for pre-replication complex proteins is modulated by transcription. *Nucleic Acids Res* **33**: 2410–2420. doi:10.1093/nar/gki539
- Nieduszynski CA, Knox Y, Donaldson AD. 2006. Genome-wide identification of replication origins in yeast by comparative genomics. *Genes Dev* **20**: 1874–1879. doi:10.1101/gad.385306
- Nojima T, Gomes T, Grosso AR, Kimura H, Dye MJ, Dhir S, Carmo-Fonseca M, Proudfoot NJ. 2015. Mammalian NET-seq reveals genome-wide nascent transcription coupled to RNA processing. *Cell* **161**: 526–540. doi:10.1016/j.cell.2015.03.027
- Peace JM, Villwock SK, Zeytounian JL, Gan Y, Aparicio OM. 2016. Quantitative BrdU immunoprecipitation method demonstrates that Fkh1 and Fkh2 are rate-limiting activators of replication origins that reprogram replication timing in G1 phase. *Genome Res* **26**: 365–375. doi:10.1101/gr.196857.115
- Petryk N, Kahli M, d'Aubenton-Carafa Y, Jaszczyszyn Y, Shen Y, Silvain M, Thermes C, Chen CL, Hyrien O. 2016. Replication landscape of the human genome. *Nat Commun* **7**: 10208. doi:10.1038/ncomms10208
- Porrua O, Boudvillain M, Libri D. 2016. Transcription termination: variations on common themes. *Trends Genet* **32**: 508–522. doi:10.1016/j.tig.2016.05.007
- Preker P, Nielsen J, Kammler S, Lykke-Andersen S, Christensen MS, Mapendano CK, Schierup MH, Jensen TH. 2008. RNA exosome depletion reveals transcription upstream of active human promoters. *Science* **322**: 1851–1854. doi:10.1126/science.1164096
- Pryde F, Jain D, Kerr A, Curley R, Mariotti FR, Vogelauer M. 2009. H3 K36 methylation helps determine the timing of Cdc45 association with replication origins. *PLoS One* **4**: e5882. doi:10.1371/journal.pone.0005882
- Raghuraman MK, Winzler EA, Collingwood D, Hunt S, Wodicka L, Conway A, Lockhart DJ, Davis RW, Brewer BJ, Fangman WL. 2001. Replication dynamics of the yeast genome. *Science* **294**: 115–121. doi:10.1126/science.294.5540.115
- Rodriguez J, Lee L, Lynch B, Tsukiyama T. 2017. Nucleosome occupancy as a novel chromatin parameter for replication origin functions. *Genome Res* **27**: 269–277. doi:10.1101/gr.209940.116
- Rundlett SE, Carmen AA, Kobayashi R, Bavykin S, Turner BM, Grunstein M. 1996. HDA1 and RPD3 are members of distinct yeast histone deacetylase complexes that regulate silencing and transcription. *Proc Natl Acad Sci* **93**: 14503–14508. doi:10.1073/pnas.93.25.14503
- Schaughency P, Merran J, Corden JL. 2014. Genome-wide mapping of yeast RNA polymerase II termination. *PLoS Genet* **10**: e1004632. doi:10.1371/journal.pgen.1004632
- Schulz D, Schwalb B, Kiesel A, Baejen C, Torkler P, Gagneur J, Soeding J, Cramer P. 2013. Transcriptome surveillance by selective termination of noncoding RNA synthesis. *Cell* **155**: 1075–1087. doi:10.1016/j.cell.2013.10.024
- Segal E, Widom J. 2009. Poly(dA:dT) tracts: major determinants of nucleosome organization. *Curr Opin Struct Biol* **19**: 65–71. doi:10.1016/j.sbi.2009.01.004
- Sequeira-Mendes J, Diaz-Urriarte R, Apedaile A, Huntley D, Brockdorff N, Gomez M. 2009. Transcription initiation activity sets replication origin efficiency in mammalian cells. *PLoS Genet* **5**: e1000446. doi:10.1371/journal.pgen.1000446
- Snyder M, Sapolsky RJ, Davis RW. 1988. Transcription interferes with elements important for chromosome maintenance in *Saccharomyces cerevisiae*. *Mol Cell Biol* **8**: 2184–2194. doi:10.1128/MCB.8.5.2184
- Soriano I, Morafraila EC, Vázquez E, Antequera F, Segurado M. 2014. Different nucleosomal architectures at early and late replicating origins in *Saccharomyces cerevisiae*. *BMC Genomics* **15**: 791. doi:10.1186/1471-2164-15-791
- Soudet J, Jolivet P, Teixeira MT. 2014. Elucidation of the DNA end-replication problem in *Saccharomyces cerevisiae*. *Mol Cell* **53**: 954–964. doi:10.1016/j.molcel.2014.02.030
- Steinmetz EJ, Conrad NK, Brow DA, Corden JL. 2001. RNA-binding protein Nrd1 directs poly(A)-independent 3'-end formation of RNA polymerase II transcripts. *Nature* **413**: 327–331. doi:10.1038/35095090
- Stinchcomb DT, Struhl K, Davis RW. 1979. Isolation and characterization of a yeast chromosomal replicator. *Nature* **282**: 39–43. doi:10.1038/282039a0
- Tudek A, Porrua O, Kabzinski T, Lidschreiber M, Kubicek K, Fortova A, Lacroute F, Vanacova S, Cramer P, Stefl R, et al. 2014. Molecular basis for coordinating transcription termination with noncoding RNA degradation. *Mol Cell* **55**: 467–481. doi:10.1016/j.molcel.2014.05.031
- Unnikrishnan A, Gafken PR, Tsukiyama T. 2010. Dynamic changes in histone acetylation regulate origins of DNA replication. *Nat Struct Mol Biol* **17**: 430–437. doi:10.1038/nsmb.1780
- Uwimana N, Collin P, Jeronimo C, Haibe-Kains B, Robert F. 2017. Bidirectional terminators in *Saccharomyces cerevisiae* prevent cryptic transcription from invading neighboring genes. *Nucleic Acids Res* **45**: 6417–6426. doi:10.1093/nar/gkx242
- van Dijk EL, Chen CL, d'Aubenton-Carafa Y, Gourvenec S, Kwapisz M, Roche V, Bertrand C, Silvain M, Legoix-Ne P, Loeillet S, et al. 2011. XUTs are a class of Xrn1-sensitive antisense regulatory non-coding RNA in yeast. *Nature* **475**: 114–117. doi:10.1038/nature10118
- van Nues R, Schweikert G, de Leau E, Selega A, Langford A, Franklin R, Iosub I, Wadsworth P, Sanguinetti G, Granneman S. 2017. Kinetic CRAC uncovers a role for Nab3 in determining gene expression profiles during stress. *Nat Commun* **8**: 12. doi:10.1038/s41467-017-00025-5
- Vogelauer M, Rubbi L, Lucas I, Brewer BJ, Grunstein M. 2002. Histone acetylation regulates the time of replication origin firing. *Mol Cell* **10**: 1223–1233. doi:10.1016/S1097-2765(02)00702-5
- Weiner A, Hsieh TH, Appleboim A, Chen HV, Rahat A, Amit I, Rando OJ, Friedman N. 2015. High-resolution chromatin dynamics during a yeast stress response. *Mol Cell* **58**: 371–386. doi:10.1016/j.molcel.2015.02.002
- Wittmann S, Renner M, Watts BR, Adams O, Huseyin M, Baejen C, El Omari K, Kilchert C, Heo DH, Kecman T, et al. 2017. The conserved protein Seb1 drives transcription termination by binding RNA polymerase II and nascent RNA. *Nat Commun* **8**: 14861. doi:10.1038/ncomms14861
- Woo H, Dam Ha S, Lee SB, Buratowski S, Kim T. 2017. Modulation of gene expression dynamics by co-transcriptional histone methylations. *Exp Mol Med* **49**: e326. doi:10.1038/emmm.2017.19
- Wyers F, Rougemaille M, Badis G, Rousselle JC, Dufour ME, Boulay J, Regnault B, Devaux F, Namane A, Seraphin B, et al. 2005. Cryptic Pol II transcripts are degraded by a nuclear quality control pathway involving a new poly(A) polymerase. *Cell* **121**: 725–737. doi:10.1016/j.cell.2005.04.030
- Xu Z, Wei W, Gagneur J, Perocchi F, Clauder-Münster S, Camblong J, Guffanti E, Stutz F, Huber W, Steinmetz LM. 2009. Bidirectional promoters generate pervasive transcription in yeast. *Nature* **457**: 1033–1037. doi:10.1038/nature07728
- Yang SC, Rhind N, Bechhoefer J. 2010. Modeling genome-wide replication kinetics reveals a mechanism for regulation of replication timing. *Mol Syst Biol* **6**: 404. doi:10.1038/msb.2010.61
- Yoshida K, Poveda A, Pasero P. 2013. Time to be versatile: regulation of the replication timing program in budding yeast. *J Mol Biol* **425**: 4696–4705. doi:10.1016/j.jmb.2013.09.020
- Yoshida K, Bacal J, Desmarais D, Padioleau I, Tsaponina O, Chabes A, Pantescio V, Dubois E, Parrinello H, Skrzypczak M, et al. 2014. The histone deacetylases Sir2 and Rpd3 act on ribosomal DNA to control the replication program in budding yeast. *Mol Cell* **54**: 691–697. doi:10.1016/j.molcel.2014.04.032

Received May 15, 2018; accepted in revised form October 31, 2018.

